NTNU
Norwegian University of
Science and Technology

Susceptibility to Hydrogen Induced Stress Cracking of centrifugal cast 25Cr Duplex Stainless Steel

Linn Cecilie Gjelseng

Materials Science and Engineering
Submission date: June 2017
Supervisor: Roy Johnsen, MTP
Co-supervisor: Mariano Iannuzzi, MTP
Atle Qvale, GE Oil & Gas
Anders Jernberg, GE Oil & Gas

Norwegian University of Science and Technology
Department of Mechanical and Industrial Engineering

Preface

As a part of the requirements of the Master's degree program at the Department of Materials Science and Engineering, the present thesis is submitted to the Norwegian University of Science and Technology (NTNU). The supervisors of this work are Professors Roy Johnsen and Mariano Iannuzzi at NTNU in collaboration with Atle Qvale and Anders Jernberg at GE Oil & Gas.

I am very grateful to all my supervisors at both NTNU and GE Oil & Gas for their steady guidance throughout the process of writing this thesis. Professors Roy Johnsen and Mariano Iannuzzi let me employ their expertise in HISC testing, without which this work would not have been the same. I am also grateful to Atle Qvale and Anders Jernberg for their input during discussions as well as for initiating the project and providing the necessary materials. Thank you all.

The engineers and other staff at NTNU and SINTEF must also be mentioned. Especially Nousha Kheramand, Trygve Schanke and Pål Skaret should be thanked for their help with the SEM, laboratory equipment and performing tests needed for the thesis, respectively. Thanks are also extended to Ann-Karin Kvernbråten for performing the hydrogen measurements used in this thesis.

Finally, I am eternally grateful to my co-students at the Department of Materials Science and Technology for making my time at NTNU such a life-changing experience.

Linn Cecilie Gjelseng
June 28. 2017, Trondheim

Abstract

Testing of the susceptibility towards hydrogen induced stress cracking (HISC) for five 25%Cr super duplex stainless steels (SDSS) under cathodic protection (CP) in seawater has been conducted. The materials were from pipes produced through different production methods; hot extrusion with and without subsequent cold drawing, manufactured from a forged bar and centrifugally cast. The testing was carried out in cortest proof rings on three test specimens pre-charged with hydrogen and one reference specimen without hydrogen until fracture occurred. Hydrogen measurements were conducted and the fracture surfaces were examined in a scanning electron microscope (SEM), and the embrittlement through thickness was indexed. The possibility of secondary cracking was also investigated using the SEM. In addition, the microstructures were examined using optical microscopy (OM) and assessed compared to the HISC testing results. The austenite spacing was also measured.

The hydrogen measurements together with the presence of secondary cracking of all test materials confirmed HISC being the fracture mechanism. The test results indicated that all SDSS materials tested are susceptible to HISC, and that the hot extruded material with no cold deformation has a higher HISC resistance while centrifugally cast materials are more prone to HISC than the other production methods. The fracture surfaces of all hydrogen charged test materials showed features indicating a reduction in ductility due to HISC as well as both ductile and brittle fracture characteristics across the surfaces. The placement of the ductile and brittle features varied, and both could be found close to the centre and edges of the fracture surfaces. The fracture surfaces for the reference specimens showed mostly ductile fracture characteristics.

The results from the HISC testing were discussed compared to available literature on the subject of HISC in SDSS, and the susceptibility of the materials from the different materials towards HISC were ranked from lowest to highest based on the overall test performance and measurements conducted. The ranking of production methods is as follows: hot extruded pipes > hot extruded pipes with subsequent cold drawing > forginged pipes > centrifugal cast pipes.

Sammendrag

Følsomheten mot hydrogenindusert spenningskorrosjon (HISC) for fem 25%Cr super duplex rustfrie stål (SDSS) utsatt for katodisk beskyttelse (CP) i sjøvann har blitt testet. Materialprøvene var fra rør produsert gjennom ulike produksjonsmetoder; varmekstrudering med og uten etterfølgende kalddeformasjon, produsert fra en smidd sylinder og sentrifugalstøping. Testingen ble utført ved stegvis økende last til brudd i cortest testringer ("Cortest proof rings") på tre prøver forladet med hydrogen og én referanseprøve uten hydrogen. Hydrogenmålinger ble gjort og bruddflatene ble undersøkt ved hjelp av et scanning elektronmikroskop (SEM). Forsprøingen grunnet hydrogen gjennom hele prøvetykkelsen ble indeksert og mulige sekundærsprekker ble undersøkt, også dette ved bruk av SEM. Mikrostrukturen til de ulike materialene ble undersøkt ved bruk av lysmikroskopi og vurdert i fohold til resultatene fra testingen for HISC. Austenittavstanden ("austenite spacing") ble også målt for materialene.

HISC ble bekreftet som bruddmekanisme for materialene gjennom hydrogenmålingene samt tilstedeværelsen av sekundærsprekker i alle materialprøvene. Testresultatene indikerer at det varmekstruderte materialet uten kalddeformasjon har høyest motstand mot HISC, mens de sentrifugalstøpte materialene har den laveste motstanden av produksjonsmetodene undersøkt i denne oppgaven. Bruddflatene til alle testmaterialene indikerte reduksjon av duktilitet grunnet HISC, samt både duktile og sprø bruddkarakeristikker ble observert for de forladde prøvene. Plasseringen av de duktile og sprø områdene varierte, og begge ble observert nær midten og mot kanten av prøvene. Referanseprøvenes bruddflater innholdt stort sett duktile bruddkarakteristikker.

Resultatene fra HISC-testingen ble diskutert i forhold til tilgjengelig litteratur om HISC i SDSS, og følsomheten til materialene for denne bruddmekanismen ble rangert fra lavest til høyest basert på den helhetlige prestasjonen i testene og de utførte målingene. Rangeringen for de ulike produksjonsmetodene er som følger: varmekstruderte rør > varmekstruderte rør med påfølgende kalddeformasjon > smidde rør > sentrifugalstøpte rør.

Contents

Nomenclature

Symbols	Explanation
α	Ferrite
α_m, α_{m+b}	Allowable SMYS factors
γ	Austenite
γ_{HISC}	Material quality factor
ε_{res}	Residual strain
σ_m, σ_{m+b}	Stresses: membrane, membrane and bending
σ_{res}	Residual stress
σ_{th}, $\sigma_{th,HISC}$	Threshold stress: reference samples, polarised samples
A, A_0, A_{min}	Area: original, minimal
$(\nabla C)_t$	Concentration gradient at time, t
D	Diffusion coefficient
D_0	Temperarure-independent pre-exponential for diffusion coefficient
$\%DB$	Ductile/brittle area ratio
d, d_0, d_{min}	Diameter: original, minimal
E, E°, E^{rev}, E_{corr}	Potential: measured, standard half-cell, reversible, corrosion
e^-	Electron
F	Faraday constant
∇G, ∇G_f°	Sum of free energies of formation: the reaction products, reactants
g	Gravitational acceleration constant
H^+	Atomised hydrogen
I, I_{corr}	Electric current, rate of corrosion
J_x	Diffusion flux for a specific direction
L_{res}	Distance from centreline of weld
M, M^{n+}	Arbitrary metal and metal ion
P_{th}	Threshold load
Q	Activities of reactants divided by the activities of products
Q_a	Activation energy for diffusion
R	Gas constant

RA	Reduction of area
RA_{air},RA_{env}	Reduction of area: reference sample, polarised sample
$\%RA$	Percent relative accuracy
T	Temperature
$\%YS$	Yield strength ratio

Abbreviations	**Explanation**
$Ag/AgCl$	Silver/Silver Chloride Reference Electrode
AYS	Actual Yield Strength
BCC	Body Centered Cubic Crystallographic Structure
BSE	Backscattered Electrons
CLT	Constant Load Testing
CP	Cathodic Protection
DSS	Duplex Stainless Steels
EDX	Energy-Dispersive X-ray analysis
FCC	Face Centered Cubic Crystallographic Structure
HAZ	Heat Affected Zone
HEDE	Hydrogen Enhanced Decohesion
HELP	Hydrogen Enhanced Local Plasticity
HISC	Hydrogen Induced Stress Cracking
OM	Optical Microscopy
RA	Reduction in Area
SD	Standard Deviation
SDSS	Super Duplex Stainless Steels
SE	Secondary Electrons
SEM	Scanning Electron Microscopy
SMYS	Specified Minimum Yield Stress
SSRT	Slow Strain Rate Testing
TLRR	Threshold Load Reduction Ratio
UTS	Ultimate Tensile Strength
YS	Yield Strength

1. Introduction

1.1. Historical Background

Over the last decades, the use of duplex and super duplex stainless steels (DSS/SDSS) in offshore installations has increased dramatically due to their excellent mechanical and corrosion resistance properties. Applications include line pipe material and manifold pipework, among others. However, in certain applications components made from DSS and SDSS may be connected to carbon steels and other alloys in need of cathodic protection. In such applications, DSS and SDSS may be exposed to cathodic protection (CP) despite having sufficient corrosion resistance. Though the general experience when using duplex stainless steels in such subsea equipment has been good, some failures has occurred as DSS and SDSS materials are susceptible to hydrogen induced stress cracking (HISC) when connected to CP systems [1].

1.2. Motivation

The motivation for this Master's thesis is the expressed desire of GE Oil & Gas for investigating whether there is a difference in the susceptibility towards HISC between materials from five of their suppliers. By performing experiments on pipe materials from the different suppliers, which differ in production methods and thus microstructures, they might reduce the risk of HISC occurring in their components by choosing materials with better performance in subsea and offshore conditions.

1.3. Aim of This Work

In this thesis, the aim will be to investigate whether there is a difference in the susceptibility towards HISC between the five 25% Cr Super Duplex materials from different production methods provided by GE Oil & Gas. The differences in susceptibility will be documented by investigating the fracture appearance of the test specimens. The investigation will include HISC testing using Cortest Proof Rings and micrographic examination using optical microscopy (OM). Scanning electrode microscopy (SEM) will be used to investigate the fracture surfaces of the test specimens used in the HISC testing.

2. Theoretical Background

Hydrogen induced stress cracking (HISC) is a form of hydrogen embrittlement. The typical degradation of a material's properties through HISC is delayed cracking at stresses below fracture strength [2]. The mechanism is caused by the combined effect of three factors, shown in Figure 2.1. These factors are atomic hydrogen, susceptible microstructure and mechanical and/or residual stresses, and they must all be present simultaneously for HISC to occur [3]. The three factors and how they interact will be explained in the first three parts of this chapter. Subsequently, the literature on the subject of HISC studied for this work will be reviewed with focus on previous HISC testing. Previous failures due to HISC will be presented along with standards created for avoiding HISC. Finally a short description of the principles behind the metallographic examination methods used in this thesis is provided.

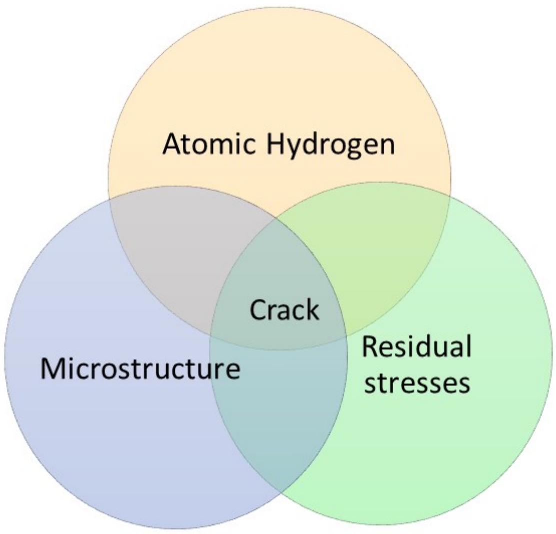

Figure 2.1: Illustration of the necessary factors for HISC to occur.

2.1. Sources of Hydrogen

There are several sources of hydrogen, where the main sources are hydrogen from applied cathodic protection (CP) and welding. For the present discussion, the most relevant source of hydrogen is CP systems [3]. In this section, hydrogen evolution on metal surfaces from CP systems will be explained, along with the electrochemistry behind the phenomenon. Finally, the diffusion of hydrogen is explained.

2.1.1. The electrochemistry of corrosion

When aiming to explain the evolution of hydrogen on a steel surface due to CP systems, one must begin with the electrochemical reactions constituting corrosion. Corrosion is the result of charge transfer reactions occurring simultaneously on a metal surface. The charge transfer reactions, also called half-cell reactions, are the oxidation reaction and the reduction reaction. The oxidation reaction involves a release of negative charge, electrons, while the reduction reaction gains an equal amount of negative charge. Thus, the result of the half-cell reactions is the overall electrochemical reaction. An illustration is presented below, with oxidation, reduction and the overall reaction represented by Equations 2.1, 2.2 and 2.3, respectively. In the equations, M is an arbitrary metal and n is the number of charge equivalents, i.e. number of electrons, (e^-), transferred [4].

$$\mathrm{M} \rightleftharpoons \mathrm{M}^{n+} + \mathrm{ne}^- \tag{2.1}$$

$$\mathrm{nH}^+ + \mathrm{ne}^- \rightleftharpoons \mathrm{nH_2\,(g)} \tag{2.2}$$

$$\mathrm{nH}^+ + \mathrm{M} \rightleftharpoons \mathrm{nH_2\,(g)} \tag{2.3}$$

Whether or not a metal corrodes in a specific environment depends on thermodynamics. Basic thermodynamics states that if the free energy, ∇G, is greater than zero, then reaction 2.3 is favoured to the right [4]. Thus, corrosion is possible. To calculate ∇G, the Nernst equation is used:

$$\nabla G = \nabla G_f^\circ + RT \cdot lnQ \tag{2.4}$$

Where ∇G_f° is the sum of free energies of formation of the reaction products minus the sum of free energies of formation of the reactants, R is the gas constant, T is the absolute temperature and Q is the product of the activities of reaction products divided by the product of the reactant's activities.

However, the potential of a corroding metal is not a thermodynamic quantity, but rather a quantity determined by the rates of the electrochemical reactions taking place on the metal[4]. Therefore, a relation between the thermodynamic calculations and electrode potentials is established by comparing measured electrode potentials with the reversible potential of a charge transfer reaction expected to occur. For this to be possible, the thermodynamic quantities ∇G and ∇G_f° must be replaced by E^{rev} and E°, respectively. E^{rev} is the reversible potential, and represents a threshold potential that must be overcome for an oxidation process to be thermodynamically possible. E° is the standard half-cell potential. The relations between the potentials and the Gibb's energies are given in Equations 2.5 and 2.6:

$$\mathrm{E}^{\mathrm{rev}} = -\frac{\nabla \mathrm{G}^{\mathrm{rev}}}{\mathrm{nF}} \tag{2.5}$$

$$\mathrm{E}^\circ = -\frac{\nabla \mathrm{G}_f{}^\circ}{\mathrm{nF}} \tag{2.6}$$

Thus, by substituting the Gibb's energies, the potential analogue of the Nernst equation emerges in Equation 2.7:

$$E^{rev} = E^\circ - \frac{RT}{nF} \cdot lnQ \tag{2.7}$$

By comparing measured potentials, E, of a metal in solution to the calculated E^{rev} in the modified Nernst equation the possibility of corrosion can be assessed [4]. The possible results of such a comparison is summarised in Table 2.1. Here, the subscript M^{n+}/M indicates that the reversible potential pertains to Equation 2.1.

Table 2.1: Possible results of E depending on E^{rev} from [4].

E	Comments concerning the possibility of corrosion
Less than $E^{rev}_{M^{n+}/M}$	Favoured to the left; corrosion will not occur.
Equal to $E^{rev}_{M^{n+}/M}$	Equilibrium.
Greater than $E^{rev}_{M^{n+}/M}$	Favoured to the right; corrosion may occur.

The possibility of corrosion can also be assessed by using an Evans diagram. In an Evans diagram as shown to the left in Figure 2.2, the range of potentials where the half-cell reactions are possible and the rate of the reactions is shown. The rate is measured in current, I. In the figure, the red line represents metal oxidation and the blue line is the evolution of hydrogen on the metal surface. The intersection between these lines represents the corrosion potential, E_{corr}, and the corrosion rate, I_{corr}.

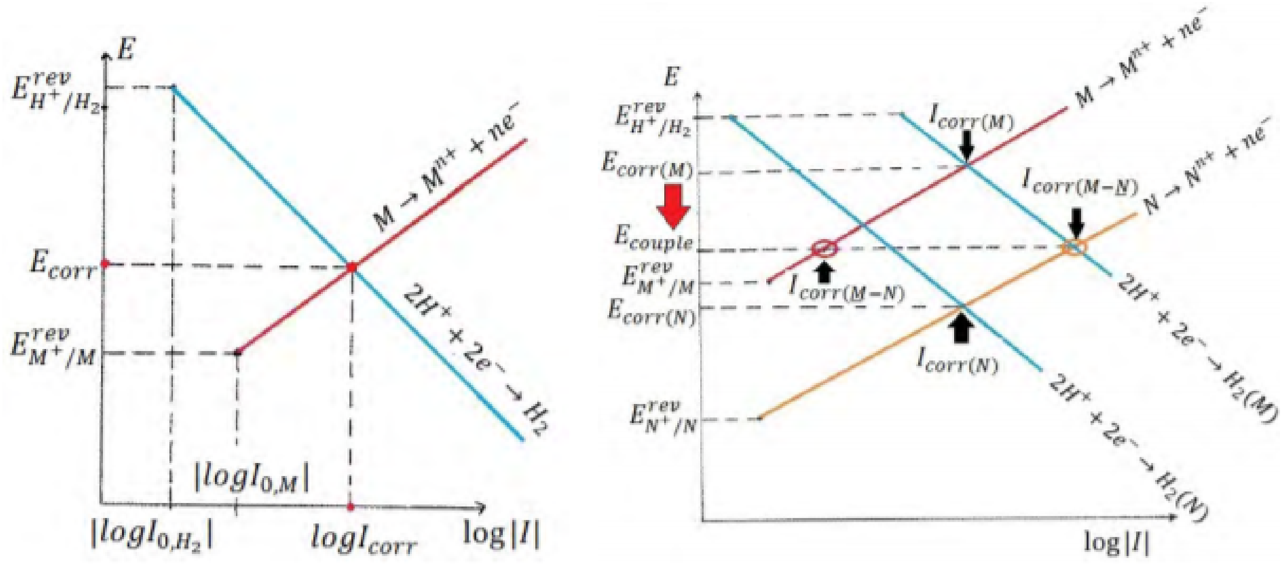

Figure 2.2: Evans diagram from [4] showing corrosion for a single metal (left) and galvanic corrosion (right).

When two metals, one more noble than the other, are in electrical contact, the overall electrochemical reaction consists of four half-cell reactions; two for each metal. In this case, the potential stabilises at an E_{couple}. At this potential, the rates of oxidation and reduction are equal. This results in the modified Evans diagram for galvanic corrosion to the right in Figure 2.2. If the potential is reduced from E_{corr} to E_{couple} as indicated by the arrow in the figure, the corrosion rate of M decreases. This is indicated by the red circle in Figure 2.2. Conversely, the corrosion rate for the less noble metal N and an increase in the corrosion rate occurs for this metal (orange circle). This is what constitutes galvanic corrosion of metals [4].

2.1.2. Cathodic protection as hydrogen source

Cathodic protection (CP) is one of the most effective ways of protecting a submerged external steel surface from corrosion. CP utilises the effect of galvanic corrosion in a positive manner by lowering the potential of a metal to a level at which the corrosion rate of the metal is significantly reduced. CP is termed a successful protection method when the rate of corrosion has been reduced to negligible values [5]. This is often achieved by galvanically connecting the surface to be protected to a less noble metal. In the case of steel, Zinc (Zn) or Aluminium (Al) alloys are commonly used. The less noble metal is termed a sacrificial anode, and will corrode in stead of the more noble steel surface.

For protecting carbon and low alloy steels, a potential of -800 $mV_{Ag/AgCl}$ is generally accepted as sufficient [6]. However, the cathodic polarisation varies depending on the distance from the anodes and the anode material. Therefore, when designing CP systems, the protective potential may vary between -800 $mV_{Ag/AgCl}$ and -1100 $mV_{Ag/AgCl}$. This corresponds to the anode potential. Hydrogen is then formed on the surface due to a cathodic reduction reaction at potentials below -800 $mV_{Ag/AgCl}$. The reactions occurring at the cathode surface are given in Equations 2.8 and 2.9:

$$2\,\mathrm{H_2O} + \mathrm{O_2} + 4\,\mathrm{e^-} \rightarrow 4\,\mathrm{OH^-} \tag{2.8}$$

$$\mathrm{H^+} + \mathrm{e^-} \rightarrow \mathrm{H^0} \tag{2.9}$$

Some of the hydrogen atoms will be absorbed by the steel surface and thus increase the content of dissolved hydrogen in the steel. If the amount of hydrogen absorbed into the steel is sufficiently high and tensile stresses are applied to the material, failure of the material due to HISC may occur. To reduce the amount of hydrogen diffusing into submerged materials, it is generally agreed in the industry that one should avoid polarised potentials more negative than -1050 to -1100 $mV_{Ag/AgCl}$ [7, 8]. However, as hydrogen evolves at -800 $mV_{Ag/AgCl}$, HISC might still occur even with this precaution.

2.1.3. Hydrogen diffusion

Hydrogen is the smallest element, consisting of only one proton and one electron. In its natural state hydrogen takes the form of H_2 gas, i.e. two hydrogen atoms bonded together. This molecule is too large to diffuse into a solid metal. Therefore, to enter a solid metal lattice, the hydrogen gas must dissociate into single atoms. These atoms are called atomic hydrogen[2]. The main diffusion mechanism for atomic hydrogen is interstitial diffusion, meaning the atoms migrate from an interstitial position in the lattice to an empty, neighbouring interstitial position [9].

In addition to dissolved hydrogen at interstitial positions, hydrogen may also be present in the microstructure at sites associated with crystalline defects, e.g. vacancies, grain boundaries or dislocations. Hydrogen at such structural heterogeneities are termed "trapped hydrogen", and trap sites are either reversible or irreversible depending on their ability to hold a hydrogen atom. At reversible traps the hydrogen may be released and hydrogen in such traps are considered mobile along with the hydrogen at interstitial lattice positions. Irreversible traps, however, hold on to the hydrogen permanently, meaning hydrogen at such sites cannot take further part in the diffusion [3].

Fick's Laws

The diffusion of hydrogen from a region of high concentration to one with a low concentration is described by Fick's first law, given in equation 2.10:

$$J_x = -D \cdot (\nabla C)_t \tag{2.10}$$

Where

J_x	=	Diffusion flux for a specific direction	$[kg/m^2s]$
D	=	Lattice diffusion coefficient	$[m^2s]$
$(\nabla C)_t$	=	Concentration gradient at a specific time t	

In ideal metals without traps, the hydrogen diffusion follows Fick's second law, equation 2.11, which describes a nonsteady-state diffusion. This law is based on Fick's first law together with the concept of mass conservation. Nonsteady-state implies that the rate decreases as an equilibrium is established[7].

$$\frac{\delta C}{\delta t} = D\left[\frac{\delta^2 C}{\delta x^2} + \frac{\delta^2 C}{\delta y^2} + \frac{\delta^2 C}{\delta z^2}\right] \tag{2.11}$$

The lattice diffusion coefficient, D, found in Fick's laws can be described by the relation:

$$D = D_0 \cdot exp\left(-\frac{Q_a}{RT}\right) \tag{2.12}$$

Where

D_0	=	Temperature-independent preexponential	$[m^2/s]$
Q_a	=	Activation energy for diffusion	$[J/mol]$
R	=	Gas constant	$[8.31(J/mol \cdot K)]$
T	=	Temperature	[K]

This coefficient is highly dependent on temperature, as seen from the relation in equation 2.12, indicating that the diffusion of hydrogen for a given concentration is similarly dependent on temperature. An increase in temperature will therefore increase the diffusion rate of hydrogen through a metal.

2.2. Super Duplex Stainless Steels

As mentioned in the introduction to this thesis, duplex stainless steels (DSS) and super duplex stainless steels (SDSS) have been used in offshore and subsea applications for some time. Below follows a description of the metallurgy and production methods for these materials.

2.2.1. Metallurgy

Duplex stainless steels are so named due to their characteristic dual phase microstructure consisting of austenite (γ) islands in a ferrite (α) matrix as illustrated in Figure 2.3. This duplex structure combines the strength, corrosion resistance and stress corrosion cracking resistance of ferrite with the toughness and weldability of austenite [10]. The phase distribution of the two phases should be as close to 50/50 as possible to achieve the desired mechanical and corrosion properties. To obtain and maintain the microstructure of duplex stainless steels, both chemical composition and heat treatment is critical [11].

DSS and SDSS contain large amounts of chromium (Cr). Other important alloying elements in DSS and SDSS include nickel (Ni) and molybdenum (Mo). The only stable phase at room temperature in pure iron is ferrite, while austenite is stable at higher temperatures. By adding so-called austenite stabilisers, such as Ni and manganese (Mn), the γ-loop in the iron-carbon phase diagram is extended, and austenite may be preserved at room temperatures. Conversely, Cr and Mo are ferrite stabilisers and addition of these elements will favour the formation of ferrite at greater temperature intervals. However, Cr added to a steel containing Ni will decelerate the kinetics of the austenite to ferrite transformation, and

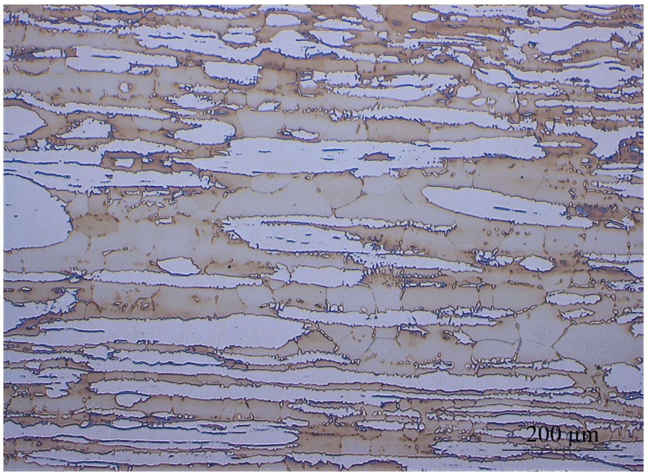

Figure 2.3: Image illustrating a duplex structure. The light areas are austenite, and the dark areas are ferrite.

austenite is easier retained at ambient temperatures. By having the correct balance between γ-forming elements, such as Ni, and the α-forming elements, such as Cr and Mo, the dual phase (α+γ) region in the Iron-Carbon phase diagram can be retained down to room temperature. Thus, in combination with heat treatment, a duplex microstructure may be achieved [11].

In addition, the alloying elements also improve the corrosion resistance of DSS and SDSS materials. Stainless steels are created by adding at least 12% of Cr, as this element creates a self-mending passive oxide layer on the steel surface. It is the amount of Cr added that defines the difference between DSS and SDSS; DSS materials contain 22% Cr while SDSS contains 25% Cr . The corrosion resistance is further increased by Mo as it eases the formation of the oxide layer created by the added Cr. The layer is also made more robust by the addition of Mo. Ni makes the oxide layer re-passivate more easily, and increases the steels corrosion resistance in several acidic environments [11].

2.2.2. Production methods

There are several possible production methods for DSS and SDSS pipes. The methods relevant for this discussion is presented below.

Forging

Forging is a manufacturing process involving mechanically deforming a component at elevated temperature. The deformation is accomplished through successive blows to the component or by continous squeezing. The forging process may be either closed or open die. During closed forging operations, a force is applied to two or more die halves, shaping the metal in the gap between them. Two die halves with simple geometric shapes are used in open die forging. Open die is often employed for larger components [9].

Centrifugal casting

One process for manufacturing seamless steel pipes is the horizontal casting process. A schematic of the process is provided in Figure 2.4. In this process, the liquid melt is poured into a preheated and rotated cylindrical, metallic mould. As the mould spins, centrifugal forces is applied as the liquid metal solidifies. The direction of solidification is from the outside diameter inwards, and the molten interior feeds the solidification front continuously. This minimises the solidification porosity and the porosity caused by shrinkage is contained to the inner diameter of the pipe. Solidification impurities such as slag and inclusions are also contained to the inner diameter due to the centrifugal forces. This part of the pipe is normally machined as a part of the manufacturing process, and the impurities will thus be removed from the pipe altogether. The machining also ensures that cast products may be supplied to much stricter tolerances on inner diameters than other products, e.g. wrought seamless pipes. Other advantages of cast products are the isotropic properties and the versatility with respect to composition as the latter can be adjusted to reach specific property requirements [12, 13].

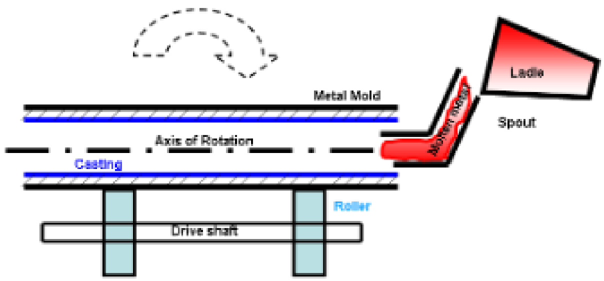

Figure 2.4: Schematic of the centrifugal casting process from [13].

Tube extrusion process
In the process of extruding tubes, the starting material is normally round steel billets. The method may be applied for manufacturing tubes up to an approximate outer diameter of 230mm. The billets may be either rolled, forged or continuously cast, and is first heated to forming temperature before being inserted into the cylindrical recipient of the extruder. Initially, the billet is pierced through the centre by a mandrel. A round-bored die is placed in the end of the recipient, and as the mandrel passes through the die it forms a gap trough which the material is extruded [14]. A schematic of the extrusion process is provided in Figure 2.5.

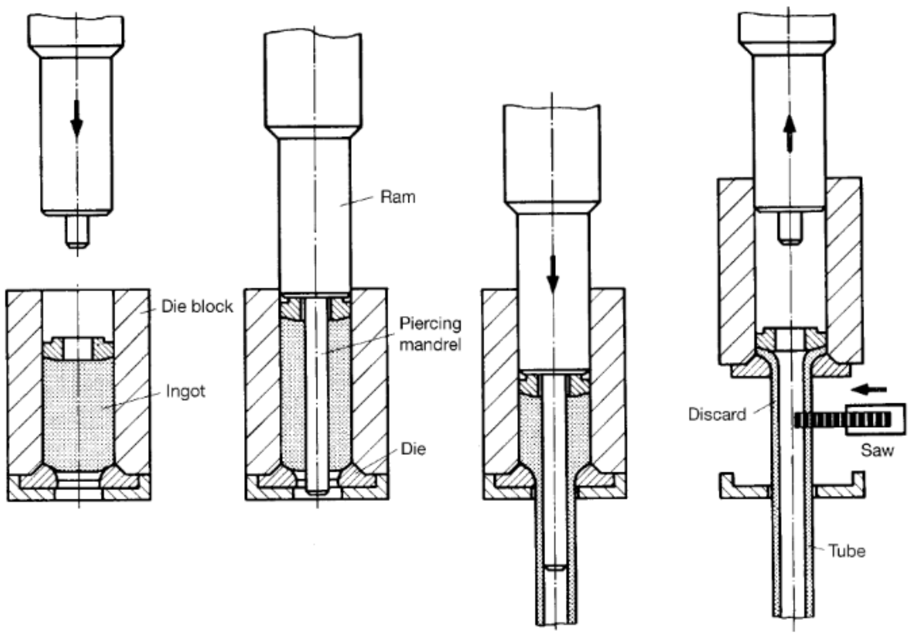

Figure 2.5: Schematic drawing of the extrusion process from [14].

Cold drawing
A sizable percentage of seamless tubes manufactured through the methods above undergo subsequent cold forming, the purpose of which is to achieve closer wall thickness and diameter tolerances. It also provides an improvement in surface finish and specific mechanical properties in the tube. Another effect of cold forming is to expand the mix of the product toward the lower end of the outer diameter and wall thickness scales. One such process is cold drawing, which may be performed in three different ways: hollow drawing, plug drawing and drawing over a mandrel. In the hollow drawing process, there is no internal

tool, meaning only the outside diameter of the tube is reduced. Also, only the outside surface is polished in the die and the reduction in wall thickness is negligible, both in terms of absolute values and tolerances [14]. Figure 2.6 illustrates the cold drawing processes.

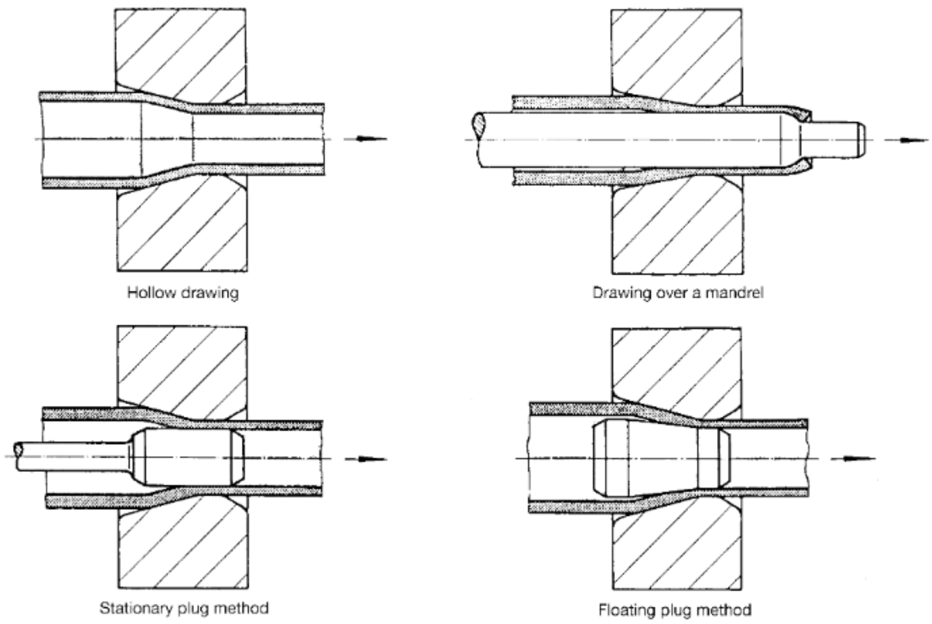

Figure 2.6: Illustration of different cold drawing processes from [14].

In plug drawing, the tube is drawn through a gap formed between a plug and the block die. The result is a reduction in the tolerances of both the outside and inside diameters, and thus also for the wall thickness. Both outside and inside surfaces are also smoothed and polished. When cold drawing over a mandrel, an inserted mandrel bar is employed to pull the tube through the die. As with plug drawing, both inside and outside diameters and the wall thickness undergo reduction. Compared to plug drawing, the possible reductions in area per draw are higher for cold drawing over a mandrel. However, the tube length is restricted by the length of the mandrel bar. In addition, to extract the mandrel the tube must be expanded slightly following the drawing process. As a result, drawing over a mandrel is normally applied for standard sizes and as a preliminary drawing process where the final dimensions are produced is several drawing operations with intermediate heat treatment [14].

When subjected to a cold forming process, the material undergoes strain hardening, meaning the yield and tensile strengths are increased while the elongation and toughness of the material decrease. This might be desirable, but a subsequent heat treatment must be performed prior to any further forming operations to recover some of the lost ductility [14].

2.3. HISC in SDSS

This section describes how HISC occurs in SDSS. From this point on, SDSS will be used as a collective term for DSS and SDSS unless otherwise specified as this material is the focus of the present discussion.

2.3.1. Hydrogen diffusion in SDSS

For the discussion presented in this work, the dual phase microstructure of DSS and SDSS is important. The ferrite phase has a body centered cubic (BCC) structure, which is an open lattice structure. Austenite, however, has a close-packed face centered cubic (FCC) lattice structure. The open BCC structure of ferrite allows for a high diffusion rate and low solubility of Hydrogen. Conversely, the close-packed FCC structure of austenite results in a decrease of the diffusion rate and increase in the solubility compared to the BCC structure [3]. Diffusion coefficients for ferritic iron and austenitic steel is provided in Table 2.2, along with the coefficients for a low alloy steel, a DSS alloy and a SDSS alloy. From the values, it is clear that the diffusion rate of hydrogen in austenite, represented by the austenitic stainless steel, is much lower than the diffusion rate of hydrogen in ferrite, represented by the pure ferrite iron.

Table 2.2: Diffusion coefficients for hydrogen in different steel types from [3].

Material	Charging conditions	Test T [C]	Diffusion coeff. [m^2/s]
Pure α-iron	-	25	$7.2x10^{-9}$
Low alloy steel (X65)	20 A/m^2 in 0.1 M NaOH	25	$1-2x10^{-9}$
DSS (SAF 2205)	$1mA/cm^2$ in 0.1 M NaOH	22	$2.8-3.0x10^{-15}$
SDSS (SAF 2507)	$1mA/cm^2$ in 0.1 M NaOH	22	$1.1x10^{-15}$
Austenitic stainless steel	-	-	$1.8-8.0x10^{-16}$

This difference in properties between the two lattice structures results in ferrite being more susceptible to hydrogen embrittlement than austenite as ferrite is more readily embrittled by small amounts of hydrogen. Several studies suggest that hydrogen enters SDSS through the ferrite phase due to the higher diffusion rate and embrittles this phase because of its low solubility of hydrogen Thus, HISC is favoured by a higher ferrite content [15, 16]. In addition, HISC is also favoured by higher temperatures. This is due to the temperature dependency of the diffusion coefficient shown in Equation 2.12, meaning that hydrogen will saturate a structure more quickly with increasing temperatures as the diffusion coefficient increases with temperature.

The presence of austenite reduces the diffusion rate of hydrogen in SDSS compared to ferritic stainless steels, as seen in Table 2.2, through several effects. The austenite islands increase the diffusion length, i.e. the distance the hydrogen atoms must travel through the structure. Also, the austenite phase boundaries act as trapping sites, thus decreasing the amount of mobile hydrogen in the material. Both of these retarding effects on hydrogen diffusion are dependent on the shape and spacing of the austenite islands[16]. The finer the grain size, i.e. the size of the islands, the stronger are the effects. This is due to the increase in grain boundary area, and thus trapping sites, with decreasing grain size. Therefore, more hydrogen is trapped at the grain boundaries and the amount of mobile hydrogen is reduced. This in turn reduces the susceptibility of fine grained SDSS materials to HISC [10, 17]. However, one study revealed that for a bimodal distribution of austenite, the fine equiaxed austenite islands appeared to be ineffective towards hindering crack initiation and propagation; the main contribution was then from the elongated grains [18].

2.3.2. Deformation and fracture

There are two possible fracture modes for metals, namely ductile or brittle. Ductile metals are characterised by extensive plastic deformation before fracture, and such fractures often exhibit a surface contour termed cup-and-cone. An example of a ductile fracture surface is provided in Figure 2.7 a. In this type of fracture, the interior region of the surface has an irregular and fibrous appearance. A brittle material is characterised by rapid crack propagation and little or no plastic deformation upon fracture. The direction of crack motion is nearly perpendicular to the direction of the applied tensile stress. This yields a fracture surface that is relatively flat, as seen in Figure 2.7 b. For most brittle crystalline materials, crack propagation occurs by cleavage. Cleavage is the process of successive and repeated breaking of atomic bonds along specific crystallographic planes. Such fractures are called transgranular as the cracks propagate through the grains [9].

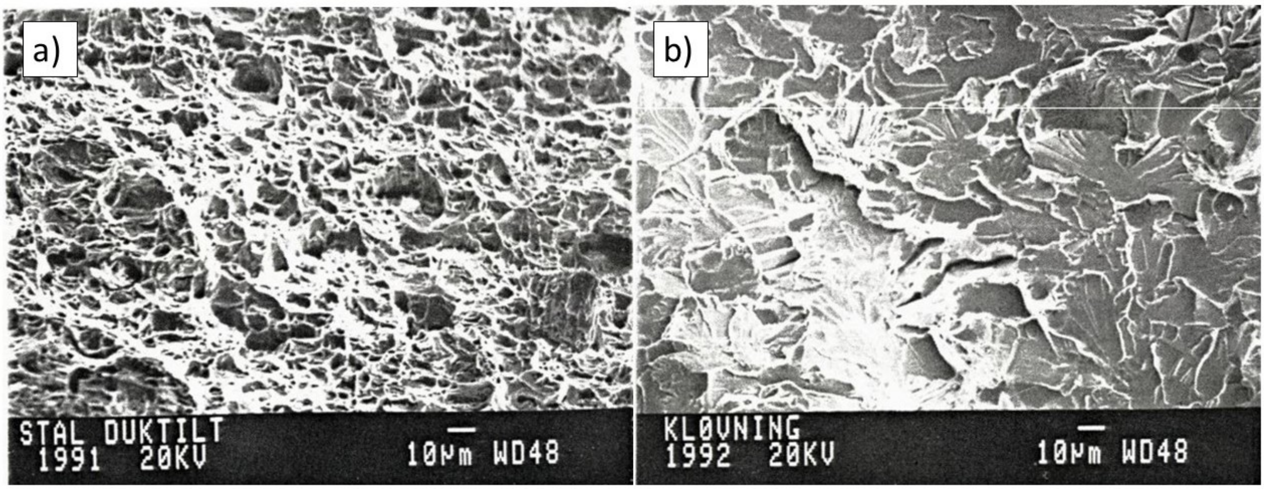

Figure 2.7: Image from [19] depicting a ductile (a) and a brittle (b) fracture surface.

Studies on cracks due to HISC suggest that a typical hydrogen crack in duplex stainless steel is characterised by brittle cleavage type fracture in the {001} plane in the ferrite phase. Under sufficient stress, the crack will overcome the critical stress required for crossing the austenite phase boundaries. This is accompanied by a change in the direction of the crack and stepwise zig-zag micro cracking along the <111> direction when entering the austenite phase [9, 16]. Secondary cracks perpendicular to the stress direction have also been documented by micrographic examination [20, 21]. When hydrogen embrittlement occurs, another fractographic feature is also observed. This feature is termed quasi-cleavage type fracture, and it involves a macroscopically brittle fracture with some local ductile fracture characteristics. It is characterised microscopically by the presence of extended voids, slip ridges and striation marks etc [22].

2.3.3. HISC fracture mechanism

When subjecting a crack to a plane opening stress it will, in mechanical terms, be described by a local stress and strain field ahead of the crack tip. The equivalent plastic strain is at its highest at the crack tip, gradually decreasing with increasing distance from this point. The hydrostatic stress field reaches its maximum a short distance ahead of the crack tip. Traditionally, hydrostatic stress is considered the main driving force for hydrogen diffusion from the bulk material towards the crack tip. Thus, hydrogen will diffuse towards the hydrostatic stress field maximum and be trapped there due to dislocation clusters [3]. No complete fracture mechanics model describing both the crack tip stress and strain with the hydrogen affected process zone exists. This is a result of the complexity of the mechanics within this zone, and some assumptions are required for the micromechanical behaviour in front of the HISC crack. The most accredited approaches for these assumptions are the hydrogen enhanced decohesion (HEDE) and the hydrogen enhanced local plasticity (HELP) models [16].

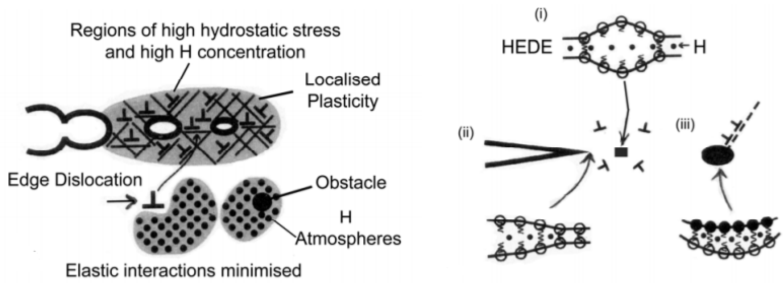

Figure 2.8: Figure from [23] explaining the HELP mechanism (left) and the HEDE mechanism (right).

HEDE is based on the theory that the cohesive strength is lowered by interstitial hydrogen due to an expansion of the metal lattice. In turn, this decreases the fracture energy, implying that the energy barrier for either grain boundary or cleavage plane decohesion is lowered by hydrogen. Fracture is then expected to initiate in the area of maximum hydrostatic stress. To the right in Figure 2.8, the weakened strength of the interatomic bonds due to hydrogen is illustrated by (i) lattice hydrogen, (ii) absorbed hydrogen and (iii) hydrogen at structural heterogeneities. On the other hand, the HELP model suggests that atomic hydrogen enhances the mobility of dislocations at the crack tip through an elastic shielding effect in preferred crystallographic planes. Thus, a fracture based on this model will initiate from slip planes at the crack tip. To the left in Figure 2.8, the HELP mechanism is illustrated by localised plasticity in regions with a high concentration of hydrogen. No matter which model one uses, the crack propagation is promoted by an increased hydrogen concentration at the crack tip [16, 23]. As the FCC crystallographic structure contains more slip planes, i. e. preferred planes, it is hypothesised that the austenite phase fractures through this mechanism, while the fracture mechanism taking place in the BCC structured ferrite phase is HEDE [24].

2.4. Previous HISC Testing

In this section, previous testing of several test parameters in relation to HISC is reviewed.

2.4.1. Materials and austenite spacing

The microstructure of SDSS materials is highly dependent on production method. Production variables such as heat treatment and cold work are two examples of how the microstructure changes with production method. Improper heat treatment may cause harmful secondary phases, which may decrease the corrosion and mechanical properties. Metallurgical changes such as dislocations, deformation bands and slip steps at the surfaces may be introduced by cold working a SDSS material. Such deformation structures influences the resistance towards hydrogen embrittlement [25]. This is due to alterations in the diffusion characteristics due to changes in the surface topography, as well as changes in the quality of the passive oxide film which may influence the amount of absorbed hydrogen.

A study conducted by Elhoud et. al. [25] found that the presence of detrimental secondary phases due to improper heat treatment weakened the resistance of a SDSS material towards intergranular and pitting corrosion. Whether such secondary phases decreases the resistance towards HISC is debated [20] and should be investigated further to find a more definitive answer. Elhoud et. al. and dos Santos et. al. [26] found that a higher degree of cold work increased the material's susceptibility towards HISC.

As previously mentioned, HISC is favoured by higher ferrite content. It is also favoured by the presence of detrimental phases, e.g. sigma [15]. Sigma phase has the approximate chemical composition FeCr and depletes the microstructure of Cr and Mo, both alloying elements that are vital for SDSS's mechanical and corrosion properties as explained earlier in the chapter. In austenitic stainless steels, sigma phase nucleates at austenite grain boundaries and usually requires ageing for up to 5h at 750°C. However, the presence of ferrite in SDSS accelerates the formation of sigma phase as it nucleates on ferrite/austenite phase boundaries in this material due to higher levels of chromium in the ferrite phase compared to the austenite. Chromium nitrides in SDSS have been investigated, both with respect to the formation of different types of chromium nitrides [27] and to their effect on HISC resistance [20], the latter by Statoil. An analysis performed with energy-dispersive X-ray (EDX)

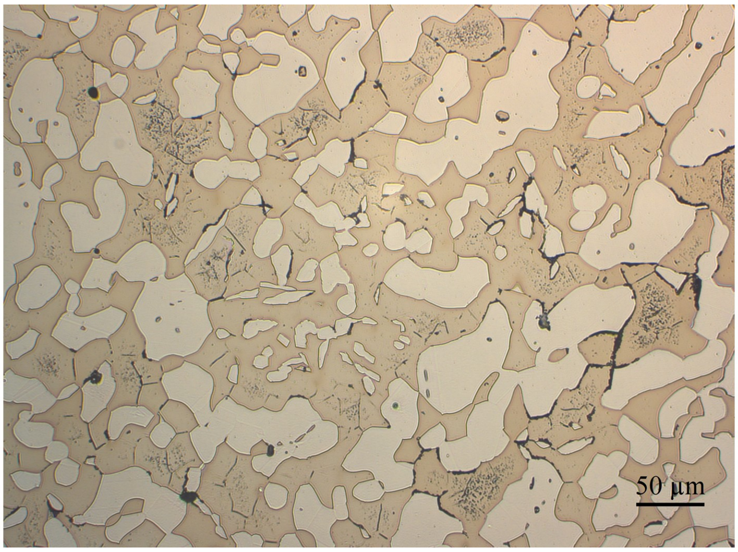

Figure 2.9: Image showing secondary phases in a SDSS structure.

shows that there are two chromium nitride precipitates that forms in SDSS, namely CrN and Cr_2N. The former forms on ferrite/austenite interphase regions, and may also form within austenite grains. A lot more is known about Cr_2N than CrN, e.g. that it tends to form during rapid cooling from elevated temperatures. During such a cooling process the solubility of N in the ferrite decreases, trapping it before it may be redistributed into the austenite phase. The morphology of Cr_2N is elongated grains, and the precipitates of this phase is generally larger than those of CrN. CrN often forms as an intergranular secondary phase in ferrite, and is often found in clusters here. Both these chromium nitride phases are enriched in Cr, N, Fe and Mo, but Cr_2N contains more chromium than, CrN, whilst the opposite holds true for the nitrogen content. This results in Cr_2N yielding larger chromium depleted regions than CrN. The result of the investigation by Statoil was an observable increase in resistance towards HISC for test specimens without nitrides compared to specimens with nitrides. It was also observed that the material with a high nitride concentration failed at stress levels below yield. Even though this result shows there are reasons for avoiding chromium nitrides, still no common requirement has been established for avoiding it as there is no standardised method for quantification of nitride content [27, 20]. An example of secondary phases in a SDSS structure is shown in Figure 2.9.

Other microstructural features decided by production methods are ferrite content, grain size and austenite spacing. Austenite spacing is the average distance between the austenite islands in the ferrite matrix, or the coarseness of the duplex microstructure [28]. When this parameter decreases the resistance towards HISC increases. This has been observed through several studies, such as Chou et al. [10] and Woolin et al. [18] According to Woolin et al., the risk of HISC may be close to eliminated by reducing the austenite spacing to below 30μm. Also, it should be mentioned that the austenite spacing is not a measure of the ferrite grain size, as this is normally substantially larger. A standard for measuring austenite spacing is provided by ASTM E-112 [29]. When relating grain size, ferrite content and austenite spacing to the production method, a ranking of materials from more susceptible to less towards HISC is as follows: forgings > rolled plates > hot isostatically pressed [17].

2.4.2. Low temperature creep

When a material is placed under static mechanical stresses it experiences the phenomenon of creep. The definition of creep is "*the time-dependent and permanent deformation of materials when subjected to a constant load or stress*"[9], and it normally occurs at elevated temperatures. When a material experiences creep, it expands in an effort to reduce the plastic strain. In most cases creep is not desired and is the limiting factor for a part's life-time. During constant load testing of environmentally assisted cracking, such as HISC, low temperature creep takes place due to the high mechanical stresses applied to the test material [9, 30].

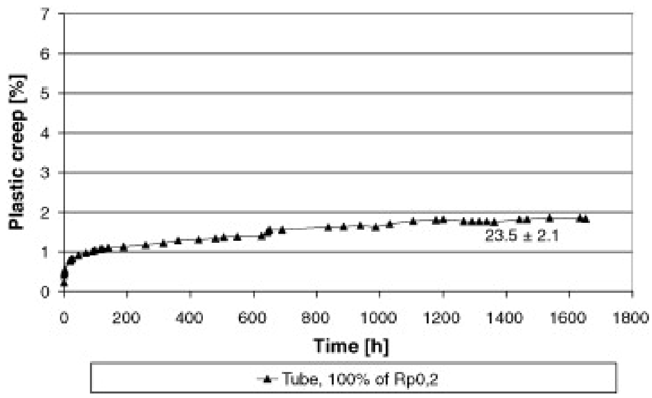

Figure 2.10: Graph from [30] showing the creep curve of an extruded SDSS material at 100% of yield strength.

Kivisäk investigated the influence of low temperature creep on the resistance towards HISC [30]. In the study, SDSS materials with fine and coarse microstructures were subjected to creep testing. A fine microstructure is generally considered to be one with austenite spacing less than 30μm, while a coarse structure has values above this limit [28]. The study by Kivisäk concluded that low temperature creep occurs at lower stress levels for materials with larger austenite spacing. Also, results from the study indicated that strain due to low temperature creep is a prerequisite for HISC to occur although the presence of low temperature creep does not initiate HISC in and of itself [30].

Hydrogen content

As hydrogen is a prerequisite for HISC to occur, the presence of hydrogen in the test material is paramount. A study on the effect of hydrogen content on the embrittlement of a DSS material [31] found a direct relation between the two, as shown in Figure 2.11. In the same figure one can also see how the electrolyte used during pre-charging influences the hydrogen content, and thus the level of embrittlement of the test material. In the study, the parameters measured to quantify the degree of embrittlement were the time to failure ratio during slow strain rate testing (SSRT) and the reduction in area ratio (RA).

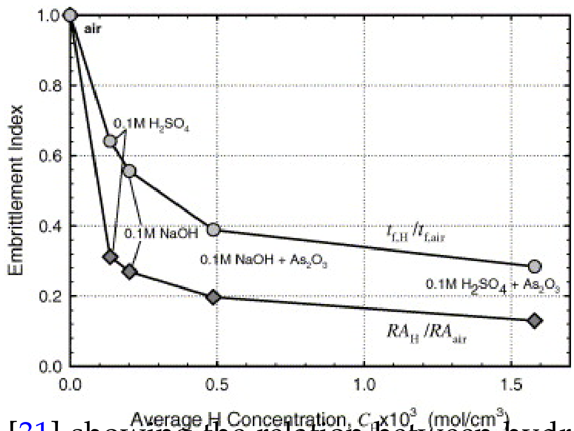

Figure 2.11: Figure from [31] showing the relation between hydrogen content and level of embrittlement for DSS.

The results of the study mentioned above shows the importance of the hydrogen content in specimens when performing HISC testing in simulated operating conditions.

Calcareous deposits

When using CP as protection against corrosion for steel surfaces in seawater, a calcareous deposit may form on the protected surface. Depending on the chemical composition of the seawater, the deposits may consist of $CaCO_3$ and $Mg(OH)_2$. According to Ou and Wu [32], such deposits reduce the hydrogen absorption of the material due to a barrier effect. For protecting steel surfaces against corrosion, the formation of calcareous deposits is therefore beneficial.

Reduction of area
When testing the influence of hydrogen embrittlement on a material it is helpful to index the amount of embrittlement of test specimens. One such embrittlement index is the reduction of area (RA). As mentioned previously in this section, Zakroczymski et al. used the RA to quantify the level of embrittlement depending on hydrogen content [31]. When investigating the susceptibility towards HISC for a material, the RA of specimens exposed to an environment containing hydrogen should be compared to the RA of specimens in air for the same material [31]. The result is then a reduction in area ratio. The studies conducted by Craidy et al. and Zakroczymski et al. [31, 24] found significant differences in RA between specimens exposed to air and hydrogen. Figure 2.12 shows the RA results from [31].

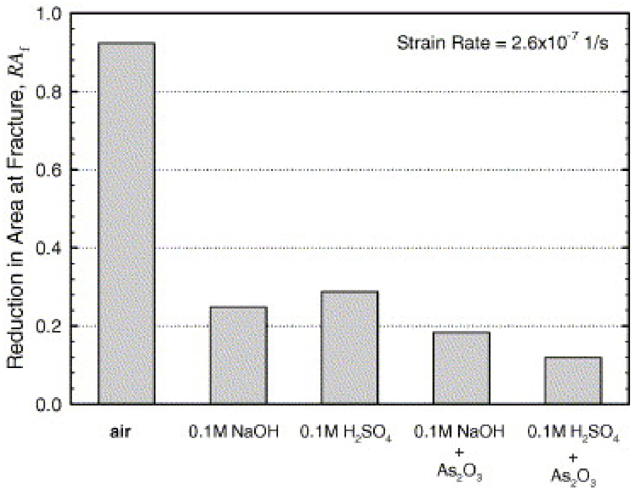

Figure 2.12: Graph from [31] showing the difference in RA between specimens exposed to air and hydrogen containing environments.

2.4.3. Shakedown

Residual stresses from manufacturing processes may be reduced through the process of shakedown. Shakedown occurs when a material is subjected to higher mechanical stress levels than those experienced in operation prior to being put into service. Upon unloading from such high stresses, shakedown causes elastic residual stresses to be lowered and the subsequent behaviour of the material is elastic up to the initial stress level. This will counteract HISC as it lowers the stress levels and thus reduces the level of plastic deformation and delays the occurrence of creep. However, the material will only experience shakedown if the operational stresses are of the same direction and occurs at the same location as the initial mechanical stress[33].

2.5. Reported Failures due to HISC in Literature

Since the oil and gas industry started using DSS and SDSS materials in subsea equipment in the last few decades, there have been several failures attributed to HISC on different subsea components. Some of these are described below to underline the risk posed by HISC in subsea and offshore installations.

2.5.1. BP Amoco Foinhaven (1996)

In 1996, BP Amoco installed a total of 181 SDSS subsea hubs on the Foinhaven field in the UK sector. During a routine pressure test of the flowline circuits approximately six months after installation, leaks were discovered in two forged connectors. Cracking was observed in the most highly stressed area of the connectors, and HISC was found to be the cause. Hydrogen had been absorbed into the material due to CP on a non-painted hub surface. A metallurgical investigation found that the failed parts had a coarse microstructure with grain size up to 180 μm and containing relatively high levels of carbon nitrides. The ferrite content was measured to approximately 50% [33].

2.5.2. Shell Garn West (2003)

Hubs constructed in a non-painted SDSS material were used to connect a manifold pipeline with the transport flowlines. The structure was protected by sacrificial anodes producing typical protection potentials of -1050 $mV_{Ag/AgCl}$. As one hub connection were restarted after a planned shutdown, it failed close to the weld to the manifold pipe. In an element close to the exposed surface of the hub, the hydrogen content was measured to 300 ppm The cracking was attributed to HISC due to presence of the three necessary factors; susceptible microstructure, access to hydrogen and sufficient stresses [1].

2.5.3. Statoil case 1 (published 2013)

An inspection of a forged SDSS subsea module that had been in service for approximately three years revealed a large crack close to the weld between two forged tee components. The failure investigation found that the crack had initiated at the weld toe, propagated through-thickness in the HAZ and base material and continued almost 180 ° circumferential before being arrested. The crack exhibited brittle, cleavage type fracture mode characteristics, and the crack propagation was mainly through the ferrite matrix. Secondary cracking was also observed and was considered indicative of HISC. The hydrogen content close to the crack initiation site was measured to approximately 10 ppm, which is a relatively low value. Further micrographic investigation revealed a relatively coarse microstructure with a ferrite content of 56%. The austenite spacing was measured to 45 μm. The investigation concluded that the failure most likely was a result of either brittle impact/overload fracture or HISC [20]. In addition, high levels of chromium nitride precipitates were present in the microstructure, which prompted the Statoil study on chromium nitride's influence on HISC previously mentioned in this work.

2.5.4. Statoil case 2 (published 2013)

Cold formed DSS and SDSS couplings for subsea umbilical hoses installed in sets of 15 were found to fail after a relatively short time in service. One coupling failed after 1,5 years, and when recovering the full set after 3 years in service, seven out of the 15 couplings contained cracks or fractures. All the failed couplings exhibited HISC fracture characteristics, such as crack initiation from multiple sites along the outer surface of the components with brittle crack propagation through the ferrite matrix. The hydrogen content was measured to approximately 40 ppm after three years in service, and approximately 50-60 ppm after five years. Even though the couplings had a fine microstructure with an austenite spacing less than 20 μm, the method for attaching them to the hoses included a swaging process. This swaging process introduced considerable cold deformation into the material as well as residual stresses [20].

2.5.5. Statoil case 3 (published 2013)

Multiple partially submerged DSS and SDSS flanges used on vertical column pipes for seawater service under CP failed in a nearly identical manner. Cracking was observed in the flange in the area close to the weld. All the cracks were detected before a complete fracture had occurred. Failure investigations revealed that all cracks exhibited brittle fracture mode characteristics with secondary cracking and propagation in the ferrite matrix. This indicated

HISC as the failure mode. The hydrogen content was measured to approximately 100 ppm, which is high value. Other common factors included intermetallic phases in some of the flanges, crack initiation occurring close to the weld start/stop area or in areas with weld repair and cracking occurring on the flange side of the weld [20].

2.6. Design Against HISC

Following the major failure on the BP Amoco Foinhaven Field, awareness of the risk HISC posed in the subsea and offshore industries was raised. To prevent HISC from occurring in subsea and offshore installations, several standards have been developed. As preveiously mentioned, HISC occurs when a susceptible material is subjected to mechanical stresses in the presence of atomic hydrogen. By removing either one of these factors, HISC may be avoided. Due to the good corrosion and mechanical properties of SDSS materials, it is not desirable to avoid using these materials and CP systems are necessary to protect components made from other materials. This results in standards focusing on the stress levels of SDSS components used offshore and subsea.

2.6.1. Result of investigation into the Foinhaven failure case

As mentioned above, the failure of two SDSS manifold hubs on the Foinhaven Field in 1996 initiated the first large investigation into HISC in the offshore industry. The investigation resulted in the development of a set of acceptance criteria for SDSS components on the field based on a material properties study and stress analyses. These criteria became the starting point for further investigations and more recent guidelines for design of SDSS components for use offshore and subsea. The acceptance criteria set by the Foinhaven investigation were as follows:

1. The critical areas of the hub can be shielded from the CP system
2. The maximum stresses during any future operational condition will not exceed the threshold for crack initiation
3. The hydrostatic strength test has caused sufficient "shakedown"

It was stated that cracking du to hydrogen embrittlement would not occur if one or more of the criteria were followed. In addition to the criteria, a long-term pressure test was developed [33].

2.6.2. DNV Recommended Practice F112

The aim of the DNV-RP-F112 is to provide the offshore and subsea industries with a "best practice" developed on the basis of the knowledge and experience at the time [28]. The standard covers all SDSS materials installed subsea with CP. In addition to recommendations on stress levels and conditions, the standard defines parameters such as CP potentials, temperature and surface characteristics and provides stress/strain design criteria. Recommendations are given on manufacturing, fabrication and testing where these factors are believed to impact the resistance towards HISC directly. As the design criteria are the most relevant for the present work, only these will be reviewed here. These criteria are divided into stress and strain criteria [28]. For both of these, materials produced through the following methods are classified as having microstructures with fine austenite spacing:

1. HIP materials.
2. Weld metal (heat affected zone, HAZ, excluded).
3. Tubes and pipes from extrusion, seamless rolling or drawing operations.
4. Rolled plates with wall thickness less than 25mm.

A fine austenite spacing is defined in this standard as less than 30μm. All other materials are classified as coarse grained with respect to austenite spacing unless the austenite spacing is measured for each component in question. The two classifications of materials are graded with a material quality factor, γ_{HISC}, which is different for the two:

$$\text{Fine grained:} \quad \gamma_{HISC} = 100\%$$
$$\text{Coarse grained:} \quad \gamma_{HISC} = 85\%$$

If a component contains girth welds, the residual stresses must be evaluated close to these unless a complete heat treatment has been performed. Estimations of the residual stresses are given within a distance L_{res} from the centreline of the weld and at weld toes, as shown below:

$$\text{Girth welds:} \quad \epsilon_{res} = 0{,}25\%$$
$$\text{Weld toes:} \quad \epsilon_{res} = 0{,}15\%$$

Linear elastic stress criteria

There are two limits for linear stress in this standard, and both are expressed as a percentage of the specified minimum yield strength (SMYS). Both must be met when designing a component for avoiding HISC. The two limits are for membrane stresses, σ_m, and membrane and bending stresses, σ_{m+b}, and are given in Equations 2.13 and 2.14.

$$\sigma_m < \alpha_m \times \gamma_{HISC} \times SMYS \tag{2.13}$$

$$\sigma_{m+b} < \alpha_{m+b} \times \gamma_{HISC} \times SMYS \tag{2.14}$$

$$\tag{2.15}$$

In the equations above, α_m and α_{m+b} are the allowable SMYS factors for SDSS components. The former equals 80% over the entire area of the component, while the latter varies depending on which part of the component the stress limits are calculated for, as seen in Table 2.3.

Table 2.3: Allowable SMYS factor for component sections

α_{m+b} = 100%	Smooth sections outside L_{res}
α_{m+b} = 90%	Smooth sections within L_{res}
α_{m+b} = 90%	Weld toe and stress raiser outside L_{res}
α_{m+b} = 80%	Within L_{res} for weld toes and stress raisers

Non-linear stress criteria

The non-linear strain criteria depends on the distance from welds, as the linear stress criteria do. In addition, the non-linear strain criteria depend on the distance from the surface of the material and the material quality. For the areas outside of L_{res}, the allowable strain is 0,30% within 5% of the wall thickness. Outside of the 5%, the allowable strain is 1% for fine grained materials and 0,60% for coarse grained materials [28].

2.7. Microstructural Examination

2.7.1. Optical microscopy

Optical microscopes (OM) are helpful when investigating the microstructure of a material. OMs develop images of a material surface by transferring a magnified image to the eye through a series of lenses that solve the details of the surface [34].

2.7.2. Scanning electron microscope

Scanning electron microscopes (SEM) are widely used for microscopical examinations of materials and surfaces. A focused electron beam is used to develop images of the chosen material or surface of interest. Upon impacting the surface of the specimen, several signals may be detected e.g. secondary electrons (SE), backscattered electrons (BSE) and characteristic X-ray radiation. These signals may be used to obtain information on the chemical composition and topography, among others, of the specimen. For fractorgraphical investigations, the topography is of importance. As the electron beam move over the specimen, SE emissions vary as a function of the specimen topography. The quality of the depth of field for SEMs is high enough that the images acquired through this method appear to be three dimensional [19].

Most materials can be investigated using SEM. Some prerequisites for specimens are conductivity and cleanliness. If the specimen has low or no electrical conductivity, the electrons in the beam will be absorbed into the material and accumulate on the surface. The charging of the surface bends the beam, resulting in poor image quality. Methods for circumventing this problem exist, but will not be discussed here as the materials in this thesis are electrical conductors. The other prerequisite, cleanliness is paramount. If there are oily substances on the specimen surface, these may evaporate due to the low pressure in the specimen chamber of SEMs and may contaminate the specimen and/or the apertures [19].

3. Materials and Experimental Methods

3.1. Test Materials

To perform the experimental work of this thesis, five different SDSS materials were provided by GE Oil & Gas. The materials are manufactured by different suppliers and are obtained through different production methods. The suppliers are Nippon Steel & Sumitomo Metal Co., Fondinox S.P.S., Tubacex Tubos Inoxidables S.A., IBF S.P.A. and Kuhn Special Steel, and the materials from each supplier will from here on be referred to as materials A, B, C, D and E, respectively. Below is provided a short description of each material, and documentation provided by the suppliers such as material certificates and heat treatment procedures are included in Appendix F.However, these material certificates are not complete; for example, not all include values such as the ferrite content of the materials. The rest of this chapter is dedicated to descriptions of the experimental methods used in the present discussion.

3.1.1. Material A

The test specimens from material A, manufactured by Nippon Steel & Sumitomo Metal Co. are from a UNS S39274 25% Cr Super Duplex Stainless Steel pipe which is obtained through hot extrusion, followed by cold drawing and subsequent heat treatment. The heat treatment is performed during the extrution process, and the temperature was 1100°C. It is directly followed by quenching in water. The chemical composition of the material is provided in Table 3.1. The ferrite content was not provided by the supplier.

Table 3.1: Chemical composition in wt% of test material A.

	C	Si	Mn	P	S	Ni	Cr	Mo	N	Cu	W
Min	0.000	0.000	0.000	0.000	0.000	6.000	24.000	2.500	0.240	0.200	1.500
Max	0.030	0.800	1.000	0.030	0.020	8.000	26.000	3.500	0.320	0.800	2.500
Comp.	0.016	0.250	0.680	0.024	0.0002	6.200	25.100	3.200	0.290	0.530	2.100

3.1.2. Material B

The second set of test specimens is from material B, manufactured by Fondinox S.P.S. The pipe from which the specimen where machined is seamless and vertically centrifugal cast

UNS S32750 25%Cr SDSS. After casting, the pipe was heat treated by solution annealing at 1130 °C followed by quenching in water. The chemical composition is given in Table 3.2. The ferrite content was reported to be 49,5% by the supplier.

Table 3.2: Chemical composition in wt% of test material B.

	C	Si	Mn	P	S	Ni	Cr	Mo	N	Cu	W
Min	0.000	0.000	0.000	0.000	0.000	6.000	24.00	4.000	0.100	-	-
Max	0.030	1.000	1.500	0.040	0.040	8.000	26.00	5.000	0.300	-	-
Comp.	0.023	0.564	0,755	0.023	0.005	7.507	25.124	4.149	0.242	-	-

3.1.3. Material C

Material C is manufactured by Tubacex Tubos Inoxidables S.A. and is a UNS S32760 25% Cr SDSS from a seamless pipe. The pipe was manufactured through hot extrusion over a mandrel followed by direct quenching in water after extrusion. The extrusion was performed at 1100°C, and thus, the extrusion also acts as a solution annealing. The ferrite content is reported as 54% by the supplier, and Table 3.3 shows the chemical composition of this material.

Table 3.3: Chemical composition in wt% of test material C.

	C	Si	Mn	P	S	Ni	Cr	Mo	N	Cu	W
Min	0.000	0.000	0.000	0.000	0.000	6.000	24.00	4.000	0.100	0.200	1.500
Max	0.030	1.000	1.500	0.040	0.040	8.000	26.00	5.000	0.300	0.800	2.500
Comp.	0.014	0.390	0,740	0.024	0.0005	6.750	25.700	3.590	0.257	0.66	0.590

3.1.4. Material D

The specimens from material D is from a UNS S 32760 25% Cr SDSS seamless pipe, with chemical composition as given in Table 3.4. The pipe was manufactured by IBF S.P.A. from a forged bar, where the bar was bored followed by honing of both inner and outer surface of the pipe. The honing step involves grinding and/or machining to achieve acceptable dimensions and surface finish. Finally, the pipe is heat treated by solution annealing at 1100°C and quenched in water. The supplier provided the ferrite content measurements, and the result of this was 49%.

Table 3.4: Chemical composition in wt% for material D

	C	Si	Mn	P	S	Ni	Cr	Mo	N	Cu	W
Min	0.000	0.000	0.000	0.000	0.000	6.000	24.00	4.000	0.100	0.200	1.500
Max	0.030	1.000	1.500	0.040	0.040	8.000	26.00	5.000	0.300	0.800	2.500
Comp.	0.016	0.490	0,550	0.025	0.0002	7.000	25.500	3.670	0.245	0.540	0.650

3.1.5. Material E

The pipe from which test material E was procured is a centrifugal cast 25% Cr SDSS seamless pipe. The supplier of this material is Kuhn Special Steel. The steel grade of the material is SEW 410 Grade 1.4471.02, which is a modification of UNS S32760 and the chemical composition of the material is provided in Table 3.5. The heat treatment performed for this material was not described in the material certificate from the supplier.

Table 3.5: Chemical composition in wt% of material from E.

	C	Si	Mn	P	S	Ni	Cr	Mo	N	Cu	W
Min	0.000	0.000	0.000	0.000	0.000	5.500	25.50	3.000	0.150	0.800	0.900
Max	0.030	1.000	2.000	0.030	0.020	8.000	28.00	4.000	0.280	1.300	1.100
Comp.	0.018	0.440	0,470	0.015	0.006	7.210	27.260	3.720	0.224	1.090	1.040

3.2. Tensile Testing

The HISC testing performed in this thesis is related to the yield strength (YS) of the test materials. Thus, it was necessary to assess the mechanical properties of each test material. Material suppliers are required to perform mechanical and chemical testing before delivering materials to their customers, so data for the materials used in this thesis was available. However, it was determined to obtain new data as the test specimens used by the supplier is of unknown location in the test materials. The dimensions of the test specimens are also unknown. In addition, to obtain all necessary data from the mechanical testing, values from the stress-strain curve is needed.

Figure 3.1: Location in test material from which test specimens were cut.

All the tensile test specimens used for obtaining stress-strain curves were cut from similar locations of the pipe materials provided, as shown in Figure 3.1. The tensile test specimens are the two smaller specimens shown in the figure. The dimensions of the tensile test specimens are provided in Figure 3.2. The cutting and machining was performed by Nomek AS in Trondheim and the tensile testing was performed by staff at the Department of Material Science and Engineering at NTNU. Two tensile tests was performed for each material, and the average value for the actual yield strength, AYS, found by the tensile test performed for this thesis was used during the subsequent HISC testing.

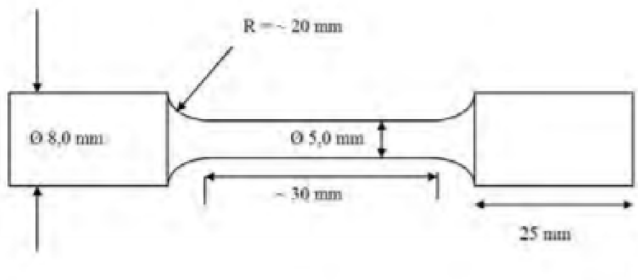

Figure 3.2: Illustration of the dimensions for the tensile test specimens.

3.3. Micrographic Examination

For examining the microstructure, suitable pieces were cut out of the test materials. Two test pieces were cut for each material; one in the direction parallel to the pipe length and one in the direction normal to the pipe length. The test pieces were then cast into an epoxy to be more manageable before being ground and polished until a mirror-like surface is achieved. The grinding and polishing procedure was performed in four steps, provided in Table 3.6.

Table 3.6: Overview of the grinding and polishing procedure used to prepare the specimens.

Step no.	Grinding/polishing disk and lubricant	Time
1	Piatto 220 grinding disk w/water	Until plane
2	Allegran 3 polishing disk w/DiaMax 6 μm Poly	10 min.
3	Daran 3μm polishing disk w/DiaMax 3 μm Poly	8 min.
4	Chemal 1μm polishing disk w/DiaMax 1 μm Poly	4 min.

Following the grinding and polishing, the specimens were etched electrolytically in two steps, as recommended for DSS and SDSS by Statoil in their standard for metallographic etching of DSS and SDSS [35]. The first step involves etching the specimens electrolytically with 20% Oxalic acid for 5 to 10 seconds with an applied potential of $5.5V$. The Oxalic acid etch makes secondary phases such as chromium nitrides visible in the structure. The second step is an electrolytical etch for 6 seconds using 20% NaOH with an applied potential of $2.5V$. This etch increases the contrast between the ferrite and austenite phases, making them visible in OM images.

3.4. Austenite Spacing

For determining the austenite spacing of the test materials, the ASTM E112 standard was applied. The austenite spacing is measured by measuring the mean length of the ferrite grains. This measurement is obtained through superimposing five parallel lines over representative micrographical image of the test material and measuring the length of the ferrite grains. For each material, four randomly selected areas were investigated, and the austenite spacing determined in this thesis is the average of those four areas. The calculation of the austenite spacing, or mean intercept length, $\overline{\ell_\alpha}$, was obtained through regular calculations of a mean value. If not otherwise specified, the austenite spacing should be measured in the through thickness direction. For the test materials in the present thesis, that is the direction normal to the pipe length.

The accuracy of the measurements are determined through statistical analysis. For the analysis, several values were calculated, the standard deviation, SD, the 95% confidence interval, $95\%CI$, and the percent relative accuracy, $\%RA$. The equations used for calculating the two latter values are provided in Equations **??** to 3.2 below.

$$95\,\%\mathrm{CI} = \frac{\mathrm{t} \cdot \mathrm{SD}}{\sqrt{\mathrm{n}}} \tag{3.1}$$

$$\%\mathrm{RA} = \frac{95\,\%\mathrm{CI}}{\bar{\ell}} \cdot {}_{100} \tag{3.2}$$

In the equations the parameters explained below are taken from ASTM E112 [29];

n = Number of measurements

t = Confidence internal multiplier as a function of n

3.5. HISC Testing

3.5.1. Experimental set up

For performing the HISC testing, four test specimens were machined from each material at similar locations as the tensile test specimens. The location from which the specimens were cut can be seen from Figure 3.1. In the figure, the HISC specimens are the larger ones. An image of the HISC specimens is provided in Figure 3.3a, and the dimensions are provided in Figure 3.3b. The specimens were exposed to a HISC favouring environment and put under mechanical stress with subsequent incremental increase in applied load. The HISC testing was performed in three consecutive steps. During all three steps, the the test materials were exposed to conditions similar to CP in seawater. To simulate such conditions, the test materials were exposed to a 3,5% NaCl solution with an impressed current of -1050 $mV_{Ag/AgCl}$. NaCl was chosen as the electrolyte, not artificial seawater, due to the latter containing Ca^{2+} and/or Mg^{2+}. Thus, possible calcareous deposits were avoided.

(a) Image of HISC test specimens.

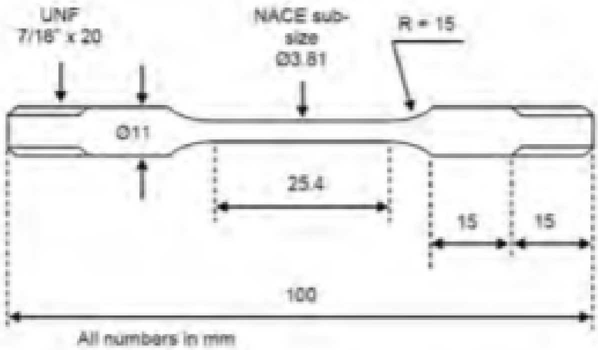

(b) Dimensions of HISC test specimens.

Figure 3.3: Illustrations of the HISC test specimens.

The first step of the HISC testing was pre-charging three of the test specimens with hydrogen at an elevated temperature for at least 10 days to ensure the presence of hydrogen in the material during the testing. The temperature was held constant at 80°C, and the water level was adjusted daily to ensure the correct concentration of 3,5% NaCl in the solution. Figure 3.4a from [36] depicts equipment and electrical set-up used for the pre-charging. The equipment and electrical set-up used in this thesis is identical to that in the thesis by K. Andersen [36]. The fourth test specimen for each test material was not pre-charged with hydrogen as these specimens were to be the reference specimens for each material.

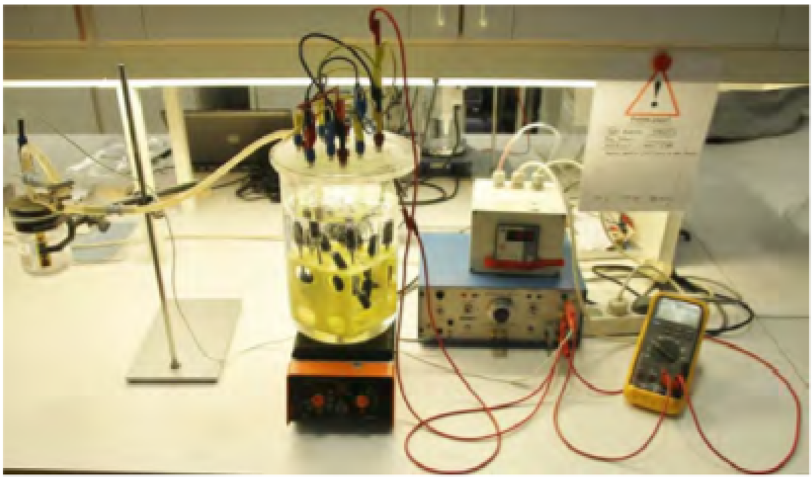

(a) Image showing the equipment used for pre-charging.

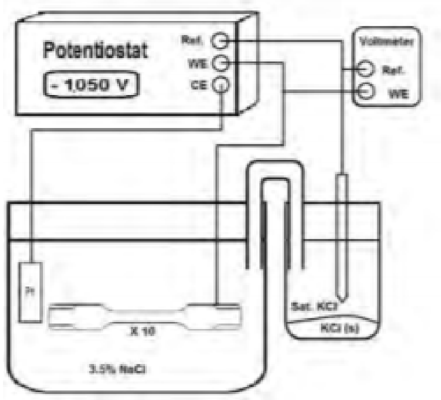

(b) Illustration of the electrical set-up for the pre-charging.

Figure 3.4: Figures from [36] showing the equipment and electrical set-up used for the pre-charging of the HISC test specimens.

After completing the pre-charging, the three specimens were mounted in individual containers and exposed to similar conditions as in the previous step, although at room temperature. The electrical set-up was similar to that of the previous step. The reference specimen for each material was also mounted in a container, only without electrolyte and polarisation. All of the test specimens were then exposed to an applied tensile load of 86% of their respective material's AYS. They were held in this state of tension for seven days.

The final step of the HISC testing involved increasing the applied tensile load incrementally. The load was increased by 4% of AYS daily from the constant load of 86% in the previous step. The incremental increase in applied load continued until fracture. Figure 3.5 shows the equipment used for the second and the final steps of the HISC testing.

3.5.2. Cortest proof rings

The equipment used for the HISC testing in this thesis is called Cortest proof rings [37]. This equipment is designed for testing of stress corrosion cracking in environments containing H_2S and HISC testing, and an image is provided in Figure 3.5.

The rings are compressed manually using the tools marked as b) and c) in Figure 3.6 while the test specimen is inserted in the individual containers. When the ring is compressed, it

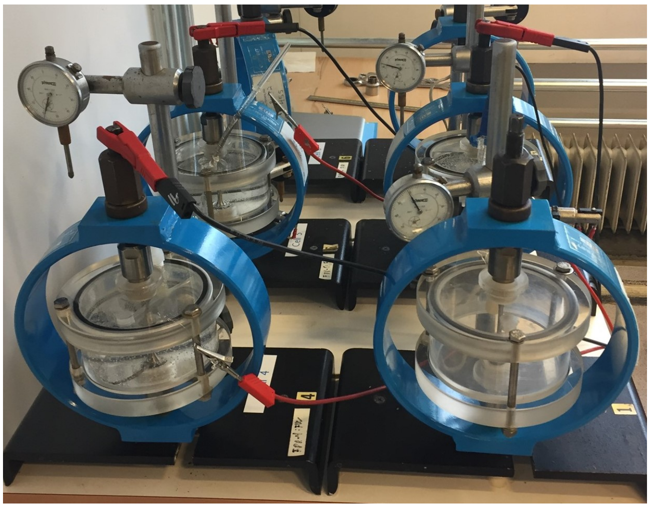

Figure 3.5: Image of Cortest proof rings used for HISC testing.

exerts a stress state of uniaxial tension and the deflection in the ring determines the load applied to the test specimen. The deflection-to-load is a linear relation and each ring is accompanied by an individual calibrated conversion chart used to calculate the ring deflection. The conversion calculations were based on the area of the most narrow cross-section.

Incidents during testing

There were some incidents during testing that should be mentioned. When pre-charging the test specimens from material C and D, two specimens went out of the electrical circuit, causing these specimens to corrode. When this was discovered, the charging process was interrupted for a short period of time to replace the corroded specimens. Upon finishing this step, the replacement specimens were left to pre-charge for the correct number of days, while the other specimens for these materials were taken out after 10 days.

Another incident occurred during the last step of testing for material D, the elongation of the reference specimen was too large with respect to the Cortest proof ring it was placed it. This caused the specimen not being able to go to fracture due to lack of room in the test ring.

3.5.3. Obtaining results from HISC testing

From the HISC testing, three values were obtained; the threshold load reduction ratio, the percentage of yield strength at fracture and the reduction in area. Below, all three are described and the calculations for all of them are explained.

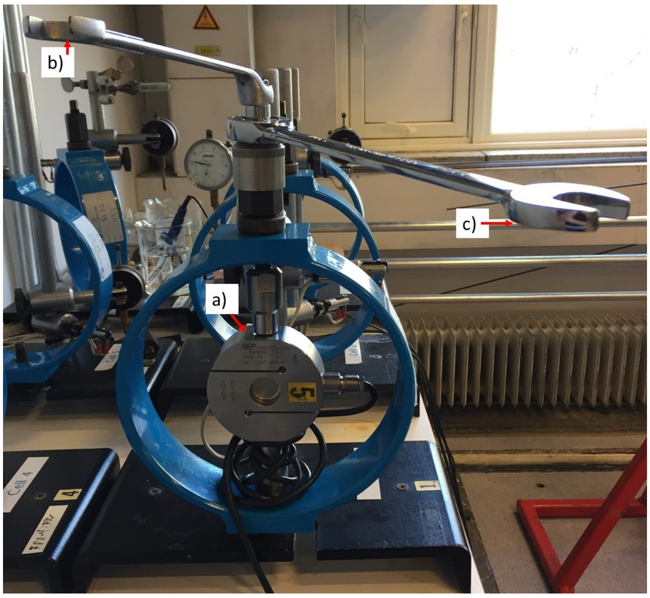

Figure 3.6: Image of load cell used for obtaining results from HISC testing.

Threshold load reduction ratio

The outer diameter of the Cortest proof rings were measured for each increase in load. Upon fracture, the individual containers where removed from the rings and replaced by a load cell, marked as a) in Figure 3.6. By inserting the load cell and compressing the ring to the same level as was held by the test specimens by using the tools shown in the figure, the load applied to the rings at any given increment was obtained. The outer diameter of interest in this thesis is the diameter to which the ring was compressed one step before fracture. This corresponds to the last load the test specimen withstood for 24 hours, or the threshold load, P_{th} in [kg] [38]. The value for P_{th} given by the load cell was converted to the threshold stress, σ_{th} [38], for the reference specimen and the HISC threshold stress, $\sigma_{th,HISC}$, for the polarised specimens using Equation 3.3. In the equation, g represents the gravitational constant equal to 9.81 m/s^2.

$$\sigma_{th}/\sigma_{th,HISC} = \frac{P_{th} \cdot g}{A_0} \tag{3.3}$$

$\sigma_{th,HISC}$ was then compared to σ_{th} for each material. This gives the threshold load reduction ratio (TLRR), a measure for each material's susceptibility to hydrogen embrittlement in percentage. The comparison was performed by implementing Equation 3.4.

$$TLRR = 100 \cdot \left[1 - \left(\frac{\sigma_{th,HISC}}{\sigma_{th}}\right)\right] \tag{3.4}$$

Yield strength ratio
The yield strength ratio, $\%YS$, is the ratio between $\sigma_{th,HISC}$ and the AYS from the stress-strain curves for each material, and the value is given as a percentage of the AYS. The calculation of %YS is provided in Equation 3.5.

$$\%YS = 100 \cdot \left[1 - \left(\frac{\sigma_{th,HISC}}{YS}\right)\right] \tag{3.5}$$

Reduction in area
RA values are obtained by comparing the original smallest cross-section of a test specimen, i.e. the smallest cross-section before testing, with the smallest cross-section of the specimen after testing. The cross-sections used for calculating the RA are obtained by measuring the diameters of the test specimens before and after testing, d_0 and d_{min} respectively, and calculating the areas A_0 and A_{min}. Finally, the areas are inserted into Equation 3.6 [24]:

$$RA = \frac{A_0 - A_{min}}{A_0} \tag{3.6}$$

As this thesis investigates the susceptibility to HISC for different materials, the RA will be reported as the RA ratio, which is the RA_{env}, for the polarised test specimens from each test material compared to the RA of the reference specimen, RA_{air}, for the same material. The resulting RA ratio for each polarised specimen will then be a relative value compared to the reference specimen for the respective material. This ratio is obtained through equation 3.7.

$$RAratio = 100 \cdot \left(1 - \frac{RA_{env}}{RA_{air}}\right) \tag{3.7}$$

3.6. Hydrogen Measurements

The hydrogen content in the test specimen where tested by staff at SINTEF Materials and Chemistry. One specimen from each test material was tested using the melt extraction technique with the H-mat 225 equipment from JUWE Laborgeräte GMbH. The test specimens were taken from the fractured samples previously used for the HISC testing. To avoid the hydrogen diffusing out of the specimens, they were contained in a freezer holding approximately -19 · C after fracture.

3.7. Fractography

To characterise the fracture surfaces of the test materials, all specimens from the HISC testing were investigated using a Scanning Electron Microscope (SEM). The SEM used for the examination was a FEI Quanta FEG 650 Environmental SEM. The method of preparation involved an ultrasonic bath for 5 minutes using acetone as the medium followed by rinsing with ethanol and air drying. During the inspection, the secondary electron detector was utilised, and the operating voltage and working distance were 20kV and 10mm, respectively.

In addition to obtaining fracture surface images, the SEM was used to measure the radius of the brittle areas of the polarised specimens. The measurements were performed to quantify the embrittlement of the specimens due to hydrogen, and the results were used for estimating the brittle area of the specimens. Three measurements for each polarised specimen were performed, and the average value for each specimen was calculated. These average values were used in further calculations. For further calculations, the reduced diameter of the specimens after HISC testing were also used. Once an estimate of the brittle area was obtained, the results were used to calculate the ratio between the ductile and brittle areas (%DB) for each specimen. The estimations for the brittle areas were also compared to the threshold load reduction ratio (TLRR) and the austenite spacing to investigate whether there was any correlation between the parameters.

Finally, the SEM was used for documentation of secondary cracking on the surfaces close to the fracture surfaces of all samples. Due to the specimen holder in the SEM, the working distance during image acquisition of secondary cracks was approximately 20mm.

4. Results

4.1. Tensile Testing

From the tensile testing, stress-strain curves for the different test materials were obtained. The stress-strain curve for material A is shown in Figure 4.1 as an example. All stress-strain curves are provided in Appendix B. Table 4.1 contains all the measured YS values for the test materials, as well as the average value used for the subsequent HISC testing. Also included in the table are ultimate tensile strength (UTS) values and the UTS/YS ratio for each material. The strain at fracture is not reported in this thesis. This is due to this test parameter not being included in the documentation obtained from the tensile testing.

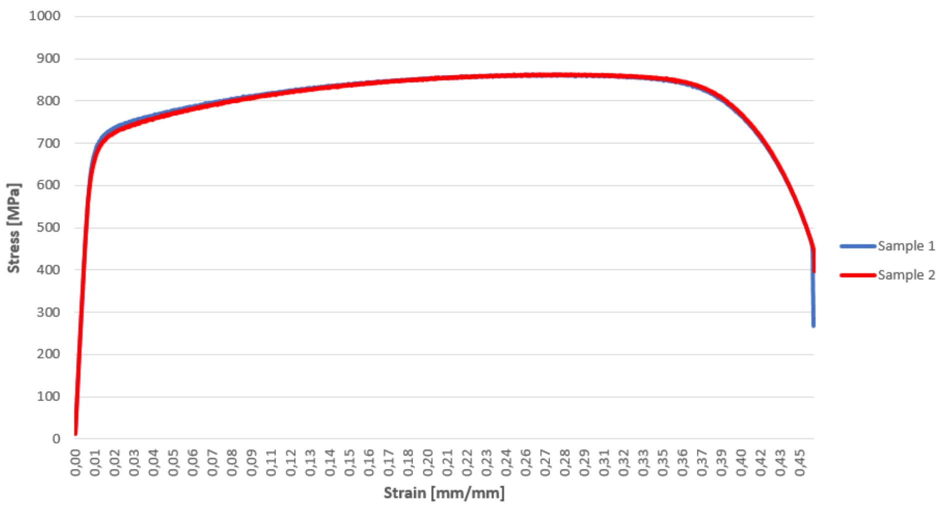

Figure 4.1: Stress-strain curve for material A.

Table 4.1: Tensile test results

Material	specimen no.	Yield strength YS [Mpa]	Ultimate tensile strength UTS [Mpa]	UTS/YS [%]
A	1	670,7	864,4	128,9
	2	656,9	864,1	131,5
	Average	663,8	864,3	130,2
	SD	9,76	0,22	1,84
B	1	574,0	820,6	143,0
	2	571,2	815,3	142,7
	Average	572,6	818,0	142,9
	SD	1,98	3,75	0,22
C	1	616,5	833,9	135,3
	2	611,5	826,7	135,2
	Average	614,0	830,3	135,2
	SD	3,54	5,09	0,10
D	1	634,7	820,7	129,3
	2	650,0	830,7	127,8
	Average	642,4	825,7	128,6
	SD	10,82	7,07	14,63
E	1	648,4	814,7	125,6
	2	617,6	813,6	131,7
	Average	633,0	814,2	128,7
	SD	21,78	1,12	4,31

4.2. Micrographic Examination

In this section, images from the micrographic examination by optical microscopy will be presented for all test materials along with a short description of the microstructure visible from the images. In all OM images presented in this thesis, the light areas represent austenite, while the dark areas represent ferrite. After the micrographical examination, the austenite spacing results are presented.

4.2.1. Material A

Figure 4.2 shows the microstructure for test material A. The image in Figure 4.2a is from the direction parallel to the pipe length at 100X magnification. From the image, a duplex structure with elongated austenite islands in a ferrite matrix is clearly visible. In addition, possible clusters of secondary phases are visible as dark clouds in some areas of the ferrite matrix, mainly in larger ferrite grains. Micrographs were also taken for the normal to pipe length direction. As seen in Figure 4.2b taken at 200X magnification, in this plane the austenite islands are more rounded. Possible secondary phases are also visible in the ferrite phase of this plane.

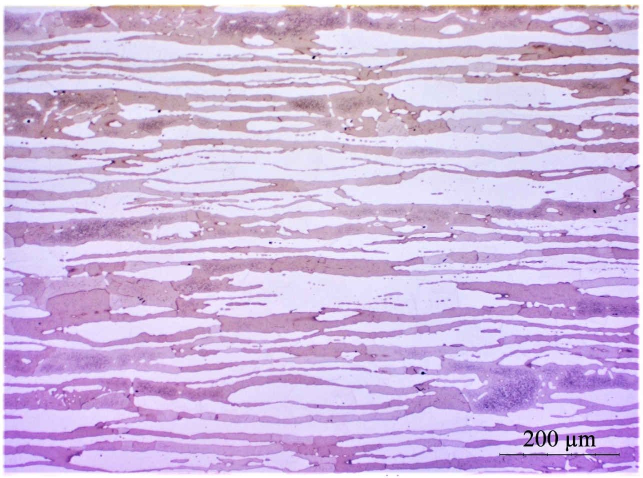

(a) Om image showing the microstructure in the parallel to pipe length direction.

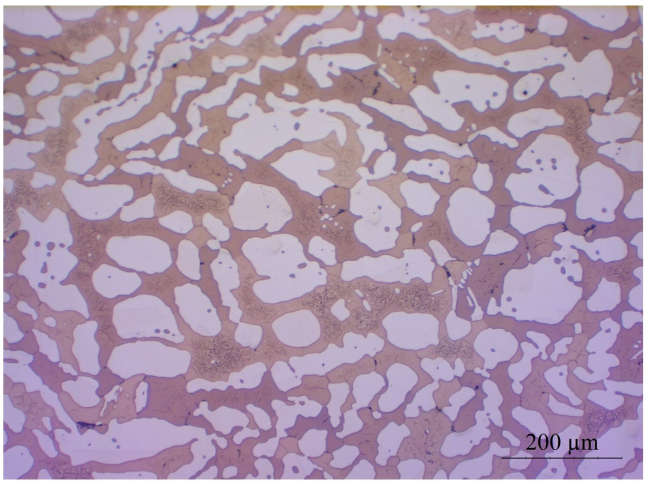

(b) OM image taken in the direction normal to pipe length

Figure 4.2: Micrographs of test material A for different directions.

4.2.2. Material B

Below, the microstructure for test material B in the direction parallel to pipe length is shown in Figure 4.3a. The structure consists of both somewhat elongated and more circular austenite islands in a ferrite matrix. In this material, as for material A, some possible secondary phases are visible in some of the larger ferrite grains.

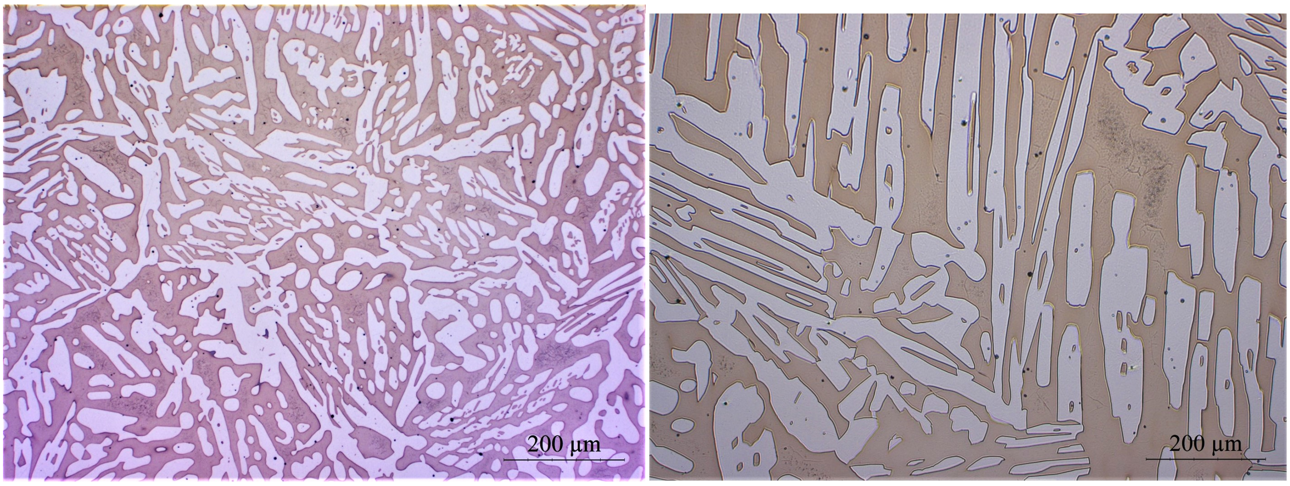

(a) Om image showing the microstructure in the parallel to pipe length direction.

(b) OM image taken in the direction normal to pipe length

Figure 4.3: Micrographs of test material B for both directions.

For the direction normal to pipe length of test material B (Figure 4.3b), the austenite islands are more elongated, and the microstructure is more needle shaped. Also in this plane, the larger ferrite grains contain some possible secondary phases.

4.2.3. Material C

Figure 4.4a depicts an image of the microstructure of test material C in the plane parallel to the pipe length, while Figure 4.4b is of the direction normal to the pipe length. The magnification of the former is 200X and 100X for the latter. The austenite islands are elongated in the parallel direction and circular in the normal direction. No secondary phases are visible in the ferrite matrix of both directions.

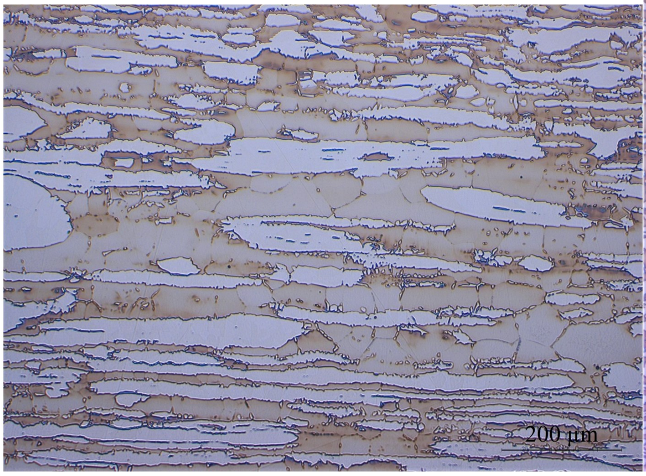

(a) Micrograph of the direction parallel to the pipe length taken at 200X magnification.

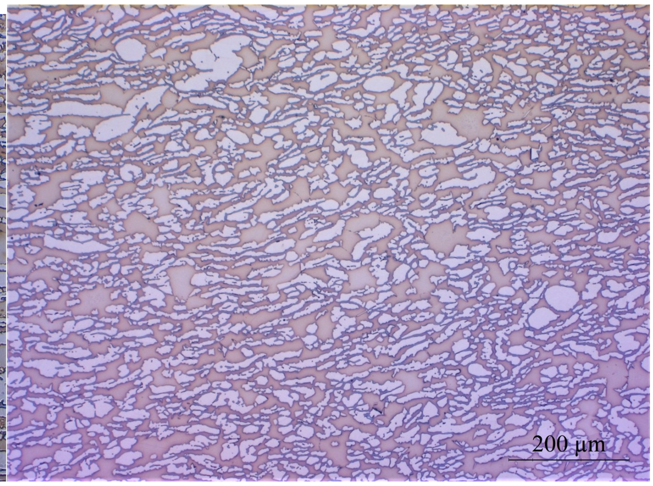

(b) OM image taken in the direction normal to pipe length

Figure 4.4: Micrographs of test material C for both directions at different magnifications.

4.2.4. Material D

OM images of test material D are provided in Figures 4.5a and 4.5b, both taken at 100X magnification. The images are of the planar direction parallel and normal to the pipe length, respectively. For the parallel direction, the austenite islands are elongated, but somewhat rounded. The duplex structure is also slightly bimodal with some clusters of smaller austenite islands between the larger, more elongated ones. As for the planar direction normal to the pipe length, the austenite islands are less elongated and more rounded. Secondary phases in the ferrite matrix are visible for both directions.

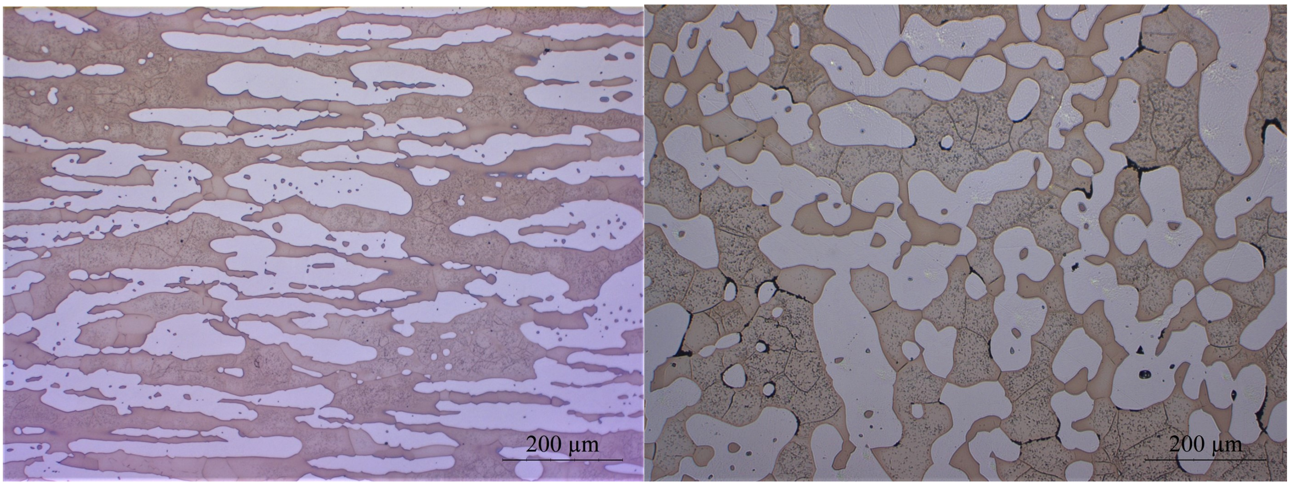

(a) Microstructure of the direction parallel to pipe length.

(b) Microstructure of the direction normal to pipe length.

Figure 4.5: Micrographs of test material D for both directions at different magnifications.

4.2.5. Material E

Figure 4.6 depicts OM images of the microstructure of test material E. As can be seen in Figure 4.6a, the microstructure in the direction parallel to the pipe length consists of both elongated and rounded austenite grains of different sizes. The ferrite grains between them are quite large. The direction normal to the pipe length has the same microstructure, as can be seen in Figure 4.6b. From this figure, secondary phases are visible on the ferrite/austenite grain boundaries as black areas.

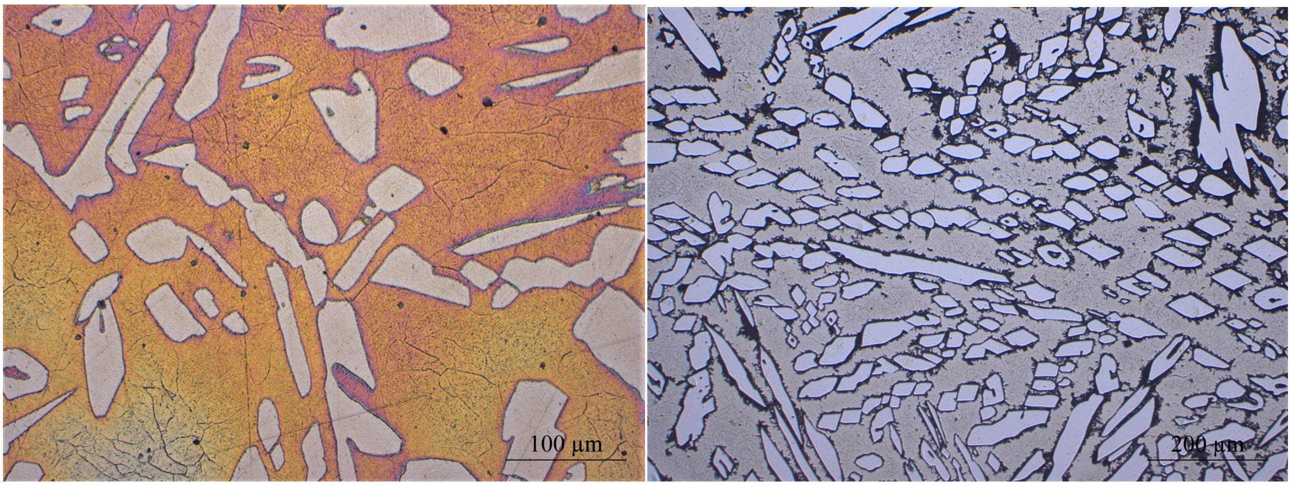

(a) Microstructure of the direction parallel to pipe length at 200X magnification.

(b) Microstructure of the direction normal to pipe length at 100X magnification.

Figure 4.6: Micrographs depicting the microstructure of test material E.

4.2.6. Austenite Spacing

The results of the austenite spacing measurements are provided in Table 4.2. From the table and Figure 4.7, material E has the highest average austenite spacing value at 51,36μm, while material C has the lowest value at 24,95μm. The results for each of the four fields used for calculating the austenite spacing for each test material is provided in Appendix C.

Table 4.2: Austenite spacing results

	Material A	Material B	Material C	Material D	Material E
Mean	27,13	26,66	24,95	47,49	51,36
SD	20,71	21,39	14,79	38,55	72,21
95%CI	9,69	10,01	6,92	18,04	33,80
%RA	35,74	37,54	27,73	37,99	65,80

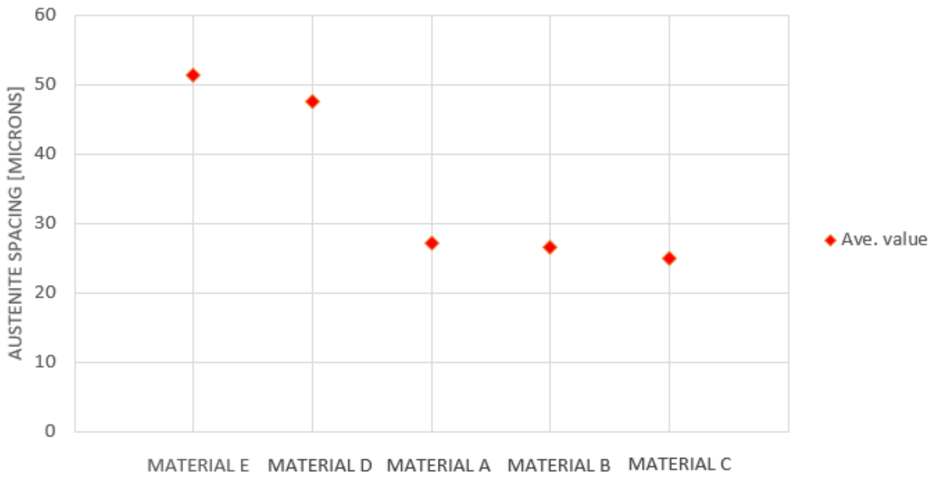

Figure 4.7: Diagram comparing the austenite spacing results sorted from highest to lowest average value.

4.3. HISC Testing

As explained in the previous chapter the HISC testing resulted in data for three different testing parameters, namely the threshold load reduction ratio (TLRR), fracture/yield strength ratio (%YS) and reduction in area. The results for these are presented below. As mentioned in the previous chapter, the reference specimen for test material D did not fracture due to lack of room in the Cortest proof ring. How this might have influenced the results will be discussed in the next chapter.

4.3.1. Threshold load reduction ratio

The TLRR values for all polarised specimens from the test materials are presented in Table 4.3. The data used for calculating the values are given in Appendix D. In Figure 4.8 the minimum, maximum and average TLRR values for the test materials are compared. As can be seen in the figure, test material C has the lowest average value or the TLRR at 7,98%. The average values for materials A and D are slightly higher at 11,50% and 10,34%, respectively, while materials B and E are quite high. The latter have average values at 23,46% and 26,10%, respectively. The standard deviation is low for all test materials. However, it is slightly higher for test material D than for the other materials.

Table 4.3: TLRR values for all polarised specimens [%].

specimen no.	Material A	Material B	Material C	Material D	Material E
1	10,00	21,03	7,07	5,00	23,90
2	10,50	23,90	8,89	12,08	25,20
3	14,00	25,44	-	13,95	29,20
Average	11,50	23,46	7,98	10,34	26,10
SD	2,18	2,24	1,29	4,72	2,26

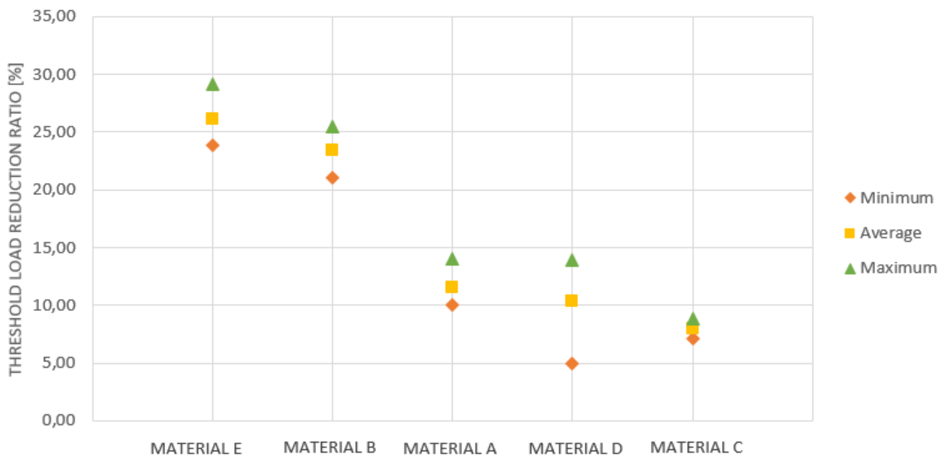

Figure 4.8: Diagram comparing the TLRR values for all test materials sorted from highest to lowest average value.

4.3.2. Yield strength ratio

The results for the %YS are given in Table 4.4. The values for $\sigma_{th,HISC}$ used for obtaining these results can be found in Appendix D under the section pertaining to the TLRR calculations. From the table, it is clear that test material E has the lowest %YS value at 94,40%. This indicates that the test specimens fractured at stress levels lower than the AYS found from the tensile tests. The highest %YS value was found for material C at 132,20%. With the exception of material D, all materials have standard deviations at 3,58 or lower, showing little variation in the results. Test material has a slightly higher SD at 6,10, which is still quite low. Figure 4.9 compares the maximum, minimum and average %YS values for the different test materials.

Table 4.4: %YS values for all polarised specimens [%].

specimen no.	Material A	Material B	Material C	Material D	Material E
1	119,10	115,76	133,50	122,81	90,40
2	123,90	120,13	130,90	113,67	95,50
3	124,70	113,42	-	111,25	97,30
Average	122,57	116,44	132,20	115,91	94,40
SD	3,03	3,41	1,84	6,10	3,58

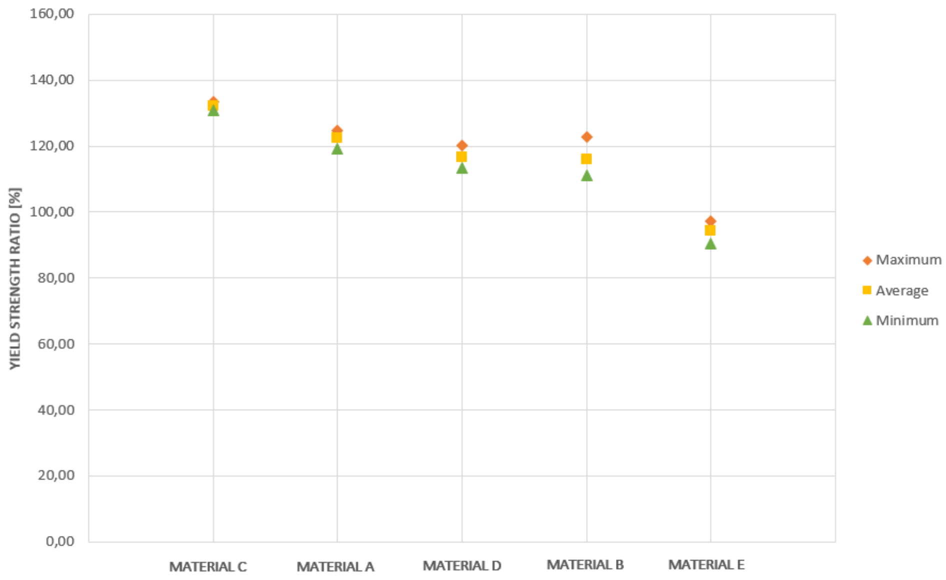

Figure 4.9: Diagram comparing the %YS values for all test materials sorted from highest to lowest average value.

4.3.3. Reduction in area

The results from the RA measurements of interest in this thesis are the relative RA_{env}/RA_{air} values. Therefore, only these values will are presented in Table 4.5. The RA values for all test specimens and the necessary variables for the calculation can be found in Appendix D. Figure 4.10 shows a diagram comparing the RA results for the different test materials. In the figure, the results are sorted by highest average value.

Table 4.5: Reduction of area ratio results [%].

specimen no.	Material A	Material B	Material C	Material D	Material E
1	72,53	85,56	59,30	9,40	94,33
2	82,18	86,32	89,30	11,85	88,34
3	85,72	87,09		12,26	96,06
Average	80,14	86,32	74,30	11,17	92,91
SD	6,83	0,77	21,21	1,55	4,05

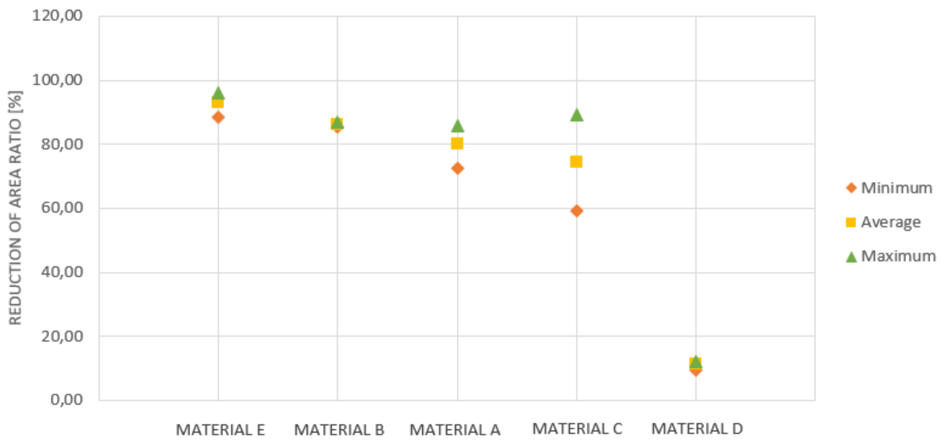

Figure 4.10: Diagram comparing the RA results.

4.4. Hydrogen Content

As mentioned in the "Materials and Experimental Methods" chapter, the hydrogen content of the materials after HISC testing was obtained by employing the melt extraction technique using the H-mat 225 equipment from JUWE Laborgeräte GMbH. The results are provided in Figure 4.11 and Table 4.6 below. From the figure, it is evident that test material C has the highest hydrogen content at 82,17ppm, while the lowest value is found for material D at 48,98ppm.

Table 4.6: Hydrogen content results

	Material A	Material B	Material C	Material D	Material E
specimen weight [g]	0,4073	0,4919	0,4216	0,4096	0,4372
Hydrogen content [ppm]	60,06	67,58	82,17	48,98	50,40

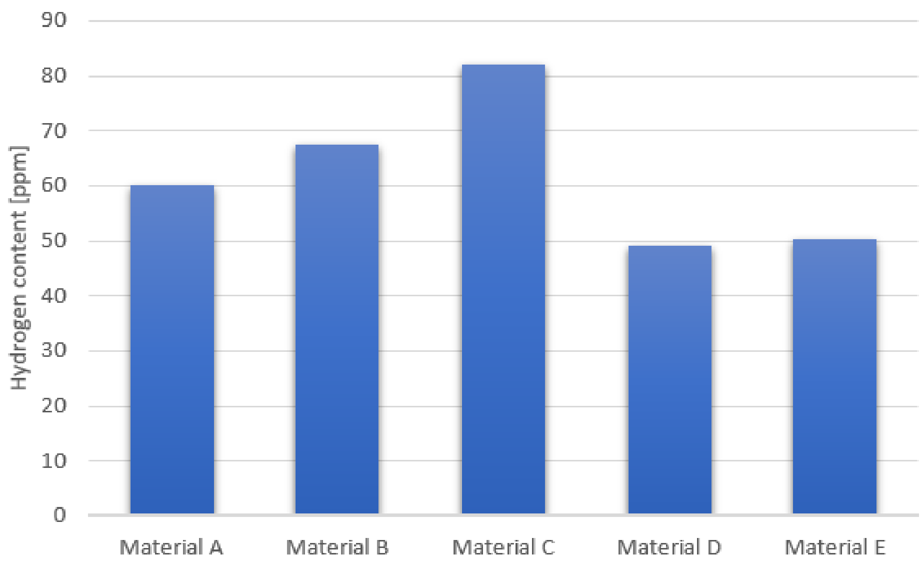

Figure 4.11: Graphical illustration of hydrogen content in the test materials.

4.5. Fractography

For the fractography, the results are obtained through the use of SEM as described in the previous chapter. In this section, SEM images of the specimens are provided along with a short description. Firstly, fracture surface examination images are provided, followed by brittle area estimation results. Finally, SEM images documenting secondary cracking are shown.

4.5.1. Fracture surface examination

Material A

In Figure 4.12, SEM images of the reference specimen for material A is shown at different magnifications. The image to the left is an overview taken at low magnification. In the image, extensive deformation of the specimen before fracture is visible as ridges in the material close to the fracture surface. Cup-and-cone characteristics, or dimples, are visible in the image to the right, which is from the center of the specimen and taken at higher magnification.

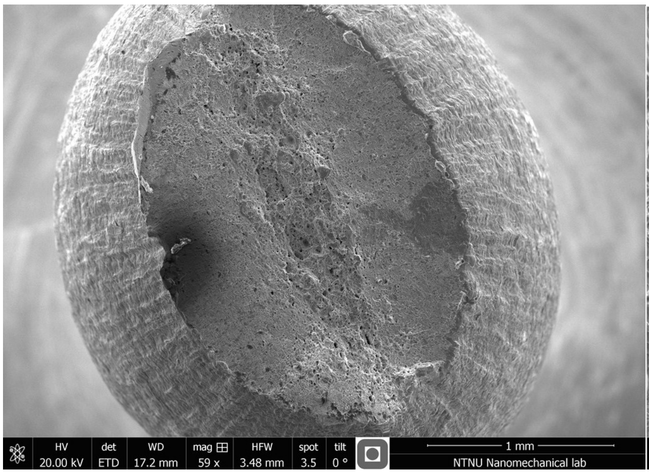

(a) Overview image of the test specimen.

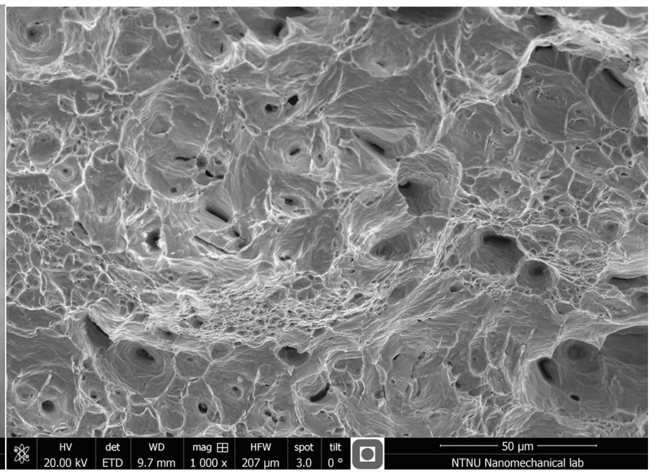

(b) Visible dimples in fracture surface.

Figure 4.12: Images showing the fracture surface of the reference specimen for material A.

Images of the fracture surface of the first polarised specimen from material A are provided in Figure 4.13. The upper left image, Figure 4.13a, shows the fracture surface at lower magnification. From this image, a ductile surface characteristic is visible towards the lower right edge of the specimen, while a more brittle cleavage-type characteristic is visible to the upper left. Figure 4.13b is of the ductile area, showing the cup-and-cone structure at higher magnification, and Figure 4.13c shows the brittle area at a higher magnification. In the latter, a cleavage in the surface is circled in red.

For the second and third polarised specimens, images taken at different magnifications are provided in Figure 4.14. The two upper images in the figure are from polarised specimen 2, while the bottom two are from polarised specimen 3. From Figures 4.14a and 4.14b, a mostly ductile fracture surface is shown for the second polarised specimen. specimen 3, Figure 4.14c, has a more mixed fracture surface character, with ductile characteristics to the left and brittle to the right of the surface. In the brittle area, a cleavage is circled in red (Figure 4.14d).

Material B

For the reference specimen for test material B, images of the fracture surface are given in Figures 4.15a and 4.15b. As for material A, the fracture surface of the reference specimen exhibit cup-and-cone characteristics. This is clearly visible from the latter figure. Evidence of

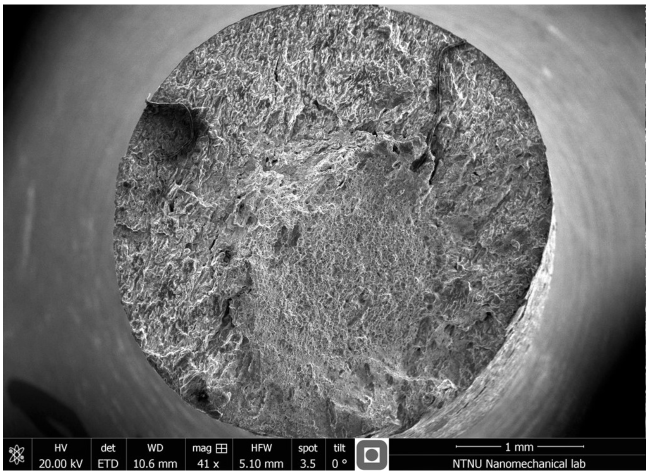

(a) Overview image of the specimen.

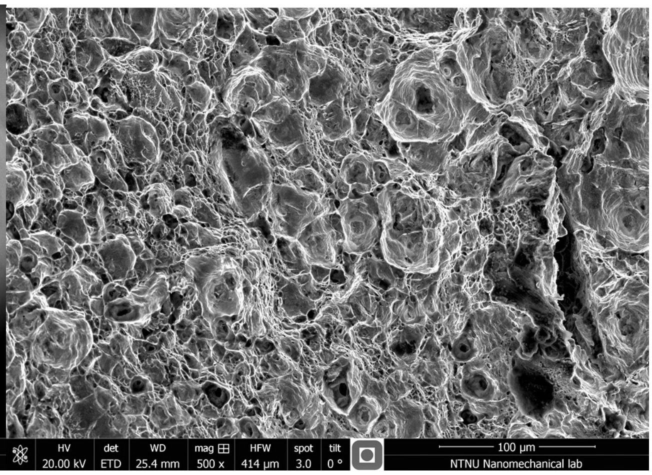

(b) Image showing the dimples in the specimen.

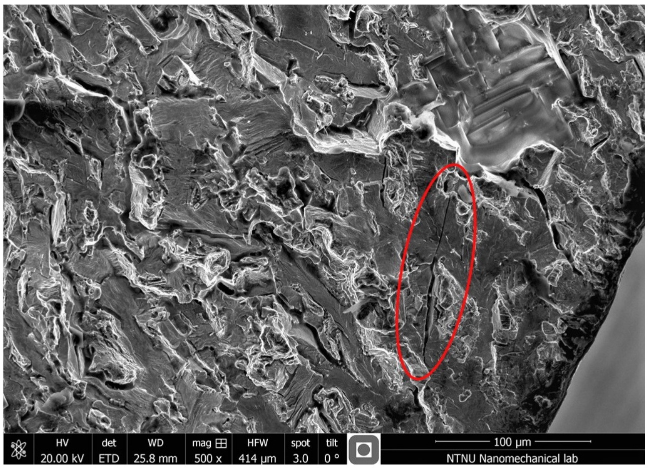

(c) Image taken at the edge of the specimen.

Figure 4.13: Images showing the fracture surface of polarised specimen 1 for material A.

deformation of the specimen before fracture can be seen from the striations on the specimen close to the fracture surface in Figure 4.15a.

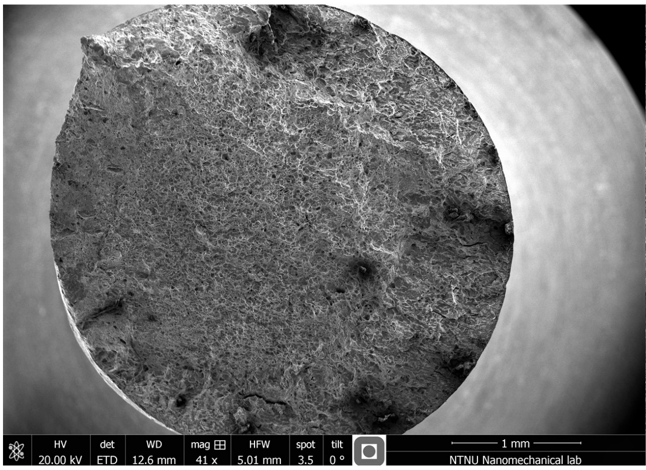

(a) Overview image of polarised specimen 2.

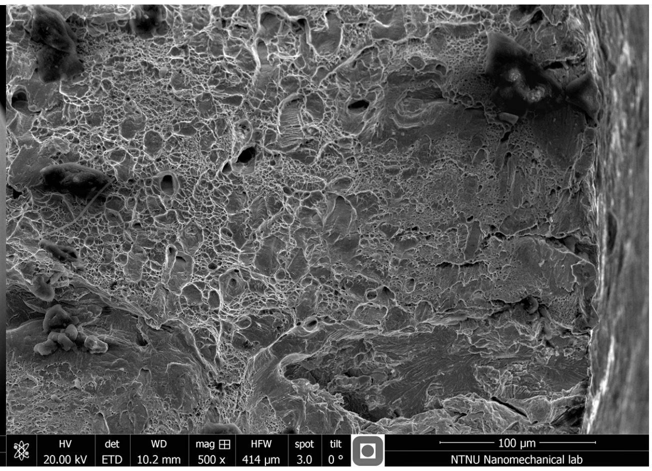

(b) Image showing the mostly ductile fracture surface.

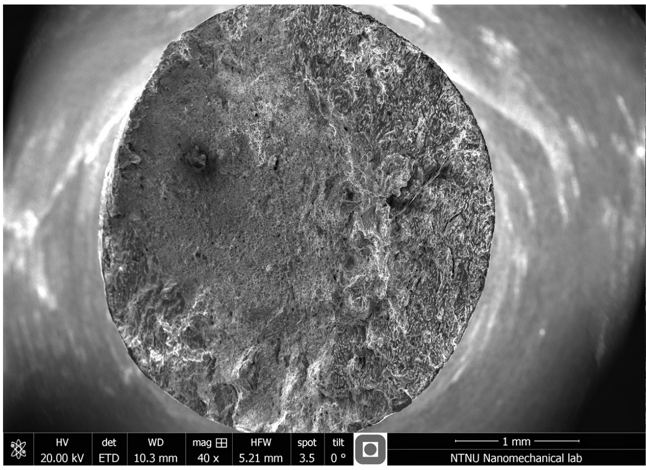

(c) Overview image of polarised specimen 3.

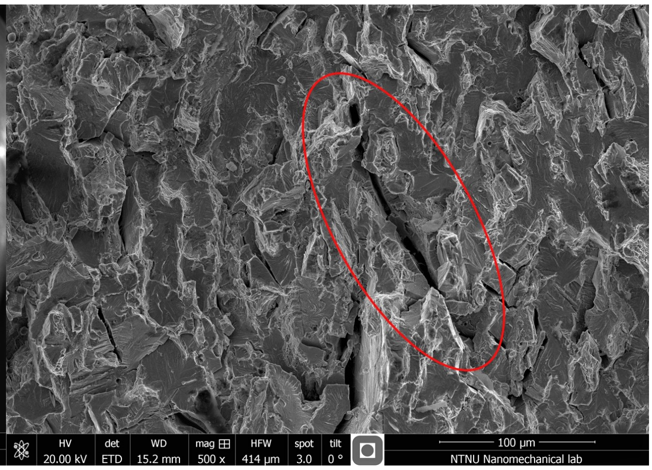

(d) Brittle cleavage-type fracture characteristic.

Figure 4.14: Images showing the fracture surface of polarised specimens 2 and 3 for material A.

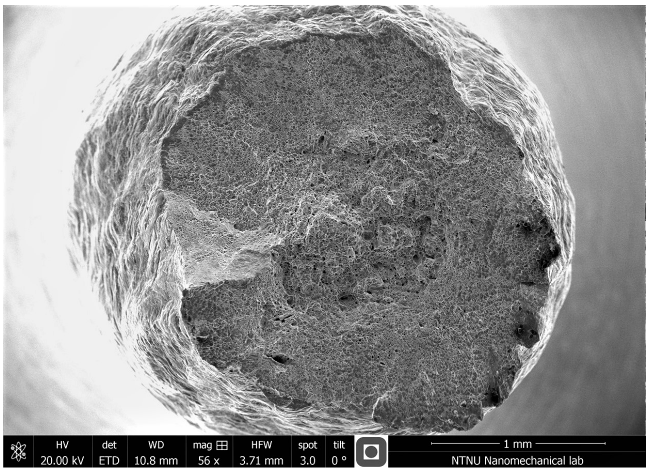

(a) Overview image of the reference specimen at low magnification.

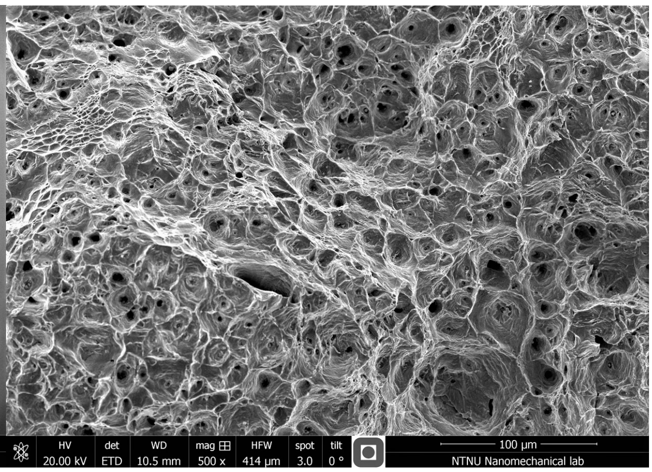

(b) Visible dimples in fracture surface at higher magnification.

Figure 4.15: Images showing the fracture surface of the reference specimen for material B.

The fracture surface characteristics of the polarised specimens are provided in Figure 4.16. The image in Figure 4.16a gives an overview of the fracture surface at lower magnification. In the image, the area showing ductile fracture characteristics is circled in red. The circle is an approximation of the ductile area. Along the edge of the surface, brittle cleavage-type fracture is present, as shown at higher magnification in Figure 4.16c. In the image, cleavages are circled in red.

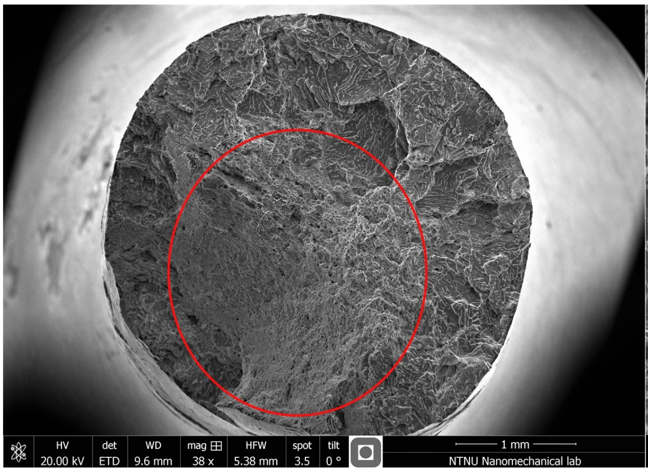

(a) Overview image of the polarised specimen.

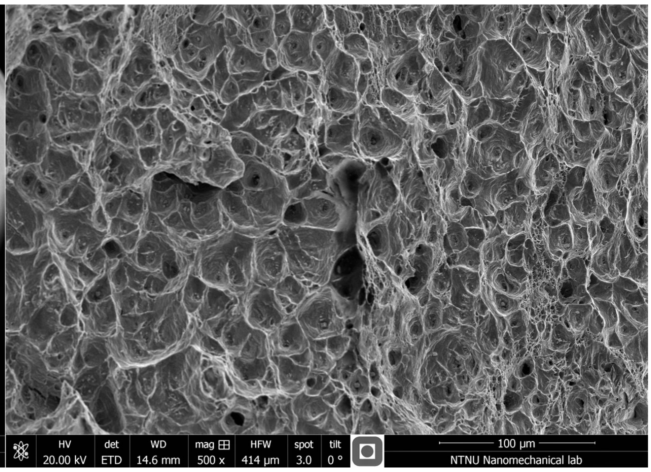

(b) Image showing the dimples in ductile area of the specimen.

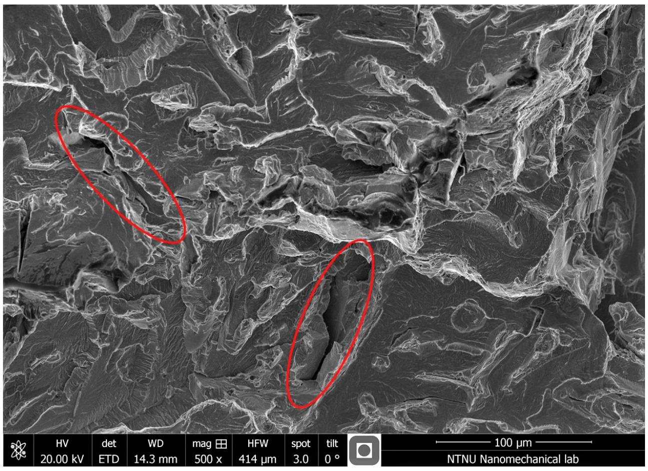

(c) Image taken at the edge of the specimen.

Figure 4.16: Images showing the fracture surface of polarised specimen 1 for material B.

Material C

Figure 4.17 depicts SEM images taken at different magnifications of the reference specimen for material C. Again, the reference specimen shows ductile fracture characteristics with deformation close to the fracture surface and clearly visible dimples.

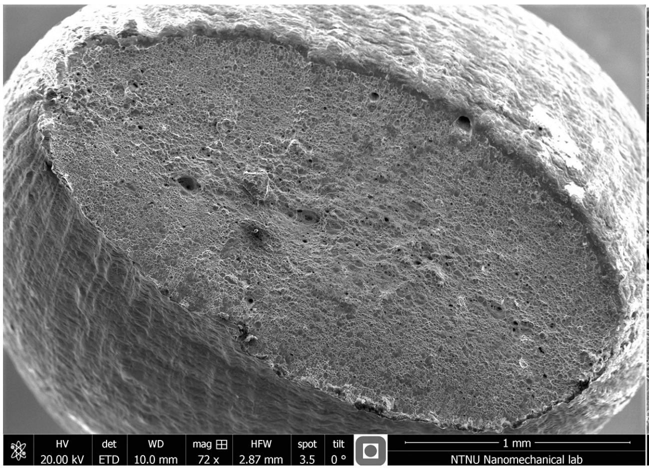

(a) Overview image of the reference specimen.

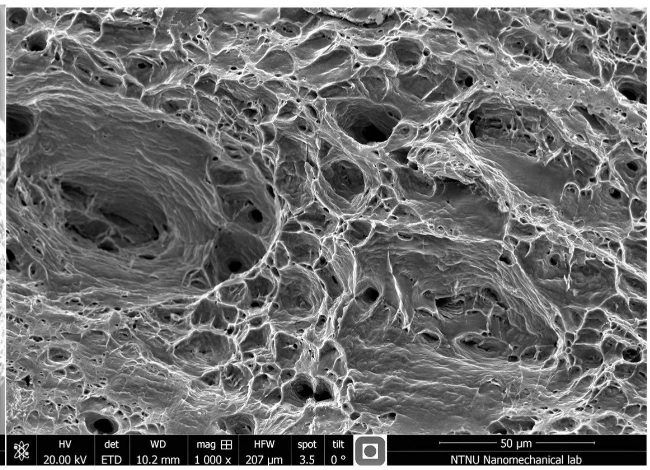

(b) Ductile characteristics visible in the fracture surface.

Figure 4.17: Images showing the fracture surface of the reference specimen for material C.

SEM images of the two polarised specimens from test material C is given in Figure 4.18. Figures 4.18a and 4.18b shows the fracture surface of polarised specimen 1 at different magnifications. A rough estimate of the area showing ductile fracture characteristics is circled in red in the former, while a cleavage is circled in the latter. Figures 4.18c and 4.18d are images of polarised specimen 2 from this material. In the former, the same mixed fracture surface characteristics are visble, and Figure 4.18d shows the dimples in the ductile area at higher magnification.

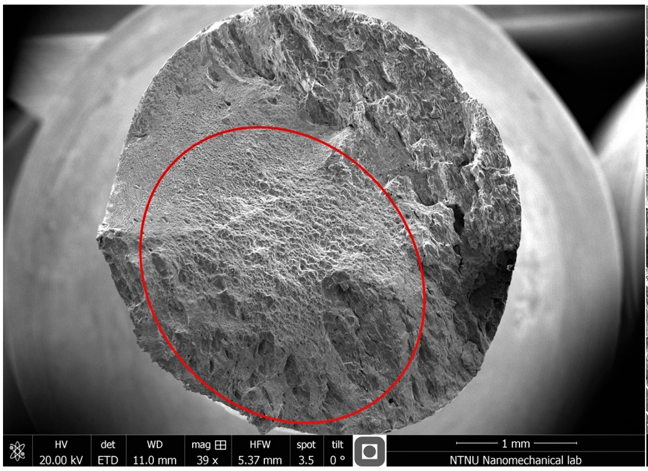

(a) Overview image of polarised specimen 1.

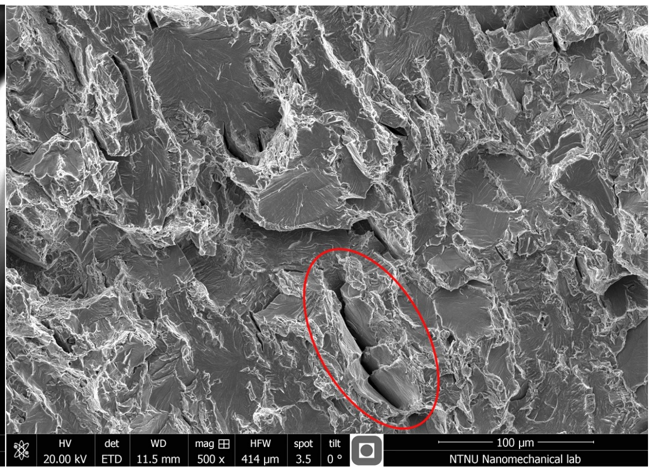

(b) Image showing brittle cleavage-type characteristics in specimen 2.

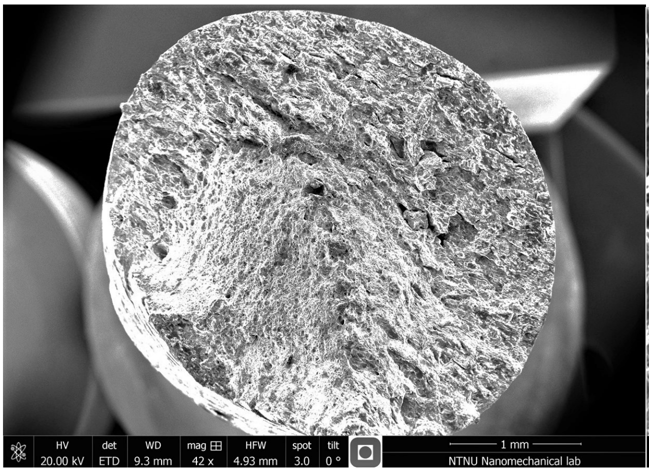

(c) Overview image of polarised specimen 2.

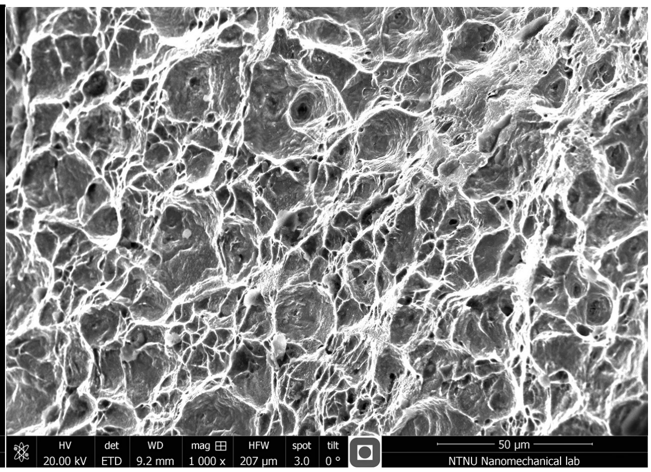

(d) Ductile cup-and-cone characteristics of polarised specimen 2.

Figure 4.18: Images showing the fracture surface of the polarised specimens for material C.

Material D

As the reference specimen for test material D did not fracture in the Cortest proof ring, no fracture surface examination was performed on that specimen. Below, representative SEM images of the polarised specimens for this material are provided. Figures 4.19a and 4.19c are overviews of polarised specimen 1 and 3, respectively. The areas showing ductile fracture characteristics are circled in red. Figure 4.19b shows the brittle area of specimen 1 at higher magnification, while Figure 4.19d shows the brittle area of specimen 3 at higher magnification.

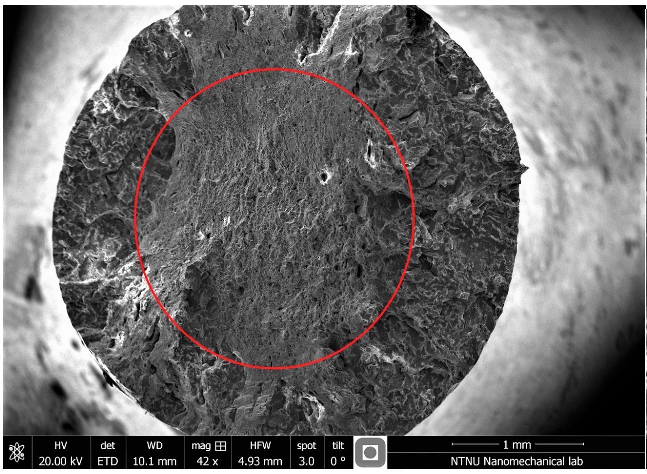

(a) Overview image of polarised specimen 1.

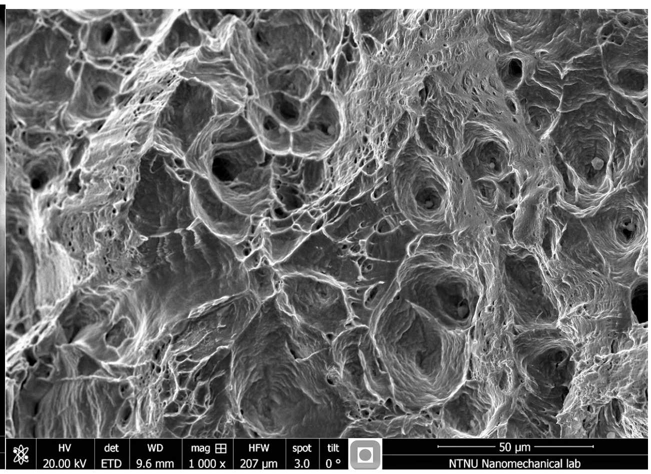

(b) Image showing ductile characteristics in specimen 1.

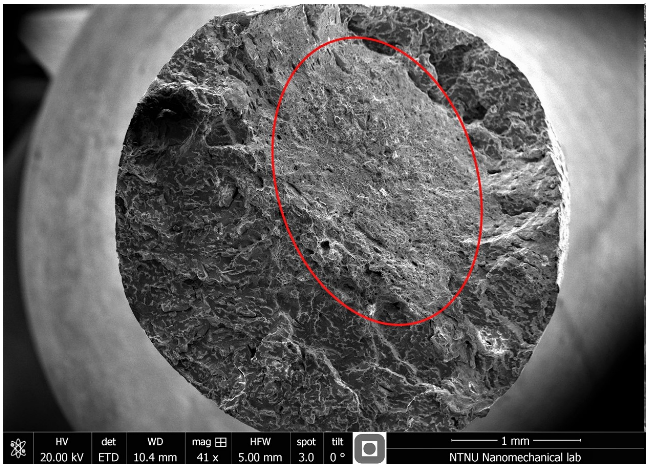

(c) Overview image of polarised specimen 3.

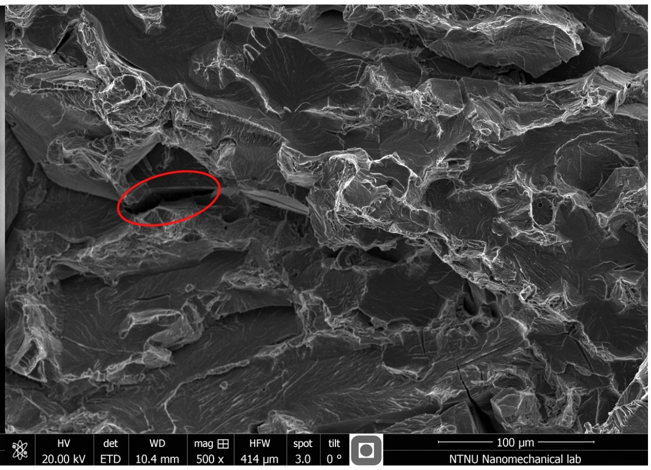

(d) Brittle characteristics of polarised specimen 3.

Figure 4.19: Images showing the fracture surface of the polarised specimens for material D.

Material E

SEM images captured of the reference specimen fracture surface for material E is given in Figure 4.20. As for the other reference specimens, deformation of the specimen is visible as striations outside the fracture surface. Ductile dimple fracture characteristics are shown at higher magnification in Figure 4.20a. In Figure 4.20c, fracture characteristics similar to cleavages are visible.

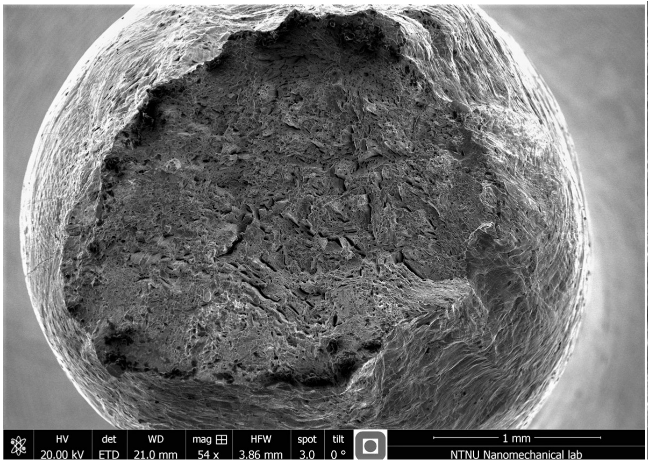

(a) Overview image of the reference specimen.

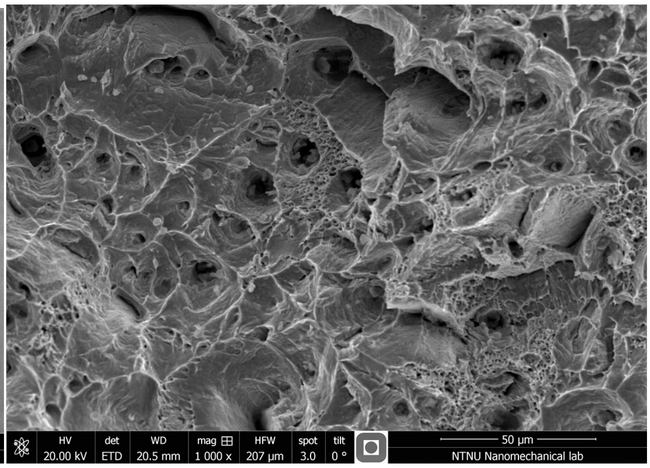

(b) Ductile characteristics visible in the fracture surface.

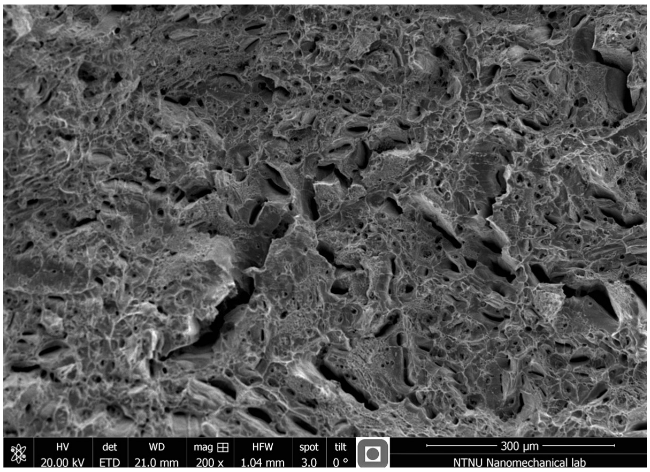

(c) Cleavage-like characteristics in the fracture surface.

Figure 4.20: Images showing the fracture surface of the reference specimen for material E.

The images in Figures 4.21 and 4.22 are of the polarised specimens for material E. In Figure 4.21a, and overview of the fracture surface for polarised specimen 1 is provided with the ductile area circled in red. Brittle fracture characteristics are shown in Figure 4.21b.

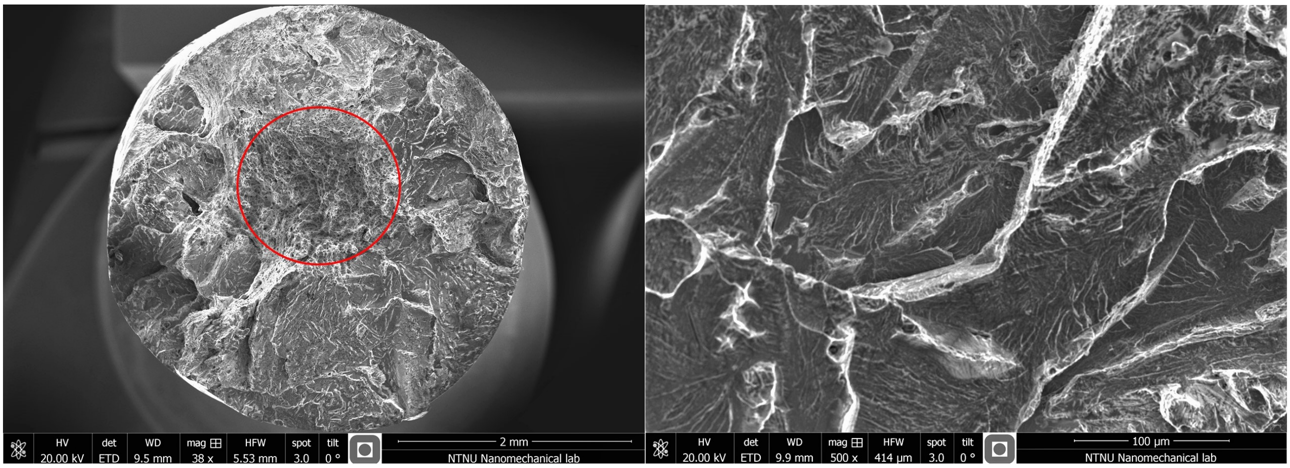

(a) Overview image of polarised specimen 1.

(b) Image showing brittle cleavage-type characteristics in specimen 1.

Figure 4.21: Images showing the fracture surface of the polarised specimen 1 for material E.

Images from polarised specimens 2 and 3 are given in Figure 4.22. In the overview image to the right in the figure the ductile area is circled in red. The dark area to the right in Figure 4.22a is due to the fracture surface not being plane, but rather having a slight angle. Figure 4.22b depicts ductile fracture characteristics of polarised specimen 3 at higher magnification.

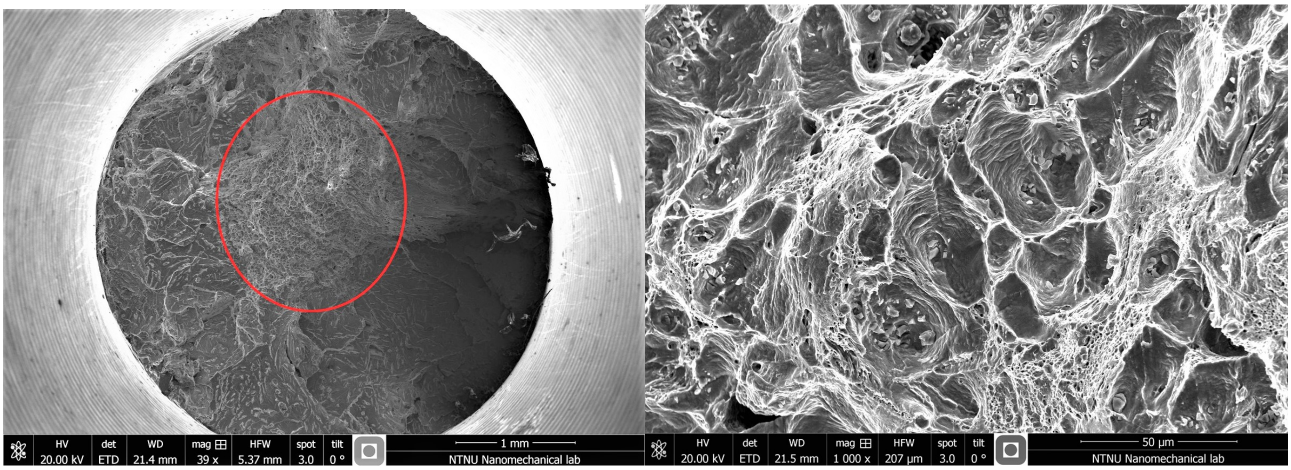

(a) Overview image of polarised specimen 3.

(b) Ductile cup-and-cone characteristics of polarised specimen 3.

Figure 4.22: Images showing the fracture surface of polarised specimens 2 and 3 for material E.

4.5.2. Brittle area measurements

All measurements for the radii of the polarised specimens are provided in Appendix E. As an example of how the measurements were obtained, a SEM image of one of the polarised specimens from test material B with the measurements is provided in Figure 4.24 below.

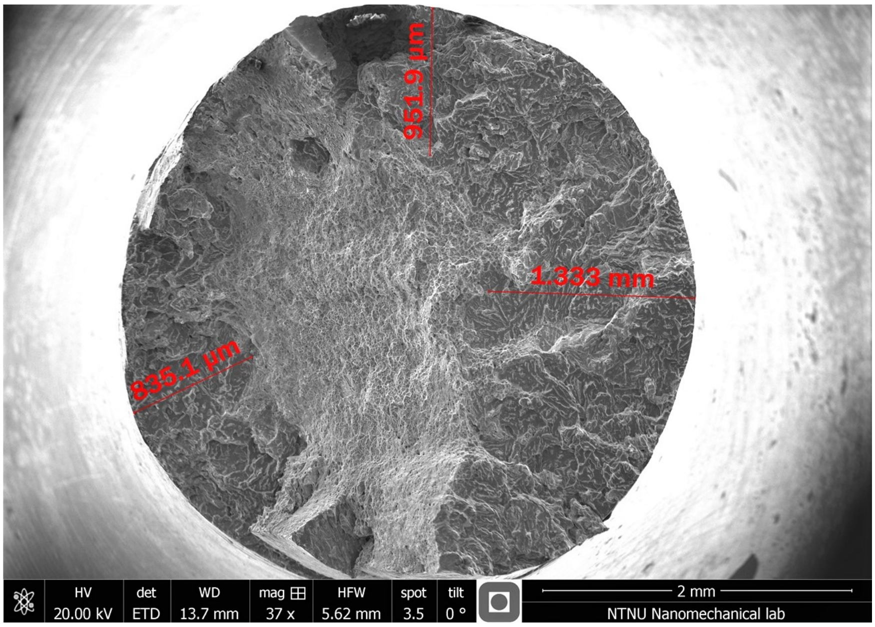

Figure 4.23: SEM image with measurements for the length of brittle area.

In Table 4.7 the average and standard deviation values for the ductile and brittle areas are provided along with the same values for the brittle/ductile ratio. From the table, it is clear that test materials B and E have the highest ratios with 77,47% and 77,58%, respectively. The lowest ratio is that of material A. In Figure 4.24 the minimum, maximum and average values for all test materials are presented, sorted from the highest average value to the lowest.

Table 4.7: Brittle/ductile ratio results

Material	Ductile area $[mm^2]$		Brittle area $[mm^2]$		%DB [%]	
Material A	Ave.	3,00	Ave.	6,57	Ave.	54,38
	SD	0,66	SD	0,68	SD	10,18
Material B	Ave.	1,84	Ave.	8,16	Ave.	77,47
	SD	0,66	SD	0,68	SD	10,18
Material C	Ave.e	2,26	Ave.	7,00	Ave.	67,65
	SD	1,11	SD	1,22	SD	13,98
Material D	Ave.	2,52	Ave.	7,45	Ave.	66,21
	SD	0,29	SD	0,41	SD	5,40
Material E	Ave.	1,95	Ave.	8,70	Ave.	77,58
	SD	0,29	SD	0,26	SD	3,76

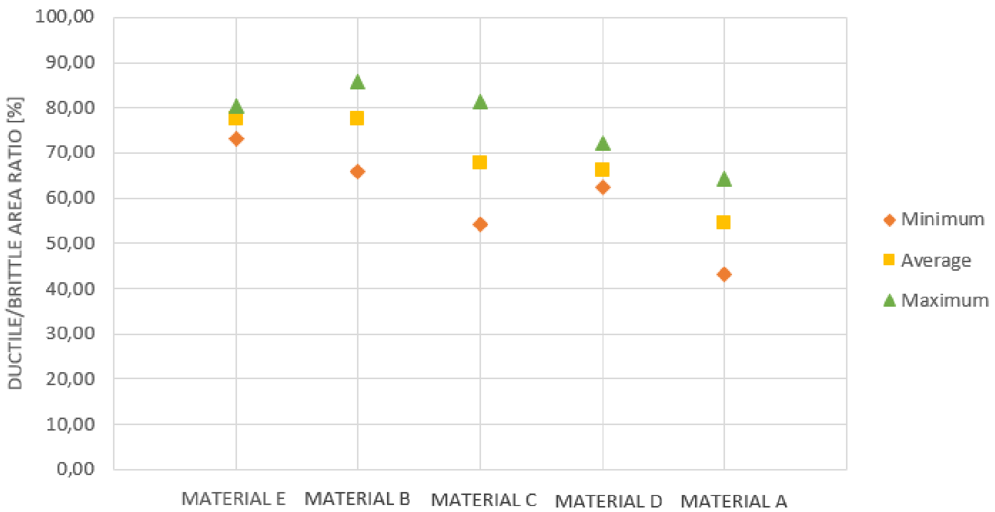

Figure 4.24: Graph showing the results for the ductile/brittle ratio estimation.

4.5.3. Secondary cracking

In the figures below, SEM images of secondary cracks for the different test materials are presented.

Material A

Figure 4.25 shows secondary cracks in the polarised test specimens from material A.

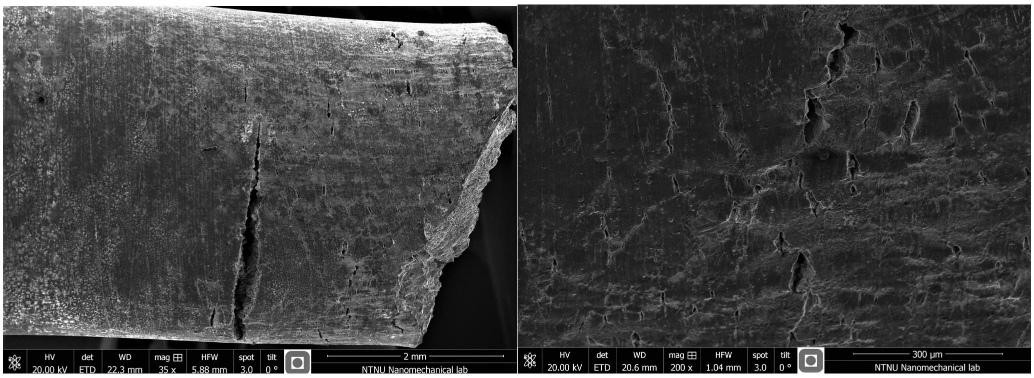

(a) Secondary cracking in material A.

(b) Secondary cracks in material A at higher magnification.

Figure 4.25: Images showing the secondary cracks in test material A.

Material B

Figure 4.26 shows secondary cracks in the polarised test specimens from material B.

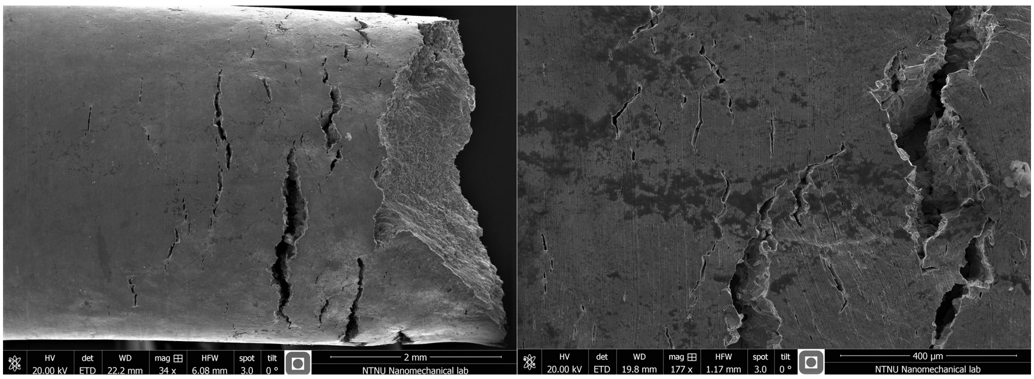

(a) Secondary cracking in material B.

(b) Secondary cracks in material B at higher magnification.

Figure 4.26: Images showing the secondary cracks in test material B at different magnifications.

Material C

Figure 4.27 Shows secondary cracking in polarised test specimens from material B.

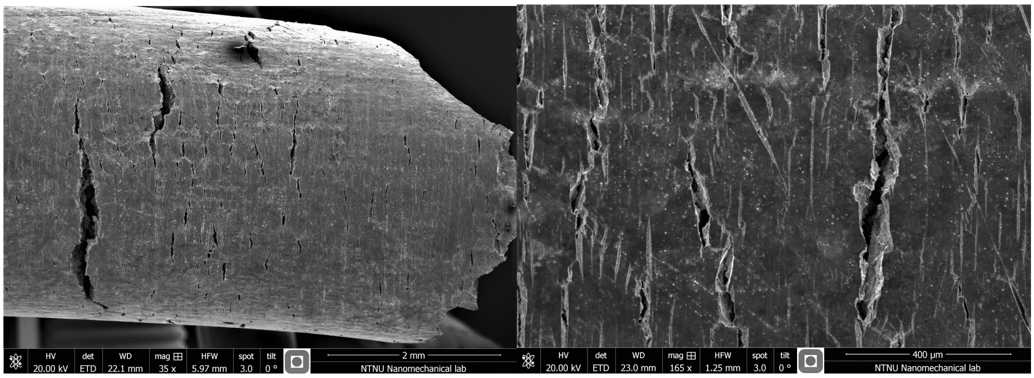

(a) Secondary cracking in material C.

(b) Secondary cracks in material C at higher magnification.

Figure 4.27: Images showing the secondary cracks in test material C.

Material D

Figure 4.28 Shows secondary cracking in polarised test specimens from material D.

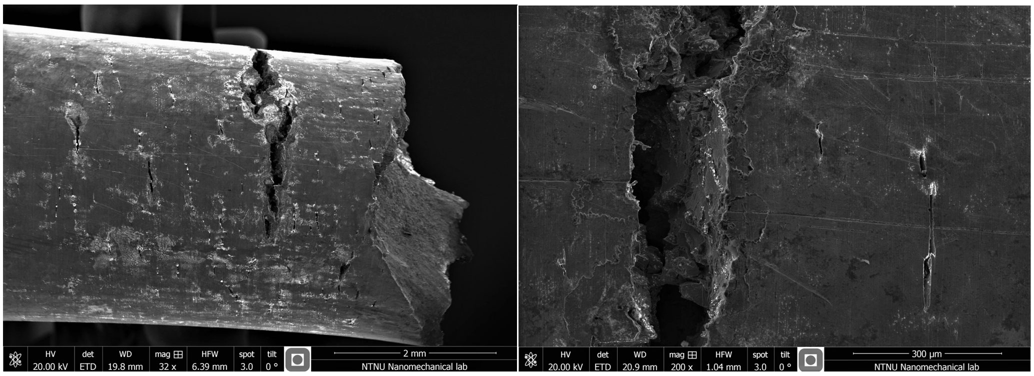

(a) Secondary cracking in material D.

(b) Secondary cracks in material D at higher magnification.

Figure 4.28: Images showing the secondary cracks in test material D.

Material E

Figure 4.29 Shows secondary cracking at different magnifications in polarised test specimens from material E.

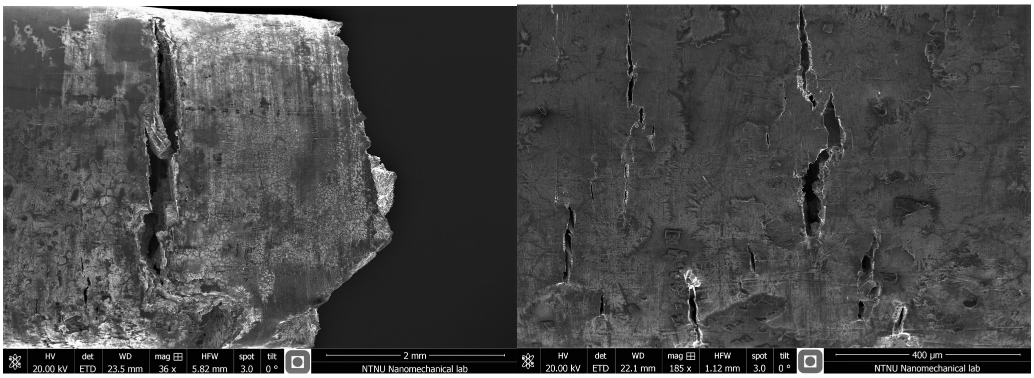

(a) Secondary cracking in material E.

(b) Secondary cracks in material E at higher magnification.

Figure 4.29: Images showing the secondary cracks in test material E.

5. Discussion

5.1. Tensile Testing

The results of the tensile tests performed in this thesis were quite consistent. Test material A was found to have the highest average YS at 663,8MPa, while material B had the lowest at 574,0 MPa. The largest difference in YS between parallels was found for test material E at approximately 31 MPa. The smallest UTS/YS ratio average was found for test material D at 128.6%, while the largest average ratio was 142.9% for test material B. It should be mentioned that test material E had a similar value to material D at 128.7%.

5.2. Metallographic Examination

5.2.1. Microstructure

The microstructure is highly dependent on production method. Materials A and C are both produced through hot extrusion, resulting in a lamellar structure with elongated austenite islands in the ferrite matrix in the direction parallel to the pipe length. This is the direction of extrusion when producing a bar or a pipe, and the microstructure is therefore as expected. However, the austenite islands of material C appear more rounded and the distance between them is greater in some areas. This difference in the microstructures of the materials is probably due to the cold work performed on test material A, and not performed for material C. For the direction normal to the pipe length, the microstructure of both materials consists of circular austenite islands.

Test materials B and E are from centrifugal cast pipes. The microstructure of material B is bimodal with small austenite grains between larger, needle shaped islands. As can be seen from Figure 4.6a, the etching appears different for material E compared to the other test materials. During etching of this specimen, the material reacted differently with the 20%NaOH etchant, and the image is therefore more coloured. The reason for this is unknown. The oxalic acid etching step was not performed in order to investigate whether the combination of the two etching steps caused the colouring of the material as it was first observed after both etching steps had been performed. However, this did not give a positive result and it seems it was the NaOH etchant the material reacted differently to. As the duplex structure is clearly visible in the image, it was decided to include it in the thesis. The microstructure for material E includes needle shaped austenite islands as do material B, but they are smaller than the ones in material B. For both directions compared to the pipe length for these materials, the ferrite grains between the austenite islands appear larger in material E versus material B.

The OM images from test material D in the direction parallel to the pipe length reveals round austenite islands which are slightly elongated with some bimodal austenite grains dispersed throughout the ferrite matrix. The austenite islands also appear quite large. For the direction normal to the pipe length, the microstructure consists of more rounded austenite islands. Also for this direction there are some bimodal austenite grains between the larger islands. The material was produced from a forged bar, and the microstructure shown in Figure 4.5bis in accordance with this production method.

The literature states that higher ferrite content promotes HISC in SDSS [15, 16]. However, as the ferrite content was only provided by the supplier for materials B, C and D, a full comparison of the effects of this value on susceptibility towards HISC between all the test materials was not possible. However, the three materials for which the ferrite content was provided are from each of the three main production routes. A preliminary comparison was therefore conducted. As mentioned in the chapter describing the materials, the ferrite contents of materials B, C and D were 49,5%, 54% and 49%, respectively. These are all close to a 50/50 phase distribution between austenite and ferrite, which is recommended for obtaining optimal mechanical and corrosion properties in SDSS [11]. How these results might have influenced the resistance towards HISC is discussed in more detail in the section on HISC testing below.

When performing the metallographic examination, features appearing to be secondary phases became visible after the electrolytic etching of materials A, B, D and E. From Figure 4.2a, clusters of these secondary phases are visible in the larger ferrite grains of material A in the direction parallel to the pipe length. The same holds true for the direction normal to the pipe length in material B (Figure 4.3b. In the direction normal to pipe length of material D, what appears to be secondary phases are visible along austenite and ferrite/austenite grain boundaries. The latter is also visible for the same direction in material E. Whether there are any secondary phases in the direction parallel to the pipe length for material E is not known as no images with oxalic etch was procured due to the problems with the etching of this material. As the secondary phase in materials A and B is found in clusters in the ferrite grains, the most probable phase is CrN.

The possible secondary phases at the austenite and austenite/ferrite grain boundaries in materials D and E could be either sigma phase or Cr_2N. For test material E, the most likely possible phase is the latter as there are no secondary phases visible in the image when etching with only NaOH. Whether or not chromium nitrides have a detrimental effect on SDSS materials with respect to HISC susceptibility is debated in the industry [20]. In addition, the extent of the secondary phase visible in the OM images is small, and would therefore not affect the performance of the materials. However, it should be noted that the features observed as possible secondary phases in the test materials might be etching artifacts, and not secondary phases at all. To ascertain whether the features are secondary phases or not, and what type of possible secondary phases, a more comprehensive analysis using EDX should be performed. This was, however, outside the scope of this work.

5.2.2. Austenite spacing

As seen from Figure 4.7, the material with the largest austenite spacing is material E with 27,13 μm. The smallest austenite spacing was found for material C with 24,95 μm. The austenite spacing of materials A and B are quite similar, with values of 27,13μm and 26,66μm, respectively. This corresponds well with the distance between the austenite islands visible in Figures 4.2 to 4.6. However, the standard deviation of the values were very high for all materials, with material C having the smallest deviation of 14,79 and material E having the largest deviation, which is 65,80. The high standard deviation results in high values for the percent relative accuracy. According to DNV-RP-F112 [28], results should only be accepted with %RA values at 10% or below. One reason for the high standard deviation and %RA is the fact that the measurements were performed by hand. Another is the bimodal microstructures; with a wide range of grain sizes in the same microstructure, deciding which grains to disregard with respect to the austenite spacing was difficult. From Table 4.2 it can be seen that the materials with a larger degree of bimodal austenite grains have larger standard deviations. As the %RA values are so high, the results of the austenite spacing measurements are not conclusive. However, they do give an indication of the real values.

5.3. Review of HISC Testing

Before reviewing and evaluating the HISC results, a few subjects should be discussed. On the whole, the testing proceeded without interruption, and the few incidents that took place were quickly corrected.

Low temperature creep
When operating the Cortest proof rings, one permanent challenge was the relaxation of the rings. The relaxation made distinguishing between measurement errors and low temperature creep difficult. An attempt to solve this was to correct for relaxation and/or creep during the second step of HISC testing. The correction involved checking the outer ring diameter every 24 hours during this step and adjusting it if necessary. However, relaxation of the rings were observed in that time interval as well. Due to no apparent permanent solution of the problem, upon fracture the threshold load was found using the last measured outer diameter the specimen held for 24h and using this when inserting the load cell.

Pre-charging of specimens from material C
During pre-charging of the specimens from material C and D, some of the specimens fell out of the electrical circuit, causing them to corrode. For material C, this happened twice. As there were only one spare test specimens for this material it was decided to move forward with the experiments using the two polarised specimens which had been pre-charged properly. Thus, when looking at the results there is one less specimen for material C than the other materials.

Reference specimen from material D
It was previously mentioned that the reference specimen from test material D did not fracture due to lack of room on the test ring. Thus, the results for this material is not necessarily accurate. When calculating the TLRR, the load used was the load at which there was no more room in the ring rather than the last load the specimen held for 24h. Also, as no necking occurred in the specimen, the measured diameter after testing was much higher than it would be at fracture. This means that in reality the TLRR and RA ratio values would be higher than the results presented below indicates. This impacts the RA ratio results the

most, as can be seen from 2.12 and Table 4.5. The %YS results are not affected by this, as the reference specimen is not used when calculating this value.

5.4. Review of HISC Results

5.4.1. Threshold load reduction ratio

As stated in the previous chapter, test material C achieved the lowest average value for the threshold load reduction ratio. A low reduction rate indicates a high resistance towards HISC, as there is less difference between threshold load for the reference and polarised specimens. The standard deviation for this material is also the lowest. However, this might be due to the fact that there were only two polarised specimens for this material as pre-charging a third specimen was not possible, as mentioned above. Test material A and D also have quite low values for the TLRR. However, the standard deviation for material A is lower, and thus the variation in the results is lower for this material. This indicates less variation of the results for material A, and thus a more accurate result. The highest values for TLRR, indicating the lowest resistance towards HISC, are for materials B and E.

Materials A and C was produced through hot extrusion, and as the materials have similar TLRR values, this indicates that the microstructure obtained through this production method is less susceptible to HISC. During manufacturing, material A was cold worked. As stated by [25] and [26], cold work decreases a material's resistance towards HISC. This explains the slight difference between the TLRR values for the two materials, along with the difference in austenite spacing measurements. Both materials contain tungsten (W), It has been suggested by the industry that W increases a material's resistance towards HISC. Unfortunately, at the time of this thesis there is no documentation on this matter.

Test material D was manufactured from a forged bar. Forged components are usually considered to have lower resistance towards HISC than materials produced through other methods which achieve finer microstructures. However, this is not seen in the results from the testing conducted in this thesis as material D performs better than the centrifugally cast materials. One possible explanation is that the material contains W, which might have increased the resistance towards HISC, along with finer austenite spacing than the two cast materials. Test material B and E, which have the highest TLRR values, are the two centrifugally cast materials. As the TLRR results are so much higher for these materials than for the other production methods, this indicates a lower resistance towards HISC for materials manufactured this way. Of these two materials, only E contains W. However, as material E has the highest TLRR value this result contradicts the industry's experience with W increasing the resistance towards HISC. On the other hand, there might be some other detrimental effects which have counteracted the positive effect of W in the material, such as the high austenite spacing.

When it comes to the effect of ferrite content on the susceptibility towards HISC, the reported values contradicts the literature as it is material C which have the largest ferrite content at 54%. A higher ferrite content should indicate a lower resistance towards HISC, but it is not the case for these results. Both materials B and D have lower ferrite content values at approximately 49% and have higher TLRR values than material C. However, as for the possible positive effect on susceptibility towards HISC of W in the microstructure, the effects of the ferrite content might have been counteracted by other microstructural features. The finer austenite spacing of material C could be the explanation for why this material performs better than the other two despite having a higher ferrite content.

5.4.2. Yield strength ratio

As seen from Table 4.4 and Figure 4.9, the highest average value for the %YS was found for test material C at 132,20%. As for the TLRR results, this indicates the highest resistance towards hydrogen embrittlement for this material. Material A also has a high %YS value at 122,57%. The fact that these materials have the highest values for this test parameter as well strengthens the indication that the microstructure for extruded pipes has a lower susceptibility towards HISC. As it is material C which again have the higher value of the two extruded pipes, it is further evidence of the cold work performed on material A reducing the resistance towards HISC. Materials B and D have quite similar average values at 116,44% and 115,91%, respectively. Again, material E has the lowest value at 94,40%. This time with quite a large margin. The difference between material E and the other materials is probably due to the larger austenite spacing for this material compared to the others. All of these results correspond reasonably well with the TLRR results, probably due to the same reasons as mentioned in the previous section.

When comparing the UTS/YS values to the %YS values, the extruded materials A and C and the forged material D have high to intermediate results for both test parameters while the centrifugally cast has the lowest results for both parameters. For both UTS/YS and %YS, material C performs slightly better than material A with UTS/YS values of 135,2% and 130,2% and %YS values of 132,2% and 122,57%, respectively. Once again, a possible explanation is the cold deformation performed on material A. Material D, however, performs best of all test materials for %UTS/YS, and has low %YS values. This variation between the two test parameters is most likely due to the large austenite spacing causing the %YS values to decrease more with respect to the UTS/YS value compared to materials A and C with finer austenite spacing. The centrifugally cast materials B and E have the lowest values for both UTS/YS and %YS. However, the large austenite spacing of material E causes a large difference in %YS values (116,44% for B and 94,40% for E) between the two materials despite the approximately equal UTS/YS values of 128,6% for B and 128,7% for E. Also for this test parameter, the large austenite spacing of material E seems to contradict the experience with W contributing positively to HISC resistance.

5.4.3. Reduction in area ratio

From the results presented in Figure 2.12, material D has the lowest RA ratio value by a large margin. The value is 11,17%. However, this result is not valid as the smallest cross-section measured for the reference specimen was so high due to the specimen's not fracturing. Thus, the RA ratio result for this material is excluded from the discussion below.

When excluding material D, it is material C which has the lowest RA ratio at 74,30%. As a low RA ratio indicates a lower level of embrittlement, this result indicates that material C has a greater resistance towards HISC. However, the standard deviation for this material is very high (21,21). One explanation for this might be the fact that only two specimens were tested for this material. On the other hand, the standard deviation is so much higher than for the other materials that this cannot be the sole reason. For materials A, B and E, the RA ratios increase by approximately 6% for each material, with material A having the lowest of the three at 80,14%. Again, the general trend of the results is the same as for the previous test parameters with centrifugally cast materials B and E showing the poorest performance with respect to resistance towards HISC.

5.5. Hydrogen Content

The hydrogen measurements provided in Figure 4.11 and Table 4.6 show that test material C has the highest hydrogen content of 82,17ppm after pre-charging and HISC testing, while test material D has the lowest hydrogen content at 48,98ppm. The intermediate results are materials B, A and E with hydrogen contents of 67,58ppm, 60,06ppm and 50,40ppm, respectively. The hydrogen contents of materials D and E are very similar with only a 0,42ppm difference. Due to the fact that the testing for hydrogen content was only performed after HISC testing was finished, it is impossible to distinguish between hydrogen absorbed during pre-charging and during the HISC testing in the Cortest proof rings. However, as hydrogen diffuses more rapidly at higher temperatures per Equation 2.12, it may be assumed that the majority of the hydrogen diffused into the material during pre-charging as this was performed at an elevated temperature, whereas the HISC testing was performed at ambient temperatures. However, most of the test specimens spent more time in the Cortest proof rings than they did during pre-charging. The time difference varied for the materials and each polarised specimen, but an average estimate is 2,5 weeks in the rings compared to 10 days in the pre-charging cell. To ascertain which step causes the most hydrogen to diffuse into the materials, hydrogen testing should be performed directly after pre-charging as well as after the HISC testing.

The ferrite content provided for materials B, C and D compared to the measured hydrogen content is in accordance with the literature [15, 16] as the material with the largest ferrite content (C) also has the largest hydrogen content. The opposite holds true for material D; it has the smallest measured ferrite and hydrogen contents. Unfortunately, a general trend for all test materials cannot be determined due to the lack of ferrite content values for materials A and E. However, the literature also [17] suggests that materials with coarser microstructures should absorb more hydrogen due to less tortuous hydrogen paths caused by a larger austenite spacing. This causes more absorption points on the surface and more continuous hydrogen diffusion in the ferrite phase. The results of the hydrogen measurements in this thesis contradicts this, as the general trend is that the test materials with the largest austenite spacing (D, E) contains the least hydrogen, and those with the finest austenite spacing (C) contains the most. This might be due to the ferrite content counteracting the positive effect of the austenite spacing. In addition, there are other factors that might cause this discrepancy between the results and literature. In general, the materials with the largest austenite spacing tended to fracture during or directly after loading from the threshold load to fracture load, while the materials with finer austenite spacing tended to fracture some time after loading. This resulted in the test specimens in the former category being moved from the Cortest proof rings to the freezer closer to the time of fracture than the latter as the specimens were not under constant observation during testing. Upon fracture, the electrical circuit was broken, and thus the hydrogen in the materials with finer microstructures had more time to diffuse out of these materials.

5.6. Fractography

5.6.1. Fracture surface examniation

As shown in the previous chapter, the reference specimens for all test materials exhibited ductile fracture characteristics. Deformation is visible close to the fracture surface, and all surfaces contained a dimpled structure over the entire cross-section. However, the reference specimen for material E also contained some fracture characteristics similar to cleavages in the center of the fracture surface as seen in Figure 4.20c. This might be due to this material having a coarser structure, and therefore a smaller degree of ductility than the other materials. The ductility of the materials prior to hydrogen exposure is also evident in the tensile testing, as the stress-strain curves drop after reaching UTS. This can be seen in Figures 5 to 9 in Appendix A. From these figures, it is evident that the drop is smaller for test material E, further confirming the poorer mechanical properties for this material. For the polarised specimens the fracture surfaces were quite different from the reference specimens. The most prominent difference was the change in fracture surface characteristics along the cross-section. With one exception, namely specimen 2 for test material C (Figure 4.18c), all polarised specimens exhibit both ductile and brittle fracture characteristics in different areas of the surface, with the brittle characteristics most often close to the edge of the fracture surface. The ductile areas can be found both close to the center of the fracture surface, as in Figure 4.19a, and close to the edge, as in Figure 4.22a. As material C has the lowest austenite spacing and the previous test parameters discussed indicates this material having a high resistance towards HISC, this might be the explanation for the mixed fracture characteristics over most of the fracture surface of the mentioned polarised specimen.

In the transition zone between the brittle and ductile areas, the surface characteristics was more mixed. For the previously mentioned specimen from material C, almost the entire fracture surface exhibits such mixed characteristics. One hypothesis is that for these areas, the austenite phase fractured through a more ductile mechanism and therefore a dimpled fracture surface [16]. Conversely, the ferrite would fracture through a more brittle mode, causing more brittle fracture characteristics. To investigate the validity of this hypothesis, a more comprehensive characterisation of the transition zones should be conducted than was within the scope of this thesis.

5.6.2. Brittle Area Estimation

It should be noted that the measurements for calculating the brittle area may not be accurate as they were obtained essentially by hand, and the exact point where the fracture surface transitioned from brittle to ductile was difficult to establish due to the mixed characteristics transition zone. However, the results of the measurements are presented as an estimate, and used as an estimated embrittlement index to investigate possible differences in embrittlement through the thickness of the test specimens.

Although the fracture surfaces for all the test materials exhibited similar fracture characteristics, there were small differences in the size of the embrittled areas, as presented in the "Results" chapter. The maximum estimated value for the brittle area was found for test material E, while the minimum value was found for material A. These values were 77,58% and 54,38%, respectively. When comparing these results with the results from the threshold load reduction ratio, they correspond somewhat. Material A has the lowest brittle/ductile area ratio, and also a low TLRR value. The same holds true for materials C and D; they both have low TLRR and %DB values. Likewise can it be observed that materials B and E have the highest values for both test parameters. This further supports the theory of hot extruded pipes having the highest resistance towards HISC and centrifugally cast pipes being more susceptible to this fracture mode.

5.6.3. Secondary cracking

The SEM images of the surface area on the side of the polarised specimens in Figures 4.25 to 4.29 show that secondary cracking has occurred for all test materials. The presence of secondary cracking along with the documented presence of hydrogen is indicative of HISC taking place in the material. Also, it means that HISC initiation has taken place on multiple points on the specimen, not only for the crack responsible for fracture of the test specimen.

5.7. Overall Test Results

The objective of this thesis was to investigate the difference in susceptibility towards HISC between the test materials provided by GE Oil & Gas. To be able to test a material's performance with respect to HISC, hydrogen must be present in the microstructure. This was achieved through the pre-charging and polarisation during HISC testing, as hydrogen was found in the material when employing the melt extraction technique. Together with the secondary cracking observed on the surfaces of the test specimens, this confirms that HISC has occurred in the materials investigated in this thesis. From the other test results obtained in this work, there is a clear trend in the resistance towards HISC between the different production methods of 25%Cr SDSS materials.

Table 5.1: Ranking of test results from best to worst with respect to HISC.

Test parameter	Test material Ranking
AYS	A - D - E - C - B
UTS/YS	D - C - A - E - B
Austenite spacing	C - B - A - D - E
TLRR	C - D - A - B - E
%YS	C - A - D - B - E
RA ratio	C - A - B - E
%DB	A - D - C - B - E
H	C - B - A - E - D

A summary of the results is provided in Table 5.1. From the rankings in the table it is clear that the materials which performed best overall with respect to resistance towards HISC are the hot extruded materials A and C, with C tending to have slightly better results. As previously mentioned, the most likely explanation for this difference is the cold work performed on material A.

When it comes to material D, which was manufactured from a forged bar, the results of the tests are very varied; however, the general trend is intermediate results with respect to the susceptibility towards HISC. Also evident from Table 5.1 is the poor performance of the centrifugally cast materials B and E. For most test parameters, these materials have the worst performance with respect to HISC. It is clear that the microstructure achieved through this production method is not optimal when exposed to CP in seawater. This is most likely closely related to the large austenite spacing found for these materials.

5.7.1. Further work

For more definitive conclusions for the investigation executed in this thesis, some further work should be conducted. For the tensile testing, the strain at fracture should be documented and discussed in relation to the HISC results. When it comes to the microstructures obtained through the different production methods, some additional testing should be done with respect to the presence and effect of secondary phases. One such test could be EDX analysis of the microstructures to confirm or refute the presence of secondary phases in the microstructures. Additional testing should also include measuring of the ferrite content as this was not reported for all test materials, and thus only a preliminary investigation could be conducted based on the values reported for materials B, C and D.

The possible positive effect of the alloying element W should also be investigated and reported on as there is no documentation on this subject at present. This could be achieved through HISC testing of materials with identical chemical composition apart from varying amounts of W. As for the austenite spacing, a method for measurement producing smaller standard deviations and thus %RA values should be employed. One possibility is to use software when conducting the measurements and determine specific limits for the size of small, bimodal austenite grains to be disregarded due to their not contributing to the trapping of hydrogen.

Pertaining to the HISC testing equipment, this was prone to relaxation, making it difficult to distinguish between relaxation of the rings and low temperature creep. To avoid this in future investigations, constant load testing using Cortest proof rings could be replaced with SSRT. This would most likely remove the relaxation aspect of the testing. In addition, the equipment should not have an upper limit for allowable elongation as the Cortest proof rings have, which resulted in the reference specimen for material D not going to fracture during testing. In addition, the electrical set-up during HISC testing should be such that the electrical circuit is not broken upon fracture of the specimen as it was for this thesis. This would result in more accurate hydrogen measurements. When it comes to hydrogen measurements, this should be performed both after pre-charging and HISC testing to be able to distinguish the hydrogen absorption during the two steps.

Additional characterisation of the transition zone found on the fracture surfaces should also be conducted to better understand the HSIC fracture mechanism. This would also enable more accuracy when indexing the embrittlement through thickness of the specimens.

6. Conclusion

Stepwise increased load testing was performed to investigate the difference in susceptibility to HISC for five 25%Cr SDSS materials obtained through different production routes. This was followed by an analysis of the fracture surfaces and measurement of hydrogen content. The microstructures were also examined using optical microscopy to document the microstructures resulting from the different production methods.

Based on the testing conducted for the materials in this thesis, the production method for 25% Cr SDSS giving the highest resistance towards HISC is hot extrusion, i.e. the materials supplied to GE Oil & Gas from Nippon Steel & Sumitomo Metal Co. and Tubacex Tubos Inoxidables S.A. This is due to the superior performance for most of the test parameters, which most likely is the result of the fine microstructure with a low degree of bimodal austenite grains and low austenite spacing values. It was also found that subsequent cold working of an extruded pipe increases the susceptibility towards HISC slightly.

Intermediate test results were obtained for the pipe from IBF S.P.A. which was manufactured from a forged bar. The highest susceptibility towards HISC was found for the centrifugally cast materials from Fondinox S.P.S. and Kuhn Special Steel. This result is attributed to the large austenite spacing and high degree of bimodal austenite grains present in the structure as bimodal austenite reduces the amount of austenite contributing to hydrogen trapping, increasing the free diffusion paths for hydrogen through the material.

References

[1] Sytze Huizinga et al. "Failure of a subsea super duplex manifold hub by HISC and implications for design". In: *CORROSION 2006*. NACE International. 2006.

[2] J Ćwiek. "Prevention methods against hydrogen degradation of steel". In: *Journal of Achievements in Materials and Manufacturing Engineering* 43.1 (2010), pp. 214–221.

[3] V. Olden, C. Thaulow, and R. Johnsen. "Modelling of hydrogen diffusion and hydrogen induced cracking in supermartensitic and duplex stainless steels". In: *Materials Design* 29.10 (2008), pp. 1934–1948.

[4] Mustafa Kemal Nisancioglu. "Corrosion Basics and Engineering". In: *Lecture Notes, Institutt for Teknisk Elektrokjemi, NTNU* (2015).

[5] David Buxton, David Gareth John, et al. "Cathodic Protection system life assessment". In: *SPE International Oilfield Corrosion Conference*. Society of Petroleum Engineers. 2008.

[6] Det Norske Veritas. "Cathodic protection design". In: *Recommended Practice DNV-RP-B401* (2005).

[7] Karl Gunnar Solheim and Jan Ketil Solberg. "Hydrogen induced stress cracking in supermartensitic stainless steels–Stress threshold for coarse grained HAZ". In: *Engineering Failure Analysis* 32 (2013), pp. 348–359.

[8] Ernest Klechka, Steven F Daily, Kevin C Garrity, et al. "Practical considerations for upper limits of cathodic protection". In: *CORROSION 2007*. NACE International. 2007.

[9] William D Callister and David G Rethwisch. "Materials Science and Engineering SI Version,-8/E." In: (2011).

[10] Shyan-Liang Chou and Wen-Ta Tsai. "Effect of grain size on the hydrogen-assisted cracking in duplex stainless steels". In: *Materials science and engineering: A* 270.2 (1999), pp. 219–224.

[11] Harry Bhadeshia and Robert Honeycombe. *Steels: microstructure and properties*. Butterworth-Heinemann, 2017.

[12] Henrik Asteman, Dietlinde Jakobi, et al. "A New Cast Alloy with High Strength and Excellent Corrosion Resistance–An Alternative to the Conventional Ni-base Alloys". In: *CORROSION 2015*. NACE International. 2015.

[13] S et. al. Venkatamaran. “Development of Centrifugally Cast 22% Cr Duplex Steel for Line Pipe”. In: *CORROSION 2014*. Vol. 4107. NACE International. 2007.

[14] K.H. Brensing and Baldur Sommer. “Steel Tube and Pipe Manufacturing Processes”. In: *Salzgitter Mannesmann Rohrenwerke* ().

[15] Thierry Cassagne, Freddy Embrittlement, et al. “A review on hydrogen embrittlement of duplex stainless steels”. In: *CORROSION 2005*. NACE International. 2005.

[16] Vigdis Olden et al. “Influence of hydrogen from cathodic protection on the fracture susceptibility of 25% Cr duplex stainless steel–Constant load SENT testing and FE-modelling using hydrogen influenced cohesive zone elements”. In: *Engineering Fracture Mechanics* 76.7 (2009), pp. 827–844.

[17] Gro Østensen Lauvstad et al. “Improved Resistance Towards Hydrogen Induced Stress Cracking (HISC) Of Hot Isostatically Pressed (HIP) Duplex Stainless Steels Under Cathodic Protection”. In: *CORROSION 2007*. NACE International. 2007.

[18] P Woollin and A Gregori. “Avoiding hydrogen embrittlement stress cracking of ferritic austenitic stainless steels under cathodic protection”. In: *ASME 2004 23rd International Conference on Offshore Mechanics and Arctic Engineering*. American Society of Mechanical Engineers. 2004, pp. 777–784.

[19] Jarle Hjelen. *Scanning elektron-mikroskopi*. SINTEF, Department of metallurgy and NTH, 1986.

[20] Mads Aursand et al. “Experiences with hydrogen induced stress cracking of duplex stainless steel components in subsea service with cathodic protection”. In: *CORROSION 2013*. NACE International. 2013.

[21] B.R.S. da Silva, F. Salvio, and D.S. dos Santos. “Hydrogen induced stress cracking in UNS S32750 super duplex stainless steel tube weld joint”. In: *International Journal of Hydrogen Energy* 40.47 (2015). Special issue on 1st International Conference on Hydrogen Storage, Embrittlement and Applications (Hy-SEA 2014), 26-30 October 2014, Rio de Janeiro, Brazil, pp. 17091–17101.

[22] Mobbassar Hassan Sk, Ruel A. Overfelt, and Aboubakr M. Abdullah. “Effects of microstructures on hydrogen induced cracking of electrochemically hydrogenated double notched tensile sample of 4340 steel”. In: *Materials Science and Engineering: A* 659 (2016), pp. 242–255.

[23] S.P. Lynch. “Pogress towards understanding mechanisms of hydrogen embrittlement and stress corrosion cracking”. In: *CORROSION 2007*. Vol. 07493. NACE International. 2007.

[24] P. Craidy, L. Briottet, and D. Santos. “Hydrogen–Microstructure–Mechanical properties interactions in super duplex stainless steel components”. In: *International Journal of Hydrogen Energy* 40.47 (2015). Special issue on 1st International Conference on Hydrogen Storage, Embrittlement and Applications (Hy-SEA 2014), 26-30 October 2014, Rio de Janeiro, Brazil, pp. 17084–17090.

[25] A. M. Elhoud, N. C. Renton, and W. F. Deans. “The effect of manufacturing variables on the corrosion resistance of a super duplex stainless steel”. In: *The International Journal of Advanced Manufacturing Technology* 52.5 (2011), pp. 451–461.

[26] Dilson Silva dos Santos et al. “On the Role of HISC on Super and Hyper Duplex Stainless Steel Tubes”. In: *OTC Brasil*. Offshore Technology Conference. 2013.

[27] Cem Oernek and Dirk L Engelberg. “Correlative EBSD and SKPFM characterisation of microstructure development to assist determination of corrosion propensity in grade 2205 duplex stainless steel”. In: *Journal of materials science* 51.4 (2016), pp. 1931–1948.

[28] Det Norske Veritas. “Design of duplex stainless steel subsea equipment exposed to cathodic protection”. In: *Recommended Practice DNV-RP-F112* (2008).

[29] ASTM Standard. “E112: Standard Test Methods for Determining Average Grain Size”. In: *West Conshocken* (1996).

[30] Ulf Kivisäkk. “Relation of room temperature creep and microhardness to microstructure and HISC”. In: *Materials Science and Engineering: A* 527.29 (2010), pp. 7684–7688.

[31] T. Zakroczymski, A. Glowacka, and W. Swiatnicki. “Effect of hydrogen concentration on the embrittlement of a duplex stainless steel”. In: *Corrosion Science* 47.6 (2005), pp. 1403–1414.

[32] Keh Chyn Ou and Jiann Kuo Wu. “Effect of calcareous deposits formation on the hydrogen absorption of steel”. In: *Materials Chemistry and Physics* 48.1 (1997), pp. 52–55.

[33] TS Taylor, T Pendlington, R Bird, et al. “Foinaven super duplex materials cracking investigation”. In: *Offshore Technology Conference*. Offshore Technology Conference. 1999.

[34] Yanjun Li. “Optical microscopy”. In: *Lecture note, NTNU* (2016).

[35] M. Aursand. “Technical note - Metallographic etching of duplex stainless steels”. In: *Statoil Document no. MAT-2010080* (2010), pp. 1–16.

[36] Kjetil Andersen. "HISC in Super Duplex Stainless Steels: A study of the relation between microstructure and susceptibility to hydrogen induced stress cracking". MA thesis. Institutt for materialteknologi, 2013.

[37] NACE Standard TM0177. "Laboratory testing of metals for resistance to sulfide stress cracking and stress corrosion cracking in H2S environments". In: *Houston, TX: NACE* (2005).

[38] ASTM F1624-12. "Standard Test Method for Measurement of Hydrogen Embrittlement Threshold in Steel by the Incremental Step Loading Technique". In: *ASTM International West Conshohocken* (2012).

Appendix A

Test Specimen Locations

Below, the test specimen locations for all materials are provided in Figures 1 to 4 with the exception of material A. The test specimens for material A were removed from the pipe material prior to work on this thesis began, and an image of the test specimens in the pipe material was therefore not acquired.

Figure 1: Image of the test specimen location for material B.

Figure 2: Image of the test specimen location for material C.

Figure 3: Image of the test specimen location for material D.

Figure 4: Image of the test specimen location for material E.

Appendix B

Stress-strain Curves

Figures 5 to 9 show the stress-strain curves obtained through tensile testing of materials A to E, respectively.

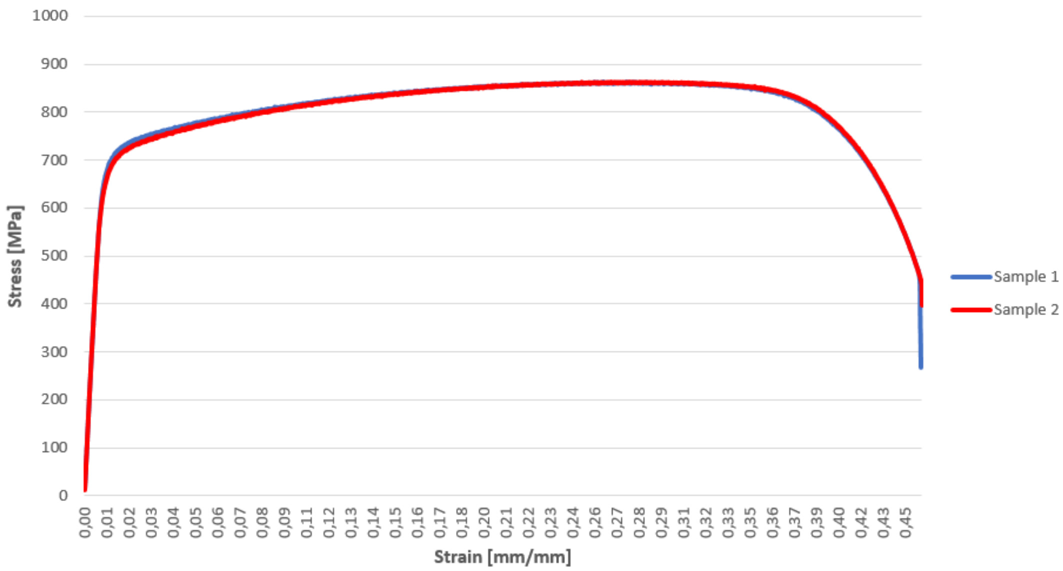

Figure 5: Stress-strain curve from tensile testing of material A.

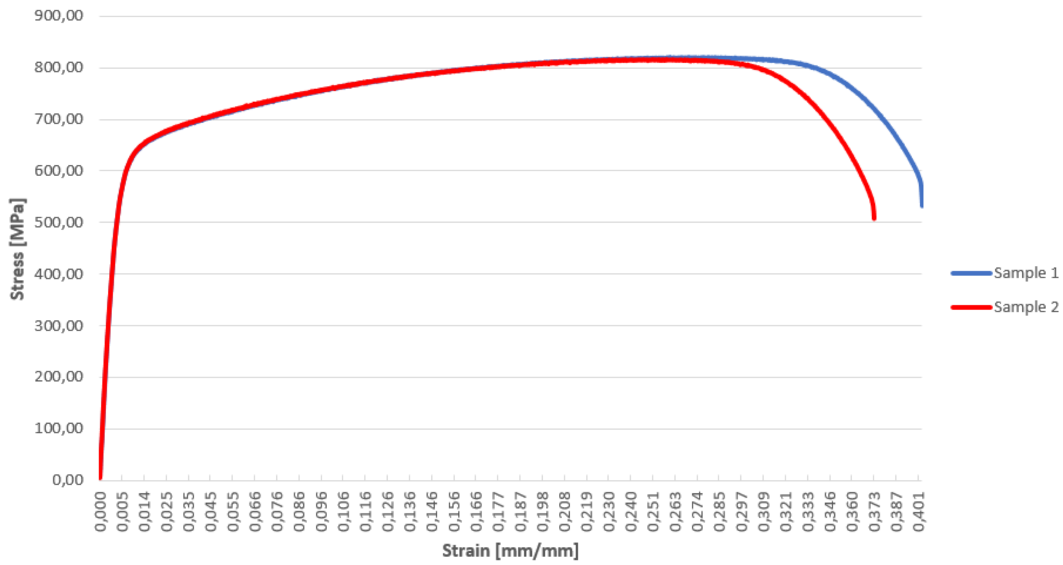

Figure 6: Stress-strain curve from tensile testing of material B.

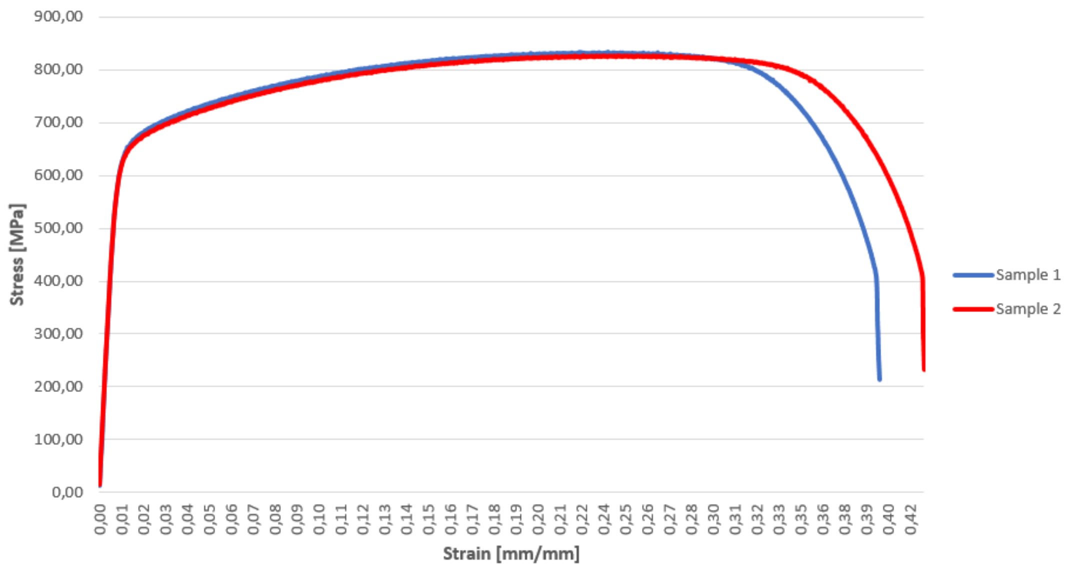

Figure 7: Stress-strain curve from tensile testing of material C.

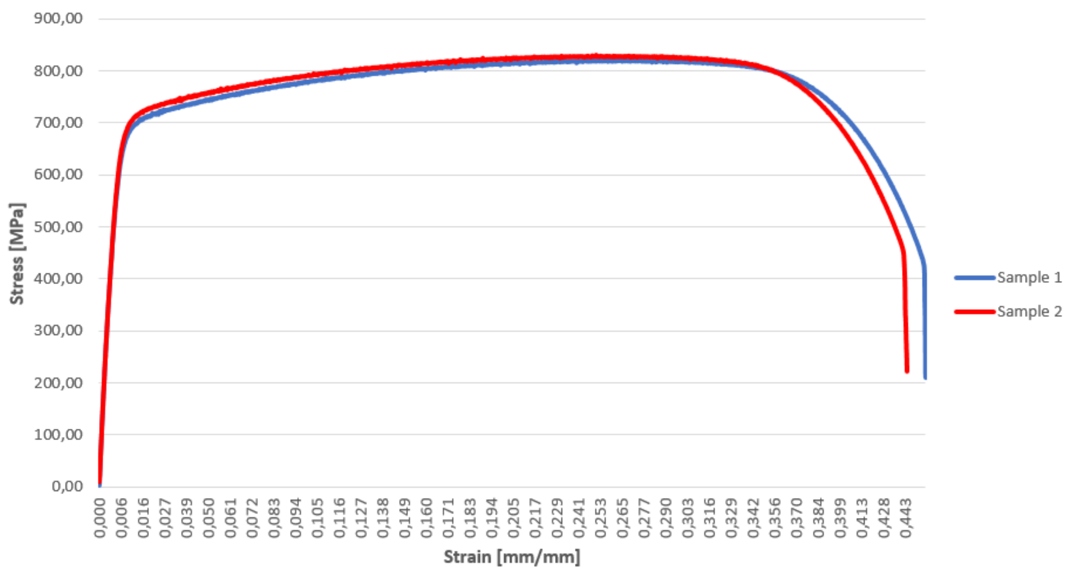

Figure 8: Stress-strain curve from tensile testing of material D.

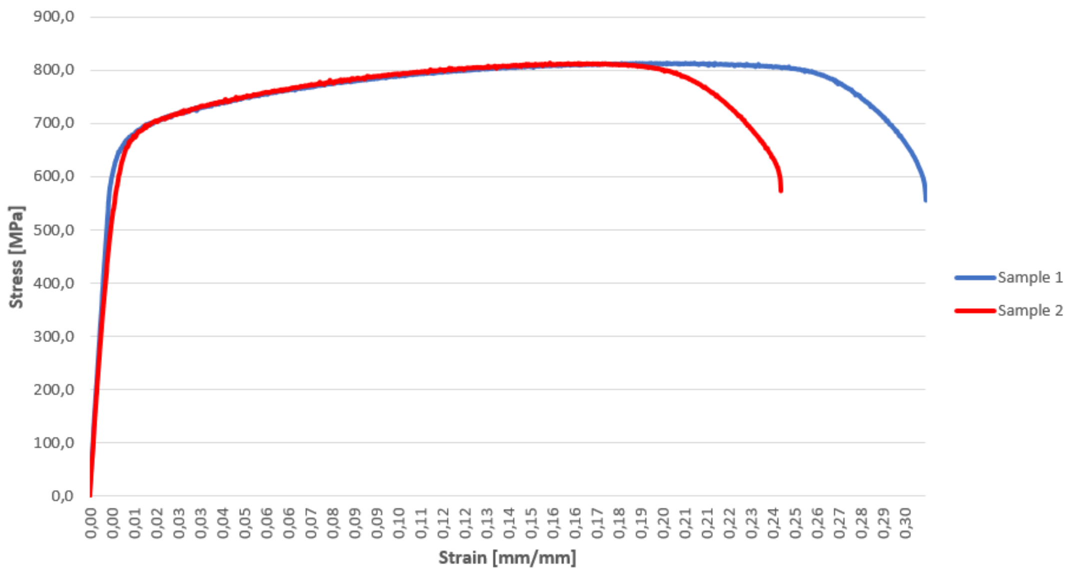

Figure 9: Stress-strain curve from tensile testing of material E.

Appendix C

Austenite Spacing Measurements

Material A

Table 1: Austenite spacing measurements for test material A

Material A				
	Area 1	Area 2	Area 3	Area 4
Mean	27,67	30,40	27,20	23,24
Min	7,22	5,15	2,06	1,03
Max	119,59	138,14	140,21	114,43
Sum	3292,49	4893,70	5249,55	4322,42
SD	21,02	22,19	20,59	19,05
Mean	**27,13**			
SD material	**20,71**			
n	20,00			
t	2,09			
95%CI	**9,69**			
%RA	**35,74**			

Material B

Table 2: Austenite spacing measurements for test material B.

Material B				
	Area 1	Area 2	Area 3	Area 4
Mean	25,67	24,38	28,68	27,92
Min	2,06	2,06	5,15	7,22
Max	156,70	128,87	121,65	89,69
Sum	3337,73	2462,29	3326,57	3797,77
SD	22,45	18,62	25,72	18,76
Mean	**26,66**			
SD material	**21,39**			
n	20,00			
t	2,09			
95%CI	**10,01**			
%RA	**37,54**			

Material C

Table 3: Austenite spacing measurements for test material B.

Material C				
	Area 1	Area 2	Area 3	Area 4
Mean	26,852	23,096	25,171	24,695
Min	7,216	7,505	8,247	7,216
Max	160,825	72,165	84,561	82,474
Sum	3222,199	2748,452	3423,242	3654,794
SD	19,102	11,686	14,527	13,828
Mean	**24,95**			
SD material	**14,786**			
n	20,00			
t	2,09			
95%CI	**6,92**			
%RA	**27,73**			

Material D

Table 4: Austenite spacing measurements for test material D.

Material D				
	Area 1	Area 2	Area 3	Area 4
Mean	51,21	46,95	49,38	42,42
Min	7,22	6,19	7,22	6,19
Max	245,37	207,23	249,48	161,87
Sum	5991,76	5680,51	5530,13	4920,53
SD	41,96	39,86	39,52	32,85
Mean	**47,49**			
SD material	**38,55**			
n	20,00			
t	2,09			
95%CI	**18,04**			
%RA	**37,99**			

Material E

Table 5: Austenite spacing measurements for test material E.

Material E				
	Area 1	Area 2	Area 3	Area 4
Mean	44,08	49,87	68,09	43,40
Min	5,15	5,15	7,22	1,03
Max	252,58	271,14	1575,26	158,78
Sum	5818,80	5236,31	5514,97	3341,89
SD	38,98	43,57	174,39	31,91
Mean	**51,36**			
SD material	**72,21**			
n	20,00			
t	2,09			
95%CI	**33,80**			
%RA	**65,80**			

Appendix D

HISC testing Calculations

Threshold Load Reduction Rate Calculation

In this section, the calculations of the TLRR values are presented in Tables 6 to 10. As explained in the chapter on experimental methods the loads obtained by using the load cell, P_{th}, is inserted into Equation 3.3, and the σ_{th} and $\sigma_{th,HISC}$ values are obtained, respectively. The TLRR values are then obtained by inserting the results from Equation 3.3 into Equation 3.4

Material A

Table 6: Calculation of TLRR values for material A.

Sample condition	d_0 [mm]	A_0 [mm^2]	P_{th} [kg]	σ_{th} [Mpa]	TLRR [%]
Reference	3,765	11,13	1043	920	
				$\sigma_{th,HISC}$ [Mpa]	
Polarised	3,765	11,13	897	791	14,0
Polarised	3,765	11,13	939	828	10,0
Polarised	3,765	11,13	933	823	10,5

Material B

Table 7: Calculation of TLRR values for material B.

Sample condition	d_0 [mm]	A_0 [mm^2]	P_{th} [kg]	σ_{th} [Mpa]	TLRR [%]
Reference	3,75	11,01	975	869	
				$\sigma_{th,HISC}$ [Mpa]	
Polarised	3,75	11,01	742	661	23,90
Polarised	3,75	11,01	727	648	25,44
Polarised	3,75	11,01	770	686	21,03

Material C

Table 8: Calculation of TLRR values for material C.

Sample condition	d_0 [mm]	A_0 [mm^2]	P_{th} [kg]	σ_{th} [Mpa]	TLRR [%]
Reference	3,745	11,01	990	882,1	
				$\sigma_{th,HISC}$ [Mpa]	
Polarised	3,745	11,01	920	819,8	7,07
Polarised	3,745	11,01	902	803,7	8,89

Material D

Table 9: Calculation of TLRR values for material D.

Sample condition	d_0 [mm]	A_0 [mm^2]	P_{th} [kg]	σ_{th} [Mpa]	TLRR [%]
Reference	3,75	11,01	932	830	
				$\sigma_{th,HISC}$ [Mpa]	
Polarised	3,74	10,98	883	789	5,00
Polarised	3,75	11,01	802	715	13,95
Polarised	3,76	11,10	826	730	12,08

Material E

Table 10: Calculation of TLRR values for material E.

Sample condition	d_0 [mm]	A_0 [mm^2]	P_{th} [kg]	σ_{th} [Mpa]	TLRR [%]
Reference	3,76	11,10	915	809	
				$\sigma_{th,HISC}$ [Mpa]	
Polarised	3,77	11,16	651	572	29,2
Polarised	3,75	11,04	693	616	23,9
Polarised	3,76	11,10	684	605	25,2

Reduction of Area Calculations

In this section, the results of the RA calculations are presented for all test specimens in the tables below. The diameters are measured values for each test specimen. The areas are obtained from the diameter measurements and used for further calculations of the RA value for each test specimen using Equation 3.6. The results from Equation 3.6 were then used in Equation 3.7 to find the RA ratios for each test material presented in the "Results" chapter. The average d_{min}, A_{min} and RA values reported in this section is the average of polarised samples only, as these values are compared to the reference sample in further calculations. It should also be noted that the RA results is presented as percentages in this appendix, while the fraction is used in Equation 3.6.

Material A

Table 11: Calculations of areas used for obtaining the RA for material A.

Sample	d_0 [mm]	A_0 [mm^2]
Reference	3,77	11,157
Polarised 1	3,76	11,098
Polarised 2		0,000
Polarised 3		0,000
Average	3,765	11,128
Sample	d_{min} [mm]	A_{min} [mm^2]
Reference	2,04	3,267
Polarised 1	3,57	10,005
Polarised 2	3,52	9,726
Polarised 3	3,38	8,968
Average	3,49	9,561

In Table 11, only two original diameters are reported as the measurements for the other two test specimens were done incorrectly. Therefore, the average value of the two diameters reported was used for further calculations.

Table 12: Calculated RA values for test specimens from material A.

Sample	RA [%]
Reference	70,642
Polarised 1	10,090
Polarised 2	12,591
Polarised 3	19,406
Average	14,029

Material B

Table 13: Calculations of areas used for obtaining the RA for material B.

Sample	d_0 [mm]	A_0 [mm^2]
Reference	3,74	10,98
Polarised 1	3,75	11,04
Polarised 2		
Polarised 3		
Average	3,745	11,01
Sample	d_{min} [mm]	A_{min} [mm^2]
Reference	2,16	3,66
Polarised 1	3,57	10,00
Polarised 2	3,56	9,95
Polarised 3	3,58	10,06
Average	3,57	10,00

In Table 13, only two original diameters are reported as the measurements for the other two test specimens were done incorrectly. Therefore, the average value of the two diameters reported was used for further calculations.

Table 14: Calculated RA values for test specimens from material B.

Sample	RA [%]
Reference	66,73
Polarised 1	9,13
Polarised 2	9,64
Polarised 3	8,62
Average	9,13

Material C

Table 15: Calculations of areas used for obtaining the RA for material C.

Sample	d_0 [mm]	A_0 [mm^2]
Reference	3,74	10,980
Polarised 1	3,75	11,039
Polarised 2	3,75	11,039
Average	3,75	11,019
Sample	d_{min} [mm]	A_{min} [mm^2]
Reference	2,31	4,189
Polarised 1	3,62	10,287
Polarised 2	3,24	8,241
Average	3,43	9,264

Table 16: Calculated RA values for test specimens from material C.

Sample	RA [%]
Reference	62,0
Polarised 1	6,6
Polarised 2	25,2
Average	15,9

Material D

Table 17: Calculations of areas used for obtaining the RA for material D.

Sample	d_0 [mm]	A_0 [mm^2]
Reference	3,75	11,04
Polarised 1	3,74	10,98
Polarised 2	3,75	11,04
Polarised 3	3,76	11,10
Average	3,745	22,08
Sample	d_{min} [mm]	A_{min} [mm^2]
Reference	3,28	8,45
Polarised 1	3,58	10,06
Polarised 2	3,59	10,12
Polarised 3	3,52	9,73
Average	3,56	9,97

Table 18: Calculated RA values for test specimens from material D.

Sample	RA [%]
Reference	61,75
Polarised 1	54,43
Polarised 2	54,18
Polarised 3	55,95
Average	55,0

Material E

Table 19: Calculations of areas used for obtaining the RA for material E.

Sample	d_0 [mm]	A_0 [mm$\hat{2}$]
Reference	3,76	11,098
Polarised 1	3,77	11,157
Polarised 2	3,75	11,039
Polarised 3	3,76	11,098
Average	3,765	11,128
Sample	d_{min} [mm]	A_{min} [mm$\hat{2}$]
Reference	2,37	4,409
Polarised 1	3,7	10,747
Polarised 2	3,63	10,344
Polarised 3	3,72	10,863
Average	3,68	10,650

Table 20: Calculated RA values for test specimens from material E.

Sample	RA [%]
Reference	60,4
Polarised 1	3,4
Polarised 2	7,0
Polarised 3	2,4
Average	4,3

Appendix E

Brittle Area Measurements

Measured Radii of brittle areas

Figures 10 to 14 show the brittle area measurements obtained using SEM. Tables 21 to 25 provide the measured radii of the brittle areas of the fracture surface for test materials A to E, respectively.

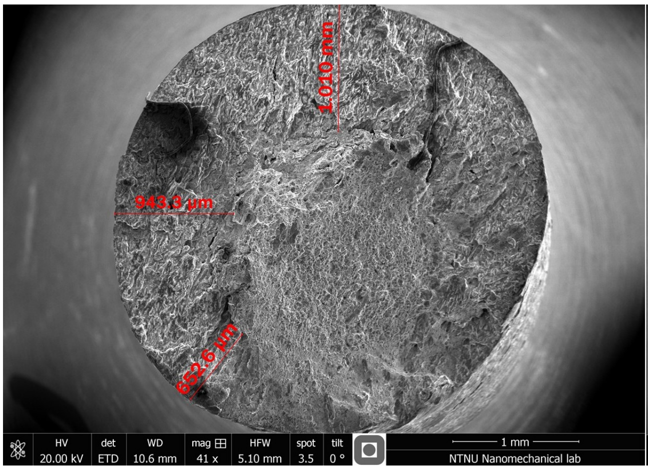

(a) Brittle area measurement for polarised sample 1.

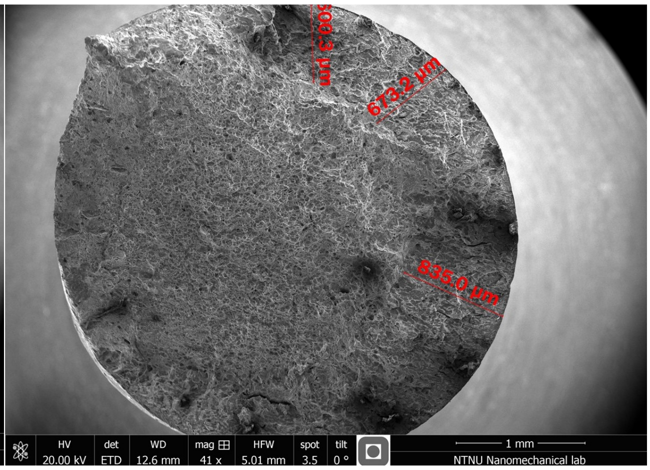

(b) Brittle area measurement for polarised sample 2.

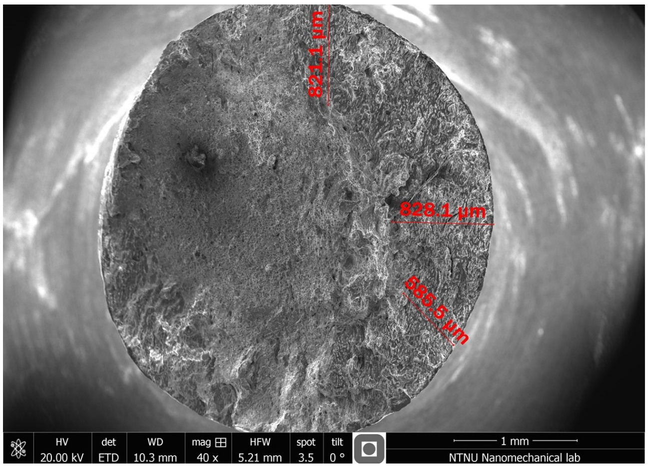

(c) Brittle area measurement for polarised sample 3.

Figure 10: Brittle area measurements for material A.

Table 21: Length of the brittle areas of the fracture surfaces for test material A in μm.

Measurem. no.	Sample 1	Sample 2	Sample 3
1	652.6	600.3	821.1
2	943.3	673.2	828.1
3	1010	835.0	585.5
Ave.	868.6	702.8	744.9

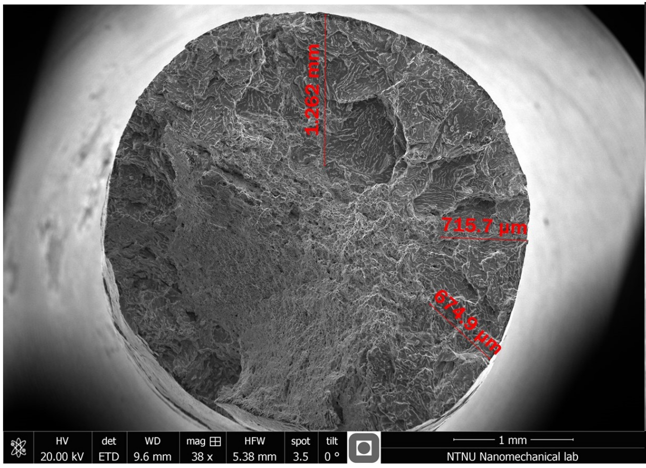

(a) Brittle area measurement for polarised sample 1.

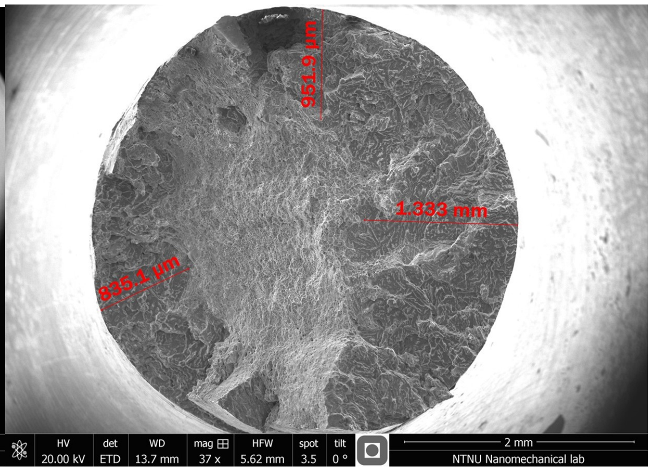

(b) Brittle area measurement for polarised sample 2.

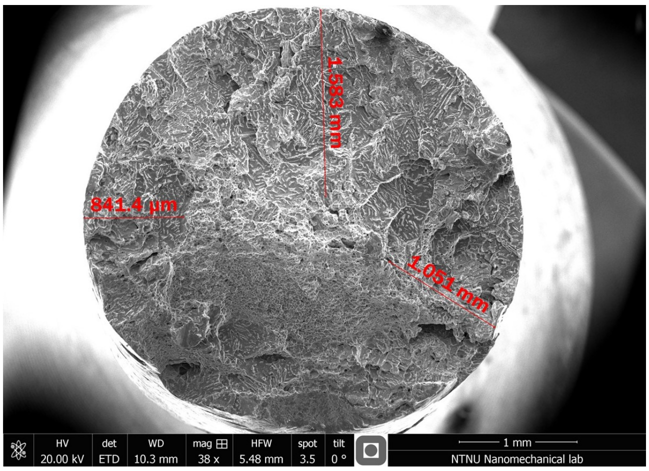

(c) Brittle area measurement for polarised sample 3.

Figure 11: Brittle area measurements for material B.

Table 22: Length of the brittle areas of the fracture surfaces for test material B in μm.

Measurem. no	Sample 1	Sample 2	Sample 3
1	1262	835.1	841.4
2	715.7	951.9	1583
3	674.9	1333	1051
Ave.	884.2	1040	1158.5

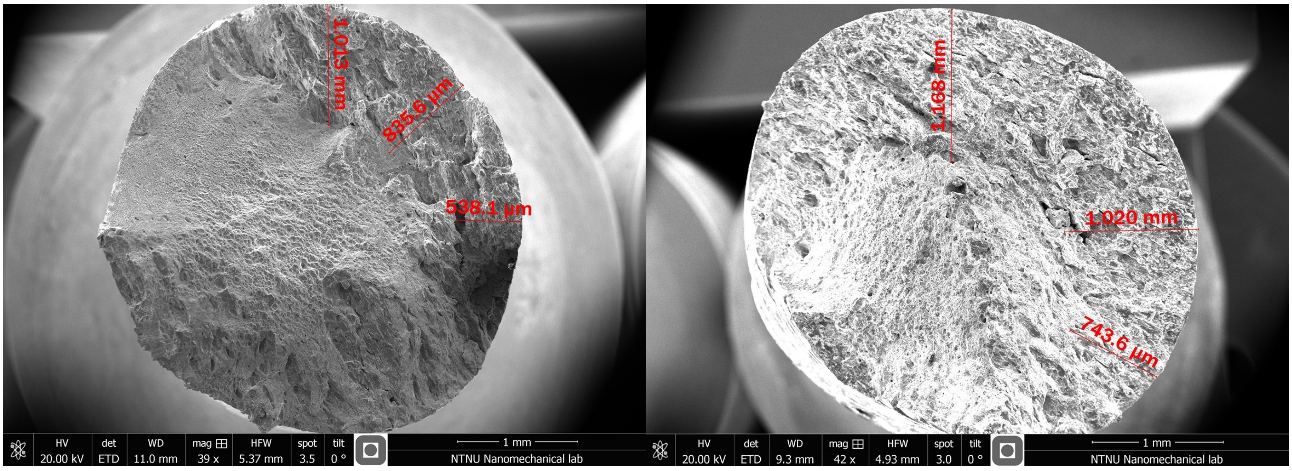

(a) Brittle area measurement for polarised sample 1.

(b) Brittle area measurement for polarised sample 2.

Figure 12: Brittle area measurements for material C.

Table 23: Length of the brittle areas of the fracture surfaces for test material C in μm.

Measurem. no.	Sample 1	Sample 2
1	1013	1168
2	835.6	1020
3	538.1	743.6
Ave.	795.6	977.2

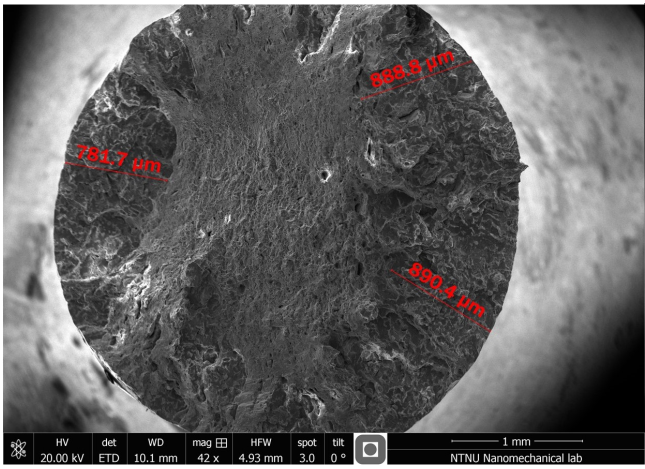

(a) Brittle area measurement for polarised sample 1.

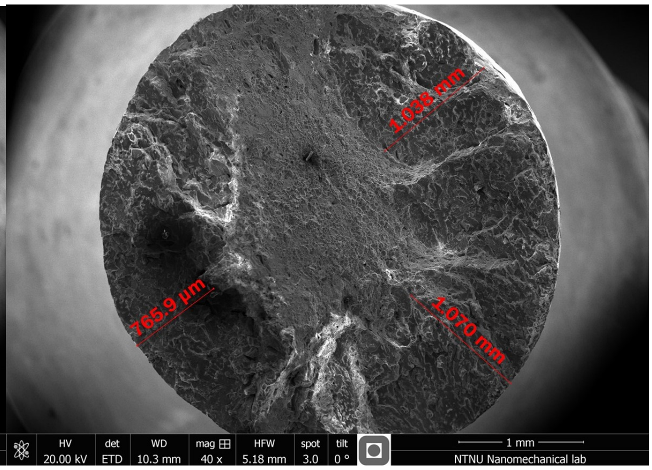

(b) Brittle area measurement for polarised sample 2.

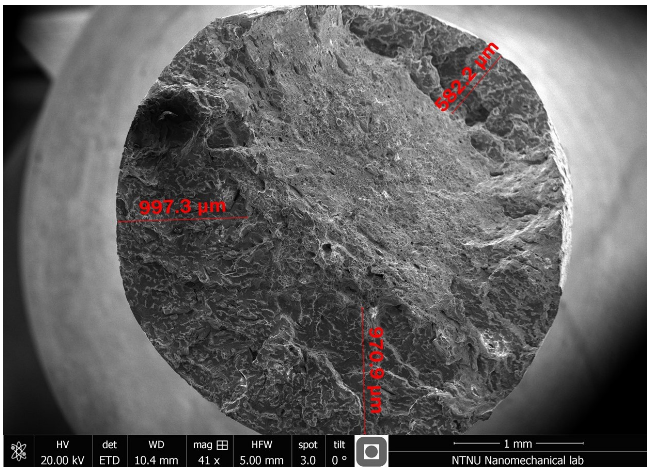

(c) Brittle area measurement for polarised sample 3.

Figure 13: Brittle area measurements for material D.

Table 24: Length of the brittle areas of the fracture surfaces for test material D in μm.

Measurem. no.	Sample 1	Sample 2	Sample 3
1	781.7	765,9	997.3
2	888.8	1070	582.2
3	890.4	1038	970,9
Ave.	853.6	958.0	850.1

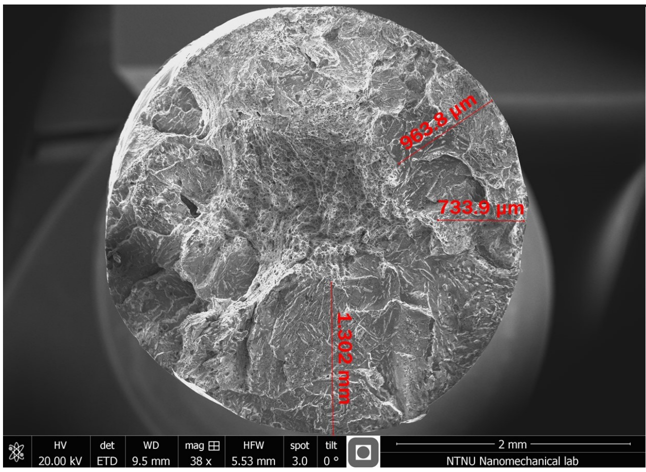

(a) Brittle area measurement for polarised sample 1.

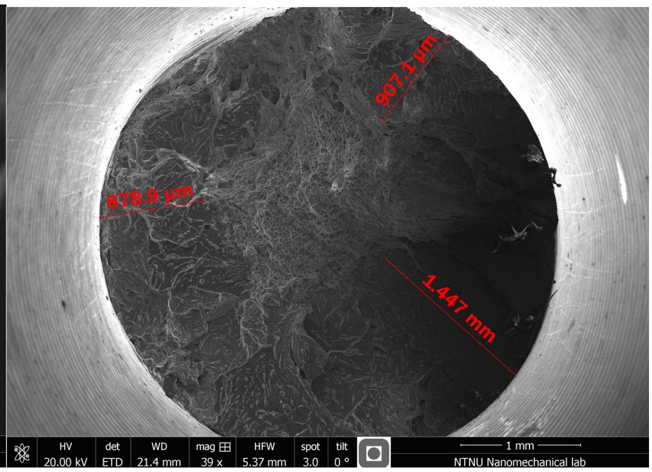

(b) Brittle area measurement for polarised sample 2.

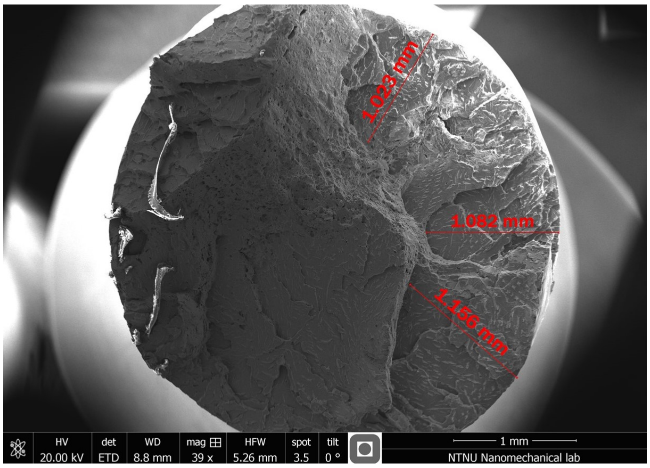

(c) Brittle area measurement for polarised sample 3.

Figure 14: Brittle area measurements for material E.

Table 25: Length of the brittle areas of the fracture surfaces for test material E in μm.

Measurem. no.	Sample 1	Sample 2	Sample 3
1	963,8	878,9	1023
2	733,9	907,1	1082
3	1302	1447	1156
Ave.	999,9	1077,7	1087,0

Ductile/brittle area ratio calculations

In this section the ductile/brittle area ratio results are provided in Tables 26 to 30. The equations used for calculating the %DB values are presented below:

$$r_d = r_{min} - r_b$$

$$A_d = \pi \cdot r_d^2$$

$$A_b = A_{min} - A_d$$

$$\%DB = 100\% \cdot \left(1 - \frac{A_d}{A_b}\right)$$

In the equations, r_{min} is the radius of the cross-section of the fracture surfaces, obtained from the measured minimum diameters, and b and d refers to values for the brittle and ductile areas of the fracture surfaces, respectively.

Table 26: Ductile/brittle area ratio calculations for material A.

Sample no.	Ad [mm^2]	Ab [mm^2]	%DB
1	2,63	7,38	64,36
2	3,53	6,20	43,08
3	2,83	6,13	53,80
Ave	3,00	6,57	54,38
SD	0,66	0,68	10,18

Table 27: Ductile/brittle area ratio calculations for material B.

Sample no.	Ad [mm^2]	Ab [mm^2]	%DB
1	2,55	7,46	65,83
2	1,72	80,23	79,11
3	1,25	8,81	85,78
Ave	1,84	8,16	77,47
SD	0,66	0,68	10,18

Table 28: Ductile/brittle area ratio calculations for material C.

Sample no.	Ad [mm^2]	Ab [mm^2]	%DB
1	3,23	7,06	54,21
2	1,30	6,94	81,31
Ave	2,26	7,00	67,65
SD	1,11	1,22	13,98

Table 29: Ductile/brittle area ratio calculations for material D.

Sample no.	Ad [mm^2]	Ab [mm^2]	%DB
1	2,75	7,31	62,32
2	2,20	7,92	72,22
3	2,60	7,13	63,52
Ave	2,52	7,45	66,21
SD	0,29	0,41	5,40

Table 30: Ductile/brittle area ratio calculations for material E.

Sample no.	Ad [mm^2]	Ab [mm^2]	%DB
1	2,27	8,48	73,23
2	1,71	8,64	80,24
3	1,88	8,99	79,12
Ave	1,95	8,70	77,58
SD	0,29	0,26	3,76

February, 2017
NIPPON STEEL & SUMITOMO METAL. CO.
AMAGASAKI WORKS

PROPERTIES OF S39274 TEST PIECES

1. Scope

NSSMC sent tensile test pieces of S39274 to Norwegian university.
Followings are properties of these samples.

2. Description of samples

Table 1 Description of samples

Size	Process	Material
OD 169.3mm × WT 25.85mm	Hot extrusion → Cold drawing → Heat treatment	S39274

3. Properties

Table 2 Chemical compositions (mass %)

	C	Si	Mn	P	S	Ni	Cr	Mo	N	Cu	W
Item 1 (Heat:F626012)	0.016	0.25	0.68	0.024	0.0002	6.2	25.1	3.2	0.29	0.53	2.10
UNS S39274	0.030 max.	0.80 max.	1.00 max.	0.030 max.	0.020 max.	6.0 /8.0	24.0 /26.0	2.5 /3.5	0.24 /0.32	0.20 /0.80	1.50 /2.50

Table 3 Tensile properties

	YS (MPa)	TS (MPa)	EL (%)
Item 1 (Heat:F626012)	660	862	39
ASTM A789-S39274	min. 550	min. 800	min. 15

FONDINOX S.p.A.
Via Marconi, 42/48
I - 26010 SERGNANO (CR)
Tel. (0373) 45651
Fax (0373) 455100
E-mail: fondinox@fondinox.com

LLOYD'S REGISTER • LRQA
ISO 9001
QMS No. 160085

Cert. N°	88357
FOGLIO	DI
BLATT - PAGE	VON - OF
FEUILLE	DE

CERTIFICATO MATERIALI - MATERIAL CERTIFICATE - WERKSTOFF PRUEFZEUGNIS - CERTIFICAT MATIERE

SEC./ACC.TO/NACH/SELON

CLIENTE / CUSTOMER / KUNDE / CLIENT: **GE OIL & GAS**

ORDINE N. / ORDER N. / BESTELLUNG N. / COMMANDE N.

EN 10204/2.2	
EN 10204/3.1	X
EN 10204/3.2	

DESCRIZIONE SPEDIZIONE - DESCRIPTION OF DELIVERY - UMFANG DER LIEFERUNG - DETAILS DU LOT

COLATA N. / HEAT NR. / SCHMELZE NR. / NO. DE COULEÈ	QUANTITÀ / QUANTITY / STUECKZAHL / QUANTITÈ	DENOMINAZIONE - DESCRIZIONE / DESCRIPTION - SIZE	GEGENSTAND - ABMESSUNG / DESIGNATION - DIMENSION
L 7628		TEST SAMPLING	

ANALISI CHIMICA - CHEMICAL ANALYSIS - HEMISCHE ZUSAMMENSETZUNG - COMPOSITION CHIMIQUE

LEGA / ALLOY / LEGIERUNG / ALLIAGE		C	Cr	Ni	Mo	Mn	Si	P	S	N
	MIN	0,000	24,000	6,000	4,000	0,000	0,000	0,000	0,000	0,100
	MAX	0,030	26,000	8,000	5,000	1,500	1,000	0,040	0,040	0,300
A995 GR 5A		0,023	25,124	7,507	4,149	0,755	0,564	0,023	0,005	0,242

PROPRIETA' MECCANICHE - MECHANICAL PROPERTIES - MECHANISCHE EIGENSCHAFTEN - ESSAIS MECANIQUES

Rp 1% (MPa)	Rp 0.2% (MPa)	Rmn (MPa)	A (%)	Z (%)	HB	Resilienza - Resilience Kerbschlagzaehigkeit - Impact T = -46°C KV JOULE	KCU JOULE	DVM JOULE	LE mmq
min =	min = 515	min = 690	min = 18	min =					
	588	809	34		237	161			
						168			
						158			

Prove speciali / Special tests / Spezifische Pruefungen / Essais Speciaux	

Trattamento termico / Heat Treatement / Termische Behandlung / Traitement Thermique	SOLUTION TREATMENT 1130°C/WATER

Osservazioni / Remarks / Bemerkungen / Observations	MELTING: ELECTRIC (INDUCTION)
	PRE=42,7
	MATERIAL ACC. TO NORSOK MDS D56 REV.5

Sergnano... 07/10/2016

Resp. laboratorio F N 3 X CATTANEO

Resp. qualità F N 2 X CARNITI

Ente collaudo

FONDINOX Via Marconi 46/48 - 26010 SERGNANO (CR) TEL. 0373 45651 FAX 0373 455100	**QUALITY CONTROL** **FERRITE CONTENT CERTIFICATE**	**88357 FC** PAGE 2 OF 2

Accordance with	ASTM E 562		
Customer	GE OIL & GAS		
Purchase Order			
Heat	L7628		
Material	A995 GR 5A		
Heat Treatment	SOLUTION ANNEALING 1130°C/WATER		
Instrument	OPTICAL METALLOGRAPHIC MICROSCOPE LEICA DM4000M LED		
Chosen of the fields	RANDOMLY		
Etching	ELECTROLITIC, OXALIC ACID + NaOH 40%		
Sample dimension	35X32X15mm		
Magnification	200X		
Grid points and shape	16	Square	
Fields	30	**Position**	½ Thk

n.	field	n.	field	n.	field	n.	field
1	56,25	**11**	37,50	**21**	40,63	**31**	-
2	53,13	**12**	31,25	**22**	65,63	**32**	-
3	43,75	**13**	46,88	**23**	68,75	**33**	-
4	43,75	**14**	37,50	**24**	50,00	**34**	-
5	37,50	**15**	50,00	**25**	37,50	**35**	-
6	62,50	**16**	50,00	**26**	53,13	**36**	-
7	68,75	**17**	56,25	**27**	56,25	**37**	-
8	56,25	**18**	46,88	**28**	31,25	**38**	-
9	50,00	**19**	50,00	**29**	50,00	**39**	-
10	50,00	**20**	56,25	**30**	46,88	**40**	-

Volume fraction Vf [%]	49,479
standard deviation s [%]	9,885
95%CI	3,691
%RA	7,459
t	2,045

Vf	± 95% CI	
49,48	3,69	%

Req.	35-55	%

LAB	QAM	THIRD PART/INSPECTOR
FONDINOX	FONDINOX	

FONDINOX Via Marconi 46/48 - 26010 SERGNANO (CR) TEL. 0373 45651 FAX 0373 455100	**QUALITY CONTROL** **METALLOGRAPHIC CERTIFICATE**	**88357 SM** PAGE 1 OF 2

Accordance with	MDS D56 REV.5
Customer	GE OIL & GAS
Purchase Order	
Heat	L7628
Material	A995 GR 5A
Heat Treatment	SOLUTION ANNEALING 1130°C/WATER
Instrument	OPTICAL METALLOGRAPHIC MICROSCOPE LEICA DM4000M LED
Etching	ELECTROLITIC, OXALIC ACID + NaOH 40%
Etching T	20 °C
Sample dimension	35X32X15mm
Magnification	200x
Position	T/2

COMMENTS	MICROSTRUCTURE FREE FROM DETRIMENTAL INTERMETALLIC PHASES AND PRECIPITATIONS
RESULTS	SATISFACTORY

LAB	QAM	THIRD PART/INSPECTOR
FONDINOX	FONDINOX	

FONDINOX	Via Marconi, 42/48 - 26010 SERGNANO (CR) Tel. +39 0373 45651 Fax +39 0373 455100 email: fondinox@fondinox.com	**CONTROLLO QUALITA'** ***QUALITY CONTROL*** **CERTIFICATO DI TRATTAMENTO TERMICO** ***HEAT TREATMENT CERTIFICATE*** **SEE CERT. 3.1 Nr. 88357**	**HT 4803** **FOGLIO** **DI** PAGE OF

CLIENTE CUSTOMER: **GE OIL & GAS**	**ORDINE N.** ORDER No.:	**COMMESSA N.** JOB No.:
COLATA HEAT: **L 7628**	**MATERIALE** ALLOY: **A995 GR 5A**	**SP. MAX. mm.** THCK MAX: **32 mm**
FORNO FURNACE: **AS BELOW INDICATED**	**COMBUSTIBILE** FUEL: **GAS**	**CICLO** CYCLE: **TT02**

TIPO TRATT. HEAT TREAT. TYPE: **SOLUTION TREATMENT 1130°C/WATER**

SPECIFICA SPECIFICATION: **ASTM APPLICABLE**

RAFFREDAMENTO IN COOLING MEDIUM: **RUNNING WATER**

CAMPO TEMP. TEMP. RANGE °C	**GRAD. SALITA** HEATING RATE °C/H MAX	**GRAD. DISCESA** COOLING RATE °C/H MAX
20-600	**580°C/h**	
600	**HOLDING 60'**	
600-1000	**133°C/h**	
1000	**HOLDING 60'**	
1000-1130	**87°C/h**	
1130	**HOLDING 240' MIN**	**WATER**

TEMP. DI REGIME HOLDING TEMP. °C: **1130**	**PERMANENZA** HOLDING TIME H: **3**
TERMOCOPPIE TERMOCOUPLES TH N°: **4**	**TIPO** TYPE: **PT/PT + RH 10%**

DIAGRAMMA TRATTAMENTO TERMICO

HT DIAGRAM

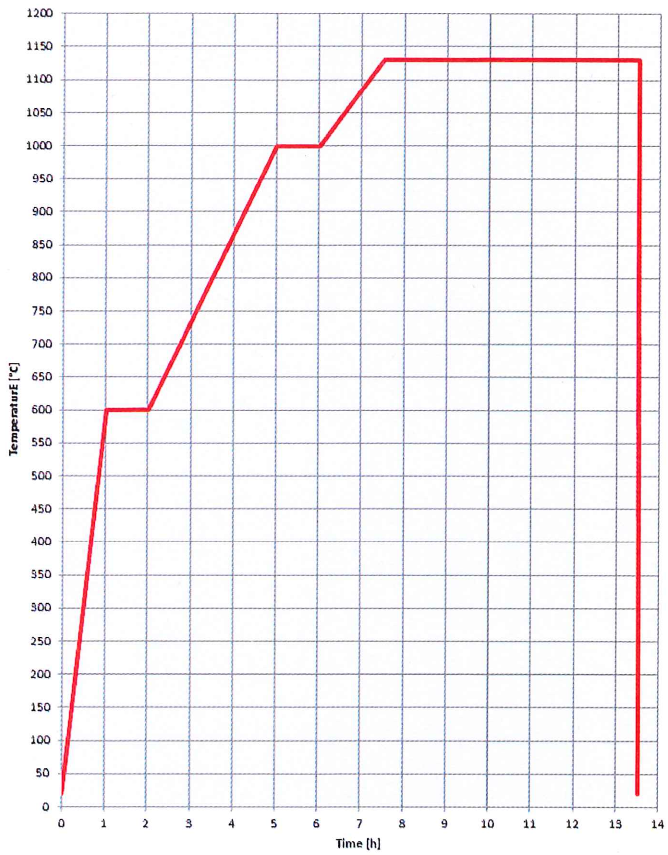

NOTE
REMARKS

NUMERO DI LOTTO DI TRATTAMENTO TERMICO HT LOT NUMBER: **15/02/16SOFIND**	SI CERTIFICA CHE IL TRATTAMENTO TERMICO RISULTA IN ACCORDO CON LA SPECIFICA SUMMENZIONATA. *WE CERTIFY THAT THE HEAT TREATMENT IS ACCORDING TO THE NAMED SPECIFICATION.*

QCMgr F N 2 X CARNITI	**DATA** Date **07/10/2016**	**ENTE ISPETTIVO** Off. Inspector	**DATA** Date

FONDINOX
Via Marconi, 42/48 - 26010 SERGNANO (CR)
Tel. +39 0373 45651
Fax +39 0373 455100
email: fondinox@fondinox.com

CONTROLLO QUALITA'
QUALITY CONTROL

CERTIFICATO PROVA DI CORROSIONE
PITTING CORROSION TEST CERTIFICATE

PCT 2515

FOGLIO DI
PAGE OF

CLIENTE: GE OIL & GAS
CUSTOMER

ORDINE N.
ORDER No.

COLATA: HEAT NUMBER	L 7628 SEE CERT. 3.1 Nr. 88357
LEGA: ALLOY	A995 GR 5A
TRATTAMENTO: HEAT TREATED	SOLUTION TREATMENT 1130°C/WATER
RIFERIMENTI: REFERENCES	ANSI/ASTM G 48, METHOD A FINISH, 120 GRIT ABRASIVE PAPER THERMAL TREATMENT: FULLY SOLUTION TREATED AT SOLUTION TREATMENT 1130°C/WATER TEST DURATION: 24 h. TEST TEMPERATURE: +50 °C

PROVINO: SPECIMEN	50 X 25 X 10
SOLUZIONE: SOLUTION	AS PER ASTM G 48
RISULTATI: RESULTS	NO WEIGHT LOSS NO PITTING AT 20X MAGNIFICATION

TEST RESULTS ACCOMPLISHE REQUIREMENTS OF

TECHNICAL DOCUMENT

QCMgr	DATA Date	ENTE ISPETTIVO Off. Inspector	DATA Date
F N X CARNITI	07/10/2016		

TUBACEX

INSPECTION CERTIFICATE
EN 10204:2004 / 3.1

Number: 577628 Page: 1 / 4	Rev: 00
Created on: Date: 24.04.2013	Modified on: 25.04.2013

TTI - TUBACEX TUBOS INOXIDABLES

Registro Mercantil de Alava, Tomo 587, Folio 189, Hoja VI 2885 - N.I.F. A-01140227
Tres cruces, 8
01400 Llodio (Alava)
SPAIN
TL: +34 946719300
FAX: +34 946725062
E-MAIL: qualitytti@tubacex.es

CUSTOMER DESCRIPTION

CLIENT SOLD TO	CLIENT SHIP TO
SFF SCANDINAVIAN FITTINGS & FLANGES A/S JACOB ASKELANDSVEI 5 4391 SANDNES NORWAY	SFF SCANDINAVIAN FITTINGS & FLANGES A/S JACOB ASKELANDSVEI 5 4391 SANDNES NORWAY

CLIENT ORDER: 278485
SALES ORDER: 129610

MATERIAL:SEAML. STAINL. STEEL TUBES/PIPES
HEAT-TREATED, PICKLED, PICKLED-PASSIVATED
GRADE: S32760,
STANDARD: ASTM A790/A790M-11
NORSOK M630 REV.5 MDS D51 REV.4
GP 29-01-02 VERSION 1.0.0
N041050-E244MA Rev.3 Piping Class Sheet PCS 1 #UD01
TOLERANCES: ASTM A999/A999M-12
RANDOM LENGTHS 4.000/7.000 MM
PLAIN ENDS,
DIMENSIONS: 168,28 X 14,27 MM - 6" SCH 120
HOT FINISHED

SFF SCANDINAVIAN FITTINGS & FLANGES AS
COMPONENT MEETS THE REQ. IN PED 97/23 ANNEX I SECT. 4.3

PROJECT: Kizomba Sattelite Phase II
CLIENT: VETCOGRAY SCANDINAVIA
CLIENT ART. CODE: N39005-P244
PRODUCT NO: 52183
Compliance with Client specification: Signed: JT
SFF Q.C. - DEPT.

Sales Item	Client Item	Delivery No	Lot No.	Heat No	Pieces	Weight	Tot Lgth	Un Lgth
10	ART.CODE:N39005-P244 - ITEM NO° 1		200097973	46836	10	3.284 KG	59,05 M	4000-7000 MM
10	ART.CODE:N39005-P244 - ITEM NO° 1		200098050	47013	10	3.220 KG	57,57 M	4000-7000 MM
10	ART.CODE:N39005-P244 - ITEM NO° 1		200098052	47024	12	4.043 KG	72,77 M	4000-7000 MM
10	ART.CODE:N39005-P244 - ITEM NO° 1		200098066	47051	26	9.170 KG	164,26 M	4000-7000 MM
10	ART.CODE:N39005-P244 - ITEM NO° 1		200098327	47045	11	3.593 KG	64,18 M	4000-7000 MM

RAW MATERIAL

Heat Nr:	Supplier	Method
46836	ACERALAVA (SPAIN)	Electric furnace+AOD
47013	ACERALAVA (SPAIN)	Electric furnace+AOD
47024	ACERALAVA (SPAIN)	Electric furnace+AOD
47045	ACERALAVA (SPAIN)	Electric furnace+AOD
47051	ACERALAVA (SPAIN)	Electric furnace+AOD

AENOR
Empresa Registrada
UNE-EN ISO 9001

AENOR
Gestión Ambiental
UNE-EN ISO 14001

Intertek
☐ Reviewed
☒ Witnessed
Initial: FCF
Date: 25/4/13
ES - 0040

L. Fdez de Nograr
Date 25.04.2013
BY TECHNOR

TUBACEX TUBOS INOXIDABLES S.A.
INGENIERIA DE CALIDAD
Iñigo Arriola Alcibar

TUBACEX

INSPECTION CERTIFICATE
EN 10204:2004 / 3.1

Number: 577628 Page: 2 / 4	Rev: 00
Created on: Date: 24.04.2013	Modified on: 25.04.2013

CHEMICAL COMPOSITION (%)

*L: Ladle C:Products

*	Heat	Seq	C	Mn	Si	P	S	Ni	Cr	Mo	Cu	W
L	46836	1	0,014	0,74	0,390	0,024	0,0005	6,75	25,70	3,59	0,66	0,590
L	47013	1	0,012	0,78	0,440	0,023	0,0005	7,00	25,60	3,61	0,63	0,610
L	47024	1	0,014	0,65	0,430	0,025	0,0006	6,95	25,55	3,63	0,66	0,610
L	47045	1	0,016	0,67	0,450	0,025	0,0005	7,00	25,65	3,60	0,64	0,610
L	47051	1	0,013	0,72	0,480	0,027	0,0004	6,85	25,45	3,61	0,66	0,600

*	Heat	Seq	N	Pren
L	46836	1	0,2570	41,6590
L	47013	1	0,2560	41,6090
L	47024	1	0,2455	41,4570
L	47045	1	0,2445	41,4420
L	47051	1	0,2470	41,3150

HEAT TREATMENT

SOLUTION ANNEALED AT 1100 °C , Direct water quenched

TENSILE TEST

Lot No.	Sample	T	Rp0.2	Rp1.0	Rm	A2"	A5	Type
		°C	MPa	MPa	MPa	%	%	
200097973	2	20	610	693	847	44	43	L
200098050	2	20	624	701	852	38	37	L
200098052	4	20	609	688	836	42	41	L
	5	20	595	684	835	36	35	L
200098066	3	20	615	697	841	36	35	L
	4	20	618	691	842	38	37	L
	5	20	614	691	844	40	39	L
200098327	2	20	613	694	839	36	35	L
	3	20	594	708	854	36	35	L

HARDNESS TEST

Lot No.	Sample	HRC1	HRC2
200097973	2	24,0	25,0
200098050	2	22,0	23,0
200098052	4	24,0	25,0
	5	24,0	25,0
200098066	3	24,0	25,0
	4	24,0	25,0
	5	24,0	25,0
200098327	2	24,0	25,0
	3	24,0	25,0

IMPACT TEST

Lot No.	Sample	T	Wspec	Ecv 1	Ecv 2	Ecv 3	Ecv AVG	Type
		°C	mm	J	J	J	J	
200097973	2	-46	10,00	220	247	248	238	L
200098050	2	-46	10,00	293	293	280	289	L
200098052	4	-46	10,00	293	231	293	272	L
	5	-46	10,00	280	261	232	258	L

AENOR Empresa Registrada UNE-EN ISO 9001

AENOR Gestión Ambiental UNE-EN ISO 14001

Intertek
☐ Reviewed
☒ Witnessed
Initial: FCF
Date: 25/4/13
ES - 0040

L. Fdez. de Nograro

Date ... 25.04.2013

84 TECHO

TUBACEX TUBOS INOXIDABLES S.A.
INGENIERIA DE CALIDAD

Iñigo Arriola Alcibar

TUBACEX

INSPECTION CERTIFICATE
EN 10204:2004 / 3.1

Number: 577628	Rev: 00
Page: 3 / 4	
Created on: Date: 24.04.2013	Modified on: 25.04.2013

IMPACT TEST

Lot No.	Sample	T	Wspec	Ecv 1	Ecv 2	Ecv 3	Ecv AVG	Type
		°C	*mm*	*J*	*J*	*J*	*J*	
200098066	3	-46	10,00	261	293	259	271	L
200098066	4	-46	10,00	249	274	250	258	L
	5	-46	10,00	293	235	220	249	L
200098327	2	-46	10,00	276	261	270	269	L
	3	-46	10,00	286	261	260	269	L

CORROSION ACCORDING TO ASTM G48A

Lot No.	Sample	T	Pits-20x	W.loss	time
		°C		*g/m2*	*Horas*
200097973	2	50	N	0,3600	24,0
200098050	2	50	N	0,1600	24,0
200098052	4	50	N	0,1000	24,0
	5	50	N	0,1300	24,0
200098066	3	50	N	0,3000	24,0
	4	50	N	0,0900	24,0
	5	50	N	0,2500	24,0
200098327	2	50	N	0,2700	24,0
	3	50	N	0,1000	24,0

FERRITE ACCORDING TO ASTM E 562

Lot No.	Sample	%Fer	Dev.Ferr
		%	*%*
200097973	2	54,02	1,91
200098050	2	53,20	2,07
200098052	4	54,56	2,43
	5	54,74	1,79
200098066	3	54,92	2,36
	4	54,55	2,20
	5	54,02	2,44
200098327	2	54,96	1,78
	3	54,39	2,16

METALURGICAL TESTS

METALLOGRAPHIC FERRITE CONTENT CHECK ACC. TO ASTM E562

- Ferrite content measured with 30 fields spread over a complete cross section, including locations near inner surface and mid thickness
- Point count conducted at 500X mag.
- Sample Electrolitically Etched using NaOH

METALLOGRAPHIC EXAMINATION

- Sample etched using NaOH ASTM E407 Etchant No.98
- Metallographic examination is conducted over the complete section.
- Examination conducted at 500X mag.

AENOR
Empresa Registrada
UNE-EN ISO 9001

AENOR
Gestión Ambiental
UNE-EN ISO 14001

Intertek
☐ Reviewed
☒ Witnessed
Initial: CCF
Date: 25/4/13
ES - 0040

L. Fdez. de Nograro

Date 25.04.2013
BY TECMOR

TUBACEX TUBOS INOXIDABLES S.A.
INGENIERIA DE CALIDAD

Iñigo Arriola Alcibar

TUBACEX

INSPECTION CERTIFICATE
EN 10204:2004 / 3.1

Number: 577628 Page: 4 / 4	Rev: 00
Created on: Date: 24.04.2013	Modified on: 25.04.2013

ETCH STRUCTURE ACC. ASTM A923 MET.A: UNAFFECTED STRUCTURE. MATERIAL FREE FROM INTERMETALLIC PHASES AND PRECIPITATES. UNIFORM STRUCTURE ACROSS FULL WALL THICKNESS

NON-DESTRUCTIVE TESTS

FERRITE CONTENT DETERMINED BY FISCHER FERRITOSCOPE TO 10% OF PRODUCTS TO BE BETWEEN 35% - 55% FERRITE CONTENT

POSITIVE MATERIAL IDENTIFICATION TEST ON EACH TUBE/PIPE BY "X-RAY-FLUORESCENCE-ANALYZER": SATISFACTORY

HYDROSTATIC PRESSURE TESTED AT 190 bar, 2750 PSI DURING 5 SEC ON EACH TUBE/PIPE: SATISFACTORY

DIMENSIONAL CHECKING ON EACH TUBE: SATISFACTORY

VISUAL INSPECTION ON EACH TUBE: SATISFACTORY

TECHNOLOGICAL TESTS

FLATTENING TEST: SATISFACTORY

MARKING

TX3 TUBACEX 168,28 X 14,27 MM - 6" SCH 120 ASTM A790 S32760 HF SMLS HEAT/ PMI-AV LOT NO/ SPAIN PROJECT: KIZOMBA PH-II CALL OFF NO.4500114582 ITEM NO.1 -ART.CODE: N39005-P244
Colour coding as follows:
- 2 stripes solid green (RAL 6010)

REMARKS

NO MERCURY, MERCURY COMPOUNDS OR MERCURY BEARING INSTRUMENTS AND/OR EQUIPMENT HAVE BEEN USED ALONG MANUFACTURING AND INSPECTION PROCESS.

NO WELDING OR WELD REPAIRS WERE MADE

MATERIAL MANUFACTURER APPROVED BY TÜV SÜD Industrie Service GmbH (NOTIFIED BODY 036)TO ISSUE CERTIFICATES OF SPECIFIC PRODUCT CONTROL IN ACCORDING TO PRESSURE EQUIPMENT DIRECTIVE 97/23/EC ANNEX 1 POINT 4.3.

MATERIAL CHARACTERISTICS COMPLY WITH POINT 7.5 OF ANNEX I TO PED BY HAVING AN ELONGATION AFTER RUPTURE AT TENSILE TEST NO LESS THAN 14% AND A BENDING RUPTURE ENERGY AT IMPACT TEST NO LESS THAN 27J AT 20ºC.

MATERIAL IS FREE OF RADIATION CONTAMINATION

AENOR Empresa Registrada UNE-EN ISO 9001

AENOR Gestión Ambiental UNE-EN ISO 14001

Intertek
☐ Reviewed
☑ Witnessed
Initial: FCF
Date: 25/4/13
ES - 0040

L. Fdez de Nograro

Date 25.04.2013

BY TECNOA

TUBACEX TUBOS INOXIDABLES S.A.
INGENIERIA DE CALIDAD

Iñigo Arriola Alcibar

TUBACEX

INSPECTION CERTIFICATE
EN 10204 3.1
Annex 1
Microphotographs

Number :	577628
Page	: 1/9
Date	: 25/04/2013

TTI - TUBACEX TUBOS INOXIDABLES, S.A.

Registro Mercantil de Alava, Tomo 587, Folio 189, Hoja VI2885 - N.I.F. A-01140227
Tres Cruces, 8
01400 Llodio (Álava)
SPAIN

Sales Order : 129610
Sales Item : 10

Standard : ASTM A790
Grade : UNS S32760
Dimensions : 6"SCH 120

Microstructure: MATERIAL FREE FROM INTERMETALLIC PHASES AND PRECIPITATES. UNIFORM STRUCTURE ACROSS FULL WALL THICKNESS.

Etchant ASTM E407 no.98

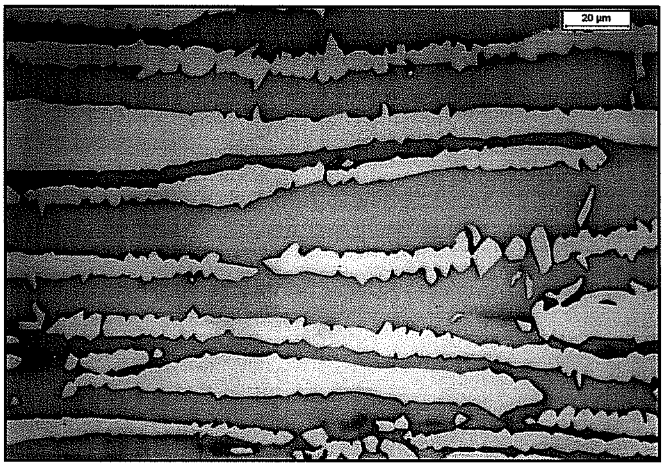

p1303465-2 Heat 46836 ferrocianuro x500.jpg

L. Fdez. de Nograro

Date 25.04.2013

BY TECHOR

Intertek
☐ Reviewed
☒ Witnessed
Initial: ECF
Date: 25/4/13
ES - 0040

TUBACEX TUBOS INOXIDABLES
INGENIERIA DE CALIDAD

Iñigo Arriola Alcibar

AENOR Empresa Registrada
AENOR Gestión Ambiental

TUBACEX

INSPECTION CERTIFICATE
EN 10204 3.1
Annex 1
Microphotographs

Number :	577628
Page :	2/9
Date :	25/04/2013

TTI - TUBACEX TUBOS INOXIDABLES, S.A.

Registro Mercantil de Alava, Tomo 587, Folio 189, Hoja VI2885 - N.I.F. A-01140227
Tres Cruces, 8
01400 Llodio (Álava)
SPAIN

Sales Order : 129610
Sales Item : 10

Standard : ASTM A790
Grade : UNS S32760
Dimensions : 6"SCH 120

Microstructure: MATERIAL FREE FROM INTERMETALLIC PHASES AND PRECIPITATES. UNIFORM STRUCTURE ACROSS FULL WALL THICKNESS.

Etchant ASTM E407 no.98

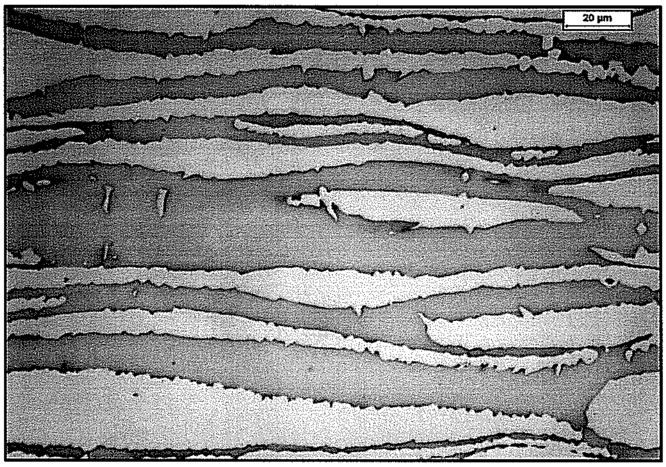

p1303459-2 Heat 47013 ferrocianuro x500.jpg

L. Fdez de Nograro

Date 25.04.2013
BY TECHOR

AENOR
Empresa Registrada

AENOR
Gestión Ambiental

Intertek
☐ Reviewed
☒ Witnessed
Initial: FCF
Date: 25/4/13
ES - 0040

TUBACEX TUBOS INOXIDABLES
INGENIERIA DE CALIDAD

Iñigo Arriola Alcibar

TUBACEX

INSPECTION CERTIFICATE
EN 10204 3.1
Annex 1
Microphotographs

Number :	577628
Page :	3/9
Date :	25/04/2013

TTI - TUBACEX TUBOS INOXIDABLES, S.A.
Registro Mercantil de Alava, Tomo 587, Folio 189, Hoja VI2885 - N.I.F. A-01140227
Tres Cruces, 8
01400 Llodio (Álava)
SPAIN

Sales Order : 129610
Sales Item : 10

Standard : ASTM A790
Grade : UNS S32760
Dimensions : 6"SCH 120

Microstructure: MATERIAL FREE FROM INTERMETALLIC PHASES AND PRECIPITATES. UNIFORM STRUCTURE ACROSS FULL WALL THICKNESS.

Etchant ASTM E407 no.98

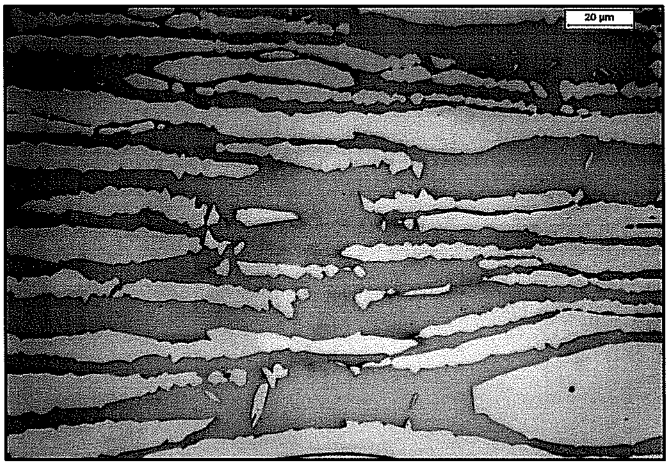

p1303464-4 heat 47024 ferrocianuro x500.jpg

L. Fdez. de Nograro

Date 25.04.2013

BV TECHOR

Intertek
☐ Reviewed
☒ Witnessed
Initial: FCF
Date: 25/4/13
ES - 0040

TUBACEX TUBOS INOXIDABLES
INGENIERIA DE CALIDAD

Iñigo Arriola Alcibar

AENOR ER Empresa Registrada
AENOR Gestión Ambiental

TUBACEX

INSPECTION CERTIFICATE
EN 10204 3.1
Annex 1
Microphotographs

Number :	577628
Page :	4/9
Date :	25/04/2013

TTI - TUBACEX TUBOS INOXIDABLES, S.A.
Registro Mercantil de Alava, Tomo 587, Folio 189, Hoja VI2885 - N.I.F. A-01140227
Tres Cruces, 8
01400 Llodio (Álava)
SPAIN

Sales Order : 129610
Sales Item : 10

Standard : ASTM A790
Grade : UNS S32760
Dimensions : 6"SCH 120

Microstructure: MATERIAL FREE FROM INTERMETALLIC PHASES AND PRECIPITATES. UNIFORM STRUCTURE ACROSS FULL WALL THICKNESS.

Etchant ASTM E407 no.98

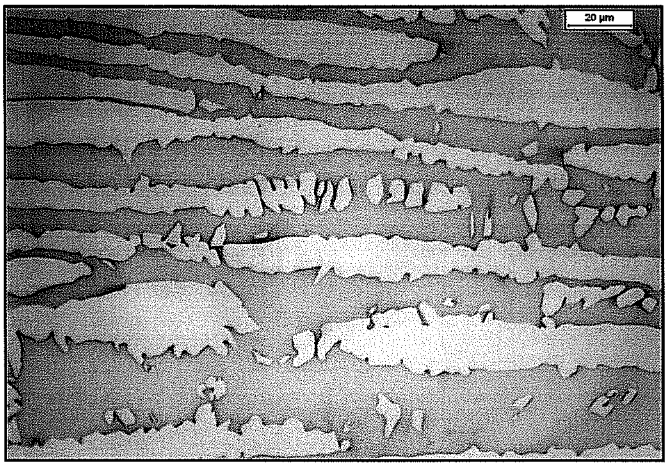

p1303464-5 heat 47024 ferrocianuro x500.jpg

L. Fdez. de Nograro

Date ...25.04.2013

BY TECNOR

Intertek
☐ Reviewed
☒ Witnessed
Initial: FCF
Date: 25/4/13
ES - 0040

TUBACEX TUBOS INOXIDABLES
INGENIERIA DE CALIDAD

Iñigo Arriola Alcibar

AENOR Empresa Registrada

AENOR Gestión Ambiental

TUBACEX

INSPECTION CERTIFICATE
EN 10204 3.1
Annex 1
Microphotographs

Number :	577628
Page :	5/9
Date :	25/04/2013

TTI - TUBACEX TUBOS INOXIDABLES, S.A.

Registro Mercantil de Alava, Tomo 587, Folio 189, Hoja VI2885 - N.I.F. A-01140227
Tres Cruces, 8
01400 Llodio (Álava)
SPAIN

Sales Order : 129610
Sales Item : 10

Standard : ASTM A790
Grade : UNS S32760
Dimensions : 6"SCH 120

Microstructure: MATERIAL FREE FROM INTERMETALLIC PHASES AND PRECIPITATES. UNIFORM STRUCTURE ACROSS FULL WALL THICKNESS.

Etchant ASTM E407 no.98

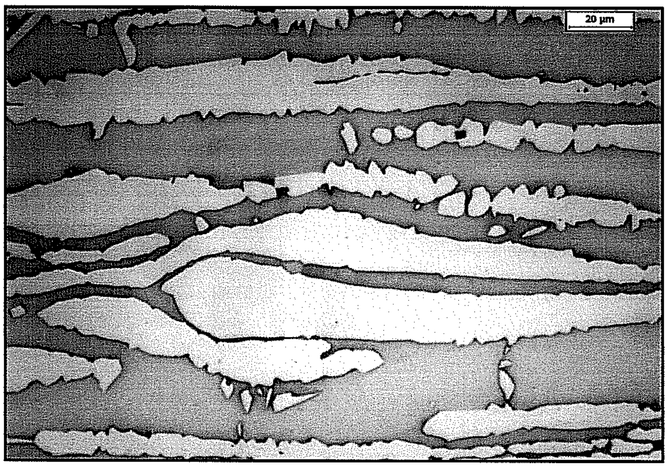

p1303463-3 Heat 47051 ferrocianuro x500.jpg

L. Fdez. de Nograro

Date 25.04.2013

BY TECHOR

Intertek
☐ Reviewed
☒ Witnessed
Initial: SCF
Date: 25/4/13
ES - 0040

TUBACEX TUBOS INOXIDABLES
INGENIERIA DE CALIDAD

Iñigo Arriola Alcibar

AENOR Empresa Registrada

AENOR Gestión Ambiental

TUBACEX

INSPECTION CERTIFICATE
EN 10204 3.1
Annex 1
Microphotographs

Number :	577628
Page :	6/9
Date :	25/04/2013

TTI - TUBACEX TUBOS INOXIDABLES, S.A.
Registro Mercantil de Alava, Tomo 587, Folio 189, Hoja VI2885 - N.I.F. A-01140227
Tres Cruces, 8
01400 Llodio (Álava)
SPAIN

Sales Order : 129610
Sales Item : 10

Standard : ASTM A790
Grade : UNS S32760
Dimensions : 6"SCH 120

Microstructure: MATERIAL FREE FROM INTERMETALLIC PHASES AND PRECIPITATES. UNIFORM STRUCTURE ACROSS FULL WALL THICKNESS.

Etchant ASTM E407 no.98

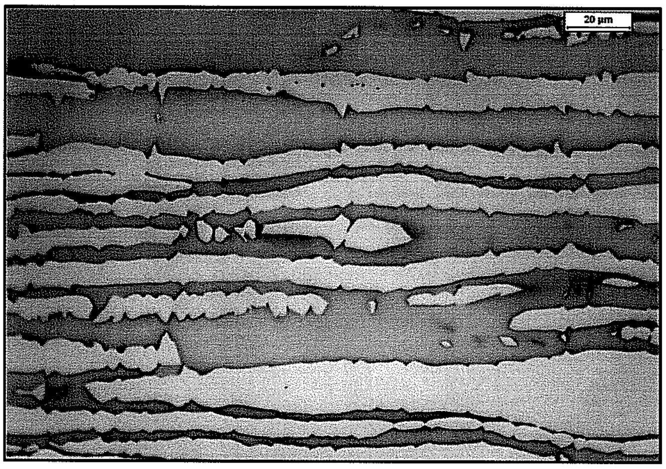

p1303463-4 Heat 47051 ferrocianuro x500.jpg

L. Fdez. de Nograro

Date 25.04.2013

BV TECMOR

Intertek
☐ Reviewed
☒ Witnessed
Initial: FCF
Date: 25/4/13
ES - 0040

TUBACEX TUBOS INOXIDABLES
INGENIERIA DE CALIDAD

Iñigo Arriola Alcibar

AENOR ER Empresa Registrada
AENOR Gestión Ambiental

TUBACEX

INSPECTION CERTIFICATE
EN 10204 3.1
Annex 1
Microphotographs

Number :	577628
Page	: 7/9
Date	: 25/04/2013

TTI - TUBACEX TUBOS INOXIDABLES, S.A.
Registro Mercantil de Alava, Tomo 587, Folio 189, Hoja VI2885 - N.I.F. A-01140227
Tres Cruces, 8
01400 Llodio (Álava)
SPAIN

Sales Order : 129610
Sales Item : 10

Standard : ASTM A790
Grade : UNS S32760
Dimensions : 6"SCH 120

Microstructure: MATERIAL FREE FROM INTERMETALLIC PHASES AND PRECIPITATES. UNIFORM STRUCTURE ACROSS FULL WALL THICKNESS.

Etchant ASTM E407 no.98

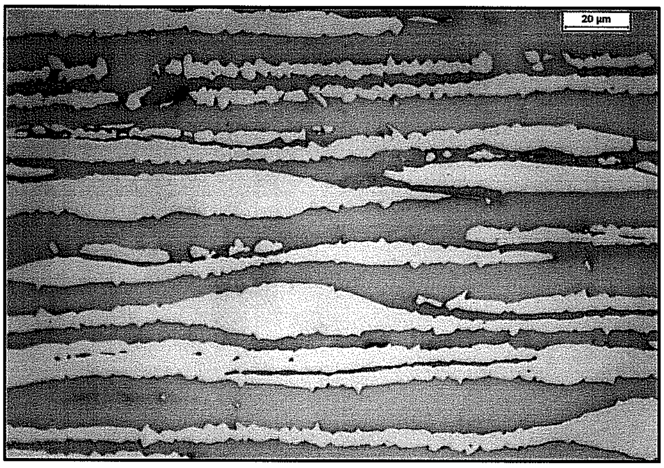

p1303463-5 Heat 47051 ferrocianuro x500.jpg

L. Fdez de Nograro

Date ..25.04.2013

BY TECNOR

AENOR
Empresa Registrada

AENOR
Gestión Ambiental

Intertek
☐ Reviewed
☒ Witnessed
Initial: FCF
Date: 25/4/13
ES - 0040

TUBACEX TUBOS INOXIDABLES
INGENIERIA DE CALIDAD

Iñigo Arriola Alcibar

TUBACEX

INSPECTION CERTIFICATE
EN 10204 3.1
Annex 1
Microphotographs

Number :	577628
Page :	8/9
Date :	25/04/2013

TTI - TUBACEX TUBOS INOXIDABLES, S.A.
Registro Mercantil de Alava, Tomo 587, Folio 189, Hoja VI2885 - N.I.F. A-01140227
Tres Cruces, 8
01400 Llodio (Álava)
SPAIN

Sales Order : 129610
Sales Item : 10

Standard : ASTM A790
Grade : UNS S32760
Dimensions : 6"SCH 120

Microstructure: MATERIAL FREE FROM INTERMETALLIC PHASES AND PRECIPITATES. UNIFORM STRUCTURE ACROSS FULL WALL THICKNESS.

Etchant ASTM E407 no.98

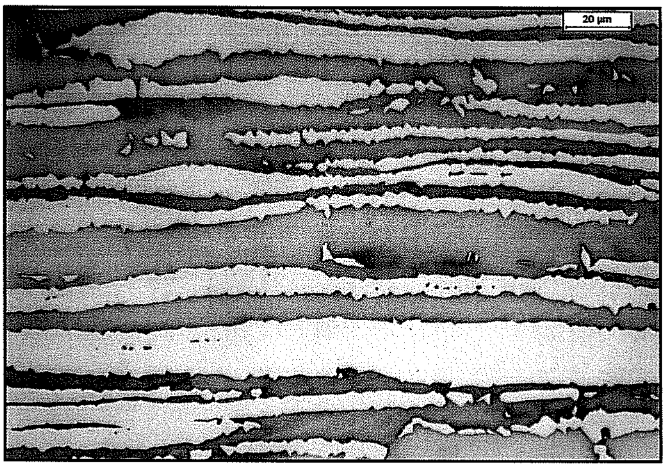

p1303460-2 Heat 47045 ferrocianuro x500.jpg

L. Fdez. de Nograro
Date 25.04.2013
BY TECNOR

AENOR
ER
Empresa Registrada

AENOR
Gestión Ambiental

Intertek
☐ Reviewed
☒ Witnessed
Initial: FCF
Date: 25/4/13
ES - 0040

TUBACEX TUBOS INOXIDABLES
INGENIERIA DE CALIDAD
Iñigo Arriola Alcibar

TUBACEX

INSPECTION CERTIFICATE
EN 10204 3.1
Annex 1
Microphotographs

Number :	577628
Page :	9/9
Date :	25/04/2013

TTI - TUBACEX TUBOS INOXIDABLES, S.A.

Registro Mercantil de Alava, Tomo 587, Folio 189, Hoja VI2885 - N.I.F. A-01140227
Tres Cruces, 8
01400 Llodio (Álava)
SPAIN

Sales Order : 129610
Sales Item : 10

Standard : ASTM A790
Grade : UNS S32760
Dimensions : 6"SCH 120

Microstructure: MATERIAL FREE FROM INTERMETALLIC PHASES AND PRECIPITATES. UNIFORM STRUCTURE ACROSS FULL WALL THICKNESS.

Etchant ASTM E407 no.98

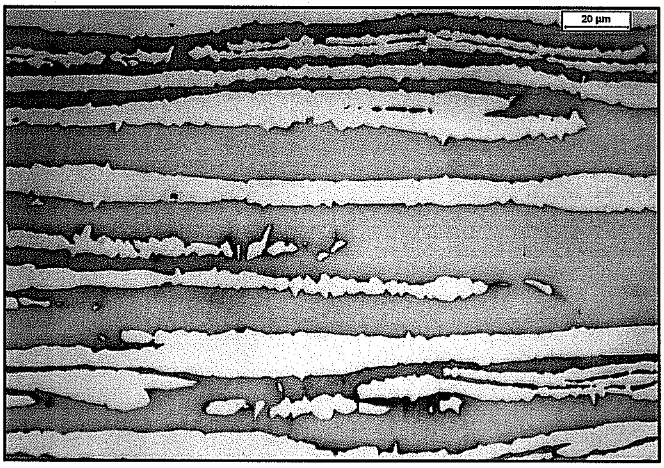

p1303460-3 Heat 47045 ferrocianuro x500.jpg

L. Fdez. de Nograro

Date 25.04.2013
BY TECMOR

AENOR
ER
Empresa Registrada

AENOR
Gestión Ambiental

Intertek
☐ Reviewed
☒ Witnessed
Initial: FCF
Date: 25/4/13
ES - 0040

TUBACEX TUBOS INOXIDABLES
INGENIERIA DE CALIDAD

Iñigo Arriola Alcibar

IBF S.P.A.
HEAD OFFICE
Via E.Berlinguer, 18 - 20040 Colnago (MI)

IBF - Pipes Division
Via Gandhi 17/19
20010 Vittuone (MI)

CHEMICAL COMPOSITION
AND MATERIAL TEST REPORT
EN 10204:2004
TYPE 3.1

MANUFACTURED IN ACCORDANCE WITH QUALITY
ASSURANCE SYSTEM APPROVED TO ISO 9001:2000,
BS EN ISO 9001:2000, UNI EN ISO 9001:2000
CERT. ISO 9001 LRC121029

MTR No.	Rev.	Date	IBF Order	Specification	Material	Finishing	Customer	Purchase Order
C070005899		06/11/2007	2007000066	ASTM A790	S32760	Smls	SFF SCANDINAVIAN FITTINGS & FL	140080 REV.02 of 29/06/2007

Si certifica che i materiali sotto elencati sono stati fabbricati e controllati e risultano conformi all'ordine del cliente e alle specifiche richiamate.
We hereby certify that the materials listed here below have been fabricated and inspected and are in compliance with the purchase order and relevant specification.

Item Description		Pcs	MU	Quantity	Tag.No.	C.I.Req.Item	DWG	Heat	HT.Lot	M.Test N°
0005 PIPE SMLS 10" SCH-120	ASTM A790 S32760 ANSI B36.10	34	MT	8,105	VENDOR NO : 052185	1		04327	H100000244	5551
0005 PIPE SMLS 10" SCH-120	ASTM A790 S32760 ANSI B36.10	36	MT	8,285	VENDOR NO : 052185	1		04327	H100000244	5551
0005 PIPE SMLS 10" SCH-120	ASTM A790 S32760 ANSI B36.10	42	MT	8,350	VENDOR NO : 052185	1		04336	H100000242	5512
0005 PIPE SMLS 10" SCH-120	ASTM A790 S32760 ANSI B36.10	45	MT	8,195	VENDOR NO : 052185	1		04335	H100000243	5513
0005 PIPE SMLS 10" SCH-120	ASTM A790 S32760 ANSI B36.10	46	MT	6,850	VENDOR NO : 052185	1		04335	H100000243	5513
0005 PIPE SMLS 10" SCH-120	ASTM A790 S32760 ANSI B36.10	48	MT	5,230	VENDOR NO : 052185	1		04335	H100000243	5513
0005 PIPE SMLS 10" SCH-120	ASTM A790 S32760 ANSI B36.10	49	MT	6,425	VENDOR NO : 052185	1		04335	H100000243	5513
0005 PIPE SMLS 10" SCH-120	ASTM A790 S32760 ANSI B36.10	50	MT	8,215	VENDOR NO : 052185	1		04347	H100000245	5567
0005 PIPE SMLS 10" SCH-120	ASTM A790 S32760 ANSI B36.10	51	MT	7,885	VENDOR NO : 052185	1		04347	H100000245	5567
0005 PIPE SMLS 10" SCH-120	ASTM A790 S32760 ANSI B36.10	52	MT	8,020	VENDOR NO : 052185	1		04347	H100000245	5567
0005 PIPE SMLS 10" SCH-120	ASTM A790 S32760 ANSI B36.10	53	MT	8,190	VENDOR NO : 052185	1		04354	H100000248	5568
0005 PIPE SMLS 10" SCH-120	ASTM A790 S32760 ANSI B36.10	54	MT	8,325	VENDOR NO : 052185	1		04354	H100000248	5568
0005 PIPE SMLS 10" SCH-120	ASTM A790 S32760 ANSI B36.10	55	MT	8,435	VENDOR NO : 052185	1		04354	H100000248	5568
0005 PIPE SMLS 10" SCH-120	ASTM A790 S32760 ANSI B36.10	57	MT	8,185	VENDOR NO : 052185	1		04347	H100000250	5577
0005 PIPE SMLS 10" SCH-120	ASTM A790 S32760 ANSI B36.10	58	MT	8,270	VENDOR NO : 052185	1		04354	H100000250	5578
0005 PIPE SMLS 10" SCH-120	ASTM A790 S32760 ANSI B36.10	59	MT	8,270	VENDOR NO : 052185	1		04354	H100000250	5578

CHEMICAL COMPOSITION

Heat	C %	Mn %	P %	S %	Si %	Ni %	Cr %	Mo %	N %	Cu %	W %	Pre %
04327	0,0160	0,5500	0,0250	0,0002	0,4900	7,0000	25,500	3,6700	0,2450	0,5400	0,6500	41,530
04335	0,0160	0,5800	0,0230	0,0002	0,5200	6,9200	25,470	3,6400	0,2530	0,5500	0,6400	41,530
04336	0,0150	0,6000	0,0260	0,0002	0,5000	6,9600	25,430	3,6900	0,2490	0,5700	0,6500	41,590
04347	0,0140	0,5000	0,0240	0,0002	0,4700	7,0300	25,500	3,6300	0,2610	0,5300	0,6400	41,660
04354	0,0140	0,5100	0,0260	0,0003	0,5000	7,0200	24,400	3,6500	0,2550	0,5400	0,6500	41,530

IBF S.p.A.
R. Colarieti
QC INSPECTOR
06/11/07

REMARKS

1) Heat Treatment details : Solution annealing at 1100°C. Holding Time:2 min/mm Quenching in water. Time from furnace to water less than 60 seconds.
2) Raw Material: by Foroni Steel Making Process: El. Furnace + AOD, see attached Certificate n° 2007/1852, 2007/1853, 2007/1891, 2007/2264, 2007/2265.
3) For Mechanical test see "T.O.S.I." reports n° 07P4676, 07P4679, 07P4680, 07P4841, 07P4842, 07P4843, 07P4845.
4) For Ferrite volume fraction metallographic determination according procedure ASTM E562 see "T.O.S.I." test report n° 07H2307, 07H2308, 07H2311, 07H2368 to 07H2372 .
5) For pitting corrosion test according ASTM G48 Met.A, see "T.O.S.I." test report n° 07H2309, 07H2310, 07H2314, 07H2376, 07H2377, 07H2379, 07H2380.
6) UT examination acc. to ASTM E213 (V NOTCH DIMENSIONS 5% WTh Max. 1.5mm): satisfactory.
7) Ferrite chechod by Ferritescope Fischer: satisfactory
8) All pipes have been passed visual and dimensional inspections in compliance with IBF Procedure IO-05.01

IBF's authorized inspection representative	Purchaser's authorized inspection representative	Inspector designated by the official regulations
PREPARED BY: Nicola Lanci / QC INSPECTOR CHECKED BY:		

IBF S.P.A.
HEAD OFFICE
Via E.Berlinguer, 18 - 20040 Colnago (MI)

IBF - Pipes Division
Via Gandhi 17/19
20010 Vittuone (MI)

CHEMICAL COMPOSITION
AND MATERIAL TEST REPORT
EN 10204:2004
TYPE 3.1

MANUFACTURED IN ACCORDANCE WITH QUALITY ASSURANCE SYSTEM APPROVED TO ISO 9001:2000.
BS EN ISO 9001:2000, UNI EN ISO 9001:2000
CERT. ISO 9001 LRC121029

MTR No.	Rev.	Date	IBF Order	Specification	Material	Finishing	Customer	Purchase Order
C070005899		06/11/2007	2007000066	ASTM A790	S32760	Smls	SFF SCANDINAVIAN FITTINGS & FL	140080 REV.02 of 29/06/2007

Si certifica che i materiali sotto elencati sono stati fabbricati e controllati e risultano conformi all'ordine del cliente e alle specifiche richiamate.
We hereby certify that the materials listed here below have been fabricated and inspected and are in compliance with the purchase order and relevant specification.

9) The pipes are in white pickled and passivated condition.
10) No weld repairs have been performed.
11) PMI 100%: Passed
12) Flattening test : Passed
13) ASTM A790-05b UNS S32760

IBF S.p.A.
R. Q...
QC INSPECTOR
06/11/07

IBF's authorized inspection representative	Purchaser's authorized inspection representative	Inspector designated by the official regulations
PREPARED BY: Nicola Lanci / QC INSPECTOR CHECKED BY:		

FORONI S.p.A.
21055 Gorla Minore (VA)
Italia

Brand

CERTIFIED MATERIAL TEST REPORT

Inspection certificate EN 10204-3.1

Cert. n° 2007/1852
Rev. 0
Date 25/6/2007
Sheet: 4

Order n°: 2007000242 + Order confirmation 2007/010114
Delivery condition: Forged, mill annealed and peeled.

Customer IBF SPA
Material: F55; UNS S32760.

Specifications: ASTM A479-06a (chemistry only).

AOD / VIDP n°	04335
VAR / ESR n°	
Steel making process:	E.F./A.O.D.

Heat Treatment: Lot n°: CTT n°:

Description:	Size	Length
Round bar	273 mm	mm

N° of pieces	Weight	Bar identification:	Forging ratio:
10	38580 Kg		5.5

Chemical analysis

% w	Heat	Product
C	0,016	✓
MN	0,58	✓
SI	0,52	✓
CR	25,47	✓
NI	6,92	✓
MO	3,64	✓
S	0,0002	✓
P	0,0230	✓
CU	0,55	✓
N	0,253	
W	0,64	
PRE	41,53	

Mechanical properties

		Test n°	5104	5104	5105	5105
	Type		[1] see remarks	[1] see remarks	[1] see remarks	[1] see remarks
Tensile properties	Position		30 mm B.S.	30 mm B.S.	30 mm B.S.	30 mm B.S.
	Direction		TRV	TRV	TRV	TRV
	Temperature	°C	20	121	20	121
	Y.S. 0,2%	MPa	599	496	604	483
	Y.S. 1%	MPa				
	U.T.S.	MPa	804	724	819	723
	Elongation	%	4D 35,3	4D 41,8	4D 36,7	4D 40,5
	Red. of Area	%	67,3	69,0	65,1	67,0
	Hardness	HB	255		262	
		HRC	21		21	
	as delivered	HRC				
Impact properties	Position		30 mm B.S.		30 mm B.S.	
	Direction		LNG		LNG	
	Temperature	°C	-46		-46	
	Charpy A	J	129		127	
			132		136	
			126		152	
	Lateral expansion	mm				
	Shear	%				
Stress-rupt.	Temperature	°C				
	Load	MPa				
	Load Increm.					
	Duration	hours				
	Elongation	%				

Other properties

	Specification:	Description:	Results:
Grain size			
[1] Ferrite content to	ASTM E562		48 % (Test n° 5104) 48 % (Test n° 5105)
[1] Corrosion test to	ASTM G48 Method A	(50°C x 24h)	Passed (Test n° 5104) Passed (Test n° 5105)
Macro examination			
[1] Microstructure test to ASTM E407 etchant #98: free from intermetallic phases and precipitates (Test n° 5104 & 5105)			
Inclusional content			
UT to	ASTM A745	QL2	Passed
Visual check			Passed
Dimensional check			Passed
P.M.I. check			Passed
Fatigue testing			

Remarks: *Material not intended for use in ... applications.*
-[1] Capability test on specimen solution annealed at 1100°C ... removed from bar prolongation.

IBF S.p.A.
10/09/07

Unless otherwise stated, listed specifications apply in the latest edition.

Material made in Italy. ***No welds, no mercury and radioactive contamination.***

The material is in compliance with the mentioned specifications. Material produced according to the Quality System described in the FORONI S.p.A. MSQ Manual.

Quality System Manual	S.C.Q. Department	R.S.Q. Inspector
MSQ Ed. 2003 Rev. 0	M.Gallina M. Gallina	[signature]

FORONI S.p.A. 21055 Gorla Minore (VA) Italia	Brand		MICROGRAPHIC EXAMINATION	Cert. n° 2007/1652 Rev. 0 Date 28/8/2007 Annex A

Center	Mid-radius	Surface
	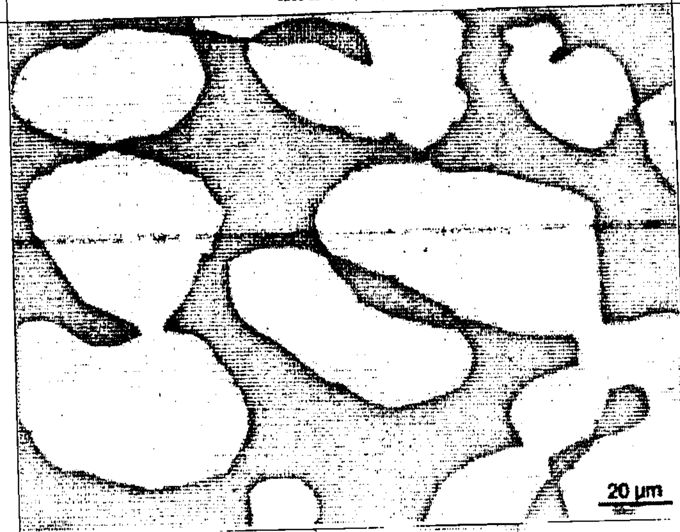	
	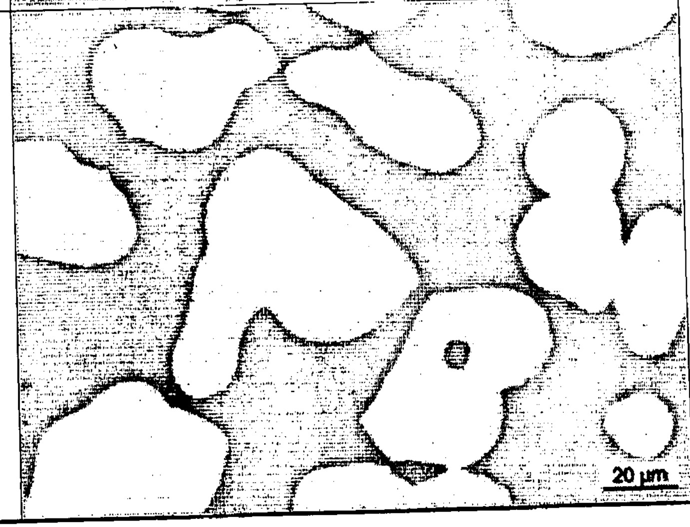	IBE S.p.A. F.CERAULO QC INSPECTOR 10/09/07

The microstructure is free from intermetallic phases and precipitates.

S.C.Q. Department	R.S.Q. Inspector
S.Pivotto	V.Gallazzi

FORONI S.p.A.
21055 Gorla Minore (VA)
Italia

Brand

CERTIFIED MATERIAL TEST REPORT

Inspection certificate EN 10204-3.1

Cert. n°: 2007/1853
Rev. 0
Date 25/6/2007
Item: 4

Order n°: 2007000242 + Order confirmation 2007/070114
Delivery condition: Forged, mill annealed and peeled.

Customer IBF SPA
Material: F55; UNS S32760.

Specifications: ASTM A479-06a (chemistry only).

AOD / VIDP n° 04336
VAR / ESR n°
Steel making process: E.F./A.O.D.

Heat Treatment: **Lot n°:** **CTT n°:**

Description: Round bar | **Size** 273 mm | **Length** mm
N° of pieces 2 | **Weight** 7665 Kg | **Bar identification:** | **Forging ratio:** 5,5

Chemical analysis

% w	Heat	Product
C	0,015	
MN	0,60	
SI	0,50	
CR	25,43	
NI	6,96	
MO	3,69	
S	0,0002	
P	0,0260	
CU	0,57	
N	0,249	
W	0,65	
PRE	41,59	

Mechanical properties

			5106	5106	5107	5107
Test n°	Type		[1] see remarks	[1] see remarks	[1] see remarks	[1] see remarks
Tensile properties	Position		30 mm B.S.	30 mm B.S.	30 mm B.S.	30 mm B.S.
	Direction		TRV	TRV	TRV	TRV
	Temperature	°C	20	121	20	121
	Y.S. 0,2%	MPa	605	491	610	475
	Y.S. 1%	MPa				
	U.T.S.	MPa	809	722	818	724
	Elongation	%	4D 33,6	4D 38,6	4D 35,6	4D 39,5
	Red. of Area	%	64,9	65,4	61,5	61,3
	Hardness	HB	255		262	
		HRC	21		21	
	as delivered	HRC				
Impact properties	Position		30 mm B.S.		30 mm B.S.	
	Direction		LNG		LNG	
	Temperature	°C	-46		-46	
	Charpy A	J	99		192	
			177		186	
			173		182	
	Lateral expansion	mm				
	Shear	%				
Stress-rupt.	Temperature	°C				
	Load	MPa				
	Load increm.					
	Duration	hours				
	Elongation	%				

Other properties

Description	Specification		Results
Grain size			
[1] Ferrite content to	ASTM E562		49 % (Test n° 5106) 48 % (Test n° 5107)
[1] Corrosion test to	ASTM G48 Method A	(50°C x 24h)	Passed (Test n° 5106) Passed (Test n° 5107)
Macro examination			
[1] Microstructure test to ASTM E407 etchant #98: free from intermetallic phases and precipitates (Test n° 5106 & 5107)			
Inclusional content			
UT to	ASTM A745	QL2	Passed
Visual check			Passed
Dimensional check			Passed
P.M.I. check			Passed
Fatigue testing			

Remarks: ***Material not intended for use in aerospace/aircraft applications.***
- [1] Capability test on specimen solution annealed at 1100°C - W.Q. removed from bar prolongation.

IDF SPA
A.CALLATERRA
QC INSPECTOR
28/09/07
Calla...

Unless otherwise stated, listed specifications apply in the latest edition.

Material made in Italy. ***No welds, no mercury and radioactive contamination.***

The material is in compliance with the mentioned specifications. Material produced according to the Quality System described in the FORONI S.p.A. MSQ Manual.

Quality System Manual	S.C.Q. Department	R.S.Q. Inspector
MSQ Ed. 2003 Rev. 0	M.Gallina M. Gallina	Gallazzi

Mod. 46 Rev. 2

FORONI S.p.A.
21055 Gorla Minore (VA)
Italia

Brand

MICROGRAPHIC EXAMINATION

Cert. n° 2007/1653
Rev. 0
Date 25/6/2007
Annex A

Center	Mid-radius	Surface
		
		

The microstructure is free from intermetallic phases and precipitates.

IBF SPA
A. CALCATERRA
QC INSPECTOR
28/09/07

S.C.Q. Department	R.S.Q. Inspector
S.Pivotto	F.Gallazzi

FORONI S.p.A.
21055 Gorla Minore (VA)
Italia

Brand

CERTIFIED MATERIAL TEST REPORT

Inspection certificate EN 10204-3.1

Cert. n° 2007/1891
Rev. 0
Date 28/6/2007

Order n°: 2007000242 + *Order confirmation* 2007/070114 — **Item:** 4
Delivery condition: Forged, mill annealed and peeled.

Customer IBF SPA
Material: F55; UNS S32760.

Specifications: ASTM A479-06a (chemistry only).

AOD / VIDP n° 04327
VAR / ESR n°
Steel making process: E.F./A.O.D.

Heat Treatment: — **Lot n°:** — **CTT n°:**

Description: Round bar — **Size** 273 mm — **Length** mm
N° of pieces 6 — **Weight** 22765 Kg — **Bar identification:** — **Forging ratio:** 5,5

Chemical analysis

% w	Heat	Product
C	0,016	
MN	0,55	
SI	0,49	
CR	25,50	
NI	7,00	
MO	3,67	
S	0,0002	
P	0,0250	
CU	0,54	
N	0,245	
W	0,65	
PRE	41,53	

Mechanical properties

		Test n°	5056	5056	5057	5057
	Type		[1] see remarks	[1] see remarks	[1] see remarks	[1] see remarks
Tensile properties	Position		30 mm B.S.	30 mm B.S.	30 mm B.S.	30 mm B.S.
	Direction		TRV	TRV	TRV	TRV
	Temperature	°C	20	121	20	121
	Y.S. 0,2%	MPa	591	473	617	484
	Y.S. 1%	MPa				
	U.T.S.	MPa	807	718	825	719
	Elongation	%	4D 35,9	4D 37,3	4D 32,8	4D 37,4
	Red. of Area	%	60,4	64,2	65,3	64,6
	Hardness	HB	255		262	
		HRC	21		22	
	as delivered	HRC				
Impact properties	Position		30 mm B.S.		30 mm B.S.	
	Direction		LNG		LNG	
	Temperature	°C	-46		-46	
	Charpy A	J	134		106	
			101		134	
			102		116	
	Lateral expansion	mm				
	Shear	%				
Stress-rupt.	Temperature	°C				
	Load	MPa				
	Load Increm.					
	Duration	hours				
	Elongation	%				

Other properties

	Specification:	Description:	Results:
Grain size			
[1] Ferrite content to	ASTM E562		50 % (Test n° 5056) 51 % (Test n° 5057)
[1] Corrosion test to	ASTM G48 Method A	(50°C x 24h)	Passed (Test n° 5056) Passed (Test n° 5057)
Macro examination			
[1] Microstructure test to ASTM E407 etchant #98: free from intermetallic phases and precipitates (Test n° 5056 & 5057)			
Inclusional content			
UT to	ASTM A745	QL2	Passed
Visual check			Passed
Dimensional check			Passed
P.M.I. check			Passed
Fatigue testing			

Remarks: ***Material not intended for use in aerospace/aircraft applications.***
- [1] Capability test on specimen solution annealed at 1100°C - W.Q. removed from bar prolongation.

Unless otherwise stated, listed specifications apply in the latest edition.

Material made in Italy. ***No welds, no mercury and radioactive contamination.***

The material is in compliance with the mentioned specifications. Material produced according to the Quality System described in the FORONI S.p.A. MSQ Manual.

Quality System Manual	S.C.Q. Department	R.S.Q. Inspector
MSQ Ed. 2003 Rev. 0	M.Gallina M. Gallina	L.Gallazzi

Mod. 48 Rev. 2

FORONI S.p.A.
21055 Gorla Minore (VA)
Italia

Brand

MICROGRAPHIC EXAMINATION

Cert. n° 2007/1891
Rev. 0
Date 28/6/2007
Annex A

	Center	Mid-radius	Surface
500 x (Test n° 5056)		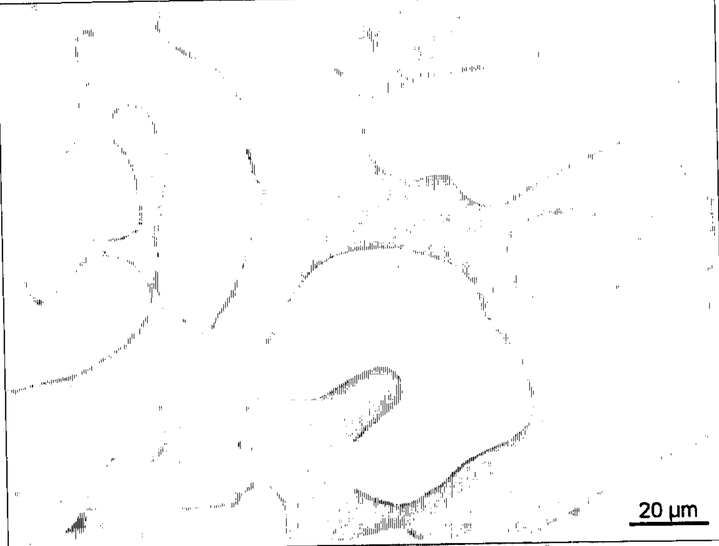	
500 x (Test n° 5057)		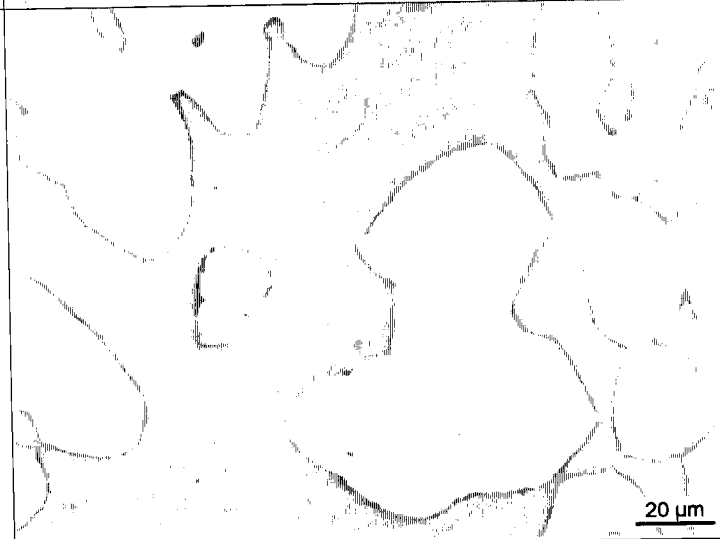	

The microstructure is free from intermetallic phases and precipitates.

S.C.Q. Department
S.Pivotto

R.S.Q. Inspector
F.Gallazzi

FORONI S.p.A.

21055 Gorla Minore (VA)
Italia

Brand

CERTIFIED MATERIAL TEST REPORT

Inspection certificate EN 10204-3.1

Cert. n. 2007/2264
Rev. 0
Date 27/7/2007

Order n°: 2007000242 + *Order confirmation* 2007 070114 **Item:** 5
Delivery condition: Forged, mill annealed and peeled

Customer IBF SPA
Material: F55 UNS S32760

Specifications: ASTM A479-06a (chemistry only)

AOD / VIDP n° 04354
VAR / ESR n°
Steel making process: E.F./A.O.D.

Heat Treatment:
Lot n°:
CTT n°:

Description: Round bar
Size 273 mm
Length mm
N° of pieces 6
Weight 23230 Kg
Bar identification:
Forging ratio: 5,5

Chemical analysis

% w	Heat	Product
C	0,014	
MN	0.51	
SI	0.50	
CR	25.40	
NI	7.02	
MO	3.65	
S	0.0003	
P	0.0260	
CU	0.54	
N	0.255	
W	0.65	
PRE	41.53	

Mechanical properties

	Test n		5209	5209	5210	5210
	Type		* see remarks	* see remarks	* see remarks	* see remarks
Tensile properties	Position		30 mm B.S.	30 mm B.S.	30 mm B.S.	30 mm B.S.
	Direction		TRV	TRV	TRV	TRV
	Temperature	°C	20	121	20	121
	Y.S. 0.2%	MPa	594	471	589	486
	Y.S. 1%	MPa				
	U.T.S.	MPa	816	725	823	739
	Elongation	%	4D 36.1	4D 39.3	4D 36.8	4D 39.1
	Red. of Area	%	60.7	62.9	61.5	65.2
	Hardness	HB	262		262	
		HRC	21		22	
	as delivered	HRC				
Impact properties	Position		30 mm B.S.		30 mm B.S.	
	Direction		LNG		LNG	
	Temperature	°C	46		46	
	Charpy A	J	166		160	
			169		118	
			129		164	
	Lateral expansion	mm				
	Shear	%				
Stress-rupt.	Temperature	°C				
	Load	MPa				
	Load Increm.					
	Duration	hours				
	Elongation	%				

Other properties

	Specification	Description	Results
Grain size			
* Ferrite content to	ASTM E562		48 % (Test n° 5209) 49 % (Test n° 5210)
* Corrosion test to	ASTM G48 Method A	(50°C x 24h)	Passed (Test n° 5209) Passed (Test n° 5210)
Macro examination			
* Microstructure test to ASTM E407 etchant #98: free from intermetallic phases and precipitates (Test n° 5209 & 5210)			
Inclusional content			
UT to	ASTM A745	QL2	Passed
Visual check			Passed
Dimensional check			Passed
P.M.I. check			Passed
Fatigue testing			

Remarks: **Material not intended for use in aerospace/aircraft applications.**
* Capability test on specimen solution annealed at 1100°C W.Q. removed from bar prolongation

IBF S.p.A
QC REVIEWED
Date: 10/10/07

Unless otherwise stated, listed specifications apply in the latest edition.

Material made in Italy. **No welds, no mercury and radioactive contamination.**

The material is in compliance with the mentioned specifications. Material produced according to the Quality System described in the FORONI S.p.A. MSQ Manual.

Quality System Manual
MSQ Ed. 2003 Rev. 0

S.C.Q. Department
M. Gallina
M. Gallina

R.S.Q. Inspector

FORONI S.p.A.
21055 Gorla Minore (VA)
Italia

Brand

MICROGRAPHIC EXAMINATION

Cert n: 2007/2264
Rev. 0
Date 27/7/2007
Annex A

Center	Mid-radius	Surface

500 x (Test n° 5209)

20 µm

500 x (Test n° 5210)

20 µm

IBF S.p.A
QC REVIEWED
Date: 10/10/07

The microstructure is free from intermetallic phases and precipitates.

S.C.Q. Department	R.S.Q. Inspector
S. Pivotto	Y. Gallazzi

FORONI S.p.A.
21055 Gorla Minore (VA)
Italia

Brand

CERTIFIED MATERIAL TEST REPORT

Inspection certificate EN 10204-3.1

Cert. n° 2007 2265
Rev. 0
Date 27/7/2007

Order n°: 2007000242 + *Order confirmation* 2007/070114 **Item:** 5
Delivery condition: Forged, mill annealed and peeled

Customer IBF SPA
Material: F55; UNS S32760

Specifications: ASTM A479 06a (chemistry only)

AOD / VIDP n° 04347
VAR / ESR n°
Steel making process: E.F./A.O.D.

Heat Treatment: | **Lot n°:** | **CTT n°:**

Description: Round bar | **Size** 273 mm | **Length** mm
N° of pieces 10 | **Weight** 37935 Kg | **Bar identification:** | **Forging ratio:** 4,6

Chemical analysis

% w	Heat	Product
C	0.014	
MN	0.50	
SI	0.47	
CR	25.50	
NI	7.03	
MO	3.63	
S	0.0002	
P	0.0240	
CU	0.53	
N	0.261	
W	0.64	
PRE	41.66	

Mechanical properties

	Test n°		5173	5173	5174	5174
	Type		* see remarks	* see remarks	* see remarks	* see remarks
Tensile properties	Position		30 mm B S	30 mm B S	30 mm B S	30 mm B S
	Direction		TRV	TRV	TRV	TRV
	Temperature	°C	20	121	20	121
	Y.S. 0.2%	MPa	582	483	591	470
	Y.S. 1%	MPa				
	U.T.S.	MPa	809	724	809	723
	Elongation	%	4D 35.2	4D 38.2	4D 36.6	4D 38.0
	Red. of Area	%	65.3	67.0	64.6	63.7
	Hardness	HB	255		255	
		HRC	21		21	
	as delivered	HRC				
Impact properties	Position		30 mm B S		30 mm B S	
	Direction		LNG		LNG	
	Temperature	°C	-46		46	
	Charpy A	J	102		125	
			86		110	
			122		111	
	Lateral expansion	mm				
	Shear	%				
Stress-rupt.	Temperature	C				
	Load	MPa				
	Load Increm					
	Duration	hours				
	Elongation	%				

Other properties

	Specification	Description	Results
Grain size			
* Ferrite content to	ASTM E562		47 % (Test n° 5173) 52 % (Test n° 5174)
* Corrosion test to	ASTM G48 Method A	(50°C x 24h)	Passed (Test n° 5173) Passed (Test n° 5174)
Macro examination			
* Microstructure test to ASTM E407 etchant #98 free from intermetallic phases and precipitates (Test n° 5173 & 5174)			
Inclusional content			
UT to	ASTM A745	QL2	Passed
Visual check			Passed
Dimensional check			Passed
P.M.I. check			Passed
Fatigue testing			

Remarks: **Material not intended for use in aerospace/aircraft applications.**
* Capability test on specimen solution annealed at 1100°C W.Q. removed from bar prolongation

IBF S.p.A
QC REVIEWED
Date: 10/10/07

Unless otherwise stated, listed specifications apply in the latest edition.

Material made in Italy. **No welds, no mercury and radioactive contamination.**

The material is in compliance with the mentioned specifications. Material produced according to the Quality System described in the FORONI S.p.A. MSQ Manual.

Quality System Manual	S.C.Q. Department	R.S.Q. Inspector
MSQ Ed. 2003 Rev. 0	M Gallina M. Gallina	Gallazzi

FORONI S.p.A.
21055 Gorla Minore (VA)
Italia

Brand

MICROGRAPHIC EXAMINATION

Cert. n° 2007/2265
Rev. 0
Date 27/7/2007
Annex A

	Center	Mid-radius	Surface
500 x (Test n° 5173)		20 µm	
500 x (Test n° 5174)		20 µm	

IBF S.p.A
QC REVIEWED
Date: 10/10/07

The microstructure is free from intermetallic phases and precipitates.

S.C.Q. Department	R.S.Q. Inspector
S. Pivotto	V. Gallazzi

ANCCP
Agenzia Nazionale Certificazione Componenti e Prodotti

Laboratorio T.O.S.I. s.r.l.

Tecnici Organizzati al Servizio delle Imprese

Sede legale e Uffici: 20025 Legnano (MI) - Via Pisacane, 46 - Tel. 0331.487210 - Fax 0331.522970
Sede operativa: 20025 Legnano (MI) - P.zza Monumento, 12 - Tel. 0331.522374-3 - Fax 0331.522462
Internet: www.laboratoriotosi.it - E-mail: labtosi@tiscalinet.it - Partita IVA e Codice Fiscale 12805730152

Laboratorio di Prova Approvato
Attestato N. 004 L
QUA 041 S

Ordine n° 570/07 **del** 08/10/07 **Rapporto di prova n°** 07P4676
Order no. of Test report no.

Cliente: IBF spa **Bolla n°** # **del** # **Data** 12/10/07
Customer Delivery note of date

Colata n°. 04327 **Materiale** ASTM A 790 UNS S32760 **Foglio** 1 **di** 1
Heat no. Material page of

Materiale ricevuto in data: # — Material recived on
Prove eseguite in data: 12/10/07 — Tests date

Macchina di prova / Test Machine						
		T1 Vickers Matsuzawa		T4 Galdabini 294J		T7 Rockwell Digi 25R
	X	T2 Brinell Wolpert	X	T5 Mohr & Federhaff 100KN		T8 Rockwell Galileo
	X	T3 Tinius Olsen 358J	X	T6 Mohr & Federhaff 600KN		

Q.tà prove (Tests q.ty)	Descrizione delle prove richieste e del materiale (Required tests and material description)
	N.3 Pipes O.D. 10" sch. 120 lot H100000244 sample **5551**
	P.O. 140080 rev.1
1	Longitudinal tensile test at room temperature according to ASTM E8 (5551-1)
1	Long. Elevated temperature tensile test at 121°C, according to ASTM E21 (5551-2)
3	Longitudinal Charpy V Notch impact test at -46°C, according to ASTM E23. (5551-3).
3	Brinell hardness test HB, according to ASTM E10.

Valori richiesti - Required

n°	Contrassegno (Specimens no. or marks)	Temp. °C	Snerv./Scost. Y.stress/strength Rs Mpa	Rottura Tensile strength Rm Mpa	Allungamento Elongation A4 %	Strizione Red. of area Z %	Resilienza KV Unitaria - Single J	Resilienza KV Media - Average J	Durezza Hardness HB	Piega Bend α/D
	5551	20	>=550	>=750	>=25				<=270	
		121	>=470							
		-46					>=35	>=45		

Valori ottenuti - Obtained

Prov. n°. Specimens no.	Forma Shape De mm X mm Di	Sez. Section mm^2	°C	Rp 0,2% Mpa	Rm Mpa	A4 %	Z %	Unitaria - Single J			Media - Average J	HB		
5551-1	Ø12,5	122,7	20	628,5	802,7	35,2						263	265	262
5551-2	Ø12,5	122,7	121	538,5										
5551-3	10,0 x 10		-46					50	48	71	56,3			

Osservazioni:
Remarks:

IBF S.p.A
N. LANCI
Q.C.

I risultati del rapporto di prova si riferiscono ai soli campioni testati
Test report values relate to the tested specimens only

Ente Autorizzato / Authorized Inspector	Esecutore / Examiner	Responsabile Laboratorio / Laboratory Responsible
☐ REV. ☐ WIT. WILDES CALLINI		

ANCCP
Agenzia Nazionale Certificazione Componenti e Prodotti

Laboratorio T.O.S.I. s.r.l.

Tecnici Organizzati al Servizio delle Imprese

Sede legale e Uffici: 20025 Legnano (MI) - Via Pisacane, 46 - Tel. 0331.487210 - Fax 0331.522970
Sede operativa: 20025 Legnano (MI) - P.zza Monumento, 12 - Tel. 0331.522374-3 - Fax 0331.522462
Internet: www.laboratoriotosi.it - E-mail: labtosi@tiscalinet.it - Partita IVA e Codice Fiscale 12805730152

Laboratorio di Prova Approvato
IIS
Attestato N. 004 L
QUA 041 S

Ordine n° 571/07 **del** 08/10/07 **Rapporto di prova n°** 07P4679
Order no. of Test report no.

Cliente: IBF spa **Bolla n°** # **del** # **Data** 15/10/07
Customer Delivery note of date

Colata n°. 04336 **Materiale** ASTM A 790 UNS S32760 **Foglio** 1 **di** 1
Heat no. Material page of

Materiale ricevuto in data: #
Material recived on

Prove eseguite in data: 15/10/07
Tests date

Macchina di prova / Test Machine						
		T1 Vickers Matsuzawa		T4 Galdabini 294J		T7 Rockwell Digi 25R
	X	T2 Brinell Wolpert	X	T5 Mohr & Federhaff 100KN		T8 Rockwell Galileo
	X	T3 Tinius Olsen 358J	X	T6 Mohr & Federhaff 600KN		

Q.tà prove / Tests q.ty	Descrizione delle prove richieste e del materiale / Required tests and material description
	N.5 Pipes O.D. 10" sch. 120 lot H100000242 sample **5512**
	P.O. 140080 rev.1
1	Longitudinal tensile test at room temperature according to ASTM E8 (5512-1)
1	Long. Elevated temperature tensile test at 121°C, according to ASTM E21 (5512-2)
3	Longitudinal Charpy V Notch impact test at -46°C, according to ASTM E23. (5512-3).
3	Brinell hardness test HB, according to ASTM E10.

Valori richiesti - Required

Contrassegno o n° provetta / Specimens no. or marks		Temp.	Snerv./Scost. Y.stress/strength	Rottura Tensile strength	Allungamento Elongation	Strizione Red. of area	Resilienza KV - Impact test KV Unitaria - Single	Media - Average	Durezza Hardness	Piega Bend
n°	Contrassegno	°C	Rs Mpa	Rm Mpa	A4 %	Z %	J	J	HB	α/D
	5512	20	>=550	>=750	>=25				<=270	
		121	>=470							
		-46					>=35	>=45		

Valori ottenuti - Obtained

Prov. n°. Specimens no.	Forma Shape De mm X mm Di	Sez. Section mm²	°C	Rp 0,2% Mpa	Rm Mpa	A4 %	Z %	Unitaria - Single J			Media - Average J	HB		
5512-1	Ø12,5	122,7	20	609,5	803,4	38,4						263	261	263
5512-2	Ø12,5	122,7	121	552,4										
5512-3	10,0 x 10		-46					62	68	70	66,7			

Osservazioni:
Remarks:

IBF S.p.A. N. LANC 2.9.1

I risultati del rapporto di prova si riferiscono ai soli campioni testati
Test report values relate to the tested specimens only

Ente Autorizzato / Authorized Inspector	Esecutore / Examiner	Responsabile Laboratorio / Laboratory Responsible
☐ REV. ☒ WIT. **WILDES CALLINI**		

ANCCP Agenzia Nazionale Certificazione Componenti e Prodotti

Laboratorio T.O.S.I. s.r.l.

Tecnici Organizzati al Servizio delle Imprese

Sede legale e Uffici: 20025 Legnano (MI) - Via Pisacane, 46 - Tel. 0331.487210 - Fax 0331.522970
Sede operativa: 20025 Legnano (MI) - P.zza Monumento. 12 - Tel. 0331.522374-3 - Fax 0331.522462
Internet: www.laboratoriotosi.it - E-mail: labtosi@tiscalinet.it - Partita IVA e Codice Fiscale 12805730152

Laboratorio di Prova Approvato — Attestato N. 004 L — QUA 041 S

Ordine n° 571/07 **del** 08/10/07 **Rapporto di prova n°** 07P4680
Order no. of Test report no.

Cliente: IBF spa **Bolla n°** # **del** # **Data** 15/10/07
Customer Delivery note of date

Colata n°. 04335 **Materiale** ASTM A 790 UNS S32760 **Foglio** 1 **di** 1
Heat no. Material page of

Materiale ricevuto in data: # (Material recived on) — **Prove eseguite in data:** 15/10/07 (Tests date)

Macchina di prova / Test Machine						
		T1 Vickers Matsuzawa		T4 Galdabini 294J		T7 Rockwell Digi 25R
	X	T2 Brinell Wolpert	X	T5 Mohr & Federhaff 100KN		T8 Rockwell Galileo
	X	T3 Tinius Olsen 358J	X	T6 Mohr & Federhaff 600KN		

Q.tà prove (Tests q.ty)	Descrizione delle prove richieste e del materiale (Required tests and material description)
	N.5 Pipes O.D. 10" sch. 120 lot H100000243 sample 5513
	P.O. 140080 rev.1
1	Longitudinal tensile test at room temperature according to ASTM E8 (5513-1)
1	Long. Elevated temperature tensile test at 121°C, according to ASTM E21 (5513-2)
3	Longitudinal Charpy V Notch impact test at -46°C, according to ASTM E23. (5513-3).
3	Brinell hardness test HB, according to ASTM E10.

Valori richiesti - Required

n°	Contrassegno (Specimens no. or marks)	Temp. °C	Snerv./Scost. (Y.stress/strength) Rs Mpa	Rottura (Tensile strength) Rm Mpa	Allungamento (Elongation) A4 %	Strizione (Red. of area) Z %	Resilienza KV - Impact test KV Unitaria - Single J	Media - Average J	Durezza (Hardness) HB	Piega (Bend) α/D
	5513	20	>=550	>=750	>=25				<=270	
		121	>=470							
		-46					>=35	>=45		

Valori ottenuti - Obtained

Prov. n°. (Specimens no.)	Forma (Shape) De mm X mm Di	Sez. (Section) mm²	°C	Rp 0,2% Mpa	Rm Mpa	A4 %	Z %	Unitaria - Single J			Media - Average J	HB		
5513-1	Ø12,5	122,7	20	623,5	810,8	37,6						263	261	263
5513-2	Ø12,5	122,7	121	546,7										
5513-3	10,0 x 10		-46					58	94	67	73,0			

Osservazioni:
Remarks:

IBF S.p.A. N. LANCI Q.C.

I risultati del rapporto di prova si riferiscono ai soli campioni testati
Test report values relate to the tested specimens only

Ente Autorizzato / Authorized Inspector	Esecutore / Examiner	Responsabile Laboratorio / Laboratory Responsible
☐ REV. ☒ WIT. WILDES CALLINI		

ANCCP Agenzia Nazionale Certificazione Componenti e Prodotti

Laboratorio T.O.S.I. s.r.l.

Tecnici Organizzati al Servizio delle Imprese

Sede legale e Uffici: 20025 Legnano (MI) - Via Pisacane, 46 - Tel. 0331.487210 - Fax 0331.522970
Sede operativa: 20025 Legnano (MI) - P.zza Monumento, 12 - Tel. 0331.522374-3 - Fax 0331.522462
Internet: www.laboratoriotosi.it - E-mail: labtosi@tiscalinet.it - Partita IVA e Codice Fiscale 12805730152

Laboratorio di Prova Approvato
Attestato N. 004 L
QUA 041 S

Ordine n° 594/07 **del** 12/10/07 **Rapporto di prova n°** 07P4841
Order no. of Test report no.

Cliente: IBF spa **Bolla n°** # **del** # **Data** 22/10/07
Customer Delivery note of date

Colata n°. 04354 **Materiale** ASTM A 790 UNS S32760 **Foglio** 1 **di** 1
Heat no. Material page of

Materiale ricevuto in data: #
Material recived on

Prove eseguite in data: 22/10/07
Tests date

Macchina di prova / Test Machine

	T1 Vickers Matsuzawa		T4 Galdabini 294J		T7 Rockwell Digi 25R
X	T2 Brinell Wolpert	X	T5 Mohr & Federhaff 100KN		T8 Rockwell Galileo
X	T3 Tinius Olsen 358J	X	T6 Mohr & Federhaff 600KN		

Q.tà prove / Tests q.ty	Descrizione delle prove richieste e del materiale / Required tests and material description
	N.2 Pipes O.D. 10" sch. 120 HT lot.H100000250 sample **5578**
	P.O. 140080 rev.1
1	Longitudinal tensile test at room temperature according to ASTM E8 (5578-1)
1	Long. Elevated temperature tensile test at 121°C, according to ASTM E21 (5578-2)
3	Longitudinal Charpy V Notch impact test at -46°C, according to ASTM E23. (5578-3).
3	Brinell hardness test HB, according to ASTM E10.

Valori richiesti - Required

n°	Contrassegno o n° provetta / Specimens no. or marks	Temp. (°C)	Snerv./Scost. Y.stress/strength Rs Mpa	Rottura Tensile strength Rm Mpa	Allungamento Elongation A4 %	Strizione Red. of area Z %	Resilienza KV Unitaria - Single J	Resilienza KV Media - Average J	Durezza Hardness HB	Piega Bend α/D
	5578	20	>=550	>=750	>=25				<=270	
		121	>=470							
		-46					>=35	>=45		

Valori ottenuti - Obtained

Prov. n°. Specimens no.	Forma Shape De mm X mm Di	Sez. Section mm²	°C	Rp 0,2% Mpa	Rm Mpa	A4 %	Z %	Unitaria - Single J			Media - Average J	HB		
5578-1	Ø12,5	122,7	20	569.1	784,6	35,2						248	252	248
5578-2	Ø12,5	122,7	121	488,6										
5578-3	10,0 x 10		-46					103	90	90	94,3			

Osservazioni:
Remarks:

I risultati del rapporto di prova si riferiscono ai soli campioni testati
Test report values relate to the tested specimens only

Ente Autorizzato ☐ REV. ☒ WIT.
Authorized Inspector
WILDES CALLINI

Esecutore
Examiner

Responsabile Laboratorio
Laboratory Responsible

LABORATORIO T.O.S.I.

ANCCP
Agenzia Nazionale Certificazione Componenti e Prodotti

Laboratorio T.O.S.I. s.r.l.

Tecnici Organizzati al Servizio delle Imprese

Sede legale e Uffici: 20025 Legnano (MI) - Via Pisacane, 46 - Tel. 0331.487210 - Fax 0331.522970
Sede operativa: 20025 Legnano (MI) - P.zza Monumento, 12 - Tel. 0331.522374-3 - Fax 0331.522462
Internet: www.laboratoriotosi.it - E-mail: labtosi@tiscalinet.it - Partita IVA e Codice Fiscale 12805730152

Laboratorio di Prova Approvato
Attestato N. 004 L
QUA 041 S

Ordine n° 581/07 **del** 09/10/07 **Rapporto di prova n°** 07P4842
Order no. of Test report no.

Cliente: IBF spa **Bolla n°** # **del** # **Data** 22/10/07
Customer Delivery note of date

Colata n°. 04347 **Materiale** ASTM A 790 UNS S32760 **Foglio** 1 **di** 1
Heat no. Material page of

Materiale ricevuto in data: # (Material recived on) — **Prove eseguite in data:** 22/10/07 (Tests date)

Macchina di prova (Test Machine)						
		T1 Vickers Matsuzawa		T4 Galdabini 294J		T7 Rockwell Digi 25R
	X	T2 Brinell Wolpert	X	T5 Mohr & Federhaff 100KN		T8 Rockwell Galileo
	X	T3 Tinius Olsen 358J	X	T6 Mohr & Federhaff 600KN		

Q.tà prove (Tests q.ty)	Descrizione delle prove richieste e del materiale (Required tests and material description)
	N.3 Pipes O.D. 10" sch. 120 HT lot.H100000245 sample **5567**
	P.O. 140080 rev.1
1	Longitudinal tensile test at room temperature according to ASTM E8 (5567-1)
1	Long. Elevated temperature tensile test at 121°C, according to ASTM E21 (5567-2)
3	Longitudinal Charpy V Notch impact test at -46°C, according to ASTM E23. (5567-3).
3	Brinell hardness test HB, according to ASTM E10.

Valori richiesti - Required

n°	Contrassegno o n° provetta (Specimens no. or marks)	Temp. °C	Snerv./Scost. (Y.stress/strength) Rs Mpa	Rottura (Tensile strength) Rm Mpa	Allungamento (Elongation) A4 %	Strizione (Red. of area) Z %	Resilienza KV Unitaria - Single J	Resilienza KV Media - Average J	Durezza (Hardness) HB	Piega (Bend) α/D
	5567	20	>=550	>=750	>=25				<=270	
		121	>=470							
		-46					>=35	>=45		

Valori ottenuti - Obtained

Prov. n°. (Specimens no.)	Forma (Shape) De mm X mm D.	Sez. (Section) mm^2	°C	Rp 0,2% Mpa	Rm Mpa	A4 %	Z %	Unitaria - Single J			Media - Average J	HB			
5567-1	Ø12,5	122,7	20	571,4	781,8	38,2						243	250	246	
5567-2	Ø12,5	122,7	121	695,6											
5567-3	10,0 x 10		-46					150	200	135	161,7				

Osservazioni:
Remarks:

I risultati del rapporto di prova si riferiscono ai soli campioni testati
Test report values relate to the tested specimens only

Ente Autorizzato Authorized Inspector	**Esecutore** Examiner	**Responsabile Laboratorio** Laboratory Responsible
☐ REV. ☒ WIT. WILDES CALLINI		LABORATORIO T.O.S.I.

ANCCP
Agenzia Nazionale Certificazione Componenti e Prodotti

Laboratorio T.O.S.I. s.r.l.

Tecnici Organizzati al Servizio delle Imprese

Sede legale e Uffici: 20025 Legnano (MI) - Via Pisacane, 46 - Tel. 0331.487210 - Fax 0331.522970
Sede operativa: 20025 Legnano (MI) - P.zza Monumento, 12 - Tel. 0331.522374-3 - Fax 0331.522462
Internet: www.laboratoriotosi.it - E-mail: labtosi@tiscalinet.it - Partita IVA e Codice Fiscale 12805730152

Laboratorio di Prova Approvato
Attestato N. 004 L
QUA 041 S

Ordine n° 581/07 **del** 09/10/07 **Rapporto di prova n°** 07P4843
Order no. of Test report no.

Cliente: IBF spa **Bolla n°** # **del** # **Data** 22/10/07
Customer Delivery note of date

Colata n°. 04354 **Materiale** ASTM A 790 UNS S32760 **Foglio** 1 **di** 1
Heat no. Material page of

Materiale ricevuto in data: #
Material recived on

Prove eseguite in data: 22/10/07
Tests date

Macchina di prova (Test Machine)						
		T1 Vickers Matsuzawa		T4 Galdabini 294J		T7 Rockwell Digi 25R
	X	T2 Brinell Wolpert	X	T5 Mohr & Federhaff 100KN		T8 Rockwell Galileo
	X	T3 Tinius Olsen 358J	X	T6 Mohr & Federhaff 600KN		

Q.tà prove (Tests q.ty)	Descrizione delle prove richieste e del materiale (Required tests and material description)
	N.3 Pipes O.D. 10" sch. 120 HT lot.H100000248 sample **5568**
	P.O. 140080 rev.1
1	Longitudinal tensile test at room temperature according to ASTM E8 (5568-1)
1	Long. Elevated temperature tensile test at 121°C, according to ASTM E21 (5568-2)
3	Longitudinal Charpy V Notch impact test at -46°C, according to ASTM E23. (5568-3).
3	Brinell hardness test HB, according to ASTM E10.

Valori richiesti - Required

Contrassegno o n° provetta (Specimens no. or marks) n°	Contrassegno	Temp. (Temp.) °C	Snerv./Scost. (Y.stress/strength) Rs Mpa	Rottura (Tensile strength) Rm Mpa	Allungamento (Elongation) A4 %	Strizione (Red. of area) Z %	Resilienza KV - Impact test KV Unitaria - Single J	Media - Average J	Durezza (Hardness) HB	Piega (Bend) α/D
	5568	20	>=550	>=750	>=25				<=270	
		121	>=470							
		-46					>=35	>=45		

Valori ottenuti - Obtained

Prov. n°. (Specimens no.)	Forma (Shape) De mm X mm Di	Sez. (Section) mm^2	°C	Rp 0,2% Mpa	Rm Mpa	A4 %	Z %	Unitaria - Single J			Media - Average J	HB			
5568-1	Ø12,5	122,7	20	602,4	803,9	39,2						242	246	246	
5568-2	Ø12,5	122,7	121	497,1											
5568-3	10,0 x 10		-46					100	141	97	112,7				

Osservazioni:
Remarks:

I risultati del rapporto di prova si riferiscono ai soli campioni testati
Test report values relate to the tested specimens only

Ente Autorizzato (Authorized Inspector)	Esecutore (Examiner)	Responsabile Laboratorio (Laboratory Responsible)
☐ REV. ☒ WIT. WILDES CALLINI		

LABORATORIO T.O.S.I. S.r.l.

ANCCP
Agenzia Nazionale Certificazione Componenti e Prodotti

Laboratorio T.O.S.I. s.r.l.

Tecnici Organizzati al Servizio delle Imprese

Sede legale e Uffici: 20025 Legnano (MI) - Via Pisacane, 46 - Tel. 0331.487210 - Fax 0331.522970
Sede operativa: 20025 Legnano (MI) - P.zza Monumento, 12 - Tel. 0331.522374-3 - Fax 0331.522462
Internet: www.laboratoriotosi.it - E-mail: labtosi@tiscalinet.it - Partita IVA e Codice Fiscale 12805730152

Laboratorio di Prova Approvato
Attestato N. 004 L
QUA 041 S

Ordine n° 587/07 **del** 10/10/07 **Rapporto di prova n°** 07P4845
Order no. of Test report no.

Cliente: IBF spa **Bolla n°** # **del** # **Data** 23/10/07
Customer Delivery note of date

Colata n°. 04347 **Materiale** ASTM A 790 UNS S32760 **Foglio** 1 **di** 1
Heat no. Material page of

Materiale ricevuto in data: #
Material recived on

Prove eseguite in data: 23/10/07
Tests date

Macchina di prova / Test Machine						
		T1 Vickers Matsuzawa		T4 Galdabini 294J		T7 Rockwell Digi 25R
	X	T2 Brinell Wolpert	X	T5 Mohr & Federhaff 100KN		T8 Rockwell Galileo
	X	T3 Tinius Olsen 358J	X	T6 Mohr & Federhaff 600KN		

Q.tà prove Tests q.ty	Descrizione delle prove richieste e del materiale Required tests and material description
	N.1 Pipe O.D. 10" sch. 120 HT lot.H100000250 sample **5577**
	P.O. 140080 rev.1
1	Longitudinal tensile test at room temperature according to ASTM E8 (5577-1)
1	Long. Elevated temperature tensile test at 121°C, according to ASTM E21 (5577-2)
3	Longitudinal Charpy V Notch impact test at -46°C, according to ASTM E23. (5577-3).
3	Brinell hardness test HB, according to ASTM E10.

Valori richiesti - Required

n°	Contrassegno o n° provetta / Specimens no. or marks	Temp. °C	Snerv./Scost. Y.stress/strength Rs Mpa	Rottura Tensile strength Rm Mpa	Allungamento Elongation A4 %	Strizione Red. of area Z %	Resilienza KV Unitaria - Single J	Resilienza KV Media - Average J	Durezza Hardness HB	Piega Bend α/D
	5577	20	>=550	>=750	>=25				<=270	
		121	>=470							
		-46					>=35	>=45		

Valori ottenuti - Obtained

Prov. n°. Specimens no.	Forma Shape De mm X mm Di	Sez. Section mm^2	°C	Rp 0,2% Mpa	Rm Mpa	A4 %	Z %	Unitaria - Single J			Media - Average J	HB			
5577-1	Ø12,5	122,7	20	599,6	812,4	39,6						245	242	242	
5577-2	Ø12,5	122,7	121	476,6											
5577-3	10,0 x 10		-46					84	104	85	91,0				

Osservazioni:
Remarks:

I risultati del rapporto di prova si riferiscono ai soli campioni testati
Test report values relate to the tested specimens only

Ente Autorizzato Authorized Inspector	**Esecutore** Examiner	**Responsabile Laboratorio** Laboratory Responsible
☐ REV. ☐ WIT. WILDES CALLINI		

LABORATORIO T.O.S.I. S.R.L.

ANCCP
Agenzia Nazionale Certificazione Componenti e Prodotti

Laboratorio T.O.S.I. s.r.l.

Tecnici Organizzati al Servizio delle Imprese

Sede legale e Uffici: 20025 Legnano (MI) - Via Pisacane, 46 - Tel. 0331.487210 - Fax 0331.522970
Sede operativa: 20025 Legnano (MI) - P.zza Monumento, 12 - Tel. 0331.522374-3 - Fax 0331.522462
Internet: www.laboratoriotosi.it - E-mail: labtosi@tiscalinet.it - Partita IVA e Codice Fiscale 12805730152

Laboratorio di Prova Approvato
Attestato N. 004 L
QUA 041 S

	Ordine n° Order no. 581/07 **del** of 09/10/07	**Rapporto di prova n°** Test report no. 07H2368
Cliente: Customer IBF SpA	**Bolla n°** Delivery note **del** of	**Data** date 18/10/07
Colata n°. Heat no. 04347	**Materiale** Material ASTM A790 UNS S32760	**Foglio** page 1 **di** of 3

Materiale ricevuto Material recived on .... **Prove eseguite** Tests date 18/10/07

ESAME MICROGRAFICO

Micrographic Examination

Sample No. **5567,** item 1 - P.O. 140080 rev.1

N. 3 Pipes OD 10" sch 120 HT Lot H100000245

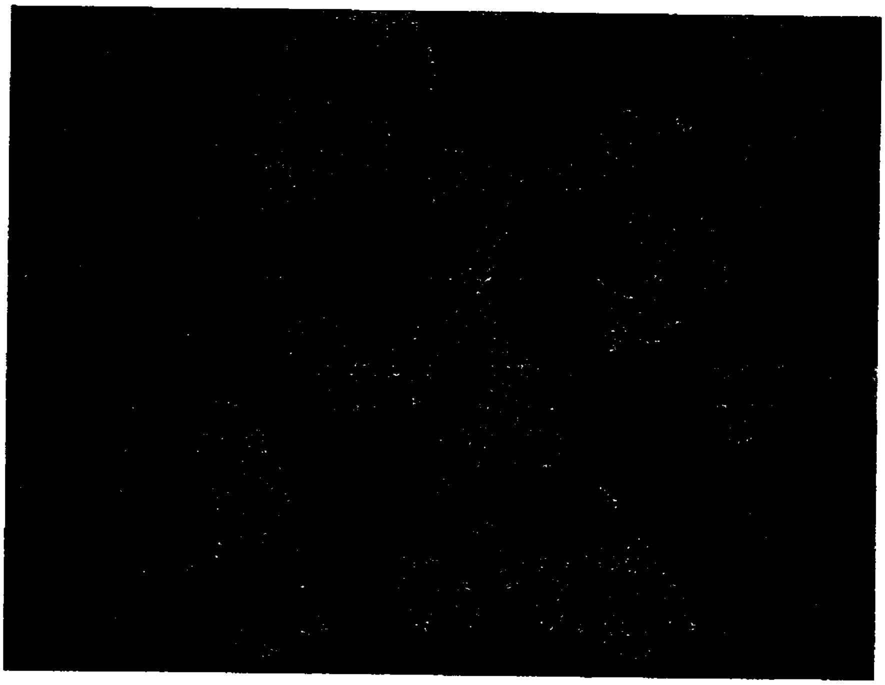

fig. 1 Magnification : 500 X

Micrographic Examination *(Esternal surface)* **: Satisfactory**

The grain boundaries are free of carbide precipitation and intermetallic phase

ASTM E562 - Determining volume fraction of ferrite = 48,4 %

Intervallo di confidenza: 0,82 Confidence interval	**Errore % : 2,24** % Error	**Deviazione standard : 2,97** Standard deviation
Campi esaminati N°: 30 Examinated fields N°	**Dimensione griglia : 30 points** Dimension grille	**Attacco: ASTM E407 # 98** Etching

I risultati del rapporto di prova si riferiscono ai soli campioni testati
Test report values relate to the tested specimen only

Ente Autorizzato Authorized Inspector ☑ REV. ☐ WIT. WILDES CALLINI	**Esecutore** Examiner	**Responsabile Laboratorio** Laboratory Responsible

ANCCP
Agenzia Nazionale Certificazione Componenti e Prodotti

Laboratorio T.O.S.I. s.r.l.

Tecnici Organizzati al Servizio delle Imprese

Sede legale e Uffici: 20025 Legnano (MI) - Via Pisacane, 46 - Tel. 0331.487210 - Fax 0331.522970
Sede operativa: 20025 Legnano (MI) - P.zza Monumento, 12 - Tel. 0331.522374-3 - Fax 0331.522462
Internet: www.laboratoriotosi.it - E-mail: labtosi@tiscalinet.it - Partita IVA e Codice Fiscale 12805730152

Laboratorio di Prova Approvato
Attestato N. 004 L
QUA 041 S

Ordine n° Order no. 581/07 **del** of 09/10/07 **Rapporto di prova n°** Test report no. **07H2368**

Cliente: Customer IBF SpA **Bolla n°** Delivery note .... **del** of .... **Data** date 18/10/07

Colata n°. Heat no. 04347 **Materiale** Material ASTM A790 UNS S32760 **Foglio** page 2 **di** of 3

Materiale ricevuto Material recived on .... **Prove eseguite** Tests date 18/10/07

ESAME MICROGRAFICO

Micrographic Examination

Sample No. **5567**, item 1 - P.O. 140080 rev.1

N. 3 Pipes OD 10" sch 120 HT Lot H100000245

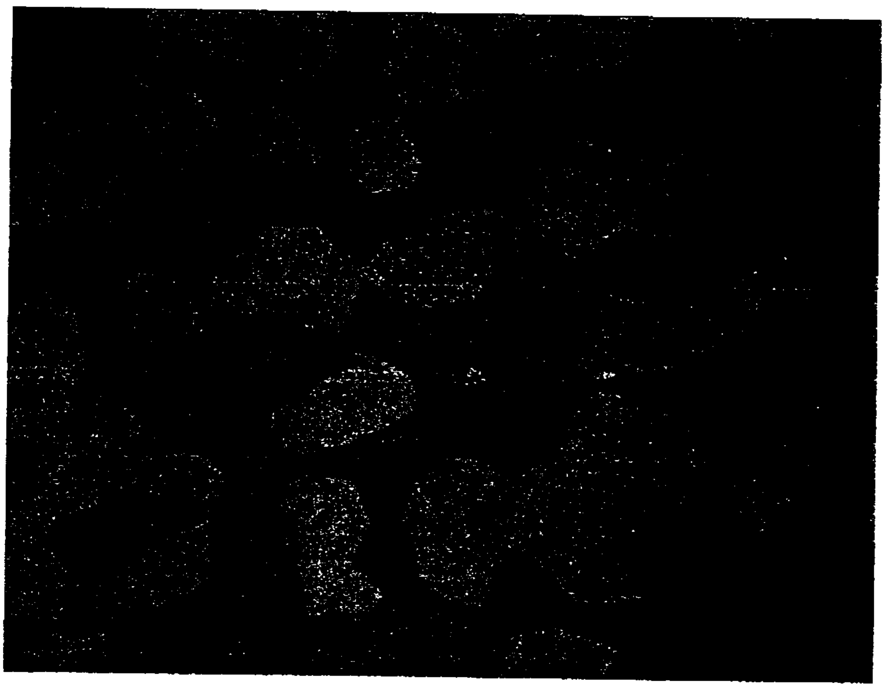

fig. 2 Magnification : 500 X

Micrographic Examination *(Half thickness)* **: Satisfactory**

The grain boundaries are free of carbide precipitation and intermetallic phase

ASTM E562 - Determining volume fraction of ferrite = 47,4 %

Intervallo di confidenza : 0,82 Confidence interval	**Errore % : 1,73** % Error	**Deviazione standard : 2,25** Standard deviation
Campi esaminati N°: 30 Examined fields N°	**Dimensione griglia : 30 points** Dimension grille	**Attacco: ASTM E407 # 98** Etching

I risultati del rapporto di prova si riferiscono ai soli campioni testati
Test report values relate to the tested speciment only

Ente Autorizzato ☒ REV. ☐ WIT. Authorized Inspector WILDES CALLINI Callini	Esecutore Examiner MBaldrello	Responsabile Laboratorio Laboratory Responsible

LABORATORIO T.O.S.I. SRL

ANCCP
Agenzia Nazionale Certificazione Componenti e Prodotti

Laboratorio T.O.S.I. s.r.l.

Tecnici Organizzati al Servizio delle Imprese

Sede legale e Uffici: 20025 Legnano (MI) - Via Pisacane, 46 - Tel. 0331.487210 - Fax 0331.522970
Sede operativa: 20025 Legnano (MI) - P.zza Monumento, 12 - Tel. 0331.522374-3 - Fax 0331.522462
Internet: www.laboratoriotosi.it - E-mail: labtosi@tiscalinet.it - Partita IVA e Codice Fiscale 12805730152

Laboratorio di Prova Approvato
Attestato N. 004 L

		Ordine n° Order no.	581/07 **del** of 09/10/07	**Rapporto di prova n°** Test report no.	**07H2368**
Cliente: Customer	**IBF** SpA	**Bolla n°** Delivery note	**del** of	**Data** date	18/10/07
Colata n°. Heat no.	04347	**Materiale** Material	ASTM A790 UNS S32760	**Foglio** page	3 **di** of 3

Materiale ricevuto Material recived on .... **Prove eseguite** Tests date 18/10/07

ESAME MICROGRAFICO

Micrographic Examination

Sample No. **5567,** item 1 - P.O. 140080 rev.1

N. 3 Pipes OD 10" sch 120 HT Lot H100000245

fig. 3 Magnification : 500 X

Micrographic Examination *(Internal surface)* **: Satisfactory**

The grain boundaries are free of carbide precipitation and intermetallic phase

ASTM E562 - Determining volume fraction of ferrite = 48,0 %

Intervallo di confidenza: 0,75 Confidence interval	**Errore % : 1,56** % Error	**Deviazione standard : 2,06** Standard deviation
Campi esaminati N°: 30 Examinated fields N°	**Dimensione griglia : 30 points** Dimension grille	**Attacco: ASTM E407 # 98** Etching

I risultati del rapporto di prova si riferiscono ai soli campioni testati
Test report values relate to the tested specimen only

Ente Autorizzato Authorized Inspector ☑ REV. ☐ WIT. WILDES CALLINI	**Esecutore** Examiner M Bardello	**Responsabile Laboratorio** Laboratory Responsible

LABORATORIO T.O.S.I.

ANCCP
Agenzia Nazionale Certificazione Componenti e Prodotti

Laboratorio T.O.S.I. s.r.l.

Tecnici Organizzati al Servizio delle Imprese

Sede legale e Uffici: 20025 Legnano (MI) - Via Pisacane, 46 - Tel. 0331.487210 - Fax 0331.522970
Sede operativa: 20025 Legnano (MI) - P.zza Monumento, 12 - Tel. 0331.522374-3 - Fax 0331.522462
Internet: www.laboratoriotosi.it - E-mail: labtosi@tiscalinet.it - Partita IVA e Codice Fiscale 12805730152

Laboratorio di Prova Approvato
Attestato N. 004 L
QUA 041 S

Annex cert. 07H2368

DETERMINAZIONE METALLOGRAFICA DELLA FERRITE ASTM E562

FERRITE VOLUME FRACTION METALLOGRAPHIC DETERMINATION ASTM E562

Sample No. **5567**, item 1 *Esternal surface*

N° FIELDS	1	2	3	4	5	6	7	8	9	10	11	12	13	14	15
POINT COUNT	14	15	14	13	14	16	15	14	16	16	14	15	15	16	16
POINT FRACT.	46,7	50,0	46,7	43,3	46,7	53,3	50,0	46,7	53,3	53,3	46,7	50,0	50,0	53,3	53,3
$(Ppi-Pp)^2$	3,1	2,4	3,1	26,1	3,1	24,0	2,4	3,1	24,0	24,0	3,1	2,4	2,4	24,0	24,0

N° FIELDS	16	17	18	19	20	21	22	23	24	25	26	27	28	29	30
POINT COUNT	14	13	13	14	14	15	14	15	13	15	14	15	15	14	15
POINT FRACT.	46,7	43,3	43,3	46,7	46,7	50,0	46,7	50,0	43,3	50,0	46,7	50,0	50,0	46,7	50,0
$(Ppi-Pp)^2$	3,1	26,1	26,1	3,1	3,1	2,4	3,1	2,4	26,1	2,4	3,1	2,4	2,4	3,1	2,4

Volume % di ferrite riscontrato (vv): 48,4
Volume frction of the ferrite

Errore% / % Error	Intervallo di confidenza / Confidence interval	Deviazione standard / Standard deviation
2,242	1,086	2,974

Sample No. **5567**, item 1 *Half thickness*

N° FIELDS	1	2	3	4	5	6	7	8	9	10	11	12	13	14	15
POINT COUNT	14	14	13	15	13	14	14	15	13	15	14	13	14	15	14
POINT FRACT.	46,7	46,7	43,3	50,0	43,3	46,7	46,7	50,0	43,3	50,0	46,7	43,3	46,7	50,0	46,7
$(Ppi-Pp)^2$	0,6	0,6	16,9	6,6	16,9	0,6	0,6	6,6	16,9	6,6	0,6	16,9	0,6	6,6	0,6

N° FIELDS	16	17	18	19	20	21	22	23	24	25	26	27	28	29	30
POINT COUNT	14	14	15	15	14	15	14	15	14	15	14	15	14	15	14
POINT FRACT.	46,7	46,7	50,0	50,0	46,7	50,0	46,7	50,0	46,7	50,0	46,7	50,0	46,7	50,0	46,7
$(Ppi-Pp)^2$	0,6	0,6	6,6	6,6	0,6	6,6	0,6	6,6	0,6	6,6	0,6	6,6	0,6	6,6	0,6

Volume % di ferrite riscontrato (vv): 47,4
Volume frction of the ferrite

Errore% / % Error	Intervallo di confidenza / Confidence interval	Deviazione standard / Standard deviation
1,735	0,823	2,254

Sample No. **5567**, item 1 *Internal surface*

N° FIELDS	1	2	3	4	5	6	7	8	9	10	11	12	13	14	15
POINT COUNT	14	15	15	15	14	15	14	16	15	15	14	14	15	14	13
POINT FRACT.	46,7	50,0	50,0	50,0	46,7	50,0	46,7	53,3	50,0	50,0	46,7	46,7	50,0	46,7	43,3
$(Ppi-Pp)^2$	1,8	4,0	4,0	4,0	1,8	4,0	1,8	28,5	4,0	4,0	1,8	1,8	4,0	1,8	21,7

N° FIELDS	16	17	18	19	20	21	22	23	24	25	26	27	28	29	30
POINT COUNT	14	15	14	14	15	14	13	14	15	14	15	14	15	14	14
POINT FRACT.	46,7	50,0	46,7	46,7	50,0	46,7	43,3	46,7	50,0	46,7	50,0	46,7	50,0	46,7	46,7
$(Ppi-Pp)^2$	1,8	4,0	1,8	1,8	4,0	1,8	21,7	1,8	4,0	1,8	4,0	1,8	4,0	1,8	1,8

Volume % di ferrite riscontrato (vv): 48,0
Volume frction of the ferrite

Errore% / % Error	Intervallo di confidenza / Confidence interval	Deviazione standard / Standard deviation
1,568	0,753	2,061

☒ REV. ☐ WIT.
WILDES CALLINI

ANCCP
Agenzia Nazionale Certificazione Componenti e Prodotti

Laboratorio T.O.S.I. s.r.l.

Tecnici Organizzati al Servizio delle Imprese

Sede legale e Uffici: 20025 Legnano (MI) - Via Pisacane, 46 - Tel. 0331.487210 - Fax 0331.522970
Sede operativa: 20025 Legnano (MI) - P.zza Monumento, 12 - Tel. 0331.522374-3 - Fax 0331.522462
Internet: www.laboratoriotosi.it - E-mail: labtosi@tiscalinet.it - Partita IVA e Codice Fiscale 12805730152

Laboratorio di Prova Approvato — Attestato N. 004 L — QUA 041 S

	Ordine n° (Order no.) 581/07 **del** (of) 09/10/07	**Rapporto di prova n°** (Test report no.) **07H2369**
Cliente: (Customer) **IBF** SpA	**Bolla n°** (Delivery note) **del** (of)	**Data** (date) 18/10/07
Colata n°. (Heat no.) 04354	**Materiale** (Material) ASTM A790 UNS S32760	**Foglio** (page) 1 **di** (of) 3

Materiale ricevuto (Material recived on) .... **Prove eseguite** (Tests date) 18/10/07

ESAME MICROGRAFICO

Micrographic Examination

Sample No. **5568**, item 1 - P.O. 140080 rev. 1

N. 3 Pipes OD 10" sch 120 HT Lot H100000248

fig. 1 Magnification : 500 X

Micrographic Examination *(Esternal surface)* **: Satisfactory**

The grain boundaries are free of carbide precipitation and intermetallic phase

ASTM E562 - Determining volume fraction of ferrite = 48,6 %

Intervallo di confidenza: 0,90 (Confidence interval)	**Errore % : 1,87** (% Error)	**Deviazione standard : 2,48** (Standard deviation)
Campi esaminati N°: 30 (Examinated fields N°)	**Dimensione griglia : 30 points** (Dimension grille)	**Attacco: ASTM E407 # 98** (Etching)

I risultati del rapporto di prova si riferiscono ai soli campioni testati
I est report values relate to the tested specimen only

Ente Autorizzato (Authorized Inspector) ☐ REV. ☐ WIT. WILDES CALLINI	**Esecutore** (Examiner) MBaratella	**Responsabile Laboratorio** (Laboratory Responsible)

ANCCP Agenzia Nazionale Certificazione Componenti e Prodotti

Laboratorio T.O.S.I. s.r.l.

Tecnici Organizzati al Servizio delle Imprese

Sede legale e Uffici: 20025 Legnano (MI) - Via Pisacane, 46 - Tel. 0331.487210 - Fax 0331.522970
Sede operativa: 20025 Legnano (MI) - P.zza Monumento, 12 - Tel. 0331.522374-3 - Fax 0331.522462
Internet: www.laboratoriotosi.it - E-mail: labtosi@tiscalinet.it - Partita IVA e Codice Fiscale 12805730152

Laboratorio di Prova Approvato - Attestato N. 004 L - QUA 041 S

Ordine n° Order no. 581/07 **del** of 09/10/07 **Rapporto di prova n°** Test report no. 07H2369

Cliente: Customer IBF SpA **Bolla n°** Delivery note ______ **del** of ______ **Data** date 18/10/07

Colata n°. Heat no. 04354 **Materiale** Material ASTM A790 UNS S32760 **Foglio** page 2 **di** of 3

Materiale ricevuto Material recived on ______ **Prove eseguite** Tests date 18/10/07

ESAME MICROGRAFICO

Micrographic Examination

Sample No. **5568,** item 1 - P.O. 140080 rev. 1

N. 3 Pipes OD 10" sch 120 HT Lot H100000248

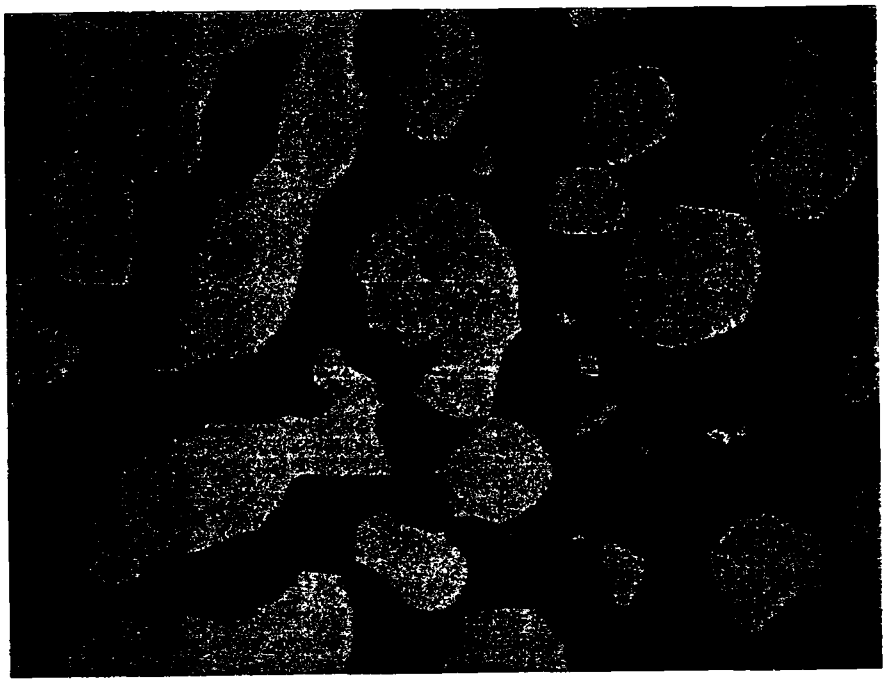

fig. 2 Magnification : 500 X

Micrographic Examination *(Half thickness)* **: Satisfactory**

The grain boundaries are free of carbide precipitation and intermetallic phase

ASTM E562 - Determining volume fraction of ferrite = 48,2 %

Intervallo di confidenza : 0,74 Confidence interval	**Errore % : 1,53** % Error	**Deviazione standard : 2,03** Standard deviation
Campi esaminati N°: 30 Examinated fields N°	**Dimensione griglia : 30 points** Dimension grille	**Attacco: ASTM E407 # 98** Etching

I risultati del rapporto di prova si riferiscono ai soli campioni testati
Test report values relate to the tested specimen only

Ente Autorizzato Authorized ☒ REV. ☐ WIT. WILDES CALLINI	**Esecutore** Examiner M Balatelli	**Responsabile Laboratorio** Laboratory Responsible

Laboratorio T.O.S.I. s.r.l.

ANCCP Agenzia Nazionale Certificazione Componenti e Prodotti

Tecnici Organizzati al Servizio delle Imprese

Sede legale e Uffici: 20025 Legnano (MI) - Via Pisacane, 46 - Tel. 0331.487210 - Fax 0331.522970
Sede operativa: 20025 Legnano (MI) - P.zza Monumento, 12 - Tel. 0331.522374-3 - Fax 0331.522462
Internet: www.laboratoriotosi.it - E-mail: labtosi@tiscalinet.it - Partita IVA e Codice Fiscale 12805730152

Laboratorio di Prova Approvato — Attestato N. 004 L — QUA 041 5

	Ordine n° Order no. 581/07 **del** of 09/10/07	**Rapporto di prova n°** Test report no. 07H2369
Cliente: Customer IBF SpA	**Bolla n°** Delivery note ______ **del** of ______	**Data** date 18/10/07
Colata n°. Heat no. 04354	**Materiale** Material ASTM A790 UNS S32760	**Foglio** page 3 **di** of 3

Materiale ricevuto Material recived on ______ **Prove eseguite** Tests date 18/10/07

ESAME MICROGRAFICO

Micrographic Examination

Sample No. **5568,** item 1 - P.O. 140080 rev. 1

N. 3 Pipes OD 10" sch 120 HT Lot H100000248

fig. 3 Magnification : 500 X

Micrographic Examination *(Internal surface)* **: Satisfactory**

The grain boundaries are free of carbide precipitation and intermetallic phase

ASTM E562 - Determining volume fraction of ferrite = 47,7 %

Intervallo di confidenza: 0,88 Confidence interval	**Errore % : 1,85** % Error	**Deviazione standard : 2,42** Standard deviation
Campi esaminati N°: 30 Examinated fields N°	**Dimensione griglia : 30 points** Dimension grille	**Attacco: ASTM E407 # 98** Etching

I risultati del rapporto di prova si riferiscono ai soli campioni testati
I est report values relate to the tested speciment only

Ente Autorizzato Authorized Inspector ☑ REV. ☐ WIT. WILDES CALLINI	**Esecutore** Examiner	**Responsabile Laboratorio** Laboratory Responsible

ANCCP
Agenzia Nazionale
Certificazione
Componenti e Prodotti

Laboratorio T.O.S.I. s.r.l.

Tecnici Organizzati al Servizio delle Imprese

Sede legale e Uffici: 20025 Legnano (MI) - Via Pisacane, 46 - Tel. 0331.487210 - Fax 0331.522970
Sede operativa: 20025 Legnano (MI) - P.zza Monumento, 12 - Tel. 0331.522374-3 - Fax 0331.522462
Internet: www.laboratoriotosi.it - E-mail: labtosi@tiscalinet.it - Partita IVA e Codice Fiscale 12805730152

Laboratorio di Prova
Approvato
Attestato
N. 004 L
QUA 041 S

Annex cert. 07H2369

DETERMINAZIONE METALLOGRAFICA DELLA FERRITE ASTM E562

FERRITE VOLUME FRACTION METALLOGRAPHIC DETERMINATION ASTM E562

Sample No. **5568**, item 1 *Esternal surface*

N° FIELDS	1	2	3	4	5	6	7	8	9	10	11	12	13	14	15
POINT COUNT	14	15	14	15	14	14	15	14	13	15	15	13	14	14	15
POINT FRACT.	46,7	50,0	46,7	50,0	46,7	46,7	50,0	46,7	43,3	50,0	50,0	43,3	46,7	46,7	50,0
$(Ppi-Pp)^2$	3,5	2,1	3,5	2,1	3,5	3,5	2,1	3,5	27,2	2,1	2,1	27,2	3,5	3,5	2,1

N° FIELDS	16	17	18	19	20	21	22	23	24	25	26	27	28	29	30
POINT COUNT	15	16	14	15	14	15	16	14	15	16	15	13	15	14	16
POINT FRACT.	50,0	53,3	46,7	50,0	46,7	50,0	53,3	46,7	50,0	53,3	50,0	43,3	50,0	46,7	53,3
$(Ppi-Pp)^2$	2,1	22,9	3,5	2,1	3,5	2,1	22,9	3,5	2,1	22,9	2,1	27,2	2,1	3,5	22,9

Volume % di ferrite riscontrato (vv): Volume frction of the ferrite	**48,6**

Errore% % Error	Intervallo di confidenza Confidence interval	Deviazione standard Standard deviation
1,872	**0,909**	**2,488**

Sample No. **5568**, item 1 *Half thickness*

N° FIELDS	1	2	3	4	5	6	7	8	9	10	11	12	13	14	15
POINT COUNT	14	15	15	14	14	15	15	14	15	14	14	15	14	13	14
POINT FRACT.	46,7	50,0	50,0	46,7	46,7	50,0	50,0	46,7	50,0	46,7	46,7	50,0	46.7	43,3	46,7
$(Ppi-Pp)^2$	2,4	3,2	3,2	2,4	2,4	3,2	3,2	2,4	3,2	2,4	2,4	3,2	2,4	23,9	2,4

N° FIELDS	16	17	18	19	20	21	22	23	24	25	26	27	28	29	30
POINT COUNT	14	16	14	14	16	14	15	14	15	16	14	14	15	14	14
POINT FRACT.	46,7	53,3	46,7	46,7	53,3	46,7	50,0	46,7	50,0	53,3	46,7	46,7	50,0	46,7	46,7
$(Ppi-Pp)^2$	2,4	26,2	2,4	2,4	26,2	2,4	3,2	2,4	3,2	26,2	2,4	2,4	3,2	2,4	2,4

Volume % di ferrite riscontrato (vv): Volume frction of the ferrite	**48,2**

Errore% % Error	Intervallo di confidenza Confidence interval	Deviazione standard Standard deviation
1,537	**0,741**	**2,030**

Sample No. **5568**, item 1 *Internal surface*

N° FIELDS	1	2	3	4	5	6	7	8	9	10	11	12	13	14	15
POINT COUNT	14	14	15	14	13	15	14	15	13	15	14	14	13	14	15
POINT FRACT.	46,7	46,7	50,0	46,7	43,3	50,0	46,7	50,0	43,3	50,0	46,7	46,7	43,3	46,7	50,0
$(Ppi-Pp)^2$	1,0	1,0	5,5	1,0	18,7	5,5	1,0	5,5	18,7	5,5	1,0	1,0	18,7	1,0	5,5

N° FIELDS	16	17	18	19	20	21	22	23	24	25	26	27	28	29	30
POINT COUNT	14	15	14	15	14	15	15	14	15	16	15	14	14	14	13
POINT FRACT.	46,7	50,0	46,7	50,0	46,7	50,0	50,0	46,7	50,0	53,3	50,0	46,7	46,7	46,7	43,3
$(Ppi-Pp)^2$	1,0	5,5	1,0	5,5	1,0	5,5	5,5	1,0	5,5	32,2	5,5	1,0	1,0	1,0	18,7

Volume % di ferrite riscontrato (vv): Volume frction of the ferrite	**47,7**

Errore% % Error	Intervallo di confidenza Confidence interval	Deviazione standard Standard deviation
1,855	**0,884**	**2,421**

☒ REV. ☐ WIT.
WILDES CALLINI
Callini

ANCCP
Agenzia Nazionale Certificazione Componenti e Prodotti

Laboratorio T.O.S.I. s.r.l.
Tecnici Organizzati al Servizio delle Imprese
Sede legale e Uffici: 20025 Legnano (MI) - Via Pisacane, 46 - Tel. 0331.487210 - Fax 0331.522970,
Sede operativa: 20025 Legnano (MI) - P.zza Monumento, 12 - Tel. 0331.522374-3 - Fax 0331.522462
Internet: www.laboratoriotosi.it - E-mail: labtosi@tiscalinet.it - Partita IVA e Codice Fiscale 12805730152

Laboratorio di Prova Approvato
Attestato N. 004 L
QUA 041 S

		Ordine n° Order no	587/07 **del** of 10/10/07	**Rapporto di prova n°** Test report no	07H2371
Cliente: Customer	IBF SpA	**Bolla n°** Delivery note	**del** of	**Data** date	18/10/07
Colata n°. Heat no	04347	**Materiale** Material	ASTM A790 UNS S32760	**Foglio** page	1 **di** of 3

Materiale ricevuto Material recived on ---------------- **Prove eseguite** Tests date 18/10/07

ESAME MICROGRAFICO
Micrographic Examination

Sample No. **5577,** item 1 - P.O. 140080 rev.1
N. 1 Pipe OD 10" sch 120 HT Lot H100000250

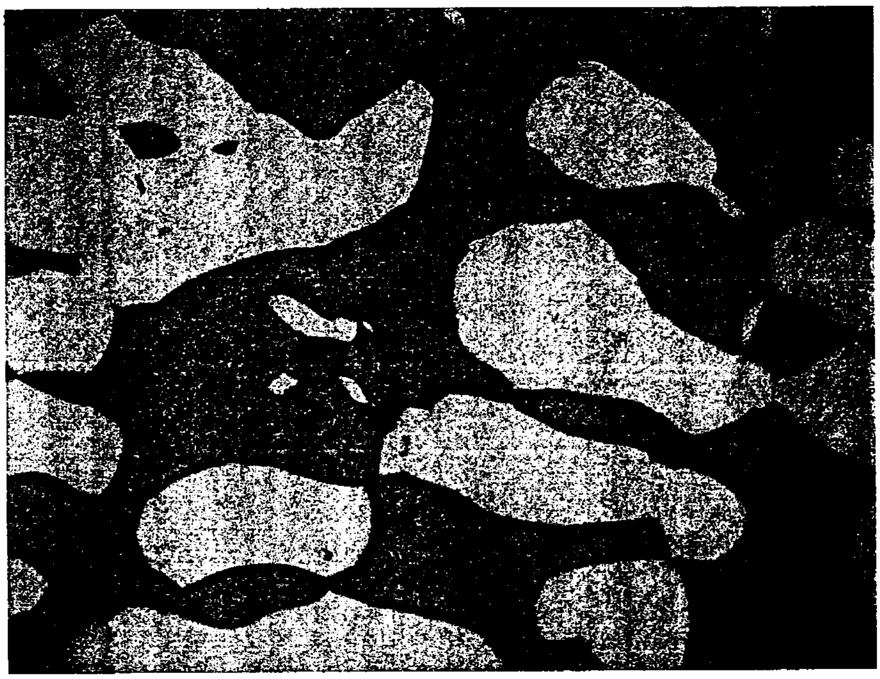

fig. 1 Magnification : 500 X

Micrographic Examination *(Esternal surface)* **: Satisfactory**
The grain boundaries are free of carbide precipitation and intermetallic phase
ASTM E562 - Determining volume fraction of ferrite = 48,8 %

Intervallo di confidenza: 1,03 Confidence interval	**Errore % : 2,12** % Error	**Deviazione standard : 2,84** Standard deviation
Campi esaminati N°: 30 Examinated fields N°	**Dimensione griglia : 30 points** Dimension grille	**Attacco: ASTM E407 # 98** Etching

I risultati del rapporto di prova si riferiscono ai soli campioni testati
Test report values relate to the tested specimen only

Ente Autorizzato ☒ REV. ☐ WIT. Authorized Inspector WILDES CALLINI	**Esecutore** Examiner MBaratelli	**Responsabile Laboratorio** Laboratory Responsible

		Ordine n° Order no.	587/07 **del** of 10/10/07	**Rapporto di prova n°** Test report no.	07H2371
Cliente: Customer	IBF SpA	**Bolla n°** Delivery note	**del** of	**Data** date	18/10/07
Colata n°. Heat no.	04347	**Materiale** Material	ASTM A790 UNS S32760	**Foglio** page	2 di of 3

Materiale ricevuto Material recived on .... — **Prove eseguite** Tests date 18/10/07

ESAME MICROGRAFICO

Micrographic Examination

Sample No. **5577,** item 1 - P.O. 140080 rev.1

N. 1 Pipe OD 10" sch 120 HT Lot H100000250

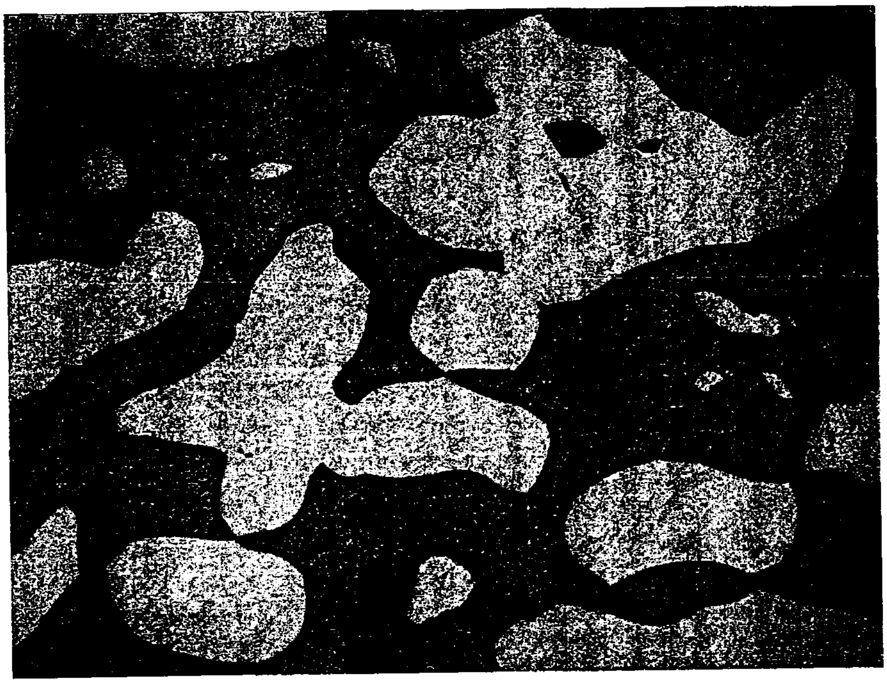

fig. 2 — Magnification : 500 X

Micrographic Examination *(Half thickness)* **: Satisfactory**

The grain boundaries are free of carbide precipitation and intermetallic phase

ASTM E562 - Determining volume fraction of ferrite = 47,8 %

Intervallo di confidenza : 0,91 Confidence interval	**Errore % : 1,91** % Error	**Deviazione standard : 2,50** Standard deviation
Campi esaminati N°: 30 Examinated fields N°	**Dimensione griglia : 30 points** Dimension grille	**Attacco: ASTM E407 # 98** Etching

i risultati del rapporto di prova si riferiscono ai soli campioni testati
Test report values relate to the tested specimen only

Ente Autorizzato Authorized Inspector ☒ REV. ☐ WIT. WILDES CALLINI	**Esecutore** Examiner M Baratelli	**Responsabile Laboratorio** Laboratory Responsible

ANCCP
Agenzia Nazionale Certificazione Componenti e Prodotti

Laboratorio T.O.S.I. s.r.l.

Tecnici Organizzati al Servizio delle Imprese

Sede legale e Uffici: 20025 Legnano (MI) - Via Pisacane, 46 - Tel. 0331.487210 - Fax 0331.522970
Sede operativa: 20025 Legnano (MI) - P.zza Monumento, 12 - Tel. 0331.522374-3 - Fax 0331.522462
Internet: www.laboratoriotosi.it - E-mail: labtosi@tiscalinet.it - Partita IVA e Codice Fiscale 12805730152

Laboratorio di Prova Approvato
Attestato N. 084 L
QLA 041 S

		Ordine n° Order no.	587/07 **del** of 10/10/07	**Rapporto di prova n°** Test report no.	07H2371
Cliente: Customer	IBF SpA	**Bolla n°** Delivery note	**del** of	**Data** date	18/10/07
Colata n°. Heat no.	04347	**Materiale** Material	ASTM A790 UNS S32760	**Foglio** page	3 **di** of 3

Materiale ricevuto Material recived on .... **Prove eseguite** Tests date 18/10/07

ESAME MICROGRAFICO

Micrographic Examination

Sample No. **5577**, item 1 - P.O. 140080 rev.1

N. 1 Pipe OD 10" sch 120 HT Lot H100000250

fig. 3 Magnification : 500 X

Micrographic Examination *(Internal surface)* : **Satisfactory**

The grain boundaries are free of carbide precipitation and intermetallic phase

ASTM E562 - Determining volume fraction of ferrite = 47,4 %

Intervallo di confidenza: 0,77 Confidence interval	**Errore % : 1,62** % Error	**Deviazione standard : 2,11** Standard deviation
Campi esaminati N°: 30 Examinated fields N°	**Dimensione griglia : 30 points** Dimension grille	**Attacco: ASTM E407 # 98** Etching

I risultati del rapporto di prova si riferiscono ai soli campioni testati
Test report values relate to the tested specimen only

Ente Autorizzato Authorized ☒ REV. ☐ WIT. WEIL DES CALLINI Callini	**Esecutore** Examiner MBaratella	**Responsabile Laboratorio** Laboratory Responsible

ANCCP
Agenzia Nazionale Certificazione Componenti e Prodotti

Laboratorio T.O.S.I. s.r.l.

Tecnici Organizzati al Servizio delle Imprese

Sede legale e Uffici: 20025 Legnano (MI) - Via Pisacane, 46 - Tel. 0331.487210 - Fax 0331.522970
Sede operativa: 20025 Legnano (MI) - P.zza Monumento, 12 - Tel. 0331.522374-3 - Fax 0331.522462
Internet: www.laboratoriotosi.it - E-mail: labtosi@tiscalinet.it - Partita IVA e Codice Fiscale 12805730152

Laboratorio di Prova Approvato
Attestato N. 004 L
QUA 041 S

Annex cert. 07H2371

DETERMINAZIONE METALLOGRAFICA DELLA FERRITE ASTM E562

FERRITE VOLUME FRACTION METALLOGRAPHIC DETERMINATION ASTM E562

Sample Nc. **5577**, item 1 *Esternal surface*

N° FIELDS	1	2	3	4	5	6	7	8	9	10	11	12	13	14	15
POINT COUNT	15	14	14	13	15	14	14	13	14	15	15	14	14	16	15
POINT FRACT.	50,0	46,7	46,7	43,3	50,0	46,7	46,7	43,3	46,7	50,0	50,0	46,7	46.7	53,3	50,0
(Ppi-Pp)²	1,5	4,4	4,4	29,6	1,5	4,4	4,4	29,6	4,4	1,5	1,5	4,4	4,4	20,8	1,5

N° FIELDS	16	17	18	19	20	21	22	23	24	25	26	27	28	29	30
POINT COUNT	15	14	17	15	15	14	16	14	16	14	15	16	14	14	15
POINT FRACT.	50,0	46,7	56,7	50,0	50,0	46,7	53,3	46,7	53,3	46,7	50,0	53,3	46,7	46,7	50,0
(Ppi-Pp)²	1,5	4,4	62,3	1,5	1,5	4,4	20,8	4,4	20,8	4,4	1,5	20,8	4,4	4,4	1,5

Volume % di ferrite riscontrato (vv): Volume frction of the ferrite	48,8

Errore% / % Error	Intervallo di confidenza / Confidence interval	Deviazione standard / Standard deviation
2,127	1,037	2,841

Sample No. **5577**, item 1 *Half thickness*

N° FIELDS	1	2	3	4	5	6	7	8	9	10	11	12	13	14	15
POINT COUNT	13	14	13	14	15	15	14	14	15	14	15	15	14	13	15
POINT FRACT.	43,3	46,7	43,3	46,7	50,0	50,0	46,7	46,7	50,0	46,7	50,0	50,0	46,7	43,3	50,0
(Ppi-Pp)²	19,7	1,2	19,7	1,2	5,0	5,0	1,2	1,2	5,0	1,2	5,0	5,0	1,2	19,7	5,0

N° FIELDS	16	17	18	19	20	21	22	23	24	25	26	27	28	29	30
POINT COUNT	15	14	16	15	13	13	15	14	15	13	15	14	15	14	16
POINT FRACT.	50,0	46,7	53,3	50,0	43,3	43,3	50,0	46,7	50,0	43,3	50,0	46,7	50,0	46,7	53,3
(Ppi-Pp)²	5,0	1,2	30,9	5,0	19,7	19,7	5,0	1,2	5,0	19,7	5,0	1.2	5.0	1,2	30,9

Volume % di ferrite riscontrato (vv): Volume frction of the ferrite	47,8

Errore% / % Error	Intervallo di confidenza / Confidence interval	Deviazione standard / Standard deviation
1,918	0,916	2,509

Sample No. **5577**, item 1 *Internal surface*

N° FIELDS	1	2	3	4	5	6	7	8	9	10	11	12	13	14	15
POINT COUNT	14	14	13	15	14	15	14	14	13	15	14	14	15	14	13
POINT FRACT.	46,7	46,7	43,3	50,0	46,7	50,0	46,7	46,7	43,3	50,0	46,7	46,7	50,0	46,7	43,3
(Ppi-Pp)²	0,6	0,6	16,9	6,6	0,6	6,6	0,6	0,6	16,9	6,6	0,6	0.6	6,6	0,6	16,9

N° FIELDS	16	17	18	19	20	21	22	23	24	25	26	27	28	29	30
POINT COUNT	16	14	15	14	15	15	14	13	15	14	15	14	13	15	14
POINT FRACT.	53,3	46,7	50,0	46,7	50,0	50,0	46,7	43,3	50,0	46,7	50,0	46,7	43,3	50.0	46,7
(Ppi-Pp)²	34,7	0,6	6,6	0,6	6,6	6,6	0,6	16,9	6,6	0,6	6,6	0,6	16,9	6,6	0,6

Volume % di ferrite riscontrato (vv): Volume frction of the ferrite	47,4

Errore% / % Error	Intervallo di confidenza / Confidence interval	Deviazione standard / Standard deviation
1,626	0,771	2,113

☒ REV. ☐ WIT.
WILDES CALLINI

ANCCP
Agenzia Nazionale Certificazione Componenti e Prodotti

Laboratorio T.O.S.I. s.r.l.

Tecnici Organizzati al Servizio delle Imprese

Sede legale e Uffici: 20025 Legnano (MI) - Via Pisacane, 46 - Tel. 0331.487210 - Fax 0331.522970
Sede operativa: 20025 Legnano (MI) - P.zza Monumento, 12 - Tel. 0331.522374-3 - Fax 0331.522462
Internet: www.laboratoriotosi.it - E-mail: labtosi@tiscalinet.it - Partita IVA e Codice Fiscale 12805730152

Laboratorio di Prova Approvato
Attestato N. 004 L
QUA 003 S

		Ordine n° Order no.	594/07 **del** of 12/10/07	**Rapporto di prova n°** Test report no.	07H2372
Cliente: Customer	IBF SpA	**Bolla n°** Delivery note	**del** of	**Data** date	10/10/07
Colata n°. Heat no.	04354	**Materiale** Material	ASTM A790 UNS S32760	**Foglio** page	1 **di** of 3

Materiale ricevuto Material recived on	**Prove eseguite** Tests date 10/10/07

ESAME MICROGRAFICO

Micrographic Examination

Sample No. **5578,** item 1 - P.O. 140080 rev.1

N. 2 Pipes OD 10" sch 120 HT Lot H100000250

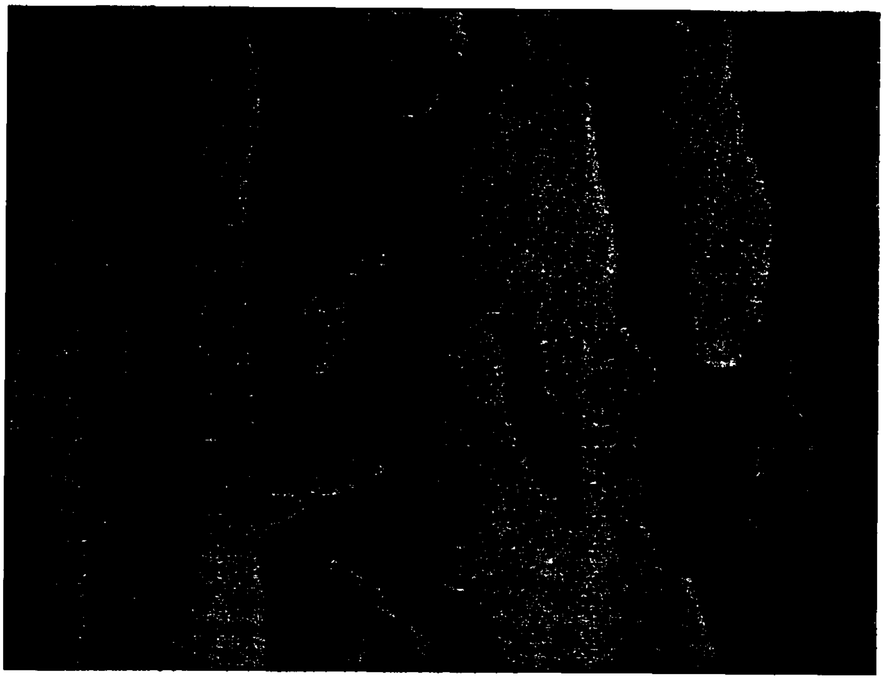

fig. 1 Magnification : 500 X

Micrographic Examination *(Esternal surface)* **: Satisfactory**

The grain boundaries are free of carbide precipitation and intermetallic phase

ASTM E562 - Determining volume fraction of ferrite = 49,1 %

Intervallo di confidenza: 1,06 Confidence interval	**Errore % : 2,16** % Error	**Deviazione standard : 2,91** Standard deviation
Campi esaminati N°: 30 Examinated fields N°	**Dimensione griglia : 30 points** Dimension grille	**Attacco: ASTM E407 # 98** Etching

I risultati del rapporto di prova si riferiscono ai soli campioni testati
Test report values relate to the tested specimen only

☒ REV. ☐ WIT.
WILDES GALLINI

Ente Autorizzato Authorized Inspector	**Esecutore** Examiner	**Responsabile Laboratorio** Laboratory Responsible
Gallini	MBattelli	

LABORATORIO T.O.S.I. SRL

ANCCP
Agenzia Nazionale Certificazione Componenti e Prodotti

Laboratorio T.O.S.I. s.r.l.

Tecnici Organizzati al Servizio delle Imprese

Sede legale e Uffici: 20025 Legnano (MI) - Via Pisacane, 46 - Tel. 0331.487210 - Fax 0331.522970
Sede operativa: 20025 Legnano (MI) - P.zza Monumento, 12 - Tel. 0331.522374-3 - Fax 0331.522462
Internet: www.laboratoriotosi.it - E-mail: labtosi@tiscalinet.it - Partita IVA e Codice Fiscale 12805730152

Laboratorio di Prova Approvato
Attestato N. 004 L
QUA 041 S

	Ordine n° Order no. 594/07 **del** of 12/10/07	**Rapporto di prova n°** Test report no. 07H2372	
Cliente: Customer **IBF** SpA	**Bolla n°** Delivery note ________ **del** of ________	**Data** date 10/10/07	
Colata n°. Heat no. 04354	**Materiale** Material ASTM A790 UNS S32760	**Foglio** page 2	**di** of 3

Materiale ricevuto Material recived on ________ **Prove eseguite** Tests date 10/10/07

ESAME MICROGRAFICO

Micrographic Examination

Sample No. **5578,** item 1 - P.O. 140080 rev.1

N. 2 Pipes OD 10" sch 120 HT Lot H100000250

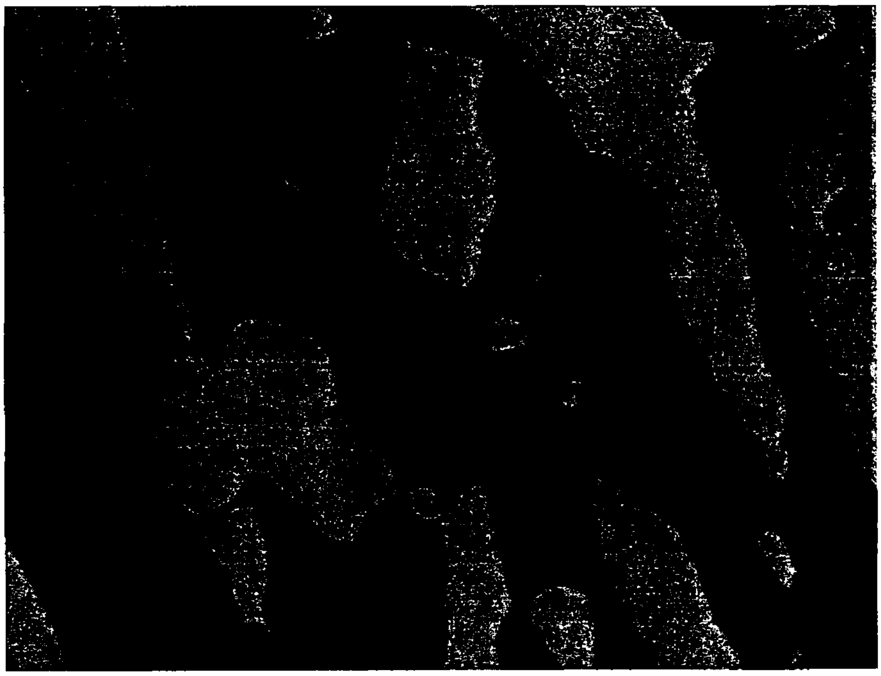

fig. 2 Magnification : 500 X

Micrographic Examination *(Half thickness)* **: Satisfactory**

The grain boundaries are free of carbide precipitation and intermetallic phase

ASTM E562 - Determining volume fraction of ferrite = 47,6 %

Intervallo di confidenza : 0,72 Confidence interval	**Errore % : 1,51** % Error	**Deviazione standard : 1,97** Standard deviation
Campi esaminati N°: 30 Examinated fields N°	**Dimensione griglia : 30 points** Dimension grille	**Attacco: ASTM E407 # 98** Etching

I risultati del rapporto di prova si riferiscono ai soli campioni testati
Test report values relate to the tested specimen only

☑ REV. ☐ WIT.

Ente Autorizzato Authorized inspector WILDES CALLINI	**Esecutore** Examiner MBaratelli	**Responsabile Laboratorio** Laboratory Responsible

LABORATORIO T.O.S.I. S.R.L.

ANCCP
Agenzia Nazionale Certificazione Componenti e Prodotti

Laboratorio T.O.S.I. s.r.l.

Tecnici Organizzati al Servizio delle Imprese

Sede legale e Uffici: 20025 Legnano (MI) - Via Pisacane, 46 - Tel. 0331.487210 - Fax 0331.522970
Sede operativa: 20025 Legnano (MI) - P.zza Monumento, 12 - Tel. 0331.522374-3 - Fax 0331.522462
Internet: www.laboratoriotosi.it - E-mail: labtosi@tiscalinet.it - Partita IVA e Codice Fiscale 12805730152

Laboratorio di Prova Approvato
Attestato N. 004 L
QUA 041 S

Ordine n° Order no. 594/07 **del** of 12/10/07		**Rapporto di prova n°** Test report no. 07H2372
Cliente: Customer IBF SpA	**Bolla n°** Delivery note ________ **del** of ________	**Data** date 10/10/07
Colata n°. Heat no. 04354	**Materiale** Material ASTM A790 UNS S32760	**Foglio** page 3 **di** of 3

Materiale ricevuto Material recived on ________ **Prove eseguite** Tests date 10/10/07

ESAME MICROGRAFICO

Micrographic Examination

Sample No. **5578,** item 1 - P.O. 140080 rev.1

N. 2 Pipes OD 10" sch 120 HT Lot H100000250

fig. 3 Magnification : 500 X

Micrographic Examination *(Internal surface)* **: Satisfactory**

The grain boundaries are free of carbide precipitation and intermetallic phase

ASTM E562 - Determining volume fraction of ferrite = 48,3 %

Intervallo di confidenza: 0,98 Confidence interval	**Errore % : 2,03** % Error	**Deviazione standard : 2,69** Standard deviation
Campi esaminati N°: 30 Examinated fields N°	**Dimensione griglia : 30 points** Dimension grille	**Attacco: ASTM E407 # 98** Etching

I risultati del rapporto di prova si riferiscono ai soli campioni testati
Test report values relate to the tested specimen only

Ente Autorizzato Authorized Inspector ☒ REV. ☐ WIT. **WILDES CALLINI**	**Esecutore** Examiner M Barbella	**Responsabile Laboratorio** Laboratory Responsible

Annex cert. 07H2372

DETERMINAZIONE METALLOGRAFICA DELLA FERRITE ASTM E562

FERRITE VOLUME FRACTION METALLOGRAPHIC DETERMINATION ASTM E562

Sample No. **5578**, item 1 *Esternal surface*

N° FIELDS	1	2	3	4	5	6	7	8	9	10	11	12	13	14	15
POINT COUNT	15	14	15	14	13	15	14	14	15	14	14	16	15	14	15
POINT FRACT.	50,0	46,7	50,0	46,7	43,3	50,0	46,7	46,7	50,0	46,7	46,7	53,3	50,0	46,7	50,0
$(Ppi-Pp)^2$	0,8	6,0	0,8	6,0	33,3	0,8	6,0	6,0	0,8	6,0	6,0	17,9	0,8	6,0	0,8

N° FIELDS	16	17	18	19	20	21	22	23	24	25	26	27	28	29	30
POINT COUNT	14	15	14	15	13	15	14	16	14	16	16	16	16	15	16
POINT FRACT.	46,7	50,0	46,7	50,0	43,3	50,0	46,7	53,3	46,7	53,3	53,3	53,3	53,3	50,0	53,3
$(Ppi-Pp)^2$	6,0	0,8	6,0	0,8	33,3	0,8	6,0	17,9	6,0	17,9	17,9	17,9	17,9	0,8	17,9

Volume % di ferrite riscontrato (vv): 49,1
Volume frction of the ferrite

Errore% / % Error	Intervallo di confidenza / Confidence interval	Deviazione standard / Standard deviation
2,168	1,065	2,916

Sample No. **5578**, item 1 *Half thickness*

N° FIELDS	1	2	3	4	5	6	7	8	9	10	11	12	13	14	15
POINT COUNT	14	14	15	14	14	14	15	14	15	14	15	14	15	14	14
POINT FRACT.	46,7	46,7	50,0	46,7	46,7	46,7	50,0	46,7	50,0	46,7	50,0	46,7	50,0	46,7	46,7
$(Ppi-Pp)^2$	0,8	0,8	6,0	0,8	0,8	0,8	6,0	0,8	6,0	0,8	6,0	0,8	6,0	0,8	0,8

N° FIELDS	16	17	18	19	20	21	22	23	24	25	26	27	28	29	30
POINT COUNT	15	14	15	14	13	15	14	15	13	14	15	14	14	15	13
POINT FRACT.	50,0	46,7	50,0	46,7	43,3	50,0	46,7	50,0	43,3	46,7	50,0	46,7	46,7	50,0	43,3
$(Ppi-Pp)^2$	6,0	0,8	6,0	0,8	17,8	6,0	0,8	6,0	17,8	0,8	6,0	0,8	0,8	6,0	17,8

Volume % di ferrite riscontrato (vv): 47,6
Volume frction of the ferrite

Errore% / % Error	Intervallo di confidenza / Confidence interval	Deviazione standard / Standard deviation
1,518	0,722	1,976

Sample No. **5578**, item 1 *Internal surface*

N° FIELDS	1	2	3	4	5	6	7	8	9	10	11	12	13	14	15
POINT COUNT	14	15	13	14	13	14	15	14	13	14	15	13	14	15	15
POINT FRACT.	46,7	50,0	43,3	46,7	43,3	46,7	50,0	46,7	43,3	46,7	50,0	43,3	46,7	50,0	50,0
$(Ppi-Pp)^2$	2,8	2,8	25,0	2,8	25,0	2,8	2,8	2,8	25,0	2,8	2,8	25,0	2,8	2,8	2,8

N° FIELDS	16	17	18	19	20	21	22	23	24	25	26	27	28	29	30
POINT COUNT	15	15	16	15	15	15	14	15	15	14	15	16	14	15	15
POINT FRACT.	50,0	50,0	53,3	50,0	50,0	50,0	46,7	50,0	50,0	46,7	50,0	53,3	46,7	50,0	50,0
$(Ppi-Pp)^2$	2,8	2,8	25,1	2,8	2,8	2,8	2,8	2,8	2,8	2,8	2,8	25,1	2,8	2,8	2,8

Volume % di ferrite riscontrato (vv): 48,3
Volume frction of the ferrite

Errore% / % Error	Intervallo di confidenza / Confidence interval	Deviazione standard / Standard deviation
2,038	0,985	2,698

☒ REV. ☐ WIT.
WILDES CALLINI

ANCCP
Agenzia Nazionale Certificazione Componenti e Prodotti

Laboratorio T.O.S.I. s.r.l.

Tecnici Organizzati al Servizio delle Imprese

Sede legale e Uffici: 20025 Legnano (MI) - Via Pisacane, 46 - Tel. 0331.487210 - Fax 0331.522970
Sede operativa: 20025 Legnano (MI) - P.zza Monumento, 12 - Tel. 0331.522374-3 - Fax 0331.522462
Internet: www.laboratoriotosi.it - E-mail: labtosi@tiscalinet.it - Partita IVA e Codice Fiscale 12805730152

Laboratorio di Prova Approvato
Attestato N. 004 L
QUA 041 S

		Ordine n° Order no.	571/07	**del** of	08/10/07
Rapporto di prova n° Test report no.	**07H2307**				
Cliente: Customer	**IBF** SpA	**Bolla n°** Delivery note	#	**del** of	#
Data date	12/10/07				
Colata n°. Heat no.	04336	**Materiale** Material	ASTM A790 UNS S32760		
Foglio page	1	**di** of	3		

Materiale ricevuto Material recived on .... **Prove eseguite** Tests date 12/10/07

ESAME MICROGRAFICO
Micrographic Examination

Sample No. **5512,** item 1 - P.O. 140080 rev.1
N. 5 Pipes OD 10" sch 120 HT Lot H1000000242

fig. 1 Magnification : 500 X

Micrographic Examination *(Esternal surface)* **: Satisfactory**
The grain boundaries are free of carbide precipitation and intermetallic phase
ASTM E562 - Determining volume fraction of ferrite = 48,7 %

Intervallo di confidenza: 0,57 Confidence interval	**Errore % : 1,18** % Error	**Deviazione standard : 1,57** Standard deviation
Campi esaminati N°: 30 Examinated fields N°	**Dimensione griglia : 30 points** Dimension grille	**Attacco: ASTM E407 # 98** Etching

I risultati del rapporto di prova si riferiscono ai soli campioni testati
Test report values relate to the tested speciment only

☑ REV. ☐ WIT.
WILDES GALLINI

Ente Autorizzato Authorized Inspector	**Esecutore** Examiner	**Responsabile Laboratorio** Laboratory Responsible

ANCCP
Agenzia Nazionale Certificazione Componenti e Prodotti

Laboratorio T.O.S.I. s.r.l.

Tecnici Organizzati al Servizio delle Imprese

Sede legale e Uffici: 20025 Legnano (MI) - Via Pisacane, 46 - Tel. 0331.487210 - Fax 0331.522970
Sede operativa: 20025 Legnano (MI) - P.zza Monumento, 12 - Tel. 0331.522374-3 - Fax 0331.522462
Internet: www.laboratoriotosi.it - E-mail: labtosi@tiscalinet.it - Partita IVA e Codice Fiscale 12805730152

Laboratorio di Prova Approvato
Attestato N. 004 L
QUA 041 S

Ordine n° Order no. 571/07 **del** of 08/10/07 **Rapporto di prova n°** Test report no. **07H2307**

Cliente: Customer **IBF** SpA **Bolla n°** Delivery note # **del** of # **Data** date 12/10/07

Colata n°. Heat no. 04336 **Materiale** Material ASTM A790 UNS S32760 **Foglio** page 2 **di** of 3

Materiale ricevuto Material recived on **Prove eseguite** Tests date 12/10/07

ESAME MICROGRAFICO

Micrographic Examination

Sample No. **5512,** item 1 - P.O. 140080 rev.1

N. 5 Pipes OD 10" sch 120 HT Lot H1000000242

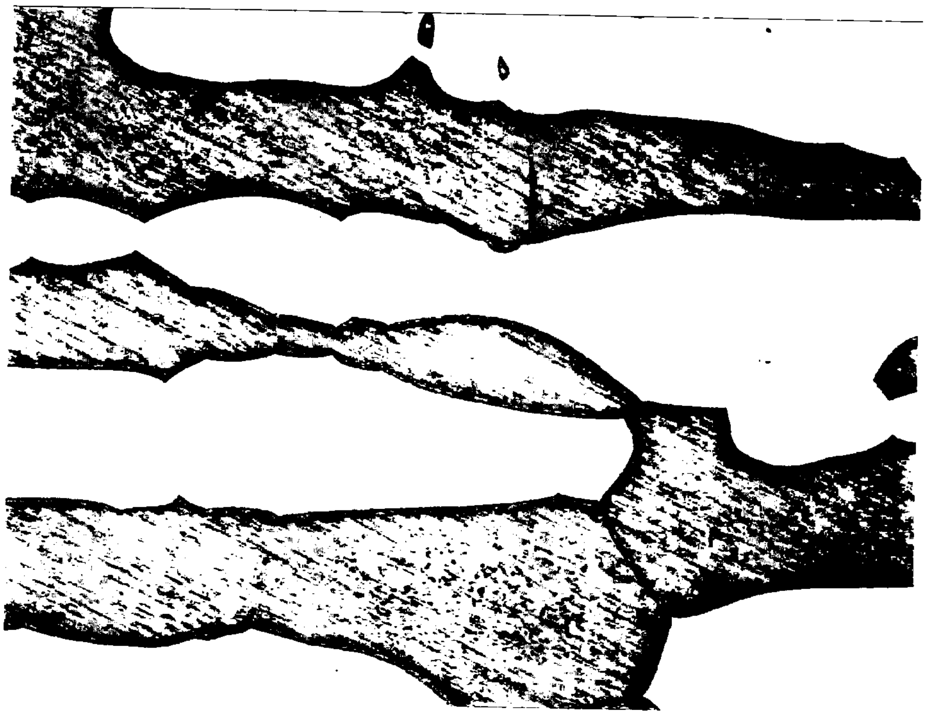

fig. 2 Magnification : 500 X

Micrographic Examination *(Half thickness)* **: Satisfactory**

The grain boundaries are free of carbide precipitation and intermetallic phase

ASTM E562 - Determining volume fraction of ferrite = 47,9 %

Intervallo di confidenza: 0,89 Confidence interval	**Errore % : 1,85** % Error	**Deviazione standard : 2,43** Standard deviation
Campi esaminati N°: 30 Examined fields N°	**Dimensione griglia : 30 points** Dimension grille	**Attacco: ASTM E407 # 98** Etching

I risultati del rapporto di prova si riferiscono ai soli campioni testati
Test report values relate to the tested speciment only

Ente Autorizzato ☐ REV. ☐ WIT. Authorized Inspector WILDES CALLINI	**Esecutore** Examiner	**Responsabile Laboratorio** Laboratory Responsible

Laboratorio T.O.S.I. s.r.l.
Tecnici Organizzati al Servizio delle Imprese
Sede legale e Uffici: 20025 Legnano (MI) - Via Pisacane, 46 - Tel. 0331.487210 - Fax 0331.522970
Sede operativa: 20025 Legnano (MI) - P.zza Monumento, 12 - Tel. 0331.522374-3 - Fax 0331.522462
Internet: www.laboratoriotosi.it - E-mail: labtosi@tiscalinet.it - Partita IVA e Codice Fiscale 12805730152

ANCCP Agenzia Nazionale Certificazione Componenti e Prodotti

Laboratorio di Prova Approvato — Attestato N. 004 L — IIS — QUA 041 S

		Ordine n° Order no.	571/07 **del** (of) 08/10/07	**Rapporto di prova n°** Test report no.	**07H2307**
Cliente: Customer	**IBF** SpA	**Bolla n°** Delivery note	# **del** (of) #	**Data** date	12/10/07
Colata n°. Heat no.	04336	**Materiale** Material	ASTM A790 UNS S32760	**Foglio** page	3 **di** (of) 3

Materiale ricevuto Material recived on — **Prove eseguite** Tests date 12/10/07

ESAME MICROGRAFICO
Micrographic Examination

Sample No. **5512,** item 1 - P.O. 140080 rev.1
N. 5 Pipes OD 10" sch 120 HT Lot H1000000242

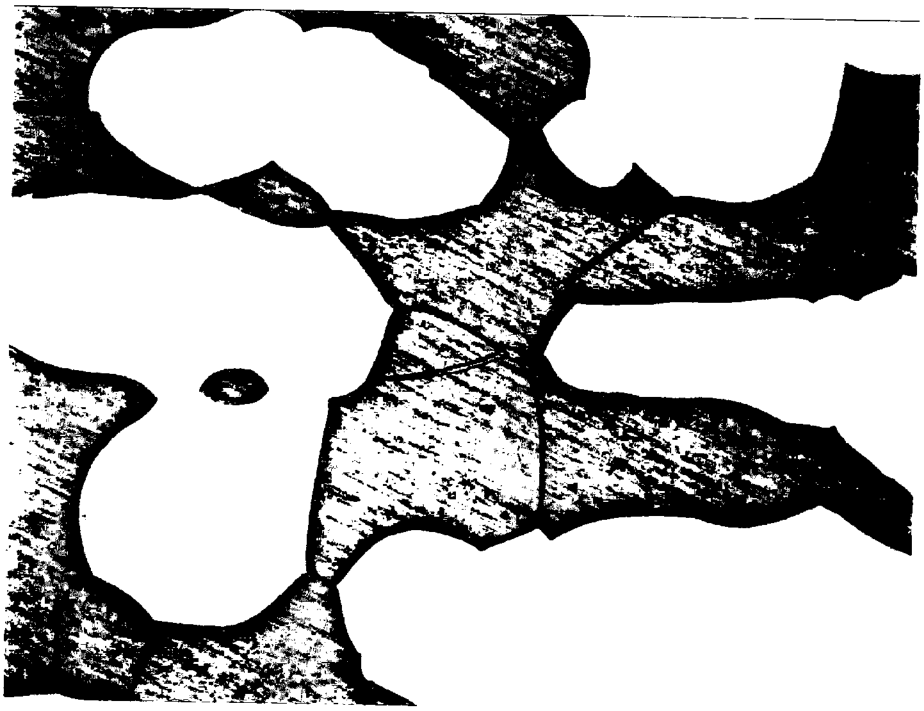

fig. 3 Magnification : 500 X

Micrographic Examination *(Internal surface)* **: Satisfactory**
The grain boundaries are free of carbide precipitation and intermetallic phase
ASTM E562 - Determining volume fraction of ferrite = 47,9 %

Intervallo di confidenza: 0,98 Confidence interval	**Errore % : 2,05** % Error	**Deviazione standard : 2,69** Standard deviation
Campi esaminati N°: 30 Examinated fields N°	**Dimensione griglia : 30 points** Dimension grille	**Attacco: ASTM E407 # 98** Etching

I risultati del rapporto di prova si riferiscono ai soli campioni testati
Test report values relate to the tested speciment only

Ente Autorizzato ☒ REV. ☐ WIT. Authorized Inspector WILDES CALLINI	**Esecutore** Examiner	**Responsabile Laboratorio** Laboratory Responsible

ANCCP
Agenzia Nazionale Certificazione Componenti e Prodotti

Laboratorio T.O.S.I. s.r.l.

Tecnici Organizzati al Servizio delle Imprese

Sede legale e Uffici: 20025 Legnano (MI) - Via Pisacane, 46 - Tel. 0331.487210 - Fax 0331.522970
Sede operativa: 20025 Legnano (MI) - P.zza Monumento, 12 - Tel. 0331.522374-3 - Fax 0331.522462
Internet: www.laboratoriotosi.it - E-mail: labtosi@tiscalinet.it - Partita IVA e Codice Fiscale 12805730152

Laboratorio di Prova Approvato
Attestato N. 004 L
QUA 041 S

Annex cert. 07H2307

DETERMINAZIONE METALLOGRAFICA DELLA FERRITE ASTM E562

FERRITE VOLUME FRACTION METALLOGRAPHIC DETERMINATION ESTM E562

Sample No. **5512**, item 1 *Esternal surface*

N° FIELDS	1	2	3	4	5	6	7	8	9	10	11	12	13	14	15
POINT COUNT	14	15	15	14	15	14	15	15	14	15	15	14	15	15	16
POINT FRACT.	46,7	50,0	50,0	46,7	50,0	46,7	50,0	50,0	46,7	50,0	50,0	46,7	50,0	50,0	53,3
$(Ppi-Pp)^2$	4,0	1,8	1,8	4,0	1,8	4,0	1,8	1,8	4,0	1,8	1,8	4,0	1,8	1,8	21,8

N° FIELDS	16	17	18	19	20	21	22	23	24	25	26	27	28	29	30
POINT COUNT	14	15	14	15	14	16	14	15	13	14	15	15	14	15	14
POINT FRACT.	46,7	50,0	46,7	50,0	46,7	53,3	46,7	50,0	43,3	46,7	50,0	50,0	46,7	50,0	46,7
$(Ppi-Pp)^2$	4,0	1,8	4,0	1,8	4,0	21,8	4,0	1,8	28,4	4,0	1,8	1,8	4,0	1,8	4,0

Volume % di ferrite riscontrato (vv): Volume frction of the ferrite	**48,7**

Errore% % Error	Intervallo di confidenza Confidence interval	Deviazione standard Standard deviation
1,183	0,576	1,576

Sample No. **5512,** item 1 *Half thickness*

N° FIELDS	1	2	3	4	5	6	7	8	9	10	11	12	13	14	15
POINT COUNT	16	14	13	15	15	14	15	15	14	15	14	14	15	14	14
POINT FRACT.	53,3	46,7	43,3	50,0	50,0	46,7	50,0	50,0	46,7	50,0	46,7	46,7	50,0	46,7	46,7
$(Ppi-Pp)^2$	29,7	1,5	20,7	4,5	4,5	1,5	4,5	4,5	1,5	4,5	1,5	1,5	4,5	1,5	1,5

N° FIELDS	16	17	18	19	20	21	22	23	24	25	26	27	28	29	30
POINT COUNT	14	14	13	15	14	15	14	15	14	16	14	13	14	15	14
POINT FRACT.	46,7	46,7	43,3	50,0	46,7	50,0	46,7	50,0	46,7	53,3	46,7	43,3	46,7	50,0	46,7
$(Ppi-Pp)^2$	1,5	1,5	20,7	4,5	1,5	4,5	1,5	4,5	1,5	29,7	1,5	20,7	1,5	4,5	1,5

Volume % di ferrite riscontrato (vv): Volume frction of the ferrite	**47,9**

Errore% % Error	Intervallo di confidenza Confidence interval	Deviazione standard Standard deviation
1,859	0,890	2,438

Sample No. **5512**, item 1 *Internal surface*

N° FIELDS	1	2	3	4	5	6	7	8	9	10	11	12	13	14	15
POINT COUNT	14	15	13	14	15	16	14	15	14	15	15	14	15	16	15
POINT FRACT.	46,7	50,0	43,3	46,7	50,0	53,3	46,7	50,0	46,7	50,0	50,0	46,7	50,0	53,3	50,0
$(Ppi-Pp)^2$	2,4	3,2	23,9	2,4	3,2	26,2	2,4	3,2	2,4	3,2	3,2	2,4	3,2	26,2	3,2

N° FIELDS	16	17	18	19	20	21	22	23	24	25	26	27	28	29	30
POINT COUNT	14	15	13	14	15	14	14	16	14	13	14	15	14	14	15
POINT FRACT.	46,7	50,0	43,3	46,7	50,0	46,7	46,7	53,3	46,7	43,3	46,7	50,0	46,7	46,7	50,0
$(Ppi-Pp)^2$	2,4	3,2	23,9	2,4	3,2	2,4	2,4	26,2	2,4	23,9	2,4	3,2	2,4	2,4	3,2

Volume % di ferrite riscontrato (vv): Volume frction of the ferrite	**48,2**

Errore% % Error	Intervallo di confidenza Confidence interval	Deviazione standard Standard deviation
2,060	0,993	2,720

☒ REV. ☐ WIT.
WILDES CALLINI

ANCCP
Agenzia Nazionale
Certificazione
Componenti e Prodotti

Laboratorio T.O.S.I. s.r.l.

Tecnici Organizzati al Servizio delle Imprese

Sede legale e Uffici: 20025 Legnano (MI) - Via Pisacane, 46 - Tel. 0331.487210 - Fax 0331.522970
Sede operativa: 20025 Legnano (MI) - P.zza Monumento, 12 - Tel. 0331.522374-3 - Fax 0331.522462
Internet: www.laboratoriotosi.it - E-mail: labtosi@tiscalinet.it - Partita IVA e Codice Fiscale 12805730152

Laboratorio di Prova Approvato
Attestato N. 004 L
IIS
QUA 041 S

		Ordine n° Order no.	571/07	**del** of	08/10/07
Cliente: Customer	**IBF** SpA	**Bolla n°** Delivery note		**del** of	
Colata n°. Heat no.	04335	**Materiale** Material	ASTM A790 UNS S32760		

Rapporto di prova n° Test report no. **07H2308**

Data date 12/10/07

Materiale ricevuto Material recived on ....

Prove eseguite Tests date 12/10/07

ESAME MICROGRAFICO

Micrographic Examination

Sample No. **5513,** item 1 - P.O. 140080 rev.1

N. 5 Pipes OD 10" sch 120 HT Lot H100000243

fig. 1 Magnification : 500 X

Micrographic Examination *(Esternal surface)* **: Satisfactory**

The grain boundaries are free of carbide precipitation and intermetallic phase

ASTM E562 - Determining volume fraction of ferrite = 46,7 %

Intervallo di confidenza: 0,90 Confidence interval	**Errore % : 1,93** % Error	**Deviazione standard : 2,47** Standard deviation
Campi esaminati N°: 30 Examinated fields N°	**Dimensione griglia : 30 points** Dimension grille	**Attacco: ASTM E407 # 98** Etching

I risultati del rapporto di prova si riferiscono ai soli campioni testati
Test report values relate to the tested speciment only

☐ REV. ☐ WIT.

Ente Autorizzato Authorized Inspector WILDES GALLINI	**Esecutore** Examiner	**Responsabile Laboratorio** Laboratory Responsible

ANCCP
Agenzia Nazionale
Certificazione
Componenti e Prodotti

Laboratorio T.O.S.I. s.r.l.

Tecnici Organizzati al Servizio delle Imprese

Sede legale e Uffici: 20025 Legnano (MI) - Via Pisacane, 46 - Tel. 0331.487210 - Fax 0331.522970
Sede operativa: 20025 Legnano (MI) - P.zza Monumento, 12 - Tel. 0331.522374-3 - Fax 0331.522462
Internet: www.laboratoriotosi.it - E-mail: labtosi@tiscalinet.it - Partita IVA e Codice Fiscale 12805730152

Laboratorio di Prova Approvato
Attestato N. 004 L
IIS
QUA 041 S

Ordine n° 571/07 **del** 08/10/07 **Rapporto di prova n°** **07H2308**
Order no. of Test report no.

Cliente: **IBF** SpA **Bolla n°** **del** **Data** 12/10/07
Customer Delivery note of date

Colata n°. 04335 **Materiale** ASTM A790 UNS S32760 **Foglio** 2 **di** 3
Heat no. Material page of

Materiale ricevuto **Prove eseguite** 12/10/07
Material recived on Tests date

ESAME MICROGRAFICO

Micrographic Examination

Sample No. **5513,** item 1 - P.O. 140080 rev.1

N. 5 Pipes OD 10" sch 120 HT Lot H100000243

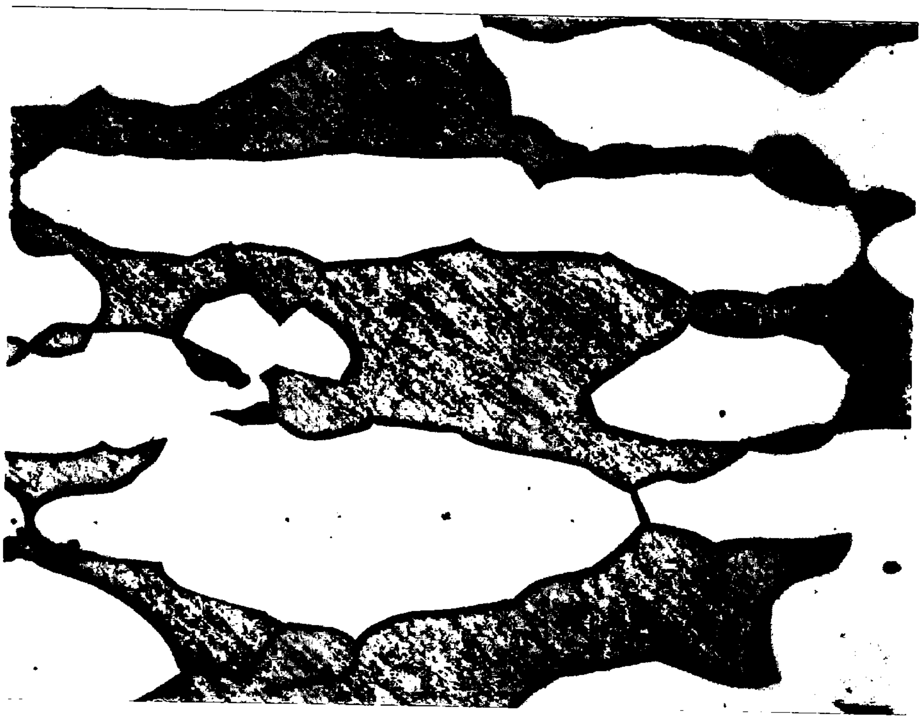

fig. 2 Magnification : 500 X

Micrographic Examination *(Half thickness)* **: Satisfactory**

The grain boundaries are free of carbide precipitation and intermetallic phase

ASTM E562 - Determining volume fraction of ferrite = 46,1 %

Intervallo di confidenza: 0,99 Confidence interval	**Errore % : 1,98** % Error	**Deviazione standard : 2,72** Standard deviation
Campi esaminati N°: 30 Examinated fields N°	**Dimensione griglia : 30 points** Dimension grille	**Attacco: ASTM E407 # 98** Etching

I risultati del rapporto di prova si riferiscono ai soli campioni testati
Test report values relate to the tested speciment only

Ente Autorizzato ☒ REV. ☐ WIT. Authorized Inspector WILDES CALLINI	**Esecutore** Examiner	**Responsabile Laboratorio** Laboratory Responsible

Ordine n° (Order no.) 571/07 **del** (of) 08/10/07 **Rapporto di prova n°** (Test report no.) **07H2308**

Cliente: (Customer) **IBF** SpA **Bolla n°** (Delivery note) **del** (of) **Data** (date) 12/10/07

Colata n°. (Heat no.) 04335 **Materiale** (Material) ASTM A790 UNS S32760 **Foglio** (page) 3 **di** (of) 3

Materiale ricevuto (Material recived on) **Prove eseguite** (Tests date) 12/10/07

ESAME MICROGRAFICO

Micrographic Examination

Sample No. **5513,** item 1 - P.O. 140080 rev.1

N. 5 Pipes OD 10" sch 120 HT Lot H100000243

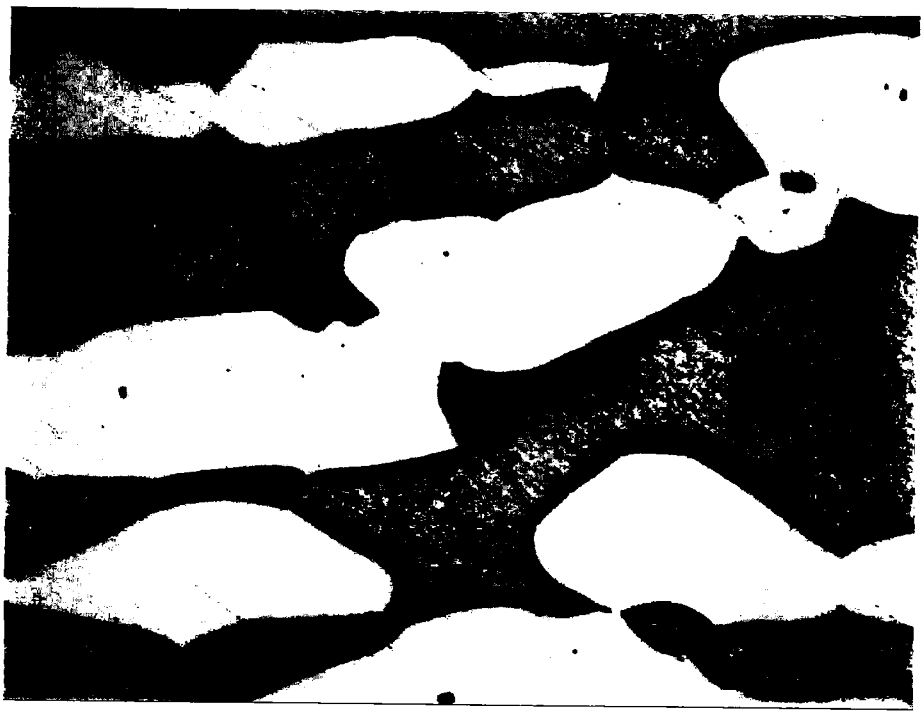

fig. 3 Magnification : 500 X

Micrographic Examination *(Internal surface)* **: Satisfactory**

The grain boundaries are free of carbide precipitation and intermetallic phase

ASTM E562 - Determining volume fraction of ferrite = 46,7 %

Intervallo di confidenza: 0,95 Confidence interval	**Errore % : 2,05** % Error	**Deviazione standard : 2,62** Standard deviation
Campi esaminati N°: 30 Examinated fields N°	**Dimensione griglia : 30 points** Dimension grille	**Attacco: ASTM E407 # 98** Etching

I risultati del rapporto di prova si riferiscono ai soli campioni testati
Test report values relate to the tested speciment only

Ente Autorizzato ☒ REV. ☐ WIT. Authorized Inspector WILDES CALLINI	**Esecutore** Examiner	**Responsabile Laboratorio** Laboratory Responsible

ANCCP
Agenzia Nazionale Certificazione Componenti e Prodotti

Laboratorio T.O.S.I. s.r.l.

Tecnici Organizzati al Servizio delle Imprese

Sede legale e Uffici: 20025 Legnano (MI) - Via Pisacane, 46 - Tel. 0331.487210 - Fax 0331.522970
Sede operativa: 20025 Legnano (MI) - P.zza Monumento, 12 - Tel. 0331.522374-3 - Fax 0331.522462
Internet: www.laboratoriotosi.it - E-mail: labtosi@tiscalinet.it - Partita IVA e Codice Fiscale 12805730152

Laboratorio di Prova Approvato
Attestato N. 004 L
QUA 041 S

Annex cert. 07H2308

DETERMINAZIONE METALLOGRAFICA DELLA FERRITE ASTM E562

FERRITE VOLUME FRACTION METALLOGRAPHIC DETERMINATION ASTM E562

Sample No. **5513**, item 1 *Esternal surface*

N° FIELDS	1	2	3	4	5	6	7	8	9	10	11	12	13	14	15
POINT COUNT	14	13	15	13	15	14	14	15	15	13	14	13	14	14	13
POINT FRACT.	46,7	43,3	50,0	43,3	50,0	46,7	46,7	50,0	50,0	43,3	46,7	43,3	46,7	46,7	43,3
$(Ppi-Pp)^2$	0,0	11,1	11,1	11,1	11,1	0,0	0,0	11,1	11,1	11,1	0,0	11,1	0,0	0,0	11,1

N° FIELDS	16	17	18	19	20	21	22	23	24	25	26	27	28	29	30
POINT COUNT	15	14	15	14	14	15	15	14	13	13	13	15	13	13	15
POINT FRACT.	50,0	46,7	50,0	46,7	46,7	50,0	50,0	46,7	43,3	43,3	43,3	50,0	43,3	43,3	50,0
$(Ppi-Pp)^2$	11,1	0,0	11,1	0,0	0,0	11,1	11,1	0,0	11,1	11,1	11,1	11,1	11,1	11,1	11,1

Volume % di ferrite riscontrato (vv): Volume frction of the ferrite	**46,7**

Errore% % Error	Intervallo di confidenza Confidence interval	Deviazione standard Standard deviation
1,938	**0,904**	**2,476**

Sample No. **5513**, item 1 *Half thickness*

N° FIELDS	1	2	3	4	5	6	7	8	9	10	11	12	13	14	15
POINT COUNT	15	14	14	13	12	13	15	14	14	13	13	14	14	13	14
POINT FRACT.	50,0	46,7	46,7	43,3	40,0	43,3	50,0	46,7	46,7	43,3	43,3	46,7	46,7	43,3	46,7
$(Ppi-Pp)^2$	15,2	0,3	0,3	7,7	37,3	7,7	15,2	0,3	0,3	7,7	7,7	0,3	0,3	7,7	0,3

N° FIELDS	16	17	18	19	20	21	22	23	24	25	26	27	28	29	30
POINT COUNT	13	14	15	14	15	15	13	14	13	15	13	14	15	14	13
POINT FRACT.	43,3	46,7	50,0	46,7	50,0	50,0	43,3	46,7	43,3	50,0	43,3	46,7	50,0	46,7	43,3
$(Ppi-Pp)^2$	7,7	0,3	15,2	0,3	15,2	15,2	7,7	0,3	7,7	15,2	7,7	0,3	15,2	0,3	7,7

Volume % di ferrite riscontrato (vv): Volume frction of the ferrite	**46,1**

Errore% % Error	Intervallo di confidenza Confidence interval	Deviazione standard Standard deviation
2,161	**0,996**	**2,728**

Sample No. **5513**, item 1 *Internal surface*

N° FIELDS	1	2	3	4	5	6	7	8	9	10	11	12	13	14	15
POINT COUNT	13	14	15	13	13	14	15	14	13	15	14	13	14	15	14
POINT FRACT.	43,3	46,7	50,0	43,3	43,3	46,7	50,0	46,7	43,3	50,0	46,7	43,3	46,7	50,0	46,7
$(Ppi-Pp)^2$	11,1	0,0	11,1	11,1	11,1	0,0	11,1	0,0	11,1	11,1	0,0	11,1	0,0	11,1	0,0

N° FIELDS	16	17	18	19	20	21	22	23	24	25	26	27	28	29	30
POINT COUNT	15	14	15	14	13	15	14	13	15	15	13	14	13	15	13
POINT FRACT.	50,0	46,7	50,0	46,7	43,3	50,0	46,7	43,3	50,0	50,0	43,3	46,7	43,3	50,0	43,3
$(Ppi-Pp)^2$	11,1	0,0	11,1	0,0	11,1	11,1	0,0	11,1	11,1	11,1	11,1	0,0	11,1	11,1	11,1

Volume % di ferrite riscontrato (vv): Volume frction of the ferrite	**46,7**

Errore% % Error	Intervallo di confidenza Confidence interval	Deviazione standard Standard deviation
2,055	**0,959**	**2,626**

☒ REV. ☐ WIT.
WILDES CALLINI

Laboratorio T.O.S.I. s.r.l.

Tecnici Organizzati al Servizio delle Imprese

Sede legale e Uffici: 20025 Legnano (MI) - Via Pisacane, 46 - Tel. 0331.487210 - Fax 0331.522970
Sede operativa: 20025 Legnano (MI) - P.zza Monumento, 12 - Tel. 0331.522374-3 - Fax 0331.522462
Internet: www.laboratoriotosi.it - E-mail: labtosi@tiscalinet.it - Partita IVA e Codice Fiscale 12805730152

ANCCP Agenzia Nazionale Certificazione Componenti e Prodotti

Laboratorio di Prova Approvato — Attestato N. 004 L — QUA 041 S

Ordine n° Order no. 570/05 **del** of 08/10/07 **Rapporto di prova n°** Test report no. **07H2311**

Cliente: Customer **IBF** SpA **Bolla n°** Delivery note **del** of **Data** date 15/10/07

Colata n°. Heat no. 04327 **Materiale** Material ASTM A790 UNS S32760 **Foglio** page 1 **di** of 3

Materiale ricevuto Material recived on **Prove eseguite** Tests date 15/10/07

ESAME MICROGRAFICO

Micrographic Examination

Sample No. **5551,** item 1 - P.O. 140080 rev.1

N. 3 Pipes OD 10" sch 120 HT Lot H100000244

fig. 1 Magnification : 500 X

Micrographic Examination *(Esternal surface)* **: Satisfactory**

The grain boundaries are free of carbide precipitation and intermetallic phase

ASTM E562 - Determining volume fraction of ferrite = 47,3 %

Intervallo di confidenza: 1,02 Confidence interval	**Errore % : 2,17** % Error	**Deviazione standard : 2,81** Standard deviation
Campi esaminati N°: 30 Examinated fields N°	**Dimensione griglia : 30 points** Dimension grille	**Attacco: ASTM E407 # 98** Etching

I risultati del rapporto di prova si riferiscono ai soli campioni testati
Test report values relate to the tested speciment only

Ente Autorizzato Authorized Inspector ☑ REV. ☐ WIT. WIEDES CALLINI	**Esecutore** Examiner	**Responsabile Laboratorio** Laboratory Responsible

Laboratorio T.O.S.I. s.r.l.
Tecnici Organizzati al Servizio delle Imprese
Sede legale e Uffici: 20025 Legnano (MI) - Via Pisacane, 46 - Tel. 0331.487210 - Fax 0331.522970
Sede operativa: 20025 Legnano (MI) - P.zza Monumento, 12 - Tel. 0331.522374-3 - Fax 0331.522462
Internet: www.laboratoriotosi.it - E-mail: labtosi@tiscalinet.it - Partita IVA e Codice Fiscale 12805730152

ANCCP Agenzia Nazionale Certificazione Componenti e Prodotti

Laboratorio di Prova Approvato — Attestato N. 004 L — IIS — QUA 041 S

Ordine n° 570/05 **del** 08/10/07 **Rapporto di prova n°** 07H2311
Order no. of Test report no.

Cliente: **IBF** SpA **Bolla n°** **del** **Data** 15/10/07
Customer Delivery note of date

Colata n°. 04327 **Materiale** ASTM A790 UNS S32760 **Foglio** 2 **di** 3
Heat no. Material page of

Materiale ricevuto — Material recived on
Prove eseguite 15/10/07 — Tests date

ESAME MICROGRAFICO
Micrographic Examination

Sample No. **5551,** item 1 - P.O. 140080 rev.1
N. 3 Pipes OD 10" sch 120 HT Lot H100000244

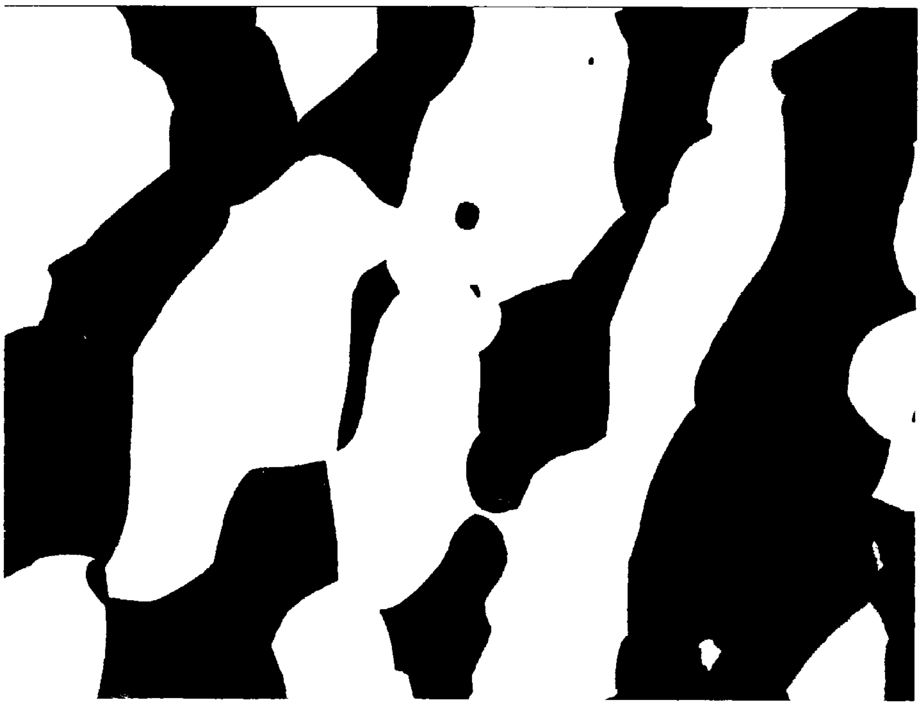

fig. 2 Magnification : 500 X

Micrographic Examination *(Half thickness)* **: Satisfactory**
The grain boundaries are free of carbide precipitation and intermetallic phase
ASTM E562 - Determining volume fraction of ferrite = 46,9 %

Intervallo di confidenza: 0,85 Confidence interval	**Errore % : 1,82** % Error	**Deviazione standard : 2,34** Standard deviation
Campi esaminati N°: 30 Examinated fields N°	**Dimensione griglia : 30 points** Dimension grille	**Attacco: ASTM E407 # 98** Etching

I risultati del rapporto di prova si riferiscono ai soli campioni testati
Test report values relate to the tested speciment only

Ente Autorizzato Authorized Inspector ☐ REV. ☐ WIT. WILDES CALLINI	**Esecutore** Examiner I. Bacchella	**Responsabile Laboratorio** Laboratory Responsible

Laboratorio T.O.S.I. s.r.l.
Tecnici Organizzati al Servizio delle Imprese
Sede legale e Uffici: 20025 Legnano (MI) - Via Pisacane, 46 - Tel. 0331.487210 - Fax 0331.522970
Sede operativa: 20025 Legnano (MI) - P.zza Monumento, 12 - Tel. 0331.522374-3 - Fax 0331.522462
Internet: www.laboratoriotosi.it - E-mail: labtosi@tiscalinet.it - Partita IVA e Codice Fiscale 12805730152

ANCCP Agenzia Nazionale Certificazione Componenti e Prodotti

Laboratorio di Prova Approvato — Attestato N. 004 L — QUA 041 S

Ordine n° Order no. 570/05 **del** of 08/10/07 — **Rapporto di prova n°** Test report no. 07H2311

Cliente: Customer **IBF** SpA — **Bolla n°** Delivery note ____ **del** of ____ — **Data** date 15/10/07

Colata n°. Heat no. 04327 — **Materiale** Material ASTM A790 UNS S32760 — **Foglio** page 3 **di** of 3

Materiale ricevuto Material recived on ____ — **Prove eseguite** Tests date 15/10/07

ESAME MICROGRAFICO
Micrographic Examination

Sample No. **5551,** item 1 - P.O. 140080 rev.1
N. 3 Pipes OD 10" sch 120 HT Lot H100000244

fig. 3 — Magnification : 500 X

Micrographic Examination *(Internal surface)* **: Satisfactory**
The grain boundaries are free of carbide precipitation and intermetallic phase
ASTM E562 - Determining volume fraction of ferrite = 47,7 %

Intervallo di confidenza: 1,03 Confidence interval	**Errore % : 2,16** % Error	**Deviazione standard : 2,83** Standard deviation
Campi esaminati N°: 30 Examinated fields N°	**Dimensione griglia : 30 points** Dimension grille	**Attacco: ASTM E407 # 98** Etching

I risultati del rapporto di prova si riferiscono ai soli campioni testati
Test report values relate to the tested speciment only

Ente Autorizzato ☒ ABS ☐ WIT. Authorized Inspector WILDES CALLINI	**Esecutore** Examiner	**Responsabile Laboratorio** Laboratory Responsible

ANCCP
Agenzia Nazionale Certificazione Componenti e Prodotti

Laboratorio T.O.S.I. s.r.l.

Tecnici Organizzati al Servizio delle Imprese

Sede legale e Uffici: 20025 Legnano (MI) - Via Pisacane, 46 - Tel. 0331.487210 - Fax 0331.522970
Sede operativa: 20025 Legnano (MI) - P.zza Monumento, 12 - Tel. 0331.522374-3 - Fax 0331.522462
Internet: www.laboratoriotosi.it - E-mail: labtosi@tiscalinet.it - Partita IVA e Codice Fiscale 12805730152

Laboratorio di Prova Approvato
Attestato N. 004 L
IIS
QUA 041 S

Annex cert. 07H2311

DETERMINAZIONE METALLOGRAFICA DELLA FERRITE ASTM E562

FERRITE VOLUME FRACTION METALLOGRAPHIC DETERMINATION ASTM E562

Sample No. **5551**, item 1 *Esternal surface*

N° FIELDS	1	2	3	4	5	6	7	8	9	10	11	12	13	14	15
POINT COUNT	14	16	15	13	15	14	14	15	15	13	14	13	14	14	13
POINT FRACT.	46,7	53,3	50,0	43,3	50,0	46,7	46,7	50,0	50,0	43,3	46,7	43,3	46,7	46,7	43,3
$(Ppi-Pp)^2$	0,4	36,1	7,1	16,0	7,1	0,4	0,4	7,1	7,1	16,0	0,4	16,0	0,4	0,4	16,0

N° FIELDS	16	17	18	19	20	21	22	23	24	25	26	27	28	29	30
POINT COUNT	15	14	15	14	14	15	15	14	16	13	13	15	13	13	15
POINT FRACT.	50,0	46,7	50,0	46,7	46,7	50,0	50,0	46,7	53,3	43,3	43,3	50,0	43,3	43,3	50,0
$(Ppi-Pp)^2$	7,1	0,4	7,1	0,4	0,4	7,1	7,1	0,4	36,1	16,0	16,0	7,1	16,0	16,0	7,1

Volume % di ferrite riscontrato (vv): Volume frction of the ferrite	**47,3**

Errore% % Error	Intervallo di confidenza Confidence interval	Deviazione standard Standard deviation
2,174	1,029	2,818

Sample No. **5551**, item 1 *Half thickness*

N° FIELDS	1	2	3	4	5	6	7	8	9	10	11	12	13	14	15
POINT COUNT	15	14	14	15	14	13	15	14	14	13	13	14	14	13	14
POINT FRACT.	50,0	46,7	46,7	50,0	46,7	43,3	50,0	46,7	46,7	43,3	43,3	46,7	46,7	43,3	46,7
$(Ppi-Pp)^2$	9,7	0,0	0,0	9,7	0,0	12,6	9,7	0,0	0,0	12,6	12,6	0,0	0,0	12,6	0,0

N° FIELDS	16	17	18	19	20	21	22	23	24	25	26	27	28	29	30
POINT COUNT	13	14	15	14	15	15	13	14	16	15	13	14	15	14	13
POINT FRACT.	43,3	46,7	50,0	46,7	50,0	50,0	43,3	46,7	53,3	50,0	43,3	46,7	50,0	46,7	43,3
$(Ppi-Pp)^2$	12,6	0,0	9,7	0,0	9,7	9,7	12,6	0,0	41,6	9,7	12,6	0,0	9,7	0,0	12,6

Volume % di ferrite riscontrato (vv): Volume frction of the ferrite	**46,9**

Errore% % Error	Intervallo di confidenza Confidence interval	Deviazione standard Standard deviation
1,828	0,857	2,347

Sample No. **5551**, item 1 *Internal surface*

N° FIELDS	1	2	3	4	5	6	7	8	9	10	11	12	13	14	15
POINT COUNT	13	14	15	16	14	14	15	14	13	15	14	13	14	15	14
POINT FRACT.	43,3	46,7	50,0	53,3	46,7	46,7	50,0	46,7	43,3	50,0	46,7	43,3	46,7	50,0	46,7
$(Ppi-Pp)^2$	18,7	1,0	5,5	32,2	1,0	1,0	5,5	1,0	18,7	5,5	1,0	18,7	1,0	5,5	1,0

N° FIELDS	16	17	18	19	20	21	22	23	24	25	26	27	28	29	30
POINT COUNT	15	14	15	14	13	15	14	13	15	15	13	14	15	15	16
POINT FRACT.	50,0	46,7	50,0	46,7	43,3	50,0	46,7	43,3	50,0	50,0	43,3	46,7	50,0	50,0	53,3
$(Ppi-Pp)^2$	5,5	1,0	5,5	1,0	18,7	5,5	1,0	18,7	5,5	5,5	18,7	1,0	5,5	5,5	32,2

Volume % di ferrite riscontrato (vv): Volume frction of the ferrite	**47,7**

Errore% % Error	Intervallo di confidenza Confidence interval	Deviazione standard Standard deviation
2,169	1,034	2,831

☐ REV. ☐ WIT.
WILDES CALLINI

ANCCP
Agenzia Nazionale Certificazione Componenti e Prodotti

Laboratorio T.O.S.I. s.r.l.

Tecnici Organizzati al Servizio delle Imprese

Sede legale e Uffici: 20025 Legnano (MI) - Via Pisacane, 46 - Tel. 0331.487210 - Fax 0331.522970
Sede operativa: 20025 Legnano (MI) - P.zza Monumento, 12 - Tel. 0331.522374-3 - Fax 0331.522462
Internet: www.laboratoriotosi.it - E-mail: labtosi@tiscalinet.it - Partita IVA e Codice Fiscale 12805730152

Laboratorio di Prova Approvato
Attestato N. 004 L
QUA 041 S

		Ordine n° Order no.	571/07	**del** of	08/10/07
Cliente: Customer	**IBF** SpA	**Bolla n°** Delivery note		**del** of	
Colata n°. Heat no.	04336	**Materiale** Material	ASTM A790 UNS S32760		

Rapporto di prova n° 07H2309
Test report no.

Data 12/10/07
date

Foglio 1 **di** 1
page of

Materiale ricevuto ....
Material recived on

Prove eseguite 12/10/07
Tests date

PROVA DI RESISTENZA ALLA CORROSIONE PER PITTING (ASTM G48 Metodo A)

Pitting Corrosion Resistance (ASTM G48 Method A)

Sample **5512** item 1
N. 5 Pipes OD 10" sch 120 HT Lot H100000242

1) Preparazione provino
Specimen preparation

a) dimensione : 27 x 12 x 26 (W Thk) mm
dimension

b) posizione Trasversale
position *Trasversal, including external and internal surfaces*

c) lucidatura : carte n. 120 a umido
polishing wetemery papers n. 120

2) Prova:
Test

a) soluzione : soluzione cloruro ferrico 6%
ferric chloride solution

b) temperatura: 50 °C
temperature

c) tempo 24 h
time

3) Valutazione
Evaluation

perdita di peso : 0,0014 g. 0,52 g/m^2
weight loss (< 4,0 g/m^2)

esame visivo (20x) : **CONFORME**
visual examination: ***satisfactory*** *no pitting at 20x magnification*

IBF S.p.A. N. LANCIA Q.C.

I risultati del rapporto di prova si riferiscono ai soli campioni testati
Test report values relate to the tested speciment only

Ente Autorizzato Authorized Inspector	**Esecutore** Examiner	**Responsabile Laboratorio** Laboratory Responsible
☒ REV. ☐ WIT. **WILDES CALLINI**	M Baiatella	

ANCCP
Agenzia Nazionale Certificazione Componenti e Prodotti

Laboratorio T.O.S.I. s.r.l.

Tecnici Organizzati al Servizio delle Imprese

Sede legale e Uffici: 20025 Legnano (MI) - Via Pisacane, 46 - Tel. 0331.487210 - Fax 0331.522970
Sede operativa: 20025 Legnano (MI) - P.zza Monumento, 12 - Tel. 0331.522374-3 - Fax 0331.522462
Internet: www.laboratoriotosi.it - E-mail: labtosi@tiscalinet.it - Partita IVA e Codice Fiscale 12805730152

Laboratorio di Prova Approvato
Attestato N. 004 L
QUA 041 S

Ordine n° 571/07 **del** 08/10/07 Order no. of		**Rapporto di prova n°** **07H2310** Test report no.
Cliente: **IBF** SpA Customer	**Bolla n°** ______ **del** ______ Delivery note of	**Data** 12/10/07 date
Colata n°. 04335 Heat no.	**Materiale** ASTM A790 UNS S32760 Material	**Foglio** 1 **di** 1 page of
Materiale ricevuto ______ Material recived on		**Prove eseguite** 12/10/07 Tests date

PROVA DI RESISTENZA ALLA CORROSIONE PER PITTING (ASTM G48 Metodo A)

Pitting Corrosion Resistance (ASTM G48 Method A)

Sample **5513** item 1

N. 5 Pipes OD 10" sch 120 HT Lot H100000243

1) Preparazione provino
Specimen preparation
   - a) dimensione : 26 x 12 x 25 (W Thk) mm
     dimension
   - b) posizione Trasversale
     position *Trasversal, including external and internal surfaces*
   - c) lucidatura : carte n. 120 a umido
     polishing wetemery papers n. 120

2) Prova:
Test
   - a) soluzione : soluzione cloruro ferrico 6%
     ferric chloride solution
   - b) temperatura: 50 °C
     temperature
   - c) tempo 24 h
     time

3) Valutazione
Evaluation

perdita di peso : 0,0012 g. — 0,48 g/m^2
weight loss — (< 4,0 g/m^2)

esame visivo (20x) : **CONFORME**
visual examination: ***satisfactory*** *no pitting at 20x magnification*

IBF S.p.A N. LANCI Q.C.

I risultati del rapporto di prova si riferiscono ai soli campioni testati
Test report values relate to the tested speciment only

Ente Autorizzato Authorized Inspector ☒ REV. ☐ WIT. WILDES CALLINI	**Esecutore** Examiner M Baratella	**Responsabile Laboratorio** Laboratory Responsible

ANCCP
Agenzia Nazionale
Certificazione
Componenti e Prodotti

Laboratorio T.O.S.I. s.r.l.

Tecnici Organizzati al Servizio delle Imprese

Sede legale e Uffici: 20025 Legnano (MI) - Via Pisacane, 46 - Tel. 0331.487210 - Fax 0331.522970
Sede operativa: 20025 Legnano (MI) - P.zza Monumento, 12 - Tel. 0331.522374-3 - Fax 0331.522462
Internet: www.laboratoriotosi.it - E-mail: labtosi@tiscalinet.it - Partita IVA e Codice Fiscale 12805730152

Laboratorio di Prova Approvato
Attestato N. 004 L
QUA 041 S

Ordine n° 570/07 **del** 08/10/07
Order no. of

Rapporto di prova n° **07H2314**
Test report no.

Cliente: **IBF** SpA
Customer

Bolla n° **del**
Delivery note of

Data 15/10/07
date

Colata n°. 04327
Heat no.

Materiale ASTM A790 UNS S32760
Material

Foglio 1 **di** 1
page of

Materiale ricevuto
Material recived on

Prove eseguite 15/10/07
Tests date

PROVA DI RESISTENZA ALLA CORROSIONE PER PITTING (ASTM G48 Metodo A)

Pitting Corrosion Resistance (ASTM G48 Method A)

Sample **5551** item 1
N. 3 Pipes OD 10" sch 120 HT Lot H100000244

1) Preparazione provino
Specimen preparation

a) dimensione : 16 x 14 x 24 (W Thk) mm
dimension

b) posizione Trasversale
position *Trasversal, including external and internal surfaces*

c) lucidatura : carte n. 120 a umido
polishing wetemery papers n. 120

2) Prova:
Test

a) soluzione : soluzione cloruro ferrico 6%
ferric chloride solution

b) temperatura: 50 °C
temperature

c) tempo 24 h
time

3) Valutazione
Evaluation

perdita di peso : 0,0009 g. 0,48 g/m^2
weight loss (< 4,0 g/m^2)

esame visivo (20x) : **CONFORME**
visual examination: ***satisfactory*** *no pitting at 20x magnification*

IBF S.p.A. MILANO Q.C.

I risultati del rapporto di prova si riferiscono ai soli campioni testati
Test report values relate to the tested speciment only

Ente Autorizzato / Authorized Inspector ☑ REV. ☐ WIT. WILDES CALLINI	Esecutore / Examiner	Responsabile Laboratorio / Laboratory Responsible
[signature]	[signature]	[signature]

Laboratorio T.O.S.I. s.r.l.

ANCCP Agenzia Nazionale Certificazione Componenti e Prodotti

Tecnici Organizzati al Servizio delle Imprese

Sede legale e Uffici: 20025 Legnano (MI) - Via Pisacane, 46 - Tel. 0331.487210 - Fax 0331.522970
Sede operativa: 20025 Legnano (MI) - P.zza Monumento, 12 - Tel. 0331.522374-3 - Fax 0331.522462
Internet: www.laboratoriotosi.it - E-mail: labtosi@tiscalinet.it - Partita IVA e Codice Fiscale 12805730152

Laboratorio di Prova Approvato — Attestato N. 004 L — QUA 041 S

Ordine n° 581/07 **del** 09/10/07 — **Rapporto di prova n°** **07H2376**
Order no. of — Test report no.

Cliente: **IBF** SpA — **Bolla n°** **del** — **Data** 19/10/07
Customer — Delivery note of — date

Colata n°. 04347 — **Materiale** ASTM A790 UNS S32760 — **Foglio** 1 **di** 1
Heat no. — Material — page of

Materiale ricevuto — **Prove eseguite** 19/10/07
Material recived on — Tests date

PROVA DI RESISTENZA ALLA CORROSIONE PER PITTING (ASTM G48 Metodo A)

Pitting Corrosion Resistance (ASTM G48 Method A)

Sample **5567** item 1
N. 3 Pipes OD 10" sch 120 HT Lot H100000245

1) Preparazione provino — *Specimen preparation*
   a) dimensione : 16 x 14 x 24 (W Thk) mm — *dimension*
   b) posizione Trasversale — *position* *Trasversal, including external and internal surfaces*
   c) lucidatura : carte n. 120 a umido — *polishing wetemery papers n. 120*

2) Prova: — *Test*
   a) soluzione : soluzione cloruro ferrico 6% — *ferric chloride solution*
   b) temperatura: 50 °C — *temperature*
   c) tempo 24 h — *time*

3) Valutazione — *Evaluation*
   perdita di peso : 0,0008 g. 0,42 g/m^2
   weight loss (< 4,0 g/m^2)

   esame visivo (20x) : **CONFORME**
   visual examination: ***satisfactory*** *no pitting at 20x magnification*

I risultati del rapporto di prova si riferiscono ai soli campioni testati
Test report values relate to the tested speciment only

Ente Autorizzato	Esecutore	Responsabile Laboratorio
Authorized Inspector ☐ REV. ☐ WIT. WILDES CALLINI	Examiner MBalatella	Laboratory Responsible

ANCCP
Agenzia Nazionale
Certificazione
Componenti e Prodotti

Laboratorio T.O.S.I. s.r.l.

Tecnici Organizzati al Servizio delle Imprese

Sede legale e Uffici: 20025 Legnano (MI) - Via Pisacane, 46 - Tel. 0331.487210 - Fax 0331.522970
Sede operativa: 20025 Legnano (MI) - P.zza Monumento, 12 - Tel. 0331.522374-3 - Fax 0331.522462
Internet: www.laboratoriotosi.it - E-mail: labtosi@tiscalinet.it - Partita IVA e Codice Fiscale 12805730152

Laboratorio di Prova Approvato
Attestato N. 004 L
QUA 041 S

Ordine n° 581/07 **del** 09/10/07 **Rapporto di prova n°** **07H2377**
Order no. of Test report no.

Cliente: **IBF** SpA **Bolla n°** **del** **Data** 19/10/07
Customer Delivery note of date

Colata n°. 04354 **Materiale** ASTM A790 UNS S32760 **Foglio** 1 **di** 1
Heat no. Material page of

Materiale ricevuto **Prove eseguite** 19/10/07
Material recived on Tests date

PROVA DI RESISTENZA ALLA CORROSIONE PER PITTING (ASTM G48 Metodo A)

Pitting Corrosion Resistance (ASTM G48 Method A)

Sample **5568** item 1
N. 3 Pipes OD 10" sch 120 HT Lot H100000248

1) Preparazione provino
Specimen preparation
   - a) dimensione : 15 x 13 x 25 (W Thk) mm
     dimension
   - b) posizione Trasversale
     position *Trasversal, including external and internal surfaces*
   - c) lucidatura : carte n. 120 a umido
     polishing wetemery papers n. 120

2) Prova:
Test
   - a) soluzione : soluzione cloruro ferrico 6%
     ferric chloride solution
   - b) temperatura: 50 °C
     temperature
   - c) tempo 24 h
     time

3) Valutazione
Evaluation
   perdita di peso : 0,0009 g. 0,50 g/m^2
   weight loss (< 4,0 g/m^2)

   esame visivo (20x) : **CONFORME**
   visual examination: ***satisfactory*** *no pitting at 20x magnification*

I risultati del rapporto di prova si riferiscono ai soli campioni testati
Test report values relate to the tested speciment only

Ente Autorizzato Authorized Inspector	**Esecutore** Examiner	**Responsabile Laboratorio** Laboratory Responsible
REV. ☐ WIT. WILDES CALLINI	MBalatella	

Mod.14.1 rev. 0 Questo documento non può essere riprodotto parzialmente senza autorizzazione scritta del Laboratorio T.O.S.I. srl

ANCCP
Agenzia Nazionale Certificazione Componenti e Prodotti

Laboratorio T.O.S.I. s.r.l.

Tecnici Organizzati al Servizio delle Imprese

Sede legale e Uffici: 20025 Legnano (MI) - Via Pisacane, 46 - Tel. 0331.487210 - Fax 0331.522970
Sede operativa: 20025 Legnano (MI) - P.zza Monumento, 12 - Tel. 0331.522374-3 - Fax 0331.522462
Internet: www.laboratoriotosi.it - E-mail: labtosi@tiscalinet.it - Partita IVA e Codice Fiscale 12805730152

Laboratorio di Prova Approvato
Attestato N. 004 L
QI A 041 S

Ordine n° 587/07 **del** 10/10/07 **Rapporto di prova n°** **07H2379**
Order no. of Test report no.

Cliente: **IBF** SpA **Bolla n°** ____ **del** ____ **Data** 19/10/07
Customer Delivery note of date

Colata n°. 04347 **Materiale** ASTM A790 UNS S32760 **Foglio** 1 **di** 1
Heat no. Material page of

Materiale ricevuto ____ **Prove eseguite** 19/10/07
Material recived on Tests date

PROVA DI RESISTENZA ALLA CORROSIONE PER PITTING (ASTM G48 Metodo A)

Pitting Corrosion Resistance (ASTM G48 Method A)

Sample **5577** item 1
N. 1 Pipe OD 10" sch 120 HT Lot H100000250

1) Preparazione provino
Specimen preparation
- a) dimensione : 20 x 13 x 23 (W Thk) mm
  dimension
- b) posizione Trasversale
  position *Trasversal, including external and internal surfaces*
- c) lucidatura : carte n. 120 a umido
  polishing wetemery papers n. 120

2) Prova:
Test
- a) soluzione : soluzione cloruro ferrico 6%
  ferric chloride solution
- b) temperatura: 50 °C
  temperature
- c) tempo 24 h
  time

3) Valutazione
Evaluation

perdita di peso : 0,0009 g. 0,44 g/m^2
weight loss (< 4,0 g/m^2)

esame visivo (20x) : **CONFORME**
visual examination: ***satisfactory*** *no pitting at 20x magnification*

I risultati del rapporto di prova si riferiscono ai soli campioni testati
Test report values relate to the tested speciment only

Ente Autorizzato Authorized Inspector	**Esecutore** Examiner	**Responsabile Laboratorio** Laboratory Responsible
☑ REV. ☐ WIT. WILDES CALLINI	MBaratella	

ANCCP
Agenzia Nazionale Certificazione Componenti e Prodotti

Laboratorio T.O.S.I. s.r.l.

Tecnici Organizzati al Servizio delle Imprese

Sede legale e Uffici: 20025 Legnano (MI) - Via Pisacane, 46 - Tel. 0331.487210 - Fax 0331.522970
Sede operativa: 20025 Legnano (MI) - P.zza Monumento, 12 - Tel. 0331.522374-3 - Fax 0331.522462
Internet: www.laboratoriotosi.it - E-mail: labtosi@tiscalinet.it - Partita IVA e Codice Fiscale 12805730152

Laboratorio di Prova Approvato
Attestato N. 004 L
QUA 041 S

Ordine n° 594/07 **del** 12/10/07 Order no. of		**Rapporto di prova n°** 07H2380 Test report no.
Cliente: IBF SpA Customer	**Bolla n°** **del** Delivery note of	**Data** 19/10/07 date
Colata n°. 04354 Heat no.	**Materiale** ASTM A790 UNS S32760 Material	**Foglio** 1 **di** 1 page of

Materiale ricevuto
Material recived on

Prove eseguite 19/10/07
Tests date

PROVA DI RESISTENZA ALLA CORROSIONE PER PITTING (ASTM G48 Metodo A)

Pitting Corrosion Resistance (ASTM G48 Method A)

Sample **5578** item 1

N. 2 Pipes OD 10" sch 120 HT Lot H100000250

1) Preparazione provino — *Specimen preparation*
   a) dimensione : 20 x 12 x 22 (W Thk) mm
      dimension
   b) posizione Trasversale
      position *Trasversal, including external and internal surfaces*
   c) lucidatura : carte n. 120 a umido
      polishing wetemery papers n. 120

2) Prova: — *Test*
   a) soluzione : soluzione cloruro ferrico 6%
      ferric chloride solution
   b) temperatura: 50 °C
      temperature
   c) tempo 24 h
      time

3) Valutazione — *Evaluation*
   perdita di peso : 0,0008 g. 0,42 g/m^2
   weight loss (< 4,0 g/m^2)

   esame visivo (20x) : **CONFORME**
   visual examination: ***satisfactory*** *no pitting at 20x magnification*

I risultati del rapporto di prova si riferiscono ai soli campioni testati
Test report values relate to the tested speciment only

Ente Autorizzato ☒ REV. ☐ WIT. Authorized Inspector WILDES CALLINI Callini	Esecutore Examiner MBaratelli	Responsabile Laboratorio Laboratory Responsible

Kuhn Special Steel
Reliable solutions. Always.

Prüfbescheinigungsart: *Inspection document:*	**cert. acc. to EN 10204: 2005 - 3.1**
Bescheinigungs-Nr.: *Document number:*	**00046446**
Rev.-Nr.: *Rev. no.:*	
Ausstellungsdatum: *Date of issue:*	**02.03.2017**
Seite: *Page:*	**1 / 2**
Auftrags-Nr.: *Order no.:*	**LS QS01/2017 Pos. 1**
Lieferschein-Nr.: *Delivery note no.:*	**LM 00172373 Pos. 10**
Fertigungs-Nr.: *Production no:*	**P1-00643455-**
KK-Artikel-Nr.: *KK part no.:*	**178996**
Bescheinigungsaussteller: *Originator of the document:*	**Qualitätsstelle**
Ansprechpartner: *Contact person:*	**Karina Nitz**
Telefon: *Telephone:*	**+49 (2195) 671-690**
Herstellerkennzeichen: *Symbol of the manuf. work:*	
Werksachverständigen-kennzeichen: *Inspector`s Stamp:*	W A

IMP / NTNU
Prof. Roy Johnsen
Richard Birkelandvei 2b

12345 Trondheim
Norwegen

Umfang der Lieferung
Extend of delivery

Bestellnummer: *Purchaser`s order no.:*	Prof.Roy Johnsen	Bestelldatum: *Date of order:*	01.03.2017
Menge: *Quantity:*	0,25 ST	Kunden-Nr.: *Customer no.:*	12559
Gegenstand: *Part:*	High-grade steel rings	Zeichnungsnummer: *Drawing no.:*	Segment *segment*
Abmessungen: *Dimensions:*	273.0 mm / 213.0 mm x 150.0 mm	Kunden-Artikel-Nr.: *Customer article no.:*	
Werkstoffnummer: *Material no.:*	1.4471.02	Werkstoff: *Material:*	GX3CrNiMoWCuN *27-6-3-1*
Spezifikation: *Specification:*	SEW 410 : 1998-07	Lieferzustand: *Delivery condition:*	+AT
Spezifikation 2: *Specification 2:*	Erstmustermaterial *first sample material*	Erzeugnisform: *Casting process:*	Schleuderguss *Centrifugal casting*
Spezifikation 3: *Specification 3:*		Erschmelzungsart: *Steel making process:*	E

Chemische Zusammensetzung: Schmelzanalyse [Gew.-%]
Chemical composition: Ladle analysis [wt.-%]

Anzahl *Qty.*	Schmelzennr. *Cast number*	C	Si	Mn	P	S	Cr	Ni	Mo	Cu	W	N	PRE	
	Min						25,50	5,50	3,00	0,80	0,90	0,150	42,0	
	Max	0,030	1,00	2,00	0,030	0,020	28,00	8,00	4,00	1,30	1,10	0,280		
1	F10689	0,018	0,44	0,47	0,015	0,006	27,26	7,21	3,72	1,09	1,04	0,224	43,1	

Klaus Kuhn Edelstahlgießerei GmbH
Otto-Hahn-Straße 12-14
42477 Radevormwald

Die Werksachverständige
Inspector
Karina Nitz

Probennummer und Wärmebehandlung
Test no. and heat treatment no.

Anzahl *No of pcs.*	Schmelzen-Nr. *Melting number*	Probennr. *Test no.*
1	F10689	151680

Zugversuch
Tensile test

Probennr. *Test no.*	T	E-Modul	Rp 0.2	Rp 1.0	Rm	A	Z	T	K_2 [J]				Härte *Hardness*			
	°C	GPa	MPa	MPa	MPa	%	%	°C	1	2	3	Ø	1	2	3	Ø
Min	RT		480		650	22										
Max	RT				850											
151680	RT		606	686	827	27	46	RT	155	132	126	137				
151680	100		549	597	700	30	62	-46	139	138	139	138				
151680	150		461	518	670	31	56	-80	56	40	62	52				
151680	200		418	475	663	34	62									

Die Prüfungen wurden nach den folgenden Normen durchgeführt:
The tests were executed acc. to the following standards:

Zugversuch: DIN EN ISO 6892-1: 2009-12
Tensile test:
Probenform: Ø 10 mm
Shape of test piece:
Probenrichtung: tangential
Direction of test piece:

Kerbschlagbiegeversuch: DIN EN ISO 148-1: 2011-01
Charpy impact test:
Probenform: V
Shape of test piece:
Probenrichtung: tangential
Direction of test piece:

Warmzugversuch: DIN EN ISO 6892-2:2011-05
Hot tensile test:
Probenform: Ø 10 mm
Shape of test piece:
Probenrichtung:
Direction of test piece:

- G48-Test Methode A-50°C-24h - OK / G48-Test Method A-50°C-24h - OK

- Schliff / Microsection (Austenite grain spacing acc. to DVN-RPF112) - OK
  15,5µm = fine

Die Lieferung wurde geprüft und entspricht den oben genannten Spezifikationen.
The products are tested and are found to be in accordance with the above specification.

Klaus Kuhn Edelstahlgießerei GmbH
Otto-Hahn-Straße 12-14
42477 Radevormwald

Die Werksachverständige
Inspector
Karina Nitz